ISGN-7

August 5-10, 2018
Warsaw, Poland

International Symposium on Growth of III-Nitrides
ISGN-7

Welcome to the 7ᵗʰ International Symposium on Growth of III-Nitrides (ISGN-7). We meet in Warsaw, the core city for GaN-related research in Poland. The conference venue is the *University of Warsaw*, located close to the *City Old Town*, and the city center. This location creates a friendly and pleasant atmosphere for our meeting. We will be given an opportunity to experience Warsaw modern metropolis spirit as well as its unforgettable history.

The ISGN-7 symposium will be focused on the recent progress and future directions in the field of bulk crystallization, thin film growth and fabrication of nanostructures of III-nitrides. These aspects will be discussed in the context of applications in optoelectronic as well as in high power electronic devices. Among excellent scientists presenting their latest research we will have the opportunity to listen to Nobel Prize Winners – Hiroshi Amano and Shuji Nakamura as well as to Sylwester Porowski, the founder of the Institute of High Pressure Physics Polish Academy of Sciences and author of pioneering work in bulk GaN crystallization from solution. We have succeeded to invite recognized colleagues to present plenary and invited lectures on very recent and outstanding achievements in the field of crystallization, fundamental properties and applications of nitride semiconductors. The plenary and invited speakers were selected by the Program Committee led by Michał Boćkowski.

I hope you will enjoy the scientific sessions as well as the social program of the Symposium. I am looking forward to meeting you in person at ISGN-7 in Warsaw.

Izabella Grzegory

Conference Chair

ISGN-7 Organizing Committee

Conference Chair

- Izabella Grzegory

Honorary Chair

- Sylwester Porowski

Conference Co-Chairs

- Tadeusz Suski
- Maria Kamińska

Program Committee

- Michał Boćkowski (Chair)
- Czesław Skierbiszewski (Co-Chair)
- Detlef Hommel (Co-Chair)
- Hiroshi Fujioka
- Yasushi Nanishi
- Akinori Koukitu
- Koichi Kakimoto
- Yusuke Mori
- Xinqiang Wang
- Euijoon Yoon
- Russell Dupuis
- Stacia Keller
- Andrew Allerman
- Jaime Freitas
- Jung Han
- Bernard Gil
- Enrique Calleja
- Ferdinand Scholz
- Bo Monemar
- Martin Kuball

International Advisory Committee

- Yasushi Nanishi (Chair)
- Andrew Allerman
- Hiroshi Amano
- Enrique Calleja
- Jen Inn Chyi
- Russell Dupuis
- Bernard Gil
- Nicolas Grandjean
- Izabella Grzegory
- Jung Han
- Sergey Ivanov
- Debdeep Jena
- Katsumi Kishino
- Hideto Miyake
- Bo Monemar
- Rachel Oliver
- Fernando Ponce
- Ferdinand Scholz
- Bo Shen
- Zlatko Sitar
- Euijoon Yoon
- Akihiko Yoshikawa

Local Committee

- Małgorzata Iwińska
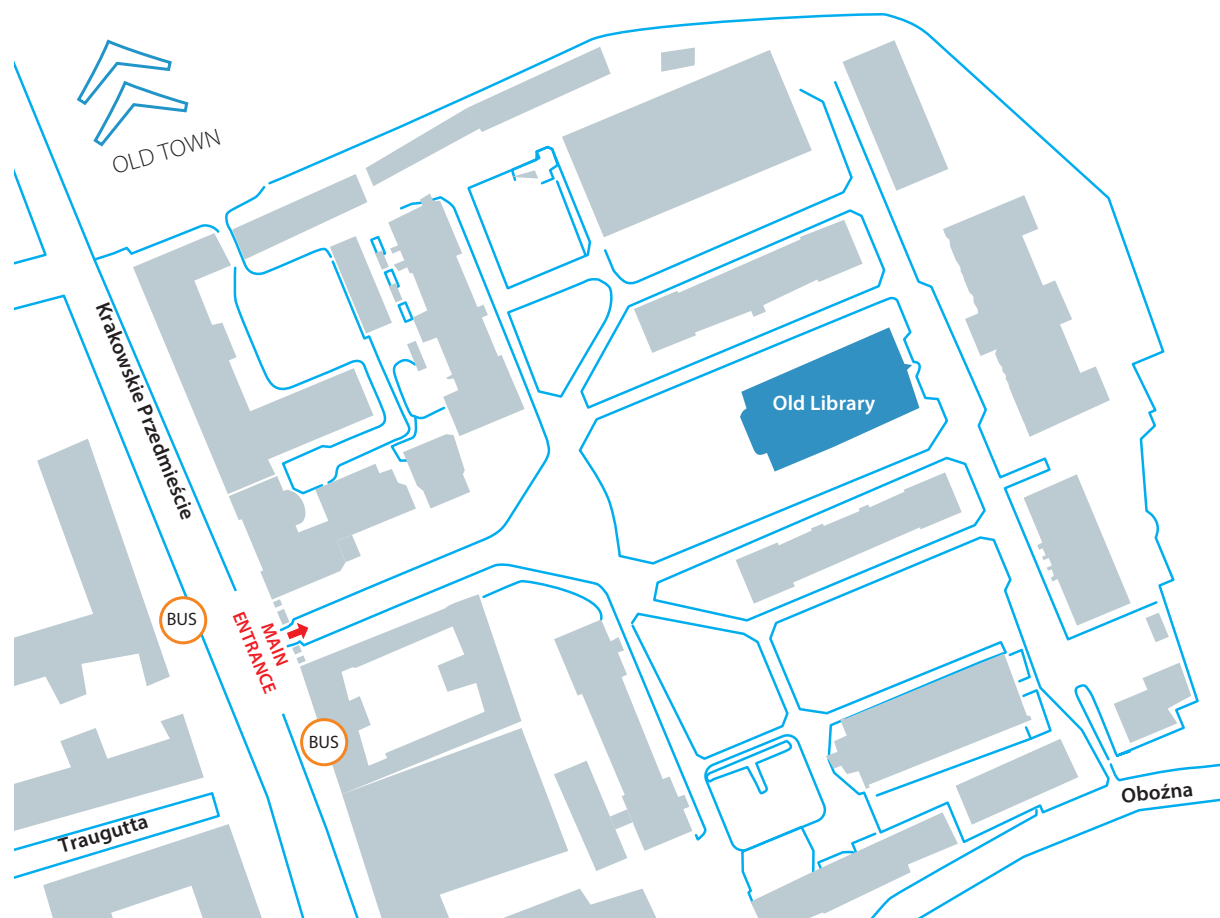- Marta Sawicka
- Aneta Drabińska
- Edyta Piskorska-Hommel

Abstract submission system

- Bartłomiej Witkowski

Conference website

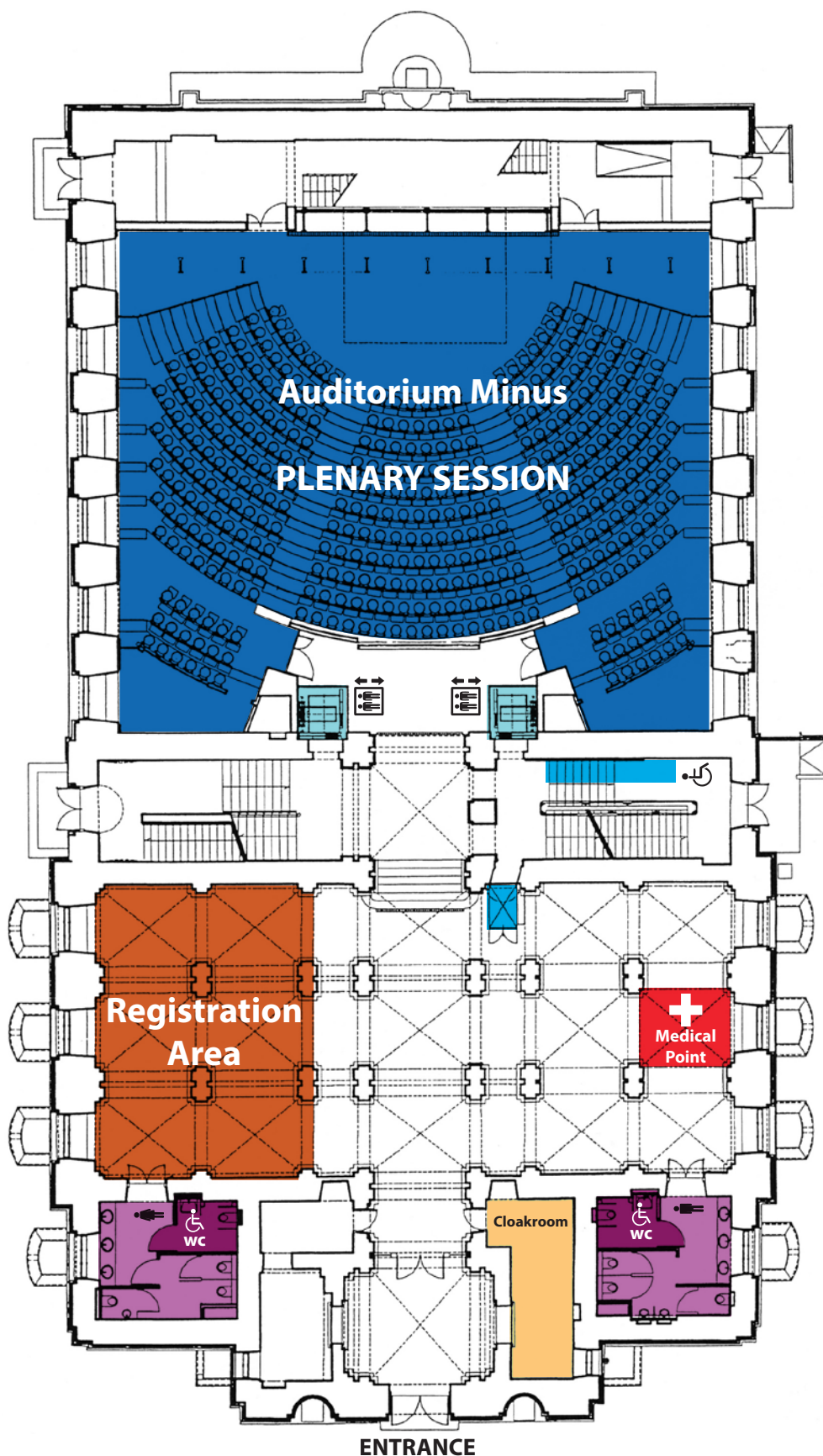- Konrad Sakowski
- Sławomir Sakowski

MAIN CAMPUS MAP

OLD TOWN

Krakowskie Przedmieście

BUS

MAIN ENTRANCE

BUS

Old Library

Oboźna

Traugutta

CONFERENCE VENUE ADDRESS
University of Warsaw
Street: Krakowskie Przedmieście 26/28
Warszawa

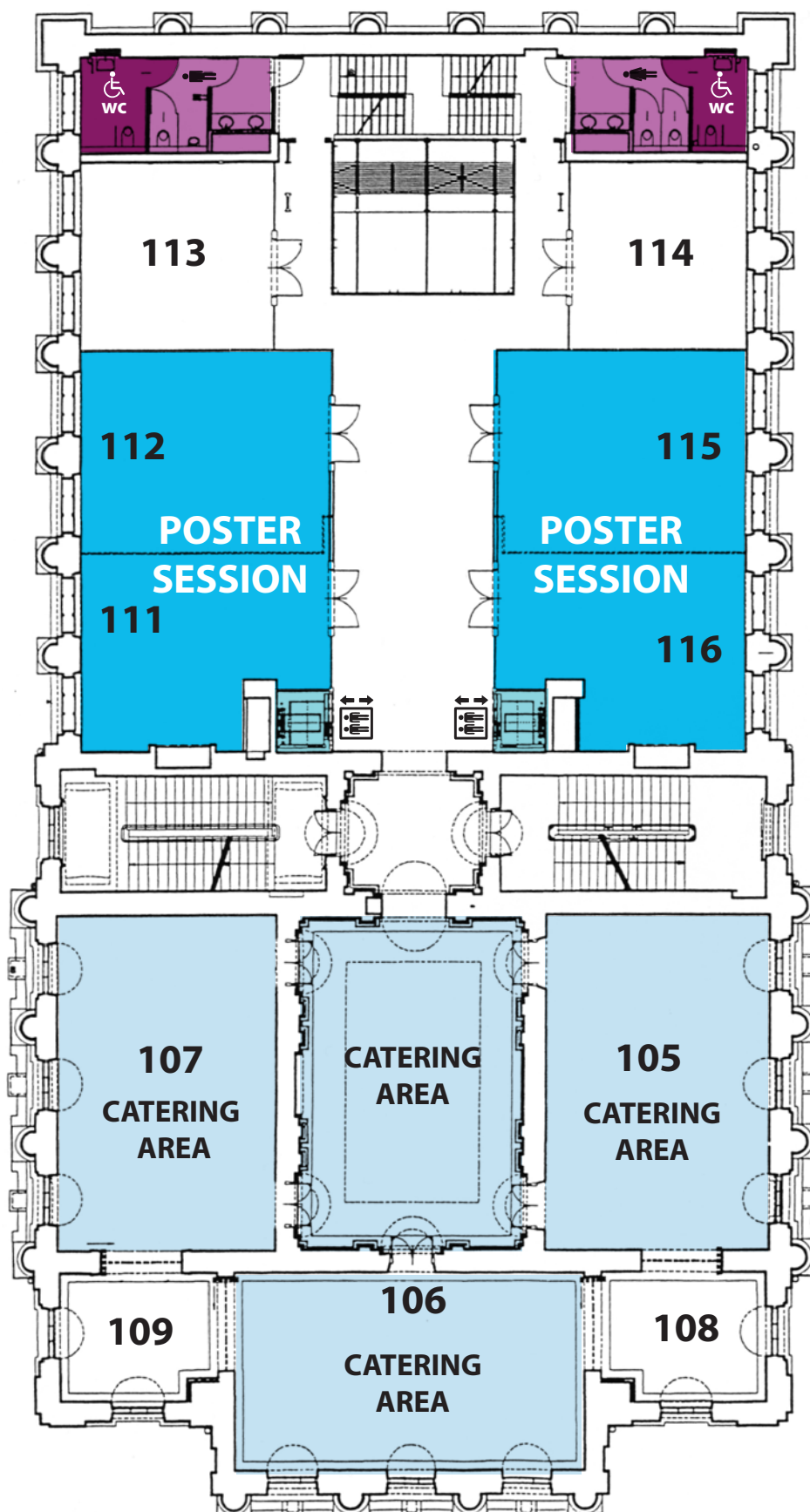wi·fi

SSiD: **ISGN7**
Password: **Warsaw2018**

Auditorium Minus

PLENARY SESSION

Registration Area

Medical Point

Cloakroom

WC

WC

ENTRANCE

113

114

112

POSTER SESSION

115

POSTER SESSION

111

116

107
CATERING AREA

CATERING AREA

105
CATERING AREA

109

106
CATERING AREA

108

WC

213

214

212

215

PARALLEL SESSION A

PARALLEL SESSION B

211

216

207
CONFERENCE OFFICE

205
COMPUTER ROOM

209

208

206
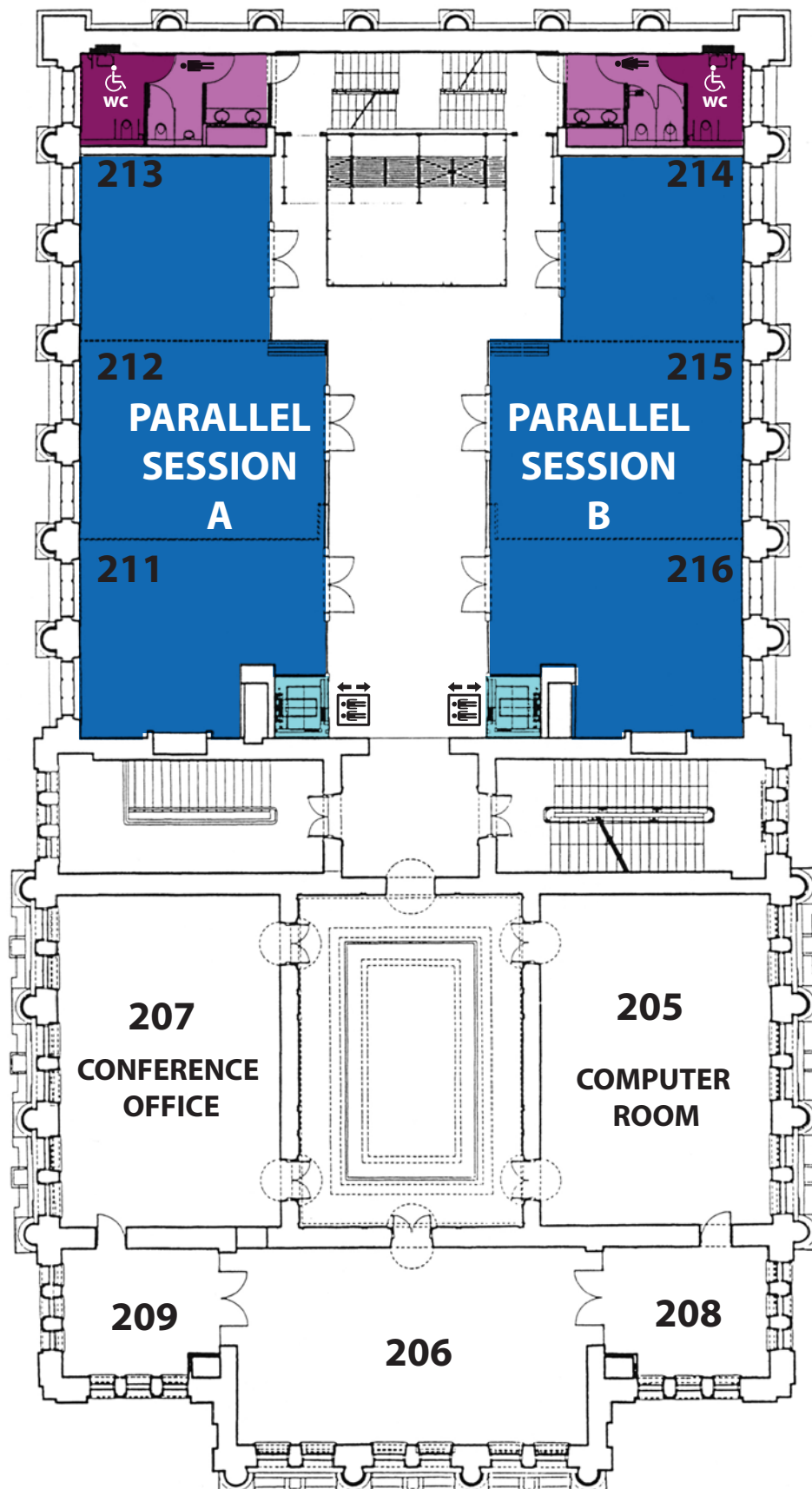
Detailed Program

SUNDAY (5ᵀᴴ AUGUST)

17.00   Registration starts (open during entire event)

18.00-20.00   Get together

MONDAY (6TH AUGUST)

08.45-09.00 **Opening Ceremony (I. Grzegory)**
Decoration of Prof. Porowski with honorary Medal for the Merited for Mazovia

09.00-10.40 **Plenary Session 1**
PS1 (chair: Y Nanishi)

09.00-09.50 **Is the phase diagram of GaN anomalous in respect to other tetrahedrally bonded semiconductors?** **PS1.1**

Sylwester Porowski

Institute of High Pressure Physics PAS, ul. Sokołowska 29/37, 01-142 Warsaw, Poland

09.50-10.40 **The invention of high efficient blue LEDs and future solid state lighting** **PS1.2**

Shuji Nakamura

Materials and ECE Departments Solid State Lighting and Energy Center University of California Santa Barbara Santa Barbara, CA 93106 USA

10.40-11.10 **Coffee break**

11.10-12.50 **Plenary Session 2**
PS2 (chair: T. Suski)

11.10-12.00 **Transformative Electronics Based on GaN and Related Materials for Realizing Sustainable Smart Society** **PS2.1**

Hiroshi Amano

Institute of Materials and Systems for Sustainability, Nagoya University, C3-1 Furo-cho, Chikusa-ku, Nagoya 464-8603, Japan

12.00-12.50 **AlGaN – a semiconductor that nature has never intended** **PS2.2**

Zlatko Sitar, P. Reddy, F. Kaess, R. Kirste, J. Tweedie, R.Collazo

North Carolina State University, Material Science and Engineering Department, Raleigh 27695, NC, USA
Adroit Materials, Inc., 991 Aviation Pkwy, Suite 800, Morrisville, NC 27560, USA.

13.00-14.00 **Lunch break**

14.00-16.00 **Parallel sessions: Growth and Characterization & Optoelectronic Devices**

Growth and Characterization - Mo1 (chair: J. Suda)

14.00-14.30 **HVPE as A New Tool for Homo-Epitaxial Growth of Highly-Pure and Thick GaN Drift Layers for Power Devices (invited)** **Mo1.1**

Hajime Fujikura, Taichiro Konno, Takehiro Yoshida and Fumimasa Horikiri

SCIOCS Co. Ltd., 880 Isagozawa-cho, Hitachi, Japan

14.30-15.00 **HVPE growth of bulk GaN, progress and challenges (invited)** **Mo1.2**

Ke Xu

Suzhou Institute of Nano-tech and Nano-bionics, Chinese Academy of Sciences
Suzhou Nanowin Science and Technology Co., Ltd. Ruoshui Road 398, Suzhou Industry Park, Suzhou 215123, P. R. China

15.00-15.30 **Recent progress in HVPE-GaN growth on ammonothermally grown GaN seeds (invited)** **Mo1.3**

T. Sochacki, M. Amilusik, M. Fijalkowski, B. Lucznik, M. Iwinska, S. Sakowski, J.L. Weyher, I. Grzegory, M. Bockowski

Institute of High Pressure Physics PAS, Sokolowska 29/37, 01-142, Warsaw, Poland

15.30-15.45 **HVPE Growth of Free-Standing GaN Wafers** **Mo1.4**

T.J. Baker, X. Luo, Y. Xie, Z. Wu

Eta Research Ltd., Shanghai, China

15.45-16.00 **Study of Low Cost Growth of Large Size Bulk GaN Crystal Growth by a New Vertical HVPE Reactor with Showerhead Nozzle** **Mo1.5**

Q. Liu, N. Fujimoto, S. Nitta, Y. Honda, H. Amano

Department of Electrical Engineering, Nagoya University, Furo-cho, Chikusa-ku, Nagoya,Japan
Institute of Materials and Systems for Sustainability, Nagoya University, Furo-cho, Chikusaku, Nagoya, Japan

Akasaki Research Center, Nagoya University, Furo-cho, Chikusa-ku, Nagoya, Japan
Venture Business Laboratory, Nagoya University, Furo-cho, Chikusa-ku, Nagoya, Japan

Optoelectronic Devices - Mo2 (chair: V. Jmerik)

| 14.00-14.30 | **Recent Progress of AlGaN Deep-UV LEDs by Increasing Light-Extraction Efficiency (invited)** | **Mo2.1** |

<u>Hideki Hirayama</u>

RIKEN, 2-1, Hirosawa, Wako, Saitama 351-0198, Japan
RIKEN Center for Advanced Photonics (RAP), 2-1, Hirosawa, Wako, Saitama 351-0198, Japan

| 14.30-15.00 | **Influence of AlN/sapphire template properties on growth and performance of AlGaN-based UV LEDs (invited)** | **Mo2.2** |

<u>S. Hagedorn</u>, A. Knauer, T. Kolbe, S. Walde, N. Susilo, C. Kuhn, D. Jaeger, M. Kneissl, M. Weyers

Ferdinand-Braun-Institut, Leibniz-Institut fuer Hoechstfrequenztechnik, Gustav-Kirchhoff-Str. 4, 12489 Berlin, Germany
Institute of Solid State Physics, Technische Universitaet Berlin, Hardenbergstr. 36, 10623 Berlin, Germany
Evatec AG, Hauptstr. 1a, 9477 Truebbach, Switzerland

| 15.00-15.30 | **375-nm Optically Pumped Vertical-Cavity Surface-Emitting Lasers with Air-Gap/Al0.05Ga0.95N Distributed Bragg Reflectors (invited)** | **Mo2.3** |

<u>Y.J. Park</u>, T. Detchprohm, K. Mehta, J. Wang, H. Jeong, Y.-S. Liu, S. Wang, S.-C. Shen, P.D. Yoder, F. Ponce, R.D. Dupuis

Center for Compound Semiconductors and School of Electrical and Computer Engineering, Georgia Institute of Technology, Atlanta, GA 30332 USA
Department of Physics and Astronomy, Arizona State University, Tempe AZ 85287 USA

| 15.30-15.45 | **Growth of InAlGaN for efficient UVB light emitting diodes** | **Mo2.4** |

<u>J. Enslin</u>, T. Teke, G. Kusch, L. Spasevski, C. Reich, B. Neuschulz, P.R. Edwards, T. Wernicke, R.W. Martin, M. Kneissl

Technische Universität Berlin, Institut für Festkörperphysik, Hardenbergstr. 36, 10623 Berlin, Germany
Ferdinand-Braun-Institut, Leibniz-Institut für Höchstfrequenztechnik, Gustav-Kirchhoff-Straße 4, 12489 Berlin, Germany

Department of Physics, SUPA, University of Strathclyde, 107 Rottenrow East, Glasgow G40NG, United Kingdom

15.45-16.00	**Three Dimensional Simulation on the Transport and Quantum Efficiency of UVC-LEDs with Random Alloy Fluctuations**	**Mo2.5**

H.H. Chen, Y.R. Wu

Graduate Institute of Photonics and Optoelectronics, National Taiwan University, Taipei, Taiwan, 10617
Industrial Technology Research Institute, Hsinchu, Taiwan.

16.00-16.30 **Coffee break**

16.30-18.30 **Parallel sessions: Growth and Characterization & Optoelectronic Devices**

Growth and Characterization - Mo3 (chair: H. Fujioka)

16.30-17.00	**Thermodynamics on HVPE of Group-III Nitrides (invited)**	**Mo3.1**

Yoshinao Kumagai

Department of Applied Chemistry, Tokyo University of Agriculture and Technology, Koganei, Tokyo, Japan
Institute of Global Innovation Research, Tokyo University of Agriculture and Technology, Koganei, Tokyo, Japan

17.00-17.15	**Defect and stress engineering in GaN layers grown by high temperature vapor phase epitaxy**	**Mo3.2**

T. Schneider, M. Förste, G. Lukin, M. Barchuk, C. Röder, C. Schimpf, E. Niederschlag, F.C. Beyer, O. Pätzold, D. Rafaja, M. Stelter

Institute for Nonferrous Metallurgy and Purest Materials TU Bergakademie Freiberg, Leipziger Straße 34, 09599 Freiberg, Germany
Institute of Materials Science, TU Bergakademie Freiberg, Gustav-Zeuner-Straße 5, 09599 Freiberg, Germany
Institute of Theoretical Physics, TU Bergakademie Freiberg, Leipziger Straße 23, 09599 Freiberg, Germany
Institute of Applied Physics, TU Bergakademie Freiberg, Leipziger Straße 23, 09599 Freiberg, Germany

17.15-17.30	**Excess Chlorine and Growth Temperature Effects of N-Polar GaN Growth via Tri-halide Vapor Phase Epitaxy and its Theoretical Study**	**Mo3.3**

N. Takekawa, D. Oozeki, A. Yamaguchi, H. Murakami, Y. Kumagai, K. Matumoto, A. Koukitu

Department of Applied Chemistry, Tokyo University of Agriculture &
Technology, Koganei, Tokyo 184-8588, Japan
TAIYO NIPPON SANSO Corporation, 10 Ohkubo, Tsukuba, 300-2611 Japan

17.30-17.45   **Carbon-doped GaN: Identification of tri-carbon defects formed at**   **Mo3.4**
substantial fraction

<u>I. Gamov</u>, E. Nowak, G. Gärtner, F. Zimmermann, F.C. Beyer, E.
Richter, M. Weyers, K. Irmscher

Leibniz-Institut für Kristallzüchtung, Max-Born-Strasse 2, 12489 Berlin,
Germany
Faculty of Technical Physics, Politechnika Poznanska, Piotrowo 3, 60-965
Poznan, Poland
Institute of Experimental Physics, TU Bergakademie Freiberg, 09599
Freiberg, Germany
Institute of Applied Physics, TU Bergakademie Freiberg, 09599 Freiberg,
Germany
Ferdinand-Braun-Institut, Leibniz-Institut für Höchstfrequenztechnik,
Gustav-Kirchhoff-Str. 4, 12489 Berlin, Germany

17.45-18.00   **Photoluminescence of Carbon-doped HVPE GaN layers**   **Mo3.5**

F. Zimmermann, G. Gärtner, K. Irmscher, I. Gamov, E. Nowak, E.
Richter, M. Weyers, J. Heitmann, <u>F.C. Beyer</u>

Institute of Applied Physics, TU Bergakademie Freiberg, Leipziger Straße 23,
D-09599 Freiberg, Germany
Institute of Experimental Physics, TU Bergakademie Freiberg, Leipziger
Straße 23, D-09599 Freiberg, Germany
Leibniz-Institut fur Kristallz¨uchtung, Max-Born-Straße 2, D-12489 Berlin,
Germany
Ferdinand-Braun-Institut, Gustav-Kirchhoff-Straße 4, D-12489 Berlin,
Germany

18.00-18.30   **A new method to achieve efficient iron doping of HVPE GaN**   **Mo3.6**
substrates (invited)

<u>J.A. Freitas</u>, Jr., J.C. Culbertson, E.R. Glaser, E. Richter, M. Weyers,
A.C. Oliveira, V.K. Garg

Naval Research Laboratory, 4555 Overlook Av. SW, Washington, USA 20375
Ferdinand-Braun-Institute, Gustav-Kirchhoff-Str. 4, 12489 Berlin, Germany
Institute of Physics, University of Brasilia, Asa Norte, 70919-970 Brasilia, DF,
Brazil

Optoelectronic Devices - Mo4 (chair: R. Dupuis)

16.30-17.00   **Plasma-assisted molecular beam epitaxy of monolayer-thick GaN/AlN heterostructures for high efficient sub-250-nm UV emitters (invited)**   **Mo4.1**

V. N. Jmerik, D. V. Nechaev, A. A. Toropov, E. A. Evropeitsev, V. I. Kozlovsky, V. P. Martovitsky, S. Rouvimov, S. V. Ivanov

Ioffe Institute, Polytekhnicheskaya str. 26, St. Petersburg 194021, Russia
Lebedev Physical Institute, Leninsky pr. 53, Moscow 119991, Russia
University of Notre Dame, Notre Dame, Indiana 46556, USA

17.00-17.15   **UVC LEDs on AlN/sapphire templates prepared by high-temperature annealing and regrowth process**   **Mo4.2**

Y. Itokazu, M. Jo, S. Minami, H. Hirayama

RIKEN, 2-1 Hirosawa, Wako, Saitama 351-0198, Japan

17.15-17.30   **Investigation of the Thermal Droop in InGaN-based Layers and UVA LEDs**   **Mo4.3**

C. DeSanti, M. Meneghini, D. Monti, H. Koch, G. Meneghesso, E. Zanoni

Dept. of Information Engineering, University of Padova, via Gradenigo 6/B, Padova, Italy
OSRAM Opto Semiconductors GmbH, Leibnizstrasse 4, 93055 Regensburg, Germany

17.30-17.45   **Investigation of crystallinity and current injection issue in 310nm-AlGaN UVB LED grown on AlN template in LP-MOVPE**   **Mo4.4**

M. Ajmal Khan, T. Matsumoto, N. Maeda, M. Jo, N. Kamata, H. Hirayama

RIKEN, 2-1 Hirosawa Wako, Saitama, 351-0198, Japan
RIKEN Center for Advanced Photonics(RAP),2-1 Hirosawa, Wako, Saitama 351-0198, Japan
Saitama University, Saitama 338-8570, Japan

17.45-18.00   **UVC emission from (11-22) AlGaN quantum wells grown by metal-organic chemical vapor deposition**   **Mo4.5**

M. Jo, Y. Itokazu, H. Hirayama

RIKEN, 2-1 Hirosawa, Wako, Saitama 351-0198, Japan

18.00-18.15   **Oxygen-induced high diffusion rate of magnesium dopant in GaN/AlGaN based UV LED heterostructures**   **Mo4.6**

P.P. Michałowski, S. Złotnik, J. Sitek, M. Rudziński

Institute of Electronic Materials Technology, Wolczynska 133, 01-919 Warsaw, Poland

TUESDAY (7TH AUGUST)

08.30-10.30 **Parallel sessions: Growth and Characterization & Optoelectronic Devices**

Growth and Characterization - Tu1 (chair: H. Murakami)

08.30-09.00 **Recent progress of in acidic ammonothermal growth of GaN crystals (invited)** **Tu1.1**

S.F. Chichibu, M. Saito, Q. Bao, D. Tomida, K. Kurimoto, K. Shima, K. Kojima, T. Ishiguro

IMRAM-Tohoku Univ., 2-2-1 Katahira, Aoba-ku, Sendai, Miyagi 980-8577, Japan
Mitsubishi Chemical Corp., 1000 Higashimamiana, Ushiku, Ibaraki 300-1295, Japan
The Japan Steel Works, Ltd., 11-1 Osaki 1-chome, Shinagawa-ku, Tokyo 141-0032, Japan

09.00-09.30 **Basic ammonothermal growth of GaN (invited)** **Tu1.2**

M. Zajac, R. Kucharski, K. Grabianska, A. Gwardys-Bak, A. Puchalski, D. Wasik, E. Litwin-Staszewska, R. Piotrzkowski, J. Z. Domagala, M. Bockowski,

Ammono Lab, Institute of High Pressure Physics, Polish Academy of Sciences, Sokolowska 29/37, 01-142 Warsaw, Poland
Faculty of Physics, University of Warsaw, Pasteura 5, 02-093, Warsaw, Poland
Institute of High Pressure Physics Polish Academy of Sciences, Sokolowska 29/37, 01-142 Warsaw, Poland
Institute of Physics, Polish Academy of Sciences, Aleja Lotników 32/46, 02-668, Warsaw, Poland

09.30-09.45 **Fabrication of GaN Crystals with Low Resistivity Grown with the Na-flux Point Seed Technique** **Tu1.3**

K. Endo, T. Yamada, H. Kubo, K. Murakami, M. Imanishi, M. Yoshimura, Y. Mori

Grad. Sch. of Eng., Osaka Univ., 2-1, Yamada-oka, Suita, Osaka, 565-0871, Japan
ILE, Osaka Univ., 2-1, Yamada-oka, Suita, Osaka, 565-0871, Japan

09.45-10.00 | **Reduction of Li impurity in the Freestanding GaN Substrate Fabricated by the Na-Flux Sapphire Dissolution Technique** | **Tu1.4**

T. Yamada, M. Imanishi, K. Murakami, K. Nakamura, M. Yoshimura, Y. Mori

Graduate School of Engineering, Osaka University, Osaka, Japan

10.00-10.15 | **The effect of undissolved carbon on GaN crystal growth in Na flux method** | **Tu1.5**

N. Takeda, T. Yamada, K. Murakami, K. Kakinouchi, M. Imanishi, Y. Mori

Graduate School of Engineering, Osaka University, 2-1, Yamada-oka, Suita, Osaka, Japan

10.15-10.30 | **Growth of GaN Single Crystal by Na Flux Method Adding Nitrogen-doped Carbon** | **Tu1.6**

Z.L. Liu, L. Shi, X.J. Su, G.Q. Ren, J.F. Wang, K. Xu

Suzhou Institute of Nano-tech and Nano-bionics, Chinese Academy of Sciences, Suzhou 215123, People's Republic of China
Suzhou Nanowin Science and Technology Co., Ltd., Suzhou 215123, People's Republic of China

Optoelectronic Devices - Tu2 (chair: D. Jena)

08.30-09.00 | **Tunnel Junctions for Next Generation III-Nitride Optoelectronics (invited)** | **Tu2.1**

Siddharth Rajan

Department of Electrical and Computer Engineering, The Ohio State University, Columbus, Ohio 43210, USA

09.00-09.30 | **Long-Living Laser Diodes Grown By Plasma Assisted Molecular Beam Epitaxy (invited)** | **Tu2.2**

Grzegorz Muziol

Institute of High Pressure Physics PAS, Sokolowska 29/37, 01-142 Warsaw, Poland

09.30-09.45 | **Structural Investigation Of InGaN/GaN Heterostructures Quantum Wells For Long Wavelength Emission** | **Tu2.3**

N. Chery, T.H. Ngo, M.P. Chauvat, B. Damilano, B. Gil, M. Morales, S. Kret, P. Ruterana

CIMAP, 6 boulevard du Marechal Juin, Université de Caen, Caen, France
L2C, Bâtiment 21 Campus Triolet, Université de Montpellier, Montpellier, France
CRHEA, Rue Bernard Gregory, Université Côte d'Azur, Valbonne, France
Institute of Physics, Polish Academy of Sciences, al. Lotników 32/46, Warsaw, Poland

| 09.45-10.00 | **AlInN/GaN DBRs for Long-wavelength GaN-based VCSELs** | **Tu2.4** |

K. Hiraiwa, W. Muranaga, J. Ogimoto, T. Akagi, T. Takeuchi, S. Kamiyama, M. Iwaya, I. Akasaki

Fac. Sci. & Eng., Meijo University, 1-501 shiogamaguchi, Tenpaku-ku, Nagoya, Japan
Akasaki Research Center, Nagoya Univ., Furo-cho, Chikusa-ku, Nagoya, Japan

| 10.00-10.15 | **Improvement of emission efficiency in green LEDs by sputtered AlN buffer layer** | **Tu2.5** |

S. Ishimoto, D.P. Han, K. Yamamoto, S. Kamiyama, T. Takeuchi, M. Iwaya, I. Akasaki

Meijo Univ., 1-501, Shiogamaguchi, Tempaku-ku, Nagoya, Japan
Akasaki Research Center, Nagoya Univ., Furou-cho, Chikusa-ku, Nagoya, Japan

| 10.15-10.30 | **Kinetic Mechanisms of InGaN(0001) by RF-MBE in the entire composition range: Phenomenological Model and Impact on Epilayer Properties** | **Tu2.6** |

E. Papadomanolaki, S.A. Kazazis, L. Lymperakis, E. Iliopoulos

Department of Physics, University of Crete, GR-70013, Heraklion, Greece
Max-Planck-Institut für Eisenforschung, 40237 Düsseldorf, Germany
Microelectronics Research Group, I.E.S.L.-FO.R.T.H., GR-71110, Heraklion, Greece

| 10.30-11.00 | **Coffee break** |

11.00-13.00 **Parallel sessions: Growth and Characterization & Electrical Devices**

Growth and Characterization - Tu3 (chair: H. Miyake)

11.00-11.30 **Growth of InN films with high electron mobility by MBE (invited)** **Tu3.1**

X. Wang, H. Liu, X. Zheng, T. Wang, P. Wang, B. Sheng, X. Rong, X. Yang, F. Xu, B. Shen

State Key Laboratory of Artificial Microstructure and Mesoscopic Physics, School of Physics, Peking University, Beijing 100871, China

11.30-12.00 **Stacking-fault-free (20-2-1) GaN on 4" sapphire substrates: a pathway to commercialize semipolar optoelectronics (invited)** **Tu3.2**

J. Song, J.W. Choi, J. Han

Department of Electrical Engineering, Yale University, New Haven, CT, USA
Saphlux Inc, Branford, CT, USA

12.00-12.15 **MOVPE grown AlN on nano-patterned sapphire substrates with different offcut angles** **Tu3.3**

S. Walde, S. Hagedorn, P.M. Coulon, P.A. Shields, G. Kusch, G. Naresh-Kumar, C. Trager-Cowan, A. Knauer, R.W. Martin, M. Weyers

Ferdinand-Braun-Institut, Leibniz-Institut fuer Hoechstfrequenztechnik, Gustav-Kirchhoff-Straße 4, 12489 Berlin, Germany
Centre of Nanoscience & Nanotechnology, University of Bath, Bath, BA2 7AY, UK,
Department of Electronic and Electrical Engineering, University of Bath, Bath, BA2 7AY, UK
Department of Physics, SUPA, University of Strathclyde, 107 Rottenrow East, Glasgow G4 0NG, UK

12.15-12.30 **Semi polar (10-11) GaN growth on silicon-on-insulator substrates for defect reduction and melt back etching suppression** **Tu3.4**

R. Mantach, G. Feuillet, P. Vennéguès, P. DeMierry, J. ZunigaPerez

Université Côte d'Azur CNRS CRHEA, Rue Bernard Gregory, Valbonne, France
Université Grenoble Alpes CEA-LETI, 17 rue des Martyrs, Grenoble, France

12.30-13.00 **InGaN quantum structures on patterned substrates (invited)** **Tu3.5**

M. Sarzyński, G. Targowski, E. Grzanka, S. Grzanka, S. Sakowski

Institute of High Pressure Physics PAS, Sokołowska 29/37, 01-142 Warsaw, Poland
TopGaN Ltd., Sokołowska 29/37, 01-142 Warsaw, Poland

Electrical Devices - Tu4 (chair: T. Palacios)

11.00-11.30   **Vertical Power Devices based on Bulk GaN Substrates (invited)**   **Tu4.1**

Isik C. Kizilyalli

Advanced Research Project Agency – Energy, U.S. Department of Energy

11.30-12.00   **Electrical characterization of homoepitaxial GaN layers for GaN vertical power devices (invited)**   **Tu4.2**

Jun Suda, Masahiro Horita

Nagoya University, Furo-cho, Chikusa-ku, Nagoya, Japan
Kyoto University, Katsura, Nishikyo-ku, Kyoto, Japan

12.00-12.15   **Characterization of Shallower Level Traps in p-GaN Grown by MOVPE Using Low Frequency Capacitance DLTS**   **Tu4.3**

Y. Tokuda, T. Kogiso, T. Narita, K. Tomita, T. Kachi

Aichi Institute of Technology, Yakusa, Toyota, Japan
Toyota Central R&D Laboratories Inc., Nagakute, Japan
Nagoya University, Chikusa-ku, Nagoya, Japan

12.15-12.30   **Accurate estimation of H1 trap concentration in n-type GaN layers**   **Tu4.4**

K. Kanegae, M. Horita, T. Kimoto and J. Suda

Kyoto Univ., Nishikyo, Kyoto City, Japan
Nagoya Univ. IMaSS, Chikusa, Nagoya City, Japan
Nagoya Univ., Chikusa, Nagoya City, Japan

12.30-13.00   **Donor states of carbon in p-type GaN grown by MOVPE (invited)**   **Tu4.5**

T. Narita, K. Tomita, Y. Tokuda, T. Kogiso, M. Horita, T. Kachi

Toyota Central R&D Labs., Inc., Yokomichi, Nagakute 480-1192, Japan
Aichi Institute of Technology, Toyota 470-0392, Japan
Kyoto University, Kyoto 615-8510, Japan
Nagoya University, Nagoya 464-8601, Japan

13.00-14.00   **Lunch break**

14.00-16.30 **Parallel sessions: Growth and Characterization & Theory**

Growth and Characterization - Tu5 (chair: **R. Collazo**)

14.00-14.30 **On the preparation of AlN single crystal boules and substrates for AlGaN devices (invited)** **Tu5.1**

Carsten Hartmann, Juergen Wollweber, Andrea Dittmr, Klaus Irmscher, Matthias Bickermann

Leibniz Institute for Crystal Growth, Max-Born-Str. 2, 12489 Berlin, Germany

14.30-15.00 **Homoepitaxy of AlN on annealed AlN/sapphire template (invited)** **Tu5.2**

H. Miyake, K. Shojiki, X. Liu, Y. Hayashi, X. Shiyu, K. Uesugi

Graduate School of Regional Innovation Studies, Mie University, Tsu, Japan
Graduate School of Engineering, Mie University, Tsu, Japan
Organization for the Promotion of Regional Innovation, Mie University, Tsu, Japan

15.00-15.15 **Di-carbon defects in AlN bulk crystals grown by physical vapor transport** **Tu5.3**

I. Gamov, C. Hartmann, A. Dittmar, J. Wollweber, M. Bickermann, I. Kogut, H. Fritze, K. Irmscher

Leibniz-Institut für Kristallzüchtung, Max-Born-Strasse 2, 12489 Berlin, Germany
Institut für Energieforschung und Physikalische Technologien, Technische Universität Clausthal, Am Stollen 19B, 38640 Goslar, Germany

15.15-15.30 **Tuning the growth of AlN epilayers on Al2O3 via TMAl preflow by MOCVD** **Tu5.4**

H. Sun, Y.J. Park, K.H. Li, T. Detchprohm, R.D. Dupuis, X. Li

King Abdullah University of Science and Technology (KAUST), Thuwal, 23955 Saudi Arabia
School of Electrical and Computer Engineering, Georgia Institute of Technology, Atlanta, Georgia 30332, USA

15.30-15.45 **Controlling the growth mode and strain of AlN grown directly on 6H-SiC(0001) substrate by metal-organic chemical vapor deposition** **Tu5.5**

H. Yoshida, S. Kimura

Corporate Research and Development Center, Toshiba Corporation, 1, Komukai-Toshiba-Cho, Saiwai-ku, Kawasaki 212-8582, Japan

15.45-16.00	**Hot-wall MOCVD growth of N-polar AlN nucleation layer on C-face vicinal and on-axis SiC substrates**	**Tu5.6**

H. Zhang, C.W. Hsu, J.T. Chen, P. Sukkaew, V. Darakchieva

Department of Physics, Chemistry and Biology (IFM), Linköping University, SE 581 83, Linköping, Sweden

16.00-16.15	**Crystal quality improvement of sputter-deposited AlN films on SiC substrates by high temperature annealing**	**Tu5.7**

K. Uesugi, Y. Hayashi, K. Shojiki, S. Xiao, K. Nagamatsu, H. Yoshida, H. Miyake

Organization for the Promotion of Regional Innovation, Mie University, Tsu, Japan
Graduate School of Regional Innovation Studies, Mie University, Tsu, Japan
Graduate School of Engineering, Mie University, Tsu, Japan

16.15-16.30	**Growth of thick AlGaN layers by HVPE method on GaN seeds**	**Tu5.8**

M. Fijalkowski, T. Sochacki, B. Lucznik, M. Amilusik, S. Sakowski, M. Iwinska, I. Grzegory, M. Bockowski

Institute of High Pressure Physics PAS, Sokolowska 29/37, 01-142 Warsaw, Poland

Theory - Tu6 (chair: J. Majewski)

14.00-14.30	**Theoretical study: Impurity incorporation in GaN MOVPE (invited)**	**Tu6.1**

Y. Kangawa, P. Kempisty, S. Krukowski, K. Shiraishi

RIAM, Kyushu University, Fukuoka 816-8580, Japan
IMaSS, Nagoya University, Nagoya 464-8603, Japan
IHPP, PAS, Sokolowska 29/37, 01-142 Warsaw, Poland

14.30-15.00	**Adsorption at nitride semiconductors surfaces - electronic aspects: surface states occupation, the equilibrium pressure, growth and doping (invited)**	**Tu6.2**

Stanisław Krukowski, Paweł Strak, Paweł Kempisty, Konrad Sakowski

Institute of High Pressure Physics, Polish Academy of Sciences, Sokołowska 29/37, 01-142 Warsaw, Poland

| 15.00-15.15 | **A Simple Theoretical Approach to Growth Mode of III-Nitride Thin Films** | **Tu6.3** |

T. Ito, T. Akiyama, K. Nakamura, A.M. Pradipto

Department of Physics Engineering, Mie University, Tsu 514-8507, Japan

| 15.15-15.30 | **AlGaN MOVPE Growth Simulation under 10-100 kPa Considering Polymer formation** | **Tu6.4** |

K. Ohkawa, K. Nakamura

Electrical Engineering, King Abdullah University of Science and Technology (KAUST), Thuwal, Saudi Arabia
Dept. Applied Physics, Tokyo University of Science, Tokyo, Japan

| 15.30-15.45 | **Relationship between the CH4 Adsorption Probability and the C Impurity Concentration in the Polar-GaN MOVPE System** | **Tu6.5** |

A. Kusaba, G. Li, M.R. vonSpakovsky, P. Kempisty, Y. Kangawa

Department of Aeronautics and Astronautics, Kyushu University, 744 Motooka, Nishi-ku, Fukuoka 819-0395, Japan
Department of Engineering Science, University of Oxford, Parks Road, Oxford OX1 3PJ, UK
Center for Energy Systems Research, Mechanical Engineering Department, Virginia Tech, Blacksburg, VA 24061, USA
Institute of High Pressure Physics, Polish Academy of Sciences, Sokolowska 29/37, 01-142 Warsaw, Poland
Research Institute for Applied Mechanics, Kyushu University, 6-1 Kasuga-koen, Kasuga, Fukuoka 816-8580, Japan
Institute of Materials and Systems for Sustainability, Nagoya University, Furo-cho, Chikusa-ku, Nagoya 464-8601, Japan

| 15.45-16.00 | **Contribution of first principles phonon calculations to thermodynamics analysis of GaN surfaces** | **Tu6.6** |

P. Kempisty, Y. Kangawa, S. Krukowski

Institute of High Pressure Physics, Sokolowska 29/37, 01-142 Warsaw, Poland
RIAM, Kyushu University, Fukuoka 816-8580, Japan
IMaSS, Nagoya University, Nagoya 464-8603, Japan

| 16.00-16.15 | **Kinetic Monte Carlo simulation of MOVPE growth/sublimation of GaN on the vicinal GaN(0001) substrate** | **Tu6.7** |

J. Endres, V. Holý, S. Daniš, M. Sarzyński

Faculty of Mathematics and Physics, Charles University, Ke Karlovu 3, 121 16 Prague, Czech Republic

Institute of High Pressure Physics PAS, ul. Sokolowska 29/37, 01-142 Warsaw, Poland

16.15-16.30   **Catalytic potential of AlN(0001) surface for N2 + H2 ammonia synthesis reaction**   **Tu6.8**

<u>P. Strak</u>, K. Sakowski, P. Kempisty, I. Grzegory, S. Krukowski

Institute of High Pressure Physics, Polish Academy of Sciences, Sokolowska 29/37, 01-142 Warsaw, Poland

16.40-17.40   **Tutorial session**
TS (chair: L. Kirste)

16.40-17.10   **Williamson-Hall Analysis on Epilayers – A critical review of common practice (invited)**   **TS1**

<u>L. Grieger</u>, J.F. Woitok

Malvern Panalytical B.V., Lelyweg 1, Almelo, The Netherlands

17.10-17.40   **X-ray Diffraction in Nitride Technology- most common mistakes and new opportunities (invited)**   **TS2**

<u>M. Leszczynski</u>, E. Grzanka, M. Krysko, J. Domagala, J. Stranska-Matejova, V. Holy

Institute of High Pressure Physics UNIPRESS, Sokolowska 29/37, 01 142 Warsaw, Poland,
TopGaN, Sokolowska 29/37, 01 142 Warsaw, Poland
Institute of Physics, Al. Lotnikow 32/46, 06-668 Warsaw, Poland
Department of Condensed Matter Physics, Faculty of Mathematics and Physics, Charles University, Ke Karlovu 5,121 16 Praha, Czech Republic.
CEITEC at Masaryk University, Kotlarska 2,611 37 Brno, Czech Republic

18.00-21.00   **Poster Session (chair: M. Bockowski)**

Po01   **Raman Spectroscopic Study of GaN Grown on (111)Si Using an AlInN Intermediate Layer by MOVPE**

T. Sugiura, S. Kawasaki, Y. Honda, T. Nonaka, D. Oikawa, T. Tsukamoto, H. Andoh, H. Amano

National Institute of Technology, Toyota College, 2-1 Eisei-cho, Toyota, Japan
Department of Electronics, Nagoya University, Furo-cho Chikusa-ku, Nagoya, Japan
Institute of Materials and Systems for Sustainability, Nagoya University, Nagoya, Japan

Po02 InGaN Band Gap Compositional Dependence Determined by Means of Photoacoustic Spectroscopy

R. Oliva, S.J. Zelewski, Ł. Janicki, K.R. Gwóźdź, J. Serafińczuk, M. Rudziński, E. Özbay, R. Kudrawiec

Dept. of Experimental Physics, Faculty of Fundamental Problems of Technology, Wroclaw Univ. of Science and Technology, Wybrzeże Wyspiańskiego 27, 50-370 Wrocław, Poland
Dept. of Quantum Technologies, Faculty of Fundamental Problems of Technology, Wroclaw University of Science and Technology, Wybrzeze Wyspianskiego 27, 50-370 Wroclaw, Poland
Faculty of Microsystem Electronics and Photonics, Wroclaw University of Science and Technology, Janiszewskiego 11/17, 50-372 Wrocław, Poland
Institute of Electronic Materials Technology, Wólczyńska 133, 01-919 Warsaw, Poland
Nanotechnology Research Center, Bilkent University, 06800 Bilkent, Turkey

Po03 TEM Investigations on High-Temperature Annealed epi-AlN on Sapphire

L. Cancellara, S. Hagedorn, S. Walde, D. Jaeger, M. Weyers, T. Markurt, M. Albrecht

IKZ, Leibniz-Institute for Crystal Growth, Max-Born-Str. 2, Berlin, Germany
Ferdinand-Braun-Institut, Gustav-Kirchhoff-Str. 4, Berlin, Germany
Evatec AG, Hauptstr. 1a, Trübbach, Switzerland

Po04 Diffusion and out-diffusion of Mn in gallium nitride.

R. Jakieła, K. Gas, M. Sawicki, A. Barcz

Institute of Physics, Polish Academy of Sciences, Lotników 32/46, Warsaw, Poland
Institute of Electron Technology, Lotników 32/46, Warsaw, Poland

Po05 Impact of Si doping in different GaN layers on luminescence properties of InGaN/GaN multiple quantum well structure

F. Hájek, M. Zíková, A. Hospodková, T. Hubáček, J. Oswald

Institute of Physics, Czech Academy of Science, Cukrovarnická 10, Prague 6, Czech Republic

Po06 Optical modulation spectroscopy of AlxGa1-xN epilayers and AlxGa1-xN/GaN quantum wells in the UV spectral range

E. Zdanowicz, W. Olszewski, S. Gorantla, K. Moszak, Ł. Janicki, D. Hommel, R. Kudrawiec

Wroclaw Research Center EIT+ Sp. z o.o., ul. Stabłowicka 147, 54-066 Wrocław, Poland
Faculty of Fundamental Problems of Technology, Wroclaw University of Science and Technology, Wybrzeże Wyspiańskiego 27, 50-370 Wrocław, Poland
Institute of Low Temperature and Structure Research, Polish Academy of Sciences W. Trzebiatowski Institute, ul. Okólna 2, 50-422 Wroclaw, Poland
Faculty of Physics, University of Wroclaw, plac Maxa Borna 9, 50-204 Wroclaw, Poland

Po07 Excess Carrier Lifetime in Ammonothermal GaN Doped with Si, Mg, and Mn

Ł. Janicki, R. Kucharski, M. Zając, R. Kudrawiec

Faculty of Fundamental Problems of Technology, Wrocław University of Science and Technology, Wybrzeże Wyspiańskiego 27, 50-370 Wrocław, Poland
AMMONO S.A., Prusa 2, 00-493 Warsaw, Poland

Po08 Influence of Depletion Layer on Spatial Distribution of Cathodoluminescence Intensity in GaN Nanowires

B. Adamowicz, M. Matys

Institute of Physics - CND, Silesian University of Technology, Konarskiego 22B, 44 -100 Gliwice, Poland
Research Center for Integrated Quantum Electronics, Hokkaido University, Kita-13 Nishi-8, Kita-ku, 060-8628 Sapporo, Japan

Po09   Influence of Macrosteps on Deep-ultraviolet Emission from AlGaN/AlGaN Multiple Quantum wells

K. Kataoka, K. Horibuchi, Y. Saito, H. Makino, K. Nagata, Y. Kimoto

Toyota Central R&D Labs., Inc., Nagakute, Aichi 480-1192, Japan
TS Opto Co. Ltd., Ichihara, Chiba 290-0067, Japan

Po10   Growth of InGaN Films by Reactive Sputtering

Q.X. Guo, K. Saito, T. Tanaka

Synchrotron Light Application Center, Department of Electrical and Electronic Engineering, Saga University, Saga 840-8502, Japan

Po11   High temperature vapor phase epitaxy for the growth of GaN layers on sapphire substrates

M. Förste, T. Schneider, G. Lukin, M. Barchuk, C. Schimpf, C. Röder, E. Niederschlag, O. Pätzold, F.C. Beyer, D. Rafaja, M. Stelter

Institute for Nonferrous Metallurgy and Purest Materials, TU Bergakademie Freiberg, 09599 Freiberg (Germany)
Institute of Materials Science, TU Bergakademie Freiberg, 09599 Freiberg (Germany)
Institute of Theoretical Physics, TU Bergakademie Freiberg, 09599 Freiberg (Germany)
Institute of Applied Physics, TU Bergakademie Freiberg, 09599 Freiberg (Germany)

Po12   Study of Indium Incorporation in OMVPE Grown 200-nm Thick InxAl1-xN Layers

S. Hasenöhrl, P. Chauhan, E. Dobročka, R. Stoklas, L. Vančo, J. Kuzmík

Institute of Electrical Engineering, Slovak Academy of Sciences, Dúbravská cesta 9, 841 04 Bratislava, Slovak Republic
Slovak University of Technology, University Science Park Bratislava Centre, Vazovova 5, 812 43 Bratislava, Slovak Republic

Po13   Structure of AlN films formed by nitriding the aluminum metal layers on the (0001) sapphire substrates

A.E. Muslimov

Federal Research Center "Crystallography and Photonics", RAS, 59 Leninskii av., Moscow, 119333, Russia

Po14   AlN layers grown by Ga-Al liquid phase epitaxy on nitrided r-plane sapphire substrate

N. Kanno, M. Adachi, H. Fukuyama

Institute of Multidisciplinary Research for Advanced Materials, Tohoku University, Sendai 980-8577, Japan

Po15   HVPE Growth Method for Thick AlN Epilayer

K.H. Kim, H.M. Kim, A.R. Park, I. Jeon, M. Yang, S.N. Yi, J.H. Lee, H.S. Ahn, C.R. Cho, S.W. Kim, N. Sawaki

Department of Electronic Materials Engineering, Korea Maritime and Ocean University, Busan 49112, Korea

Compound Semiconductor Fabrication Technology Center, Korea Maritime and Ocean University, Busan 49112, Korea
Department of Nano Fusion Technology, Pusan National University, Busan 46241, Korea
Department of Physics, Andong National University, Andong 36729, Korea
Department of Electrical and Electronics Engineering, AIT, Aichi 470-0392, Japan

Po16 Mg-doped AlN Epilayer Grown by Mixed Source HVPE Method

S.W. Kim, K.H. Kim, K.B. Park, I. Jeon, J.H. Lee, M. Yang, S.N. Yi, H.S. Ahn, C.R. Cho, S.W. Kim, N. Sawaki

Department of Electronic Materials Engineering, Korea Maritime and Ocean University, Busan 49112, Korea
Compound Semiconductor Fabrication Technology Center, Korea Maritime and Ocean University, Busan 49112, Korea
Department of Nano Fusion Technology, Pusan National University, Busan 46241, Korea
Department of Physics, Andong National University, Andong 36729, Korea
Department of Electrical and Electronics Engineering, AIT, Aichi 470-0392, Japan

Po17 The Growth of High Al Composition AlxGa1-xN Epilayers

J.S. Yu, K.H. Kim, S.W. Kim, I. Jeon, M. Yang, S.N. Yi, J.H. Lee, H.S. Ahn, C.R. Cho, S.W. Kim, N. Sawaki

Department of Electronic Materials Engineering, Korea Maritime and Ocean University, Busan 49112, Korea
Compound Semiconductor Fabrication Technology Center, Korea Maritime and Ocean University, Busan 49112, Korea
Department of Nano Fusion Technology, Pusan National University, Busan 46241, Korea
Department of Physics, Andong National University, Andong 36729, Korea
Department of Electrical and Electronics Engineering, AIT, Aichi 470-0392, Japan

Po18 Characteristics of Epilayers in Light Emitting Diode Grown by HVPE Method

J.H. Lee, K.B. Park, J.S. Yu, K.H. Kim, I. Jeon, M. Yang, S.N. Yi, H.S. Ahn, C.R. Cho, S.W. Kim, N. Sawaki

Department of Electronic Materials Engineering, Korea Maritime and Ocean University, Busan 49112, Korea
Compound Semiconductor Fabrication Technology Center, Korea Maritime and Ocean University, Busan 49112, Korea
Department of Nano Fusion Technology, Pusan National University, Busan 46241, Korea
Department of Physics, Andong National University, Andong 36729, Korea
Department of Electrical and Electronics Engineering, AIT, Aichi 470-0392, Japan

Po19 Characteristics of aluminum nitride films on hexagonal boron nitride buffer layers using various growth methods through metal organic chemical vapor deposition

M. Han, B.D. Ryu, K.B. Ko, C.H. Jo, T.V. Cuong, C.H. Hong

School of Semiconductor and Chemical Engineering, Chonbuk National University, Jeonju, 561-756, South Korea
NTT Hi-Tech Institute, Nguyen Tat Thanh University, 298-300 A Nguyen Tat Thanh Street, Ho Chi Minh City, Vietnam

Po20 Synchrotron radiation x-ray topography and defect selective etching analysis of threading dislocations in HVPE-GaN

J.L. Weyher, T. Sochacki, S. Sintonen, M. Boćkowski

Institute of High Pressure Physics Polish Academy of Sciences, Sokolowska 29/37, 01-142 Warsaw, Poland

IQE Cardiff, UK

Po21 Crystallization of Thin GaN Layers by HVPE Method on Native and Foreign Substrates

M. Oklej, T. Sochacki, M. Amilusik, M. Fialkowski, M. Iwinska, B. Lucznik, M. Bockowski

Chemical Scientific Club of UKSW, Cardinal Stefan Wyszynski University. Mathematics and Natural Sciences Department School of Exact Sciences. ul. Woycickiego 1/3, 01-938 Warszawa, Poland
Institute of High Pressure Physics Polish Academy of Sciences, Sokolowska 29/37, 01-142 Warsaw, Poland

Po22 Highly resistive HVPE-GaN grown on native seeds – investigation and comparison of different dopants

M. Iwinska, Tomasz Sochacki, Boleslaw Lucznik, Michal Fijalkowski, Mikolaj Amilusik, Elzbieta Litwin-Staszewska, Ryszard Piotrzkowski, and Michal Bockowski

Institute of High Pressure Physics Polish Academy of Sciences, Sokolowska 29/37, 01-142 Warsaw, Poland

Po23 Highly conductive HVPE-GaN grown on native seeds – investigation and comparison of different dopants

B. Lucznik, M. Iwinska, T. Sochacki, M. Fijalkowski, M. Amilusik, H. Teisseyre, M. Bockowski

Institute of High Pressure Physics Polish Academy of Sciences, Sokolowska 29/37, 01-142 Warsaw, Poland
Insitite of Physics, Polish Academy of Sciences, Al. Lotnikow 32/46, 02-668 Warsaw, Poland

Po24 Vacancy defects in Si and Ge doped HVPE-GaN investigated by positron annihilation spectroscopy

I. Prozheev, F. Tuomisto, M. Iwinska, M. Bockowski

Department of Applied Physics, Aalto University, Finland
Institute of High Pressure Physics, Polish Academy of Sciences, Warsaw, Poland

Po25 Growth of 2-inch HVPE-GaN doped with Si – numerical simulations and experiments

S. Sakowski, T. Sochacki, M. Amilusik, P. Kempisty, M. Fijałkowski, B. Łucznik, M. Iwińska, M. Boćkowski

Institute of High Pressure Physics Polish Academy of Sciences, Sokolowska 29/37, 01-142 Warsaw, Poland

Po26 Homoepitaxial Semi Polar Growth of GaN on Ammono Seeds by HVPE

M. Amilusik, T. Sochacki, M. Fijalkowski, B. Lucznik, M. Iwinska, I. Grzegory, M. Bockowski

Institute of High Pressure Physics Polish Academy of Sciences, Sokolowska 29/37, 01-142 Warsaw, Poland

Po27 GaN crystallization from iron based solution at 1 and 6 GPa pressures – investigation of critical points of this experimental approach

B. Sadovyi, I. Petrusha, P. Sadovyi, I. Dziecielewski, S. Porowski, V. Turkevich, A. Nikolenko, B. Tsykaniuk, V. Strelchuk, I. Grzegory

Institute of High Pressure Physics Polish Academy of Sciences, Sokolowska 29/37, 01-142 Warsaw, Poland
V. Bakul Institute for Superhard Materials of the National Academy of Sciences of Ukraine, 2, Avtozavodska str., 04074 Kyiv, Ukraine
V. Lashkaryov Institute of Semiconductor Physics, National Academy of Sciences of Ukraine, 45, prospekt Nauky, 03028 Kyiv, Ukraine

Po28 Influence of electron concentration on chemo-mechanical polishing rate of gallium nitride wafers

G. Kamler, G. Nowak, T. Sochacki, M. Amilusik, I. Dzięcielewski, I. Grzegory, M. Boćkowski

Institute of High Pressure Physics Polish Academy of Sciences, Sokolowska 29/37, 01-142 Warsaw, Poland

Po29 Growth of low Threading Dislocation Density GaN single crystal during the Na-flux Point Seed Method at low supersaturation

Y. Sawada, T. Yamada, K. Murakami, K. Kakinouchi, K. Nakamura, K. Okumura, T. Kitamura, M. Imanishi, M. Yoshimura, Y. Mori

Grad. Sch. of Eng., Osaka Univ., 2. ILE, Osaka Univ. Yamadaoka 2-1, Suita, Osaka 565-0871, Japan

Po30 Effect of AlN Cap Protection on the Decomposition of High-Temperature Annealed GaN

M. Masłyk, E. Kamińska, O. Dyczewska, R. Jakieła, E. Dynowska, M. Wzorek, K. Gołaszewska-Malec

Institute of Electron Technology, al. Lotników 32/46, 02-668 Warsaw, Poland
Institute of Physics, Polish Academy of Sciences, al. Lotników 32/46, 02-668 Warsaw, Poland

po32 Increasing scintillator active region thickness by InGaN/GaN QW number

T. Vaněk, A. Hospodková, T. Hubáček, K. Kuldová, J. Oswald, J. Pangrác, F. Dominec, M. Zíková, A. Vetushka

Technical University of Liberec, Studentská 2, CZ-46117, Liberec, Czech Republic
Institute of Physics CAS, v.v.i., Cukrovarnická 10, Prague 6 162 00, Czech Republic

Po32 Effect of dust contamination on GaN/InGaN multiple quantum well growth morphology

K. Kuldová, T. Kretková, R. Novotný, F. Dominec, F. Hájek, J. Pangrác, A. Hospodková

Institute of Physics, Czech Academy of Sciences v.v.i., Cukrovarnická 10, 16200 Praha 6, Czech Republic

Po33 Inhomogeneous Luminescence of InGaN/GaN Quantum Wells: Effect of Growth Temperature, Carrier Gas and the Buffer Layer Growth

F. Dominec, K. Kuldová, M. Zíková, J. Pangrác, A. Hospodková

Institute of Physics, Czech Academy of Sciences, Cukrovarnická 10,165 00 Prague 6, Czech Republic

Po34 Effects of Nitrogen Radical Irradiation on InN Growth by RF-MBE

F.B. Abas, R. Fujita, S. Mouri, Y. Nanishi, T. Araki

Ritsumeikan University, 1-1-1 Noji-higashi, Kusatsu, Japan

Po35 **Influence of Different InGaN/(In)GaN Growth Modes on Indium Incorporation and Quality of Layers**

T. Hubáček, A. Hospodková, J. Pangrác, M. Zíková, J. Oswald, K. Kuldová, E. Hulicius

Faculty of Mechatronics, Informatics and Interdisciplinary Studies, Technical University of Liberec, Studentská 2, CZ-46117, Liberec, Czech Republic
Institute of Physics, CAS, v.v.i., Cukrovarnická 10, CZ-16200, Prague 6, Czech Republic

Po36 **Use of Low Temperature Buffer Layer to Suppress the Contamination of InGaN/GaN Quantum Wells**

M. Zíková, A. Hospodková, J. Pangrác, T. Hubáček, F. Dominec, J. Oswald, K. Kuldová, E. Hulicius

Institute of Physics, Czech Academy of Sciences, Cukrovarnická 10, 162 00 Prague 6, Czech Republic

Po37 **UV Emitting Defects in Hexagonal Boron Nitride**

K.P. Korona, T. Korona, A.M. Witowski, M. Chojecki, A.K. Dąbrowska, K. Pakuła, J. Borysiuk, A. Wysmołek, R. Stępniewski

Institute of Experimental Physics, Faculty of Physics, University of Warsaw, ul. Pasteura 5, 02-093 Warsaw, Poland
Quantum Chemistry Laboratory, Faculty of Chemistry, University of Warsaw, ul. Pasteura 1, 02-093 Warsaw, Poland

Po38 **MOVPE Growth and Surface Morphology Investigation of High Quality GaN, Al0.14Ga0.86N Epilayers and Al0.14Ga0.86N/GaN Superlattice**

W. Olszewski, S. Gorantla, K. Moszak, J. Stoever, R. Szukiewicz, D. Hommel

Wroclaw Research Center EIT+ Sp. z o.o., ul. Stablowicka 147, 54-066 Wroclaw, Poland
Faculty of Physics, University of Wroclaw, plac Maxa Borna 9, 50-204 Wroclaw, Poland
Institute of Low Temperature and Structure Research, Polish Academy of Sciences W. Trzebiatowski Institute, ul. Okolna 2, 50-422 Wroclaw, Poland
Leibniz Institute for Crystal Growth, Max-Born-Str. 2, D-12489 Berlin, Germany

Po39 **Plasma-assisted MBE and structural properties of AlGaN nanorods selectively grown on µ-cone patterned c-sapphire substrates**

A.N. Semenov, D.V. Nechaev, D.A. Kirilenko, S.I. Troshkov, V.N. Jmerik, S.V. Ivanov

Ioffe Institute of RAS, Polytekhnicheskaya 26, St. Petersburg 194021, Russia

Po40 **Morphology and Electrical Properties of InGaN:Mg/InGaN:Si Tunnel Junctions Grown by Plasma-assisted Molecular Beam Epitaxy**

M. Żak, M. Siekacz, K. Nowakowski-Szkudlarek, A. Feduniewicz-Żmuda, C. Skierbiszewski

Institute of High Pressure Physics Polish Academy of Sciences, ul. Sokołowska 29/37, 01-142 Warsaw, Poland
Gdańsk Uniwersity of Technology, ul. Gabriela Narutowicza 11/12, 80-233 Gdańsk, Poland
TopGaN Ltd, ul. Sokołowska 29/37, 01-142 Warsaw, Poland

Po41 **Influence of Mg-doped Layers on Internal Optical Losses in InGaN Laser Diodes**

M. Hajdel, G. Muzioł, K. Nowakowski-Szkudlarek, M. Siekacz, A. Feduniewicz-Żmuda, P. Wolny, C. Skierbiszewski

Institute of High Pressure Physics Polish Academy of Sciences, ul. Sokołowska 29/37, 01-142 Warsaw, Poland

Gdańsk Uniwersity of Technology, ul. Gabriela Narutowicza 11/12, 80-233 Gdańsk, Poland
TopGaN Ltd, ul. Sokołowska 29/37, 01-142 Warsaw, Poland

Po42 **Comparison between MBE-grown InGaN/GaN Blue LEDs with Standard p-contact and Tunnel Junction p-contact**

Shyam Bharadwaj, Kevin Lee, Henryk Turski, Huili Xing,Debdeep Jena

Cornell University, Ithaca, USA
Institute of High Pressure Physics, Warsaw, Poland

Po43 **Kelvin probe force microscopy study of High electron mobility transistors**

A. Minj, M.P. Chauvat, O. Patard, P. Gamarra, C. Lacam, C. Dua, S.L. Delage, and P. Ruterana

CIMAP, UMR 6252, CNRS-ENSICAEN-CEA-UCBN, 6, Bd Maréchal Juin, 14050 Caen, France
III-V Lab, 1 Avenue Augustine Fresnel, Campus Polytechnique, 91767 Palaiseau, France

Po44 **Probing piezoelectric polarization and hole trapping induced surface band bending at interface dislocations in InGaN/GaN heterostructures**

A. Minj, M.A. Fazio, D. Cavalcoli, M.P. Chauvat, Q.T. Li, N. Garro, A. Cros, P. Ruterana

CIMAP, UMR 6252, CNRS-ENSICAEN-CEA-UCBN, 6, Bd Maréchal Juin, 14050 Caen, France
Department of Physics and Astronomy, University of Bologna, Viale Berti Pichat 6/2, 40127 Bologna, Italy
Institute of Materials Science (ICMUV), Universidad de Valencia, P.O. Box 22085, E-46071 Valencia, Spain

Po45 **Stress and surface defects control for optimization of AlGaN/GaN/Si(111) HEMT-type structures properties**

T. Szymanski, M. Wosko, B. Paszkiewicz, R. Paszkiewicz

Faculty of Microsystem Electronics and Photonic, Wroclaw University of Science and Technology, Janiszewskiego 11/17, 50-372 Wroclaw, Poland

Po46 **On-chip near-ultraviolet multicomponent system toward the internet of things**

Y. Jiang, J.L. Yuan, C. Qin, Y.J. Wang

Peter Grünberg Research Centre, Nanjing University of Posts and Telecommunications, Nanjing, 210003, China

Po47 **Monte Carlo simulation of carbon incorporation in GaN MOVPE**

S. Yamamoto, Y. Inatomi, A. Kusaba, P. Kempisty, Y. Kangawa

Department of Aeronautics and Astronautics, Kyushu University, Fukuoka 819-0395, Japan
IMaSS, Nagoya University, Nagoya 464-8603, Japan
IHPP, PAS, Sokolowska 29/37, 01-142 Warsaw, Poland
RIAM, Kyushu University, Kasuga, Fukuoka 816-8580, Japan

Po48 **Migration Energy of a N Atom around Ga Vacancy in GaN**

M. Oda

Department of Applied Physics, Wakayama University, Japan

Po49 **Compositional Dependence of Band Gaps in III-Nitride Semiconductor Superlattices**

T. Kawamura, T. Akiyama, Y. Kangawa

Graduate School of Engineering, Mie University, 1577 Kurimamachiya-cho, Tsu, Japan
Research Institute for Applied Mechanics, Kyushu University, 6-1 Kasuga-koen, Kasuga,
Fukuoka, Japan

Po50 Electronic and Thermodynamic Properties of the AlN/diamond Interfaces – a DFT Studies

R. Hrytsak, P. Kempisty, S. Krukowski, M. Sznajder

Institute of High Pressure Physics, Polish Academy of Sciences, Sokołowska 29/37, 01-142
Warsaw, Poland
Faculty of Mathematics and Natural Sciences, University of Rzeszów, Pigonia 1, 35-959
Rzeszów, Poland

Po51 On determination of the dominant recombination mechanisms from time resolved photoluminescence in nitride semiconductor heterostructures

K. Sakowski, P. Strak, K. Koroński, K. Sobczak, J. Borysiuk, K. P. Korona, A. Suchocki,
E. Monroy, A. Kaminska, S. Krukowski

Institute of High Pressure Physics, Polish Academy of Sciences, Sokolowska 29/37, 01-142
Warsaw, Poland
Institute of Physics, Polish Academy of Sciences, Al. Lotników 32/46, 01-142 Warsaw, Poland
Faculty of Chemistry, Biological and Chemical Research Centre, University of Warsaw
Faculty of Physics, University of Warsaw, Pasteura 5, 02-093 Warsaw, Poland
Université Grenoble-Alpes, CEA, INAC-Pheliqs, 17 av. des Martyrs, 38000 Grenoble, France
Cardinal Stefan Wyszynski University, College of Science, Department of Mathematics and
Natural Sciences, Dewajtis 5, 01-815 Warsaw, Poland

Po52 Effective approach for calculating absolute surface energies of polar and semipolar planes for group-III nitrides under MOVPE conditions

T. Akiyama, Y. Seta, K. Nakamura, T. Ito

Department of Physics Engineering, Mie University, 1577 Kurima-Machiya, Tsu 514-8507, Japan

WEDNESDAY (8TH AUGUST)

08.30-10.10   **Plenary Session 3**
PS3 (chair: I. Grzegory)

08.30-09.20   **Recent Progress of GaN Growth by Na-flux Method**   **PS3.1**

Yusuke Mori, Masayuki Imanishi, Masashi Yoshimura

Graduate School of Engineering, Osaka University, 2-1, Yamada-oka, Suita, Osaka, Japan

09.20-10.10   **Acceptors in Nitrides: Doping, Compensation, and Impact on Device Performance**   **PS3.2**

Chris G. Van de Walle

Materials Department, University of California, Santa Barbara, USA

10.10-10.30   **Coffee break**

10.30-13.00   **Parallel sessions: Characterization & Theory**

Characterization - We1 (chair: M. Leszczynski)

10.30-11.00   **Defect Structure Analysis of GaN Substrates by Synchrotron X-Ray Diffraction Techniques (invited)**   **We 1.1**

L. Kirste, T.N. TranThi, A.N. Danilewsky, T. Sochacki, M. Boćkowski, J. Baruchel

Fraunhofer Institute for Applied Solid State Physics (IAF), Freiburg, Germany
European Synchrotron Radiation Facility (ESRF), Grenoble, France
Crystallography, Albert-Ludwigs University, Freiburg, Germany
Institute of High Pressure Physics PAS, Warsaw, Poland

11.00-11.30   **Multi-microscopy of defects in nitride semiconductors (invited)**   **We1.2**

T.J. O'Hanlon, F.C. Massabuau, M.J. Kappers, R.A. Oliver

Department of Materials Science and Metallurgy, University of Cambridge, 27 Charles Babbage Road, Cambridge, CB3 0FS

11.30-12.00   **Spontaneous formation of quantum wells, ordering and composition fluctuations in (11-22) semipolar AlGaN/GaN heterostructures grown by plasma enhanced MBE (invited)**   **We1.3**

H.P. Lei, M.P. Chauvat, S. Kret, E. Monroy, <u>P. Ruterana</u>

Key Laboratory of Materials Physics, Institute of Solid State Physics, Chinese Academy of Sciences, Hefei 230031, China
CIMAP, 6 boulevard du Marechal Juin, Université de Caen, Caen, France
Institute of Physics, Polish Academy of Sciences, al. Lotników 32/46, Warsaw, Poland
CEA Grenoble, INAC/SP2M, 25 Rue des Martyrs 38042, Grenoble Cedex 9, France

12.00-12.15   **Observation of Dislocations in AlN Single Crystal by Using Synchrotron X-Ray Topography, Etch Pit Method and Transmission Electron Microscope**   **We1.4**

<u>Y. Yao</u>, Y. Sugawara, Y. Ishikawa, D. Yokoe, N. Okada, R. Inomoto, K. Tadatomo, Y. Takahashi, K. Hirano

Japan Fine Ceramics Center (JFCC), 2-4-1 Mutsuno, Atsuta, Nagoya, Japan
Yamaguchi Univ., 2-16-1 Tokiwadai, Ube, Yamaguchi, Japan
Nihon Univ., 7-24-1 Narashinodai, Funabashi, Japan
High Energy Accelerator Research Organization (KEK), 1-1 Ooho, Tsukuba, Japan

12.15-12.30   **Investigation of Stacking Faults in Zincblende GaN Grown on 3C-SiC on Si templates with TEM and XRD**   **We1.5**

<u>L.Y. Lee</u>, P. Vacek, M. Frentrup, M.J. Kappers, R.A. Oliver, D.J. Wallis

Department of Materials Science and Metallurgy, University of Cambridge, 27 Charles Babbage Rd, Cambridge, CB3 0FS, United Kingdom
Centre for High Frequency Engineering, University of Cardiff, 5 The Parade, Newport Road, Cardiff, CF24 3AA, United Kingdom

12.30-12.45   **Nanobeam X-ray Diffraction Analysis of Local Lattice Distortions in the Growth Direction of a Modified Na-Flux GaN Bulk Crystal**   **We1.6**

<u>K. Shida</u>, S. Takeuchi, T. Tohei, M. Imanishi, M. Imade, Y. Mori, K. Sumitani, Y. Imai, S. Kimura, A. Sakai

Graduate School of Engineering Science, Osaka University, 1-3 Machikaneyama-cho, Toyonaka, Osaka, Japan
Graduate School of Engineering, Osaka University, 2-1 Yamadaoka, Suita, Osaka, Japan
Japan Synchrotron Radiation Research Institute (JASRI), 1-1-1 Koto, Sayo, Hyogo, Japan

12.45-13.00   **Strain relaxation in InGaN/GaN epilayers by formation of V-pit defects: XRD experiments and numerical simulations**   **We1.7**

J. Stranska-Matejova, L. Horak, P. Minarik, V. Holy, A. Hospodkova, E. Grzanka, J. Domagala, M. Leszczynski

Faculty of Mathematics and Physics, Charles University, Ke Karlovu 5, 121 16 Prague, Czech Republic
Institute of Physics, Czech Academy of Sciences, Cukrovarnicka 10/112, 162 00 Prague, Czech Republic
Institute of High Pressure Physics, Polish Academy of Sciences, Sokolowska 29/37, 01-142 Warsaw, Poland
Institute of Physics,Polish Academy of Sciences, Al. Lotnikow 32/46, Warsaw, Poland

Theory - We2 (chair: S. Krukowski)

10.30-11.00   **Optical Properties of 1 ML GaN in AlN: What Happens Beyond the Envelope Function Approach (invited)**   **We2.1**

A. A. Toropov, E. A. Evropeitsev, M. O. Nestoklon, D. S. Smirnov, V. N. Jmerik, D. V. Nechaev, S. Rouvimov, T. V. Shubina, B. Gil, S. V. Ivanov

Ioffe Institute, Politekhnicheskaya 26, 194021 St Petersburg, Russia
University of Notre Dame, Notre Dame, 46556 Indiana, USA
Université Montpellier 2, L2C, UMR 5221, 34095 Montpellier Cedex 5, France

11.00-11.30   **First Principles and Thermodynamic Studies on GaN MOVPE Processes**   **We2.2**

Y. Okawachi, K. Sekiguchi, K. Chokawa, M. Araidai, M. Shoji, Y. Shigeta, Y. Kangawa, K. Kakimoto, K. Shiraishi **(invited)**

Graduate School of Engineering, Nagoya University, Furo-cho, Chikusa-ku, Nagoya 464-8603, Japan
Institute of Materials and Systems for Sustainability, Nagoya University, Furo-cho, Chikusaku, Nagoya 464-8603, Japan
Center for Computational Sciences, University of Tsukuba, 1-1-1 Tennodai, Tsukuba 305-8577, Japan
Research Institute for Applied Mechanics, Kyushu University, 6-1 Kasuga-koen, Kasuga, 816-8580, Japan

11.30-12.00 — **Compensation in Si-doped AlN: Mechanisms and opportunities (invited)** — **We2.3**

Douglas L. Irving, Joshua S. Harris, Jonathon N. Baker, Shun Washiyama, M. Hayden Breckenridge, Pramod Reddy, Ramon Collazo, and Zlatko Sitar

Department of Materials Science and Engineering, North Carolina State University, Raleigh, NC, USA
Adroit Materials, Cary, NC, USA

12.00-12.15 — **A theoretical model for carbon incorporation during step-flow growth of GaN by MOVPE** — **We2.4**

Y. Inatomi, Y. Kangawa

Department of Aeronautics and Astronautics, Kyushu University, Fukuoka 812-0395, Japan
RIAM, Kyushu University, Fukuoka 816-8580, Japan
IMaSS, Nagoya University, Nagoya 464-8601, Japan

12.15-12.30 — **Perovskite Solar Cells with n-type GaN Electrodes** — **We2.5**

M. Wierzbowska, M. Sarzyński, I. Dzięcielewski, J. Weyher1, B.-E. Cohen and L. Etgar

Institute of High Pressure Physics, Polish Academy of Sciences, Sokołowska 29/37, 01-142 Warsaw, Poland
Institute of Chemistry, The Center for Nanoscience and Nanotechnology, The Casali Center for Applied Chemistry, The Hebrew University of Jerusalem, Israel

12.30-13.00 — **Morphology and Electronic Structure of Carbon Doped Hexagonal Boron Nitride (invited)** — **We2.6**

A. Jamróz, J.A. Majewski

Faculty of Physics, University of Warsaw, ul. Pasteura 5, 02-093 Warszawa

13.00-14.00 — **Lunch break**

14.00-18.00 — **Excursion**

19.30-22.00 — **Gala Dinner**

THURSDAY (9TH AUGUST)

09.00-11.00   **Parallel sessions: Electrical Devices & Characterization**

Electrical Devices - Th1 (chair: T. Anderson)

09.00-09.30   **GaN Nanostructures (or how to Take Transistor Linearity to new Levels) (invited)**   **Th1.1**

Sameer Joglekar, Ujwal Radhakrishna, Qingyun Xie, and <u>Tomás Palacios</u>

Massachusetts Institute of Technology 77 Massachusetts Ave., Bldg. 39-567, Cambridge

09.30-10.00   **Growth, Physics, and Applications of Tunneling Nitride Structures (invited)**   **Th1.2**

<u>Debdeep Jena</u>, Jimy Encomendero, Samuel Bader, Alex Chaney, Henryk Turski, Yongjin Cho, Grace Huili Xing

Cornell University, Ithaca, USA

10.00-10.15   **High Reliability and Frequency Performances of InAlN/GaN HFETs**   **Th1.3**

<u>Z.H. Feng</u>, Y.J. Lv, Y.L. Fang, Y.G. Wang, X.B. Song, S.J. Cai

National Key Laboratory of ASIC, Hebei Semiconductor Research Institute, Shijiazhuang, China

10.15-10.30   **Demonstration of GaN vertical double implanted MOSFET**   **Th1.4**

<u>R. Tanaka</u>, S. Takashima, K. Ueno, H. Matsuyama, M. Edo, K. Nakagawa

Fuji Electric Co., Ltd., 1, Fuji-machi, Hino-city, Tokyo 191-8502, Japan
Univ. of Yamanashi, 7-32, Miyamae-cho, Kofu, Yamanashi 400-8511, Japan

10.30-10.45   **Optimized Ohmic Contacts For InAlGaN/GaN HEMTs**   **Th1.5**

<u>F. Bouazzaoui</u>, M.P. Chauvat, M. Zegaoui, F. Medjdoub, P. Gamarra, S. Kret, P. Ruterana

CIMAP, 6 boulevard du Marechal Juin, Université de Caen, Caen, France
Institute of Electronics, Microelectronics and Nanotechnology (IEMN), Av. Poincaré,Villeneuve d'Ascq, France;
III-V Lab, 1 Avenue Augustin Fresnel, Campus Polytechnique, Palaiseau, France

Institute of Physics, Polish Academy of Sciences, al. Lotników 32/46, Warsaw, Poland

10.45-11.00	**Improving the Performance of AlInN/GaN and AlInGaN/GaN HEMTs by Using a Triethylgallium-Grown Channel Layer and Barrier**	**Th1.6**

I. Sanyal, Y.C. Lee, Y.C. Lin, J.I. Chyi

Department of Electrical Engineering, National Central University, Taiwan R.O.C
Centre for Applied Sciences, Academia Sinica, Taiwan R.O.C

Characterization - Th2 (chair: M. Kamińska)

09.00-09.30	**Characterization of Threading Dislocations in Thick GaN Films Using Multiphoton-Excitation Photoluminescence (invited)**	**Th2.1**

Tomoyuki Tanikawa, Kazuki Ohnishi, Tatsuya Fujita and Takashi Matsuoka

Institute for Materials Research, Tohoku University, Katahira 2-1-1, Aoba-ku, Sendai, Japan

09.30-10.00	**Observation of Dislocation Propagation in GaN on GaN Structure with a Multiphoton Excitation Photoluminescence Microscope (invited)**	**Th2.2**

A. Tanaka, K. Nagamatsu, S. Usami, M. Kushimoto, M. Deki, S. Nitta, Y. Honda, H. Amano

Institute of Materials and Systems for Sustainability (IMaSS), Nagoya University, Furo-cho, Chikusa-ku, Nagoya, Japan
National Institute for Materials Science (NIMS), Namiki, Tsukuba, Japan
Department of Electrical Engineering and Computer Science, Nagoya University, Furo-cho, Chikusa-ku, Nagoya, Japan
Akasaki Research Center, Nagoya University, Furo-cho, Chikusa-ku, Nagoya, Japan
Venture Business Laboratory, Nagoya University, Furo-cho, Chikusa-ku, Nagoya, Japan

10.00-10.30	**Evaluation of Structural Disorder and In-Gap States of III-V nitrides by Photothermal Deflection Spectroscopy (invited)**	**Th2.3**

M. Sumiya, K. Fukuda, Y. Nakano, S. Ueda, L. Sang, H. Iwai, T. Yamaguchi, T. Onuma, T. Honda

National Institute for Materials Science, Tsukuba Ibaraki, 305-0044, Japan
Kougakuin Univ., Hachioji, Tokyo 192-0015, Japan

Chubu Univ., Kasugai Aichi, 487-8501, Japan

10.30-10.45	**Origin of the Yellow Luminescence in Be-doped GaN revealed by hydrostatic pressure studies**	**Th2.4**

A. Kaminska, H. Teisseyre, J.L. Lyons, D. Jarosz, M. Bockowski, A. Suchocki, C.G. VandeWalle

Institute of Physics, Polish Academy of Sciences, Aleja Lotnikow 32/46, PL-02-668 Warsaw, Poland
Cardinal Stefan Wyszynski University, College of Science, Department of Mathematics and Natural Sciences, Dewajtis 5, 01-815 Warsaw, Poland
Institute of High Pressure Physics, Polish Academy of Sciences, Sokolowska 29/37, 01-142 Warsaw, Poland
Center for Computational Materials Science, Naval Research Laboratory, Washington, DC 20375, USA
Materials Department, University of California, Santa Barbara, CA 93106-5050 USA

10.45-11.00	**Imaging of Surface Plasmon Polaritons of 2D Plasmons of InN Nanostructures having Surface Electron Accumulation**	**Th2.5**

K.K. Madapu, S.K. Dhara

Surface and Nanoscience Division, Indira Gandhi Centre for Atomic Research, Homi Bhabha National Institute, Kalpakkam-603102, India

11.00-11.15   **Coffee break**

11.15-13.00   **Parallel sessions: Electrical Devices & Nanowires**

Electrical Devices - Th3 (chair:C.Skierbiszewski)

11.15-11.45	**Navy Application of Wide Bandgap (WBG) semiconductors enabling future Power and Energy Systems (invited)**	**Th3.1**

Travis J. Anderson, Lynn Petersen

U.S. Naval Research Laboratory, 4555 Overlook Ave SW, Washington, DC USA
Office of Naval Research, 875 N Randolph St, Arlington, VA USA

11.45-12.15	**Vertical Power Devices Enabled by Bulk GaN Substrates (invited)**	**Th3.2**

Travis J. Anderson, Lunet E. Luna, James C. Gallagher, Jennifer K. Hite, Alan G. Jacobs, Boris N. Feigelson, Karl D. Hobart, and Fritz J. Kub

U.S. Naval Research Laboratory, 4555 Overlook Ave SW, Washington, DC USA

12.15-12.30   **Characterizations of high-temperature Mg ion implantation in GaN**   **Th3.3**

<u>M. Takahashi</u>, K. Sone, A. Tanaka, S. Usami, Y. Ando, M. Deki, M. Kushimoto, S. Nitta, Y. Honda, H. Amano

Dept. of Electronics, Nagoya Univ, Furo-cho, Chikusa-ku, Nagoya, 464-8603, JAPAN,
Nagoya Univ. IMaSS, Furo-cho, Chikusa-ku, Nagoya, 464-8603, JAPAN,
NIMS, 1-2-1 Sengen, Tsukuba, Ibaraki 305-0047, JAPAN
Nagoya Univ. Akasaki Research Center, Furo-cho, Chikusa-ku, Nagoya, 464-8603, JAPAN,
Nagoya Univ. VBL, Furo-cho, Chikusa-ku, Nagoya, 464-8603, JAPAN

12.30-12.45   **Non-cap thermal activation process of Mg-ion implanted Ga-polar GaN using ultra high pressure N2 annealing**   **Th3.4**

<u>H. Sakurai</u>, S. Yamada, M. Omori, Y. Furukawa, H. Suzuki, M. Boćkowski, J. Suda, T. Kachi

IMaSS, Nagoya University, Aichi 464-8603, Japan
Dept. of Electronics, Grad. School of Engineering, Nagoya Univ., Aichi 464-8603, Japan
ISET, ULVAC, Inc., Chigasaki, Kanagawa 253-8543, Japan
Institute of High Pressure Physics Polish Academy of Sciences, 01-142 Warsaw, Poland

12.45-13.00   **Improvement of Electrical Stability of ALD-Al2O3/GaN Interface by UV/O3 Oxidation and Postdeposition Annealing**   **Th3.5**

<u>M. Deki</u>, K. Sone, K. Watanabe, F. Miura, K. Nagamatsu, A. Tanaka, M. Kushimoto, S. Nitta, Y. Honda, H. Amano

Inst. of Materials and Systems for Sustainability, Nagoya University, Nagoya, Japan
Dept. of Electrical Engineering and Computer Science, Nagoya University, Nagoya, Japan
National Institute for Materials Science, Namiki, Tsukuba, Japan
Akasaki Research Center, Nagoya University, Nagoya, Japan
Venture Business Laboratory, Nagoya University, Nagoya, Japan

Nanowires - Th4 (chair: Xinqiang Wang)

11.15-11.30   **Fabrication and characterization of GaN-nanowires optoelectronic devices**   **Th4.1**

<u>M. Takebayashi</u>, N. Sone, A. Suzuki, K. Nokimura, K. Sasai, S. Kamiyama, T. Takeuchi, M. Iwaya, I. Akasaki

Meijo Univ., 1-501, Shiogamaguchi, Tempaku-ku, Nagoya, Japan
Akasaki Research Center, Nagoya Univ., Furou-cho, Chikusa-ku, Nagoya, Japan

11.30-11.45   **Optical simulation of GaInN-based multi-quantum-shell (MQS)-Light-Emitting-Diodes (LEDs)**   **Th4.2**

M. Terazawa, M. Ohya, S. Kamiyama, T. Takeuchi, M. Iwaya, I. Akasaki

Meijo Univ., 501 Icchoume, Shiogamaguchi, Tenpaku-ku, Nagoya-shi, Aichi, Japan
Akasaki Research Center, Nagoya Univ., Furou-cho, Chikusa-ku, Nagoya-shi, Aichi, Japan

11.45-12.00   **Self-Induced InGaN Nanowires with a Controlled Indium Composition and Selective Area Growth of InN by HVPE**   **Th4.3**

G. Avit, M. Zeghouane, Y. André, C. Bougerol, E. Gil, D. Castelucci, P. Ferret, E. Roche, J. Leymarie, F. Médard, V.G. Dubrovskii, A. Trassoudaine

Université Clermont Auvergne, CNRS SIGMA Clermont, Institut Pascal, F-63000 Clermont-Ferrand, France
Université Grenoble Alpes, F-38000 Grenoble, France
CNRS, Institut Néel, F-38042 Grenoble, France
CEA LETI, Département Optique et Photonique, F-38000 Grenoble, France
ITMO University, Kronverkskiy prospekt 49, 197101, St Petersburg, Russia

12.00 -12.15   **Study on emission wavelength control of GaInN multi-quantum-shell/GaN nanowire**   **Th4.4**

N. Goto, K. Sasai, K. Iida, N. Sone, A. Suzuki, K. Nokimura, M. Takebayashi, H. Murakami, M. Terazawa, S. Kamiyama, T. Takeuchi, M. Iwaya, I. Akasaki

Meijo Univ., 501 Icchoume, Shiogamaguchi, Tenpaku-ku, Nagoya-shi, Aichi, Japan
Akasaki Research Center, Nagoya Univ., Furou-cho, Chikusa-ku, Nagoya-shi, Aichi, Japan

12.15-12.30   **Device fabrication of GaInN-based multi-quantum-shell LEDs**   **Th4.5**

A. Suzuki, H. Murakami, K. Nokimura, M. Takebayashi, K. Sasai, N. Goto, N. Sone, S. Kamiyama, T. Takeuchi, M. Iwaya, I. Akasaki

Meijo Univ., 1-501, Shiogamaguchi, Tenpaku-ku, Nagoya, Japan
Akasaki Research Center, Nagoya Univ., Furou-cho, Chikusa-ku, Nagoya, Japan

| 12.30-12.45 | **Green/Yellow/Red Emission From m-plane Core-shell InGaN/GaN Nanowires** | **Th4.6** |

<u>A. Kapoor</u>, N. Guan, L. Mancini, C. Bougerol, F.H. Julien, J.P. Barnes, M. Tchernycheva, C. Durand, J. Eymery

Univ. Grenoble Alpes, CEA, INAC-PHELIQS, 38000 Grenoble, France
Center of Nanoscience and Nanotechnologies (C2N), UMR 9001 CNRS, Paris, France
Univ. Grenoble Alpes, CEA, INAC-MEM, 38000 Grenoble, France
Univ. Grenoble Alpes, CNRS, Institut Néel, 38000 Grenoble, France
Univ. Grenoble Alpes, CEA, LETI, DTSI, SCMC, F-38000 Grenoble, France.

| 12.45-13.00 | **Insights into the Quantum Efficiency and Recombination Dynamics of InGaN/GaN Core-Shell Microrod LED Structures** | **Th4.7** |

<u>H. Zhou</u>, P. Henning, F. A. Ketzer, L. Nicolai, H. Spende, J. Hartmann, A. Vogt,A. Avramescu, S. Fündling, H.-H. Wehmann, M. Hanke, A. Trampert, M. Straßburg, H.-J. Lugauer, A. Hangleiter, T. Voss, A. Waag

Institut für Halbleitertechnik and Laboratory for Emerging Nanometrology, Technische Universität Braunschweig, 38092 Braunschweig, Germany
epitaxy competence center ec2, Hans-Sommer-Straße 66, 38106 Braunschweig, Germany
Institut für Angewandte Physik, Technische Universität Braunschweig, 38106 Braunschweig, Germany
Paul-Drude-Institut für Festkörperelektronik, Hausvogteiplatz 5-7, 10117 Berlin, Germany
OSRAM Optosemiconductors GmbH, Leibnizstraße 4, 93055 Regensburg, Germany

| 13.00-14.00 | **Lunch break** |

| 14.00-16.00 | **Parallel sessions: Growth and Characterization & Optoelectronic Devices and Growth** |

Growth and Characterization - Th5 (chair: J. Hite)

| 14.00-14.15 | **In-situ observation of AlN growth on levitated Ni-Al droplet** | **Th5.1** |

<u>Y. Yamagata</u>, S. Hamaya, M. Adachi, A.J. Loach, J.S. Fada, L.G. Wilson, J.W. Carter, R.H. French, H. Fukuyama

Institute of Multidisciplinary Research for Advanced Materials (IMRAM), Tohoku University, 2-1-1 Katahira, Aoba-ku, Sendai 980-8577, Japan.
Department of Materials Science and Engineering, Case Western Reserve University, 10900 Euclid Avenue, Cleveland, Ohio 44106-7204, USA.

Department of Mechanical and Aerospace Engineering, Case Western Reserve University, 10900 Euclid Avenue, Cleveland, Ohio 44106-7204, USA.

14.15-14.30	**Effect of Reaction Temperature on AlN Formation at Interface of Al Layer Deposited on GaN Substrate**	**Th5.2**

M. Noorprajuda, M. Ohtsuka, M. Adachi, H. Fukuyama

Institute of Multidisciplinary Research for Advanced Materials (IMRAM), Tohoku University, 2-1-1, Katahira, Aoba-ku, Sendai 980-8577, Japan

14.30-14.45	**Evolution of morphology and crystalline quality of sputtered AlN films with high-temperature annealing**	**Th5.3**

Y. Mogami, S. Motegi, A. Osawa, K. Osaki, Y. Tanioka, A. Maeoka, M. Jo, N. Maeda, H. Yaguchi, H. Hirayama

RIKEN, 2-1 Hirosawa, Wako, Saitama 351-0198, Japan
Saitama University, 255 Shimo-Okubo, Sakura-ku, Saitama 338-8570, Japan
SCREEN Finetech Solutions Co. Ltd., 2426-1 Mikami, Yasu, Shiga 520-2323, Japan

14.45-15.00	**Characteristics of highly conductive p-type GaN films prepared by pulsed sputtering**	**Th5.4**

T. Fudetani, K. Ueno, A. Kobayashi, H. Fujioka

Institute of Industrial Science, The University of Tokyo, 4-6-1 Komaba, Meguro, Tokyo, Japan
JST-ACCEL, 5 Sanbancho, Chiyoda, Tokyo, Japan

15.00-15.15	**Improvement of electron mobility of polycrystalline InN on glass substrates by AlN buffer layers**	**Th5.5**

M. Sakamoto, A. Kobayashi, K. Ueno, H. Fujioka

Institute of Industrial Science, The University of Tokyo, 4-6-1 Komaba, Meguro, Tokyo, Japan
JST-ACCEL, 5 Sanbancho, Chiyoda, Tokyo, Japan

15.15-15.30	**Structural and Electrical Properties of AlN and AlGaN Prepared by Pulsed Sputtering**	**Th5.6**

Y. Sakurai, K. Ueno, A. Kobayashi, H. Miyake, H. Fujioka

Institute of Industrial Science, the University of Tokyo, 4-6-1 Komaba, Tokyo, Japan
Graduate School of Regional Innovation, Mie University, Mie 514-8507, Japan

ACCEL, Japan Science and Technology Agency (JST), 5 Sanbancho, Chiyoda, Tokyo, Japan

| 15.30-15.45 | **Surface Morphology Control and Si-Doping of MOVPE-Grown High-Al-Content AlGaN Layers** | **Th5.7** |

<u>M. Tollabi Mazraehno</u>, M.P. Hoffmann, L. Cancellara, C. Frankerl, B. Neuschulz, M.J. Davies, C. Brandl, T. Wernicke, M. Albrecht, M. Kneissl, H.-J. Lugauer

Institute of Solid State Physics, Technische Universität Berlin, Hardenbergstr. 36, 10623 Berlin, Germany
Leibniz-Institut für Kristallzüchtung, Max-Born-Str. 2, 12489 Berlin, Germany
OSRAM Opto Semiconductors GmbH, Leibnizstr. 4, 93055 Regensburg, Germany

| 15.45-16.00 | **Effects of N2 and H2 carrier gases on the growth of AlGaN epilayers on Si(110) substrates by MOCVD** | **Th5.8** |

<u>X.Q. Shen</u>, T. Takahashi, M. Shimizu, H. Okumura

National Institute of Advanced Industrial Science and Technology (AIST) Tsukuba, Ibaraki 305-8568, Japan

Optoelectronic Devices and Growth - Th6 (chair: J. Freitas)

| 14.00-14.30 | **Significantly enhanced performance for AlGaN UV LED by employing a thin BAIN electron blocking layer (invited)** | **Th6.1** |

W. Guo, K. Liu, Z.H. Zhang, H. Sun, K. Liu, <u>X. Li</u>

King Abdullah University of Science and Technology (KAUST), Thuwal, 23955, Saudi Arabia
Hebei University of Technology, Tianjin, 300401, China.

| 14.30-14.45 | **Green - blue InGaN/GaN LED array obtained by lateral band-gap engineering.** | **Th6.2** |

<u>P.A. Dróżdż</u>, M. Sarzyński, K.P. Korona, R. Czernecki, T. Suski

Faculty of Physics, University of Warsaw, Pasteura 5, 02-093 Warsaw, Poland
Institute of High Pressure Physics "Unipress", Polish Academy of Sciences, Sokołowska 29/37, 01-142 Warsaw, Poland

| 14.45-15.00 | **InAlN growth peculiarities on vicinal GaN substrates** | **Th6.3** |

<u>M. Sawicka</u>, M. Siekacz, G. Muziol, A. Feduniewicz-Żmuda, J. Smalc-Koziorowska, M. Kryśko, Ž. Gačević, E. Calleja, C. Skierbiszewski

Institute of High Pressure Physics Polish Academy of Sciences, Sokołowska 29/37, 01-142 Warsaw, Poland
TopGaN Sp. z o.o., Sokołowska 29/37, 01-142 Warsaw, Poland
ISOM-ETSIT Universidad Politécnica de Madrid, Avda. Complutense s/n, 28040 Madrid, Spain

15.00-15.15	**Germanium doping of Cubic AlxGa1-xN Grown by Molecular Beam Epitaxy**	**Th6.4**

<u>M. Deppe</u>, F. Tacken, T. Henksmeier, J.W. Gerlach, D. Reuter, D.J. As

University of Paderborn, Department of Physics, Warburger Str. 100,

33098 Paderborn, Germany
Leibniz Institute of Surface Engineering (IOM), Permoserstr. 15, 04318 Leipzig, Germany

15.15-15.30	**Material Redistribution during Thermal Annealing of GaN Nanocolumns and Conditions for Their Maskless Overgrowth by MOVPE**	**Th6.5**

<u>V.Z. Zubialevich</u>, P. Pampili, P.J. Parbrook

Tyndall National Institute, University College Cork, T12 R5CP Cork, Ireland
School of Engineering, University College Cork, Cork, Ireland

15.30-15.45	**Surface-enhanced Raman scattering in graphene induced by AlxGa1-xN/GaN axial heterostructure nanowire substrate**	**Th6.6**

<u>J. Kierdaszuk</u>, M. Tokarczyk, K.M. Czajkowski, A. Krajewska, Z.R. Zytkiewicz, G. Kowalski, T.J. Antosiewicz, M. Kamińska, A. Wysmołek, A. Drabińska

Faculty of Physics, University of Warsaw, Pasteura 5, Warsaw, Poland
Institute of Electronic Materials Technology, Wólczyńska 133, Warsaw, Poland
Institute of Optoelectronics, Military University of Technology, Kaliskiego 2, Warsaw, Poland
Institute of Physics, Polish Academy of Sciences, Lotników 32/46, Warsaw, Poland

15.45-16.00	**Two-step epitaxial growth of GaN nanowires by MOVPE**	**Th6.7**

<u>K. Sasai</u>, N. Goto, N. Iida, N. Sone, A. Suzuki, K. Nokimura, M. Takebayasi, H. Murakami, S. Kamiyama, T. Takeuchi, M. Iwaya, I. Akasaki

Meijo Univ., 501 Icchoume, Shiogamaguchi, Tenpaku-ku, Nagoya-shi, Aichi, Japan

Akasaki Research Center, Nagoya Univ., Furou-cho, Chikusa-ku, Nagoya-shi, Aichi, Japan

16.00-16.30 **Coffee break**

16.30-18.30 **Parallel sessions: Electrical Devices & Boron Nitride and Related Materials**

Electrical Devices - Th7 (chair: M. Deki)

16.30-17.00 **EdgeFET Devices Fabricated on 2DEG GaN/AlGaN Heterostructures for Basic and Applied Sciences (invited)** **Th7.1**

G. Cywiński, P. Sai, D.B. But, P. Prystawko, M. Grabowski, P. Kruszewski, I. Yahniuk, P. Wiśniewski, B. Stonio, M. Słowikowski, B. Grzywacz, G.S. Simin, K. Nowakowski-Szkudlarek, J. Przybytek, S.L. Rmyantsev, W. Knap

Institute of High Pressure Physics PAS, ul. Sokolowska 29/37, 01-142, Warsaw, Poland
CEZAMAT, Warsaw University of Technology, 02-822, Warsaw, Poland
National Research University of Information Technologies, St. Petersburg, 197101, Russia
Department of Electrical Engineering, University of South Carolina, Columbia, 29208, USA
Laboratoire Charles Coulomb, University of Montpellier, CNRS, Montpellier, 34095, France

17.00-17.15 **AlGaN/GaN EdgeFET Based on Two Lateral Schottky Barrier Gates as Terahertz Detector** **Th7.2**

P. Sai, D.B. But, P. Prystawko, I. Yahniuk, P. Wiśniewski, B. Stonio, M. Słowikowski, B. Grzywacz, K. Nowakowski-Szkudlarek, J. Przybytek, S.L. Rumyantsev, W. Knap, G. Cywiński

Institute of High Pressure Physics PAS, ul. Sokolowska 29/37, 01-142, Warsaw, Poland
CEZAMAT, Warsaw University of Technology, 02-822, Warsaw, Poland
National Research University of Information Technologies, St. Petersburg, 197101, Russia
Laboratoire Charles Coulomb, University of Montpellier, CNRS, Montpellier, 34095, France

17.15-17.30 **A Study on 2DEG Properties of AlGaN/GaN Structures Formed on Stepped GaN Surfaces for Vertical Power Devices** **Th7.3**

A. Yamamoto, K. Kanatani, S. Makino, M. Kuzuhara

Graduate School of Engineering, University of Fukui, 3-9-1 Bunkyo, Fukui 910-8507, Japan

17.30-17.45	**Modified Small-Signal Model for High Frequency GaN-on-Si HEMT with the Leaky Buffer**	**Th7.4**

Y.T. Ho, K.C. Hsu, L.C. Chang, C.H. Wu

Graduate Institute of Photonics and Optoelectronics, National Taiwan University,
Graduate Institute of Electronics Engineering, National Taiwan University, No. 1, Sec. 4, Roosevelt Road, Taipei City, 10617, Taiwan (R.O.C)

17.45-18.00	**Schottky Barrier Diodes Fabricated on Miscut m-plane Substrates**	**Th7.5**

Y. Ando, K. Nagamatsu, A. Tanaka, M. Deki, O.1. Barry, S. Usami, M. Kushimoto, S. Nitta, Y. Honda, H. Amano

Department of Electrical Engineering and Computer Science, Nagoya University, Furo-Cho, Chikusa-ku, 464-8603 Nagoya, Japan
Institute of Materials and Systems for Sustainability, Nagoya University, Furo-Cho, Chikusa-ku, 464-8603 Nagoya, Japan
National Institute for Materials Science, 1-1, Namiki, 305-0044 Tsukuba, Japan
Akasaki Research Center, Furo-Cho, Chikusa-ku, 464-8603 Nagoya, Japan
Venture Business Laboratory, Furo-Cho, Chikusa-ku, 464-8603 Nagoya, Japan

18.00-18.15	**AlGaN/GaN HEMT Heterostructures Grown by Ammonia and Combined Plasma-Assisted/Ammonia MBE on Sapphire Substrates**	**Th7.6**

E.V. Lutsenko, M.V. Rzheutski, A.G. Vainilovich, I.E. Svitsiankou, V.A. Shulenkova, G.P. Yablonskii, A.N. Alexeev, S.I. Petrov, A.Y. Alyamani

Institute of Physics of NAS of Belarus, 68 Nezalezhnasti Ave. 220072, Minsk, Belarus
SemiTEq JSC, 27 Engels Ave. 194156, Saint-Petersburg, Russia
KACST, National Nanotechnology Center. P.O. BOX 6086, 11442 Riyadh, Saudi Arabia

Boron Nitride and Related Materials - Th8 (chair: D. Hommel)

16.30-16.45	**MOCVD of Boron Nitride Films on Sapphire**	**Th8.1**

J. M.Baranowski and P.A.Caban, P.P.Michalowski, J.Gaca, M.Wójcik and P.Ciepielewski

Institute of Electronic Materials Technology, Warsaw, POLAND

16.45-17.00   **Investigation of MOVPE Boron Nitride Growth**   **Th8.2**

K. Pakuła, M. Tokarczyk, A. Dąbrowska, J. Borysiuk, G. Kowalski, K. Korona, A. Wysmołek, R. Stępniewski

Faculty of Physics, University of Warsaw, Pasteura 5, 02-093 Warsaw, Poland

17.00-17.15   **Growth of BN thin films by MBE: effect of post thermal annealing**   **Th8.3**

F. Liu, P. Wang, X. Rong, T. Wang, Z. Chen, B. Sheng, X. Zheng, S. Sheng, F. Xu, B. Shen, X. Wang

State Key Laboratory for Artificial Microstructure and Mesoscopic Physics, Schoolof Physics, Peking University, Beijing 100871, China

17.15-17.45   **Excitonic spectra of ultra-thin epitaxial boron nitride layers grown by MOCVD (invited)**   **Th8.4**

A. Grempka, P. Tatarczak, M. Wojtczak, A. Dąbrowska, K. Pakuła, M. Tokarczyk, G. Kowalski, J. Borysiuk, R. Stępniewski, A. Wysmołek

Faculty of Physics, University of Warsaw, Pasteura 5, 02-093 Warsaw, Poland

17.45-18.00   **Novel BAlN/AlxGa1-xN heterostructures for optical and power devices**   **Th8.5**

H. Sun, K.H. Li, Y.J. Park, T. Detchprohm, R.D. Dupuis, X. Li

King Abdullah University of Science and Technology (KAUST), Thuwal, 23955 Saudi Arabia
School of Electrical and Computer Engineering, Georgia Institute of Technology, Atlanta, Georgia 30332, USA

18.00-18.15   **Nitrogen Plasma Effects on MBE Growth of GaN on Graphitic Substrate**   **Th8.6**

U. Ooe, S. Arakawa, S. Mouri, Y. Nanishi, T. Araki

Ritsumeikan University, Nojihigashi1-1-1, Kusatsu, Shiga, Japan

18.15-18.30   **New AlScN growth and annealing for used as lattice matched substrate for deep UV LEDs**   **Th8.7**

Jason Schmitt, Peng Lu, Mark Kennard, Dominik Jaeger, Lutz Kriste

Nitride Solutions INC, 3333 W. Pawnee St, Wichita, KS USA
Evatec AG, Hauptstrasse 1a, CH-9477 Trubbach, Switzerland

Fraunhofer Institute for Applied Solid State Physics, Tullastrasse 72, 79108 Freiburg, Germany

FRIDAY (10TH AUGUST)

08.30-10.15   **Parallel sessions: Characterization & Electrical Devices**

Characterization - Fr1 (chair: R. Oliver)

08.30-09.00   **InGaN still to be discovered (invited)**   **Fr1.1**

M. Anikeeva, T. Schulz, L. Lymperakis, C. Freysoldt, P. Wolny, M. Sawicka, C. Cheze, F. Bertram, G. Schmidt, F. Mahler, J. Tomm, C. Skierbiszewski, J. Christen, Neugebauer, M. Albrecht

Leibniz-Institut für Kristallzüchtung, Max-Born-Str. 2, Berlin, Germany
Max-Planck-Institut für Eisenforschung, Düsseldorf, Germany
Institute for High Pressure Physics, Polish Academy of Sciences, Poland
Paul-Drude-Institut, Berlin, Germany
Otto von Guericke Universität Magdeburg, Magdeburg, Germany
Max-Born-Institut, Berlin, Germany

09.00-09.30   **Differences in the mechanism of strain relaxation of InGaN buffer**   **Fr1.2**
                    layers deposited on GaN/sapphire templates and GaN bulk
                    substrates (invited)

J. Smalc-Koziorowska, J. Moneta, E. Grzanka, G. Staszczak, G. Targowski, T. Suski

Institute of High Pressure Physics, PAS, Sokołowska 29/37, 01-142 Warsaw, Poland
TopGaN Ltd. Sokołowska 29/37, 01-142 Warsaw, Poland
Leibniz Institute for Crystal Growth, Max-Born-Str. 2, 12489 Berlin, Germany

09.30-09.45   **Investigation of the spontaneous crystallographic degradation in**   **Fr1.3**
                    nearly lattice-matched InAlN layers to GaN

R. Mohamad, H. Benammar, P. Gamarra, C. Lacam, S. Kret, J. Chen, P. Ruterana

CIMAP, ENSICAEN 6 boulevard du Marechal Juin and Pôle universitaire d'Alençon, Campus de Damigny, 61250 DAMIGNY, Université de Caen Normandie, Caen, France
III-V Lab, 1 Avenue Augustin Fresnel, Campus Polytechnique, Palaiseau, France
Institute of Physics, Polish Academy of Sciences, al. Lotników 32/46, Warsaw, Poland

09.45-10.00 **The Upper Limit for InGaN Plastic Relaxation – Could We Obtain** **Fr1.4**
Fully Relaxed InGaN Layer?

J. Moneta, E. Grzanka, M. Siekacz, M. Albrecht, J. Smalc-Koziorowska

Leibniz Institute for Crystal Growth, Max-Born-Str. 2, 12489 Berlin, Germany
Institute of High Pressure Physics, Polish Academy of Sciences, Sokolowska 29/37, 01-142 Warsaw, Poland
Top GaN Ltd, Sokolowska 29/37, 01-142 Warsaw, Poland

10.00-10.15 **Structural Studies of the Processes Occurring During Thermal** **Fr1.5**
Annealing of InGaN Quantum Wells

A. Lachowski, E. Grzanka, J. Smalc-Koziorowska, S. Grzanka, Ł. Marona, R. Czarnecki, G. Staszczak, S. Kret, M. Leszczyński

Institute of High Pressure Physics, Polish Academy of Sciences, Sokolowska 29/37, 01-142 Warsaw, Poland
TopGaN Ltd., Sokolowska 29/37, 01-142 Warsaw, Poland
Faculty of Materials Science and Engineering, Warsaw University of Technology, Wołoska 141, 02-507 Warsaw, Poland
Institute of Physics, Polish Academy of Sciences, Al.Lotnikow 29/37, 02-668 Warsaw,Poland

Electrical Devices - Fr2 (chair: G. Cywinski)

08.30-09.00 **Ultralow-sheet-resistance high-electron-mobility transistor** **Fr2.1**
structures with strain-controlled high-Al-composition AlGaN
barrier (invited)

A. Yamada, J. Kotani, N. Nakamura

Fujitsu Laboratories Ltd., 10-1 Morinosato-Wakamiya, Atsugi, Kanagawa, 243-0197, Japan

09.00-09.15 **Leakage current analysis for individual dislocations in the** **Fr2.2**
modified Na-flux GaN bulk single crystal

T. Hamachi, S. Takeuchi, T. Tohei, M. Imanishi, Y. Mori, A. Sakai

Graduate School of Engineering Science, Osaka University, 1-3 Machikaneyama-cho, Toyonaka, Osaka, Japan
Graduate School of Engineering, Osaka University, 2-1 Yamadaoka, Suita, Osaka, Japan

09.15-09.30   **Dependency of the reverse leakage current on the MOVPE growth pressure of vertical p–n diodes on a GaN free-standing substrate**   **Fr2.3**

S. Usami, A. Tanaka, H. Fukushima, Y. Ando, M. Deki, M. Kushimoto, S. Nitta, Y. Honda, H. Amano

Dept. of Electronics, Nagoya Univ, Furo-cho, Chikusa-ku, Nagoya, 464-8603, JAPAN,
Nagoya Univ. IMaSS, 3 NIMS, 4 Nagoya Univ. ARC, 5 Nagoya Univ. VBL

09.30-09.45   **Reduction of Carrier Concentration Increase near the Surface of Silicon Substrate after GaN Growth**   **Fr2.4**

K. Matsumoto, T. Ono, Y. Honda, K. Torigoe, M. Kushimoto, H. Amano

SUMCO Corporation, 1-52 Kubara, Yamashiro-cho, Imari 849-4256, Japan
Department of Electrical Engineering and Computer Science
Institute of Materials and Systems for Sustainability
Venture Business Laboratory
Akasaki Research Center,
Nagoya University, Chikusa-ku, Nagoya 464-8603, Japan

09.45-10.00   **RF-Loss Suppression of AlGaN/GaN-on-Si HEMT With Superlattice Buffer**   **Fr2.5**

Y.E. Jeng, K.C. Hsu, L.C. Chang, Y.T. Ho, C.H. Wu

Graduate Institute of Photonics and Optoelectronics, National Taiwan University, Taipei 106, Taiwan
Graduate Institute of Electronics Engineering, National Taiwan University, Taipei 106, Taiwan

10.00-10.15   **Growth and Characterization of InAlN/AlGaN Heterostructures**   **Fr2.6**

J.S. Xue, J.C. Zhang, Y. Hao

Key Laboratory of Wide Bandgap Semiconductor Materials and Devices, School of Microelectronics, Xidian University, Xi'an, People's Republic of China

10.15-10.45   **Coffee break**

10.45-12.15   **Parallel sessions: Growth and Characterization & Optoelectronic Devices**

Growth and Characterization - Fr3 (chair: J. Baranowski)

10.45-11.15   **Determination of the Fermi Level in Doped GaN by Contactless Electroreflectance (invited)**   **Fr3.1**

Ł. Janicki, R. Kudrawiec

Faculty of Fundamental Problems of Technology, Wrocław University of Science and Technology, Wybrzeże Wyspiańskiego 27, 50-370 Wrocław, Poland

11.15-11.30   **Alloying as an effective way to increase Mg incorporation into GaN**   **Fr3.2**

H. Turski, G. Muzioł, P. Wolny, M. Siekacz, K. Nowakowski-Szkudlarek, A. Feduniewicz-Żmuda, C. Skierbiszewski

Institute of High Pressure Physics, PAS, Sokolowska 29/37, 01-142 Warsaw, Poland
Top GaN Ltd., Sokolowska 29/37, 01-142 Warsaw, Poland

11.30-11.45   **Self-Compensation of Carbon in AlGaN**   **Fr3.3**

B. Rackauskas, M.J. Uren, S. Stoffels, M. Zhao, S. Decoutere, M. Kuball

Center for Device Thermography and Reliability, University of Bristol, UK
Inter-University Micro-Electronics Centre, Belgium

11.45-12.15   **Controlling Si Doping Limits in Al Rich AlGaN: Knee Behavior and Low Doping Limits (invited)**   **Fr3.4**

R. Collazo, P. Reddy, S. Washiyama, F. Kaess, R. Kirste, S. Mita, Z. Sitar

Department of Materials Science and Engineering, North Carolina State University, Raleigh, NC 27695-7919, USA.
Adroit Materials, Inc., 2054 Kildaire Farm Rd., Cary NC 27518, USA

Optoelectronic Devices - Fr4 (chair: S. Chichibu)

10.45-11.15 **Growth and Device Characterization of III-N Deep-Ultraviolet Avalanche Photodiodes and Arrays (invited)** **Fr4.1**

<u>M.-H. Ji</u>, M. Bakhtiary-Noodeh, H. Jeong, J. Kim, T. Detchprohm, S.-C. Shen, P. Ghuman, S. Babu, A.K. Sood, R.D. Dupuis

Center for Compound Semiconductors and School of Electrical and Computer, Georgia Institute of Technology, Atlanta, Georgia 30332, USA
Center for Compound Semiconductors and School of Materials Science and Engineering, Georgia Institute of Technology, Atlanta, Georgia 30332, USA
Materials and Devices Advanced Research Institute, LG Electronics, Seoul, South Korea
NASA Earth Science Technology Office, Goddard Space Flight Center, Greenbelt, MD 2077
Magnolia Optical Technologies, Inc., Woburn, MA 01801, USA

11.15-11.30 **Alternative Growth Approaches of p-Type Doped AlGaN Epitaxial Structures** **Fr4.2**

<u>S. Zlotnik</u>, K. Rosiński, J. Sitek, P.P. Michałowski, M. Rudziński

Institute of Electronic Materials Technology, Wolczynska 133, 01-919 Warsaw, Poland

11.30-11.45 **Design of InGaN/GaN MQW structure for scintillator applications** **Fr4.3**

<u>A. Hospodková</u>, T. Hubáček, M. Zíková, F. Dominec, J. Oswald, K. Kuldová, F. Hájek, T. Vaněk, V. Jarý

Institute of Physics, CAS, Cukrovarnická 10, Praha 6, Czech Republic
Crytur, s r.o., Na Lukách 2283, Turnov, Czech Republic

11.45-12.15 **Burying surface defects in InGaN underlayer to increase blue LED efficiency (invited)** **Fr4.4**

Camille Haller, Wei Liu, Jean-François Carlin, Gwénolé Jacopin, Denis Martin, Raphaël Butté, and <u>Nicolas Grandjean</u>

Institute of Physics, Ecole polytechnique fédérale de Lausanne (EPFL), Switzerland

12.30-13.00 **Closing Ceremony** (chair: I. Grzegory and Y. Nanishi)

13.00-14.00 **Lunch**

Plenary lecture

Is the phase diagram of GaN anomalous in respect to other tetrahedrally bonded semiconductors?

Sylwester Porowski

Institute of High Pressure Physics Polish Academy of Sciences,
ul. Sokołowska 29/37, 01-142 Warsaw, Poland

Establishing of phase diagrams of III-N semiconductors is still an important challenge. In this lecture, further discussion on phase diagrams and structural transitions in tetrahedrally bonded semiconductors with particular emphasis of GaN, will be presented. Comprehensive experimental data and the most important theoretical predictions are comprised in an effort to bring up a generalized universal scheme that explains melting that may or may not be accompanied by the change of the coordination number. The scheme considers the "anomalous" melting temperature pressure dependence for GaN. Principal possibility of GaN melting into low density semiconducting liquid is demonstrated and challenges on the way to experimental observation of such a liquid phase are disputed. Prospects of future experiments that can provide reliable information on the nature of atomic bonding for different GaN phases are laid out.

Plenary lecture

The invention of high efficient blue LEDs and future solid state lighting

Shuji Nakamura

Materials and ECE Departments Solid State Lighting and Energy Center University of California Santa Barbara Santa Barbara, CA 93106 USA

In 1970's and 80's, an efficient blue and green light-emitting diodes (LED) were the last missing elements for solid-state display and lighting technologies due to the lack of suitable materials. By that time, III-nitride alloys was regarded the least possible candidate due to various "impossible" difficulties. However, a series of unexpected breakthroughs in 1990's totally changed people's view angle. Finally, the first high efficient blue LEDs were invented and commercialized at the same time of 1993. Nowadays, III-nitride-based LEDs have become the most widely used light source in many applications. Laser lighting using blue/violet lasers is also coming as a future lighting with an ultimate point light source.

Plenary lecture

Transformative Electronics Based on GaN and Related Materials for Realizing Sustainable Smart Society

Hiroshi Amano

Institute of Materials and Systems for Sustainability, Nagoya University, C3-1 Furo-cho, Chikusa-ku, Nagoya 464-8603, Japan

In this presentation, an open innovation platform for transformative electronics based on GaN and related materials being built at a Nagoya University will be explained.

In the 2020s, nitride semiconductors such as BN, AlN, GaN, InN, and their alloys and heterostructures, are expected to play a key role in realizing next-generation personal information systems and social infrastructures. In Japan, the total emission of greenhouse gases decreased from 1.393 billion tons CO_2 equivalent ($BtCO_2$) in 2005 to 1.321 $BtCO_2$ in 2015, which is a 0.53% reduction per year. If this rate of reduction continues, we can expect the emission in 2030 to be 1.22 $BtCO_2$. On the basis of the Paris Agreement, the government of Japan has set targets for the total emission of greenhouse gases of 1.07 $BtCO_2$ in 2030 and 0.29 $BtCO_2$ in 2050. By 2020, more than 70% of general lighting systems in Japan, traditionally based on conventional incandescent lamps or fluorescent lamps, will have been replaced with LED lamps, by which the total electricity consumption can be reduced by about 7%. Conventional personal display systems such as LCD displays with LED backlight units and OLED displays have the problem of low efficiency because both displays have to use color filters. Direct-full color emission based on micro-LED pixels will be the key technology for next-generation high-efficiency personal information systems. We are trying to accelerate the reduction of CO_2 emission by developing new direct display systems using GaN-based nanorod technology. Nitride semiconductors are thought to be the only semiconducting materials that can be used in high power microwave and mm-wave devices, which will be employed in next-generation ultra-broadband 5G wireless communication systems. The energy loss of all electric power circuits such as inverters and converters can be reduced to one-tenth by replacing Si-based MOSFETs and IGBTs with GaN-based transistors and diodes. In future, many everyday objects are likely to be connected to the Internet, referred to as the Internet of Things (IoT). A concern about the IoT is the possibility of each system running out of battery power. If we can connect objects to achieve communication and energy transmission wirelessly regardless of the time and place, this concern can be addressed and we can realize a sustainable smart society. Therefore, realizing the Internet of Energy (IoE) is the first priority in achieving an IoT society. In future, the mobility of humans, such as by vehicles and airplanes, will be increasingly driven by electricity. In order that electric vehicles and airplanes can replace conventional vehicles, in addition to safe and large-capacity batteries, wireless energy transmission systems are essential. For next-generation wireless energy transmission devices it is necessary to realize both high-power and high-frequency operation.

To realize such novel devices and systems, we are trying to develop an open innovation platform. Details of our new space, "Center for Integrated Research of Future Electronics (CIRFE) Transformative Electronics Facilities and Commons", known as C-TEFs and C-TECs, will be explained.

Plenary lecture

AlGaN – a semiconductor that nature has never intended

P. Reddy[1], F. Kaess[1], R. Kirste[2], J. Tweedie[2], R.Collazo[1], Z. Sitar[1, 2]

[1]*North Carolina State University, Material Science and Engineering Department, Raleigh 27695, NC, USA*
[2]*Adroit Materials, Inc., 991 Aviation Pkwy, Suite 800, Morrisville, NC 27560, USA.
Email:sitar@ncsu.edu / Phone: (919) 515-8637*

Although most challenges in growing of high crystalline quality AlGaN alloys and controlling its composition have been overcome over the past few years, achieving control of n and p electrical conductivity over all doping levels of interest has proven to be challenging, particularly for high Al-content alloys. AlGaN exhibits a decrease in free carrier concentration as the dopant concentration increases above a critical doping concentration. This behavior is attributed to the formation of compensating defects due to the lowering of their formation energy during doping. These compensators not only significantly reduce the number of free carriers (sometimes to zero) but also contribute to impurity scattering, limiting the carrier mobility.

A novel scheme to control point defects in wide bandgap semiconductors is presented. The scheme uses minority carrier generation during the growth process to change the position of the quasi Fermi levels in a semiconductor, and, thus, increase the formation energy of compensating defects, leading to a decrease in their incorporation. Using AlGaN as a model system, we demonstrated that the electrical properties of this material could be enhanced by one to two orders of magnitude, rendering it semiconducting.

In n- and p-doped AlGaN films grown by MOCVD, point defects such as hydrogen, carbon, nitrogen or metal vacancies and their corresponding complexes lead to dopant compensation, resulting in a high resistivity and a low mobility in these films. Generally, the energy of formation of a point defect is a function of the process conditions, as described by the chemical potentials of the species involved. In addition, the energy of formation of charged point defects is also a function of the Fermi energy, or the electrochemical potential. We have developed a non-equilibrium process scheme in which the Fermi level is controlled by external excitation in a steady-state condition. We introduce the generation of minority carriers by an external excitation source for control and enhancement of doping capabilities during growth and even during post-growth processing.

This presentation will focus on the details of the theoretical background and related phenomena. The proposed point defect control scheme is of great interest for all wide bandgap materials in which compensation is the main limiting factor in obtaining the desired free carrier concentrations and conductivity. Samples were characterized using SIMS, photoluminescence, Hall measurements, XRD and TEM. The passivation and selfcompensation of Mg acceptors by H and VN was significantly reduced by controlling the Fermi level. The H concentration was reduced by an order of magnitude and no post growth annealing was needed to activate the samples. In Si doped (n-type) AlGaN, Si donor compensation by acceptor defects (e.g. C or VGa/Al) was reduced by up to two orders of magnitude. A significant reduction in PL intensity related to compensating defects was also observed in these n-type films.

Invited lecture

HVPE as A New Tool for Homo-Epitaxial Growth of Highly-Pure and Thick GaN Drift Layers for Power Devices

Hajime Fujikura, Taichiro Konno, Takehiro Yoshida and Fumimasa Horikiri

SCIOCS Co. Ltd., 880 Isagozawa-cho, Hitachi, Japan

Recent advancement in high-quality GaN substrates has made it possible to realize GaN-based vertical power devices with high breakdown voltages by homo-epitaxy. Most of these proto-type devices have been grown using MOCVD. However, there exist several inherent drawbacks in MOCVD-method as an epitaxial growth tool for GaN-based vertical power devices. In order to achieve high voltage blocking capability in power device operation, growth of thick (several 10 μm) n-GaN drift layer with precise carrier concentration control below 10^{16} cm^{-3} is required. However, presence of residual carbon in the MOCVD-grown crystal ($>=10^{16}$ cm^{-3}) makes it difficult to grow such a highly pure n-GaN drift layer. Its slow growth rate around several μm/h will also become obstacle to cost-effective fabrication of vertical GaN power devices.

Both of the above drawbacks can be overcome by using HVPE instead of MOCVD because of the use of carbon-free raw materials (Ga metal and NH$_3$) and its extremely high growth rate over 100 μm/h. However, almost no effort has been made to apply HVPE to the growth of GaN-based vertical power devices up to date, probably because of widely held beliefs on HVPE method, such as a high background donor concentrations (Si and O, instead of C) and difficulties in achieving smooth as-grown surface and uniform thickness.

In this talk, we will show a new possibility of HVPE-method as a tool for homo-epitaxial growth of highly-pure and thick GaN drift layers for power devices. An appropriate gas-flow design of our HVPE system enabled us to grow GaN layers with smooth as-grown surfaces with excellent thickness uniformity. Additionally, surface instability due to macrostep formation often observed for GaN homo-epitaxy even by MOCVD was found to be suppressed easily in HVPE after growth optimization (**Fig.1**). Removal of quartz parts from the HVPE system markedly reduced the concentration of residual impurities (Si, O, C and so on) to below the limits of detection by SIMS analysis. Slight Si doping to this high-purity layer enabled us to control carrier concentration over a wide range down to 1×10^{15} cm^{-3} (**Fig.2**) with a maximum mobility of 1150 cm^2/V·s. Amounts of residual deep levels in the lightly Si-doped layers were estimated to be in the 10^{14} cm^{-3} range or less by C-V, Hall-effect, SIMS, and PL measurements.
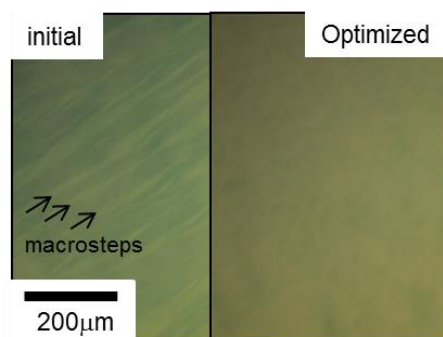
Fig.1 Optical microscope images of homo-epitaxial GaN layers (t=30μm) grown by HVPE with different conditions.
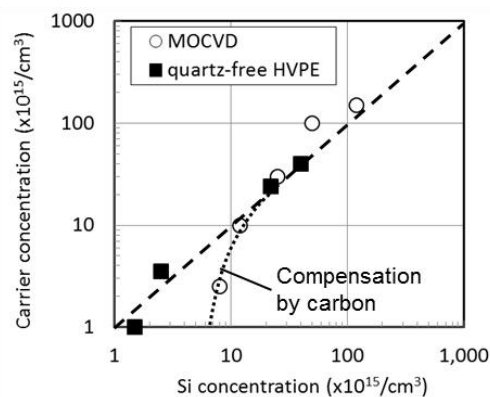
Fig.2 Relationships between carrier and Si concentrations for Si-doped GaN layers grown by the quartz-free HVPE and conventional MOCVD.

HVPE growth of bulk GaN, progress and chanllenging

Ke Xu[1,2]

[1]Suzhou Institute of Nano-tech and Nano-bionics, Chinese Academy of Sciences
[2]Suzhou Nanowin Science and Technology Co., Ltd.
Ruoshui Road 398, Suzhou Industry Park, Suzhou 215123, P. R. China

Growth technologies of bulk GaN substrate have been developed very fast, including Hydride Vapor Phase Epitaxial Growth (HVPE), Ammonothermal method, Na-flux method, due to its rapidly increased demands in fabrication of laser diodes, power electronic devices [1]. More than 6 inch GaN substrate grown by HVPE was also reported. However, the challenges in fabricating high-quality and low-cost bulk GaN substrate still exist, such as dislocation density reduction, n-type doping, semi-insulating substrate, bowing control, and surface preparation, etc. In this work, the recent progress in bulk GaN substrate growth by HVPE in our group are reported, including 4~6-inch bulk GaN growth, doping with Si, Ge and Fe. The bulk GaN by HVPE has dislocation density in 105cm-2 order, and background electron concentration in the order of 1016cm-3, and electron mobility of around 1300V·s/cm2. Finally, we summarized the latest device progress on GaN substrate, including LED, laser diode, high electron mobility transistors, and other electron devices. We believe homoepitaxial growth technology will boost the next rapid growth of nitride semiconductor industry.

[1]. Xu Ke, Wang Jianfeng and Ren Guoqiang, Progress in bulk GaN growth, Chinese Phys. B, Vol.24, pp6, 2015

[2]. M Bockowski, M Iwinska, M Amilusik, M Fijalkowski, B Lucznik and T Sochack, Challenges and future perspectives in HVPE GaN growth on ammonothermal GaN seeds, Semicond. Sci. Tech. 31(2016), 093002

Invited lecture

Recent progress in HVPE-GaN growth on ammonothermally grown GaN seeds

T. Sochacki, M. Amilusik, M. Fijalkowski, B. Lucznik, M. Iwinska, S. Sakowski, J.L. Weyher, I. Grzegory, and M. Bockowski

Institute of High Pressure Physics PAS, Sokolowska 29/37, 01-142, Warsaw, Poland

It was shown that the ammonothermally grown GaN crystals (Am-GaN) can be successfully used as seeds for the Hydride Vapor Phase Epitaxy (HVPE). Crack-free and up to 2-mm-thick HVPE-GaN layers were obtained. Free-standing (F-S) HVPE-GaN crystals sliced from Am-GaN seeds show high structural as well as optical, electrical, and thermal qualities [1].

Since the structural properties of the F-S HVPE-GaN crystals are not different from the excellent structural properties of the Am-GaN seeds, F-S HVPE-GaN can be successfully used as a seed for further HVPE-GaN growth. It is feasible to multiply the ammonothermally grown GaN by the HVPE technology. The F-S HVPE-GaN crystals can also be used as seeds for the ammonothermal growth [2].

In this paper the state of the art of HVPE-GaN growth on Am-GaN seeds will be demonstrated. Bulk growth (up to 2 mm) and growth of thin (up to 100 μm) unintentionally doped GaN layers will be analyzed. Particular attention will be paid to strain generation in the new-grown material. It will be shown that strain appears due to the lattice mismatch between the Am-GaN seed and the HVPE-GaN layer. Additional strain derives from HVPE-GaN wings crystallized on the edges of the HVPE-GaN grown in the c direction. The wings grow in non-polar and semi-polar directions. Due to a difference in free carrier concentration, the lattice constants of the wings are much larger than the lattice constants of the HVPE-GaN layer. Possibilities of avoiding the influence of lateral growth and ways to minimize its impact will be presented.

New directions and strategies in the development of the HVPE-GaN growth will be discussed. Today, the main goal is to develop a method for uniform doping by donors and acceptors without any co-doping effect. Due to the high purity of the HVPE-GaN, the free carriers can be easily compensated at a very low level of doping. Thus, high-quality and highly resistive HVPE-GaN can be obtained. On the other hand, high-quality HVPE-GaN with the free electron concentration of the order of 5×10^{18} cm^{-3} is also crystallized.

[1] T. Sochacki et al. Appl. Phys. Expr. 6, 075504 (2013)
[2] R. Kucharski et al. JCG 427 (2015) 1–6

HVPE Growth of Free-Standing GaN Wafers

Troy J. Baker, Xiaoju Luo, Yu Xie, and Zecheng Wu

Eta Research Ltd., Shanghai, China

HVPE can be used to grow free-standing GaN wafers, which are usually grown on and separated from sapphire substrates, but there are many challenges to developing an entire production process. These challenges include separation of the GaN wafer from the substrate, overcoming cracking and pit formation in the GaN wafer, and reducing the dislocation density and curvature of the GaN wafer. Some examples of HVPE methods used to produce free-standing wafers include TiN nano-masking[1], PEC etched GaN nanowires[2], GaAs substrates with a SiO_2 patterned mask[3], and millimeter thick boule growth[4].

Eta Research has self-developed HVPE equipment and processes to achieve free-standing GaN wafers. In Fig. 1, a complete free-standing 4" GaN wafer is shown. The wafer is crack-free, has a low density of pits, XRD 002 and 102 rocking curve FWHMs below 100 arcsec, and lattice curvature radius larger than 10 m. After the HVPE growth, the wafer must be shaped on the edges and polished. Due to the undesirable edge effects, a 4" substrate can be used to produce a finished GaN wafer cut down to 3" or 2" diameter.

This paper will review the characteristics of free-standing GaN wafers grown using a unique HVPE method including XRD rocking curves, wafer curvature, cracking, and pit density. The effects of the HVPE process will be discussed. Data will be shown for as-grown GaN wafers compared to cut and polished GaN wafers.
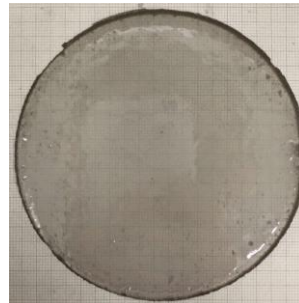
Fig. 1. Free-standing GaN wafer grown using Eta Research's HVPE method.

[1] Y. Oshima, T. Eri, M. Shibata, H. Sunakawa, K. Kobayahi, T. Ichihashi, and A. Usui, *J. Appl. Phys.* **42**, L1 (2003).
[2] K. Xu, J. F. Wang, and G. Q. Ren, *Chin. Phys. B* **24**, 066105 (2015).
[3] K. Motoki, T. Okahisa, N. Matsumoto, M. Matsushima, H. Kimura, H. Kasai, K. Takemoto, K. Uematsu, T. Hirano, M. Nakayama, S. Nakahata, M. Ueno, D. Hara, Y. Kumagai, A. Koukitu, and H. Seki, *Jpn. J. Appl. Phys.* **40**, L140 (2001).
[4] K. Fujito, S. Kubo, H. Nagaoka, T. Mochizuki, H. Namita, and S. Nagao, *J. Cyrstal Growth* **311**, 3011 (2009).

Study of Low Cost Growth of Large Size Bulk GaN Crystal Growth by a New Vertical HVPE Reactor with Showerhead Nozzle

Qiang Liu[1], Naoki Fujimoto[2], Shugo Nitta[2], Yoshio Honda[2], Hiroshi Amano[2,3,4]

[1]*Deptment of Electrical Engineering, Nagoya University, Furo-cho, Chikusa-ku, Nagoya, Japan*
[2]*Institute of Materials and Systems for Sustainability, Nagoya University, Furo-cho, Chikusa-ku, Nagoya, Japan*
[3]*Akasaki Research Center, Nagoya University, Furo-cho, Chikusa-ku, Nagoya, Japan*
[4]*Venture Business Laboratory, Nagoya University, Furo-cho, Chikusa-ku, Nagoya, Japan*

GaN is a promising material which can mostly reduce the electric power conversion loss and help to achieve energy-saving society. It is important to make large size, high quality free-standing GaN wafers. Hydride Vapor Phase Epitaxy (HVPE) has the potential to achieve massive industrialization. To achieve large size, thick GaN crystal with low cost, it is important to realize long-time continuous growth with crystal thickness uniformity and high Ga utilization rate. We developed a new facedown vertical HVPE reactor to approach these goals. In our reactor, an optimized showerhead nozzle configuration, barrier gas lines and independently controlled inner/outer gas system were employed. In this research, we were trying to improve Ga utilization rate by analyzing the relationship between the flow and growth rate with both experiment and simulation.

The showerhead nozzle configuration of the reactor is shown in Fig.1. The nozzles on showerhead are separated into inner (inside dash line circle zone) and outer (outside dash line zone) two zones for both GaCl line and NH_3 line, and the flow of each line can be controlled independently. The typical growth condition is at growth temperature of 1058 °C, pressure of 1 atm, V/III ratio of 20, and growth time of 1 hour. Figure 2 shows the crystal thickness distribution along radius from center to edge grown with typical condition but with different flow on each line. This result demonstrated that the growth rate is mainly determined by the GaCl supply rate. The flow in the reactor is further analyzed by the aid of HVPE reactor simulator (Virtual Reactor of STR Group, Inc.). The simulation result demonstrated that the GaCl concentration near wafer surface determine the growth rate. And it is also indicated by the simulation that by decreasing distance between showerhead and wafer, developing design of showerhead nozzle configuration, and optimizing inner/outer flow balance can further improve the Ga utilization rate.
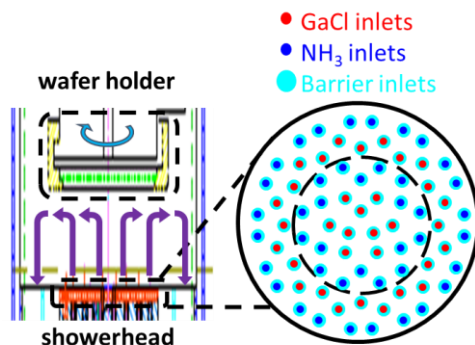
Fig.1 Schematic of the new vertical reactor with showerhead nozzle
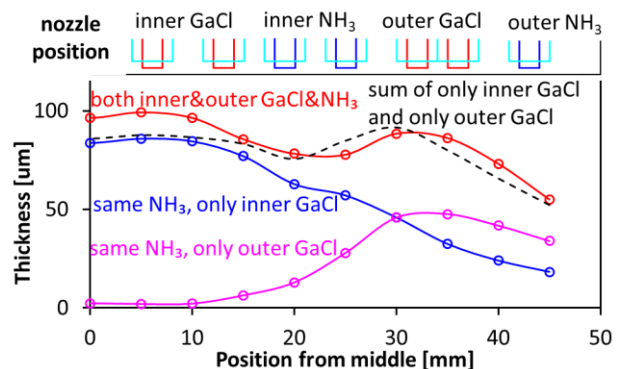
Fig.2 Growth rate of 3 experiments with different inner/outer flow

Recent Progress of AlGaN Deep-UV LEDs by Increasing Light-Extraction Efficiency

Hideki Hirayama [1,2]

[1]*RIKEN, 2-1, Hirosawa, Wako, Saitama 351-0198, Japan*
[2]*RIKEN Center for Advanced Photonics (RAP), 2-1, Hirosawa, Wako, Saitama 351-0198, Japan*

AlGaN deep ultraviolet light-emitting diodes (DUV-LEDs) are attracting a great deal of attention, since they have the potential to be used in a wide variety of applications, such as for sterilization, water purification, UV curing, and in the medical and biochemistry fields. As a result of recent developments in AlGaN DUV LEDs, high internal quantum efficiencies (IQE) of more than 60-80% have been achieved by reducing the threading dislocation density (TDD) of the AlN, and/or by the introduction of AlN single crystal wafers. However, the wall-plug efficiency (WPE) of AlGaN DUV-LEDs still remains below 2%. The target for the efficiency of AlGaN DUV-LEDs is to go beyond an efficiency of 20%, which would make them comparable to low-pressure mercury lamps. A significant problem is that the light-extraction efficiency (LEE) is still quite low because of heavy UV absorption through the p-GaN contact-layer. Usual LEE is still below 10%.

In this work, we demonstrate an external quantum efficiency (EQE) of over 20% and WPE over 10% in an AlGaN DUV-LEDs by increasing LEE. In order to increase LEE of DUV LEDs, we introduced a transparent p-AlGaN contact layer, a highly reflective p-type electrode and AlN template buffer fabricated on patterned sapphire substrate (PSS). We used high-Al-content (Al=70%) p-AlGaN contact layers for 270 nm UVC LEDs. The transparency of the p-AlGaN contact layer was more than 97%. As a highly-reflective p-type electrode, we used Rh. By introducing a transparent contact layer and a highly-reflective electrode, EQE was increased by approximately 3 times. We also observed the efficiency increase by about 1.7 times by introducing AlN template fabricated on PSS and by conducting encapsulation with resin. Maximum EQE was 20.3 % for a 275 nm UVC LED measured under room temperature DC current condition. The UV output power with 50 mW current was 44 mW. Recently we also succeeded in reducing an applying voltage and obtained the record WPE of 10.8% from the DUV LED with lens. We also demonstrated the increase of LEE by introducing highly-reflective photonic crystal fabricated on the p-AlGaN transparent contact layer.
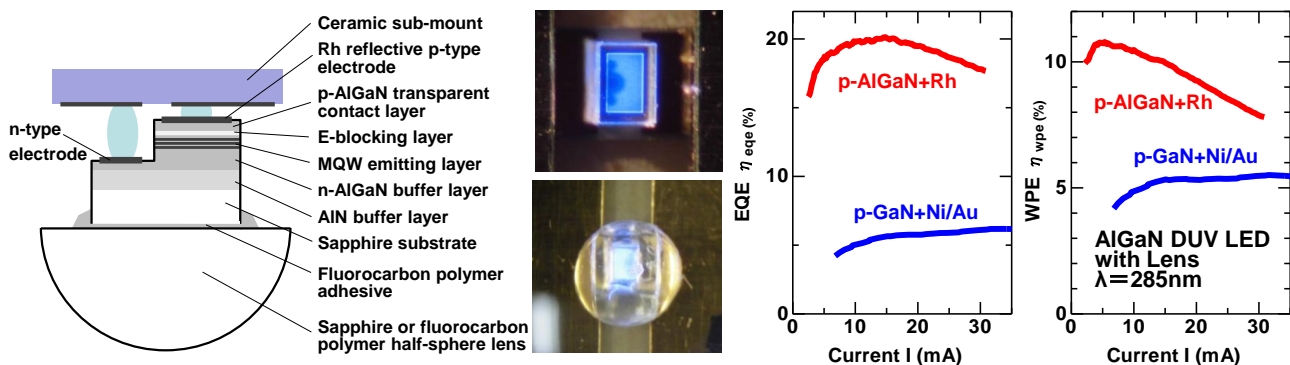
Fig. 1. Structure, photo images, EQE and WPE characteristics of AlGaN DUV LEDs with lens, comparing between transparent p-AlGaN contact layer and p-GaN contact layer. (The LED samples were supplied by DOWA Electronics Materials Co. Ltd.)

Invited lecture

Influence of AlN/sapphire template properties on growth and performance of AlGaN-based UV LEDs

S. Hagedorn [1], **A. Knauer** [1], **T. Kolbe** [1], **S. Walde** [1], **N. Susilo** [2], **C. Kuhn** [2], **D. Jaeger** [3], **M. Kneissl** [2], **and M. Weyers** [1]

[1] *Ferdinand-Braun-Institut, Leibniz-Institut fuer Hoechstfrequenztechnik, Gustav-Kirchhoff-Str. 4, 12489 Berlin, Germany*
[2] *Institute of Solid State Physics, Technische Universitaet Berlin, Hardenbergstr. 36, 10623 Berlin, Germany*
[3] *Evatec AG, Hauptstr. 1a, 9477 Truebbach, Switzerland*

AlGaN-based ultraviolet (UV) light emitting diodes (LEDs) with emission in the UVC and UVB spectral range enable a wide field of applications such as medical diagnostics and phototherapy, gas sensing, UV curing and water disinfection. Unfortunately, the external quantum efficiencies (EQE) of such LEDs are relatively low. To enhance the EQE AlN base layers are required that allow for growth of uniform and low defect density LED heterostructures. Up to now low defect density bulk AlN substrates are only available with small diameters ($< 2"$) and are still fairly expensive. Therefore, considerable efforts have been made to grow several micrometer thick AlN base layers by metalorganic vapor phase epitaxy (MOVPE) on c-plane sapphire substrates. Unfortunately, this approach leads to high densities of threading dislocations (TDD) and thus non-radiative recombination centers in the active region of LEDs. Consequently, the TDD in AlN has to be reduced. This is usually done by dislocation annihilation with increasing AlN layer thickness, facing the challenge of strain relief without cracking while providing a smooth AlN surface. Typical TDDs that can be reached with our MOVPE processes are plotted against AlN layer thickness in Fig. 1. By costly photolithographic surface patterning, etching and subsequent epitaxial lateral overgrowth (ELO), increased layer thicknesses and TDDs as low as 10^9 cm^{-2} can be reached.

To obtain favorable material quality already at lower AlN layer thickness, we also applied the method of high-temperature annealing (HTA) at about 1700°C to MOVPE grown and sputtered AlN/sapphire following the method of Miyake et al. [1, 2]. To monitor the AlN template and LED heterostructure growth process, in-situ measurements of wafer curvature and 405 nm light reflectivity were carried out. In this paper we will show how AlN/sapphire template properties influence the heterostructure growth, e.g., by changing the strain state due to dislocation climbing and by varying in-plane lattice constant of AlN base layers. Also the impact of patterned AlN/sapphire interfaces on the light extraction and hence on the EQE will be taken into consideration.

Fig. 1: TDD against layer thickness for MOVPE grown AlN on sapphire with and without ELO process. Value reached by HTA of AlN/sapphire and subsequent MOVPE overgrowth (red box).

[1] H. Miyake, G. Nishio, S. Suzuki, K. Hiramatsu, H. Fukuyama, J. Kaur, and N. Kuwano, *Appl. Phys. Express* **9**, 025501 (2016).
[2] N. Susilo, S. Hagedorn, D. Jaeger, H. Miyake, U. Zeimer, C. Reich, B. Neuschulz, L. Sulmoni, M. Guttmann, F. Mehnke, C. Kuhn, T. Wernicke, M. Weyers, and M. Kneissl, *Appl. Phys. Lett.* **112**, 041110 (2018).

Invited lecture

375-nm Optically Pumped Vertical-Cavity Surface-Emitting Lasers with Air-Gap/Al$_{0.05}$Ga$_{0.95}$N Distributed Bragg Reflectors

Young Jae Park[1], Theeradetch Detchprohm[1], Karan Mehta[1], Jialin Wang[1], Hoon Jeong[1], Yuh-Shiuan Liu[1], Shuo Wang[2], Shyh-Chiang Shen[1], P. Douglas Yoder[1], Fernando Ponce[2] and Russell D. Dupuis[1]

[1] *Center for Compound Semiconductors and School of Electrical and Computer Engineering, Georgia Institute of Technology, Atlanta, GA 30332 USA*
[2] *Department of Physics and Astronomy, Arizona State University, Tempe AZ 85287 USA*

Nitride-based vertical-cavity surface-emitting lasers (VCSELs) at wavelengths λ<400 nm have attracted enormous interest over the past few years as they have the advantages of lower threshold current, circular and low-divergent beam, high efficiency during operation, arraying capability, low temperature sensitivity and low production cost. UV VCSELs can be used in many applications for optical sources such as optical storage, decontamination, optically pumped solid-state lasers and compact chip-scale atomic clocks. In this report, we describe our recent work on GaN-based UV VCSELs lasing at ~370 nm. In this work, optically pumped VCSELs with a 1λ thick optical cavity lasing at 375 nm have been demonstrated from Al$_x$Ga$_{1-x}$N based multi-quantum-well structures using a pulsed excimer laser source. To realize a high-reflectivity mirror on the bottom of the cavity, air-gap/Al$_{0.05}$Ga$_{0.95}$N DBRs with a large refractive index contrast have been employed. The AlGaN-GaN VCSEL epitaxial structures in this work are grown on (0001) sapphire by metalorganic chemical vapor deposition (MOCVD) in an AIXTRON CCS 3x2 high-temperature reactor. A semiconductor-based distributed Bragg reflector (DBR) composed of five periods of air-gap/Al$_{0.05}$Ga$_{0.95}$N was introduced as the bottom mirror while the top mirror was an e-beam-deposited dielectric DBR consisting of ten pairs of λ/4 HfO$_2$/SiO$_2$. The bottom DBR structure consisted of five periods of 277 nm n^+Al$_{0.05}$Ga$_{0.95}$N (n = 2E+19 cm^{-3}, sacrificial layer)/103.6 nm Al$_{0.05}$Ga$_{0.95}$N (unintentionally doped) grown on a 3 μm thick GaN template. Following that, an Al$_{0.10}$Ga$_{0.90}$N spacer layer, an MQW active region of five-pairs of InGaN quantum well and AlGaN quantum barrier, and a thin Al$_{0.1}$Ga$_{0.9}$N cap layer were grown. The etching channel was formed using optical lithography process followed by deep plasma dry etching. Subsequently, the n^+Al$_{0.05}$Ga$_{0.95}$N layers were transformed into air-gap layers through a conductivity-selective electrochemical etching process. The fabricated VCSEL structures were optically pumped at 300K under pulsed conditions using a 248nm KrF excimer laser. The lowest threshold incident power density measured at a room temperature was estimated to be ~270 kW/cm^2. The achieved optically pumped VCSEL demonstrates the possibility that the airgap/Al$_x$Ga$_{1-x}$N DBRs can be used as a mirror for injection laser devices. More details about the growth process, DBR fabrication and optical characterization will be presented.

Figure 1: Vertical-cavity laser emission spectra with the optical excitation pump power densities below and above threshold at room temperature

Growth of InAlGaN for efficient UVB light emitting diodes

J. Enslin [1], T. Teke [1], G. Kusch [3], L. Spasevski [3], C. Reich [1], B. Neuschulz [1], P. R. Edwards [3], T. Wernicke [1], R. W. Martin [3] and M. Kneissl [1,2]

[1] *Technische Universität Berlin, Institut für Festkörperphysik, Hardenbergstr. 36, 10623 Berlin, Germany*
[2] *Ferdinand-Braun-Institut, Leibniz-Institut für Höchstfrequenztechnik, Gustav-Kirchhoff-Straße 4, 12489 Berlin, Germany*
3 *Department of Physics, SUPA, University of Strathclyde, 107 Rottenrow East, Glasgow G40NG, United Kingdom*

Although AlGaN-based light emitting diodes emitting in the UVB spectral region between 280 nm and 320 nm can be used for a variety of applications such as plant growth lighting and the treatment of psoriasis, they still suffer from relatively poor external quantum efficiencies (EQE) [1]. One way to improve the EQE of these devices is to increase the radiative recombination efficiency within the active region. In recent years the effect of localized indium in quaternary $In_xAl_yGa_{1-x-y}N$ layers has been used to increase the recombination efficiency [2, 3]. However, detailed studies of the impact of indium incorporation and of the influence of the In-content on the internal quantum efficiency, polarization fields and carrier localization are still missing. In order to investigate the indium incorporation and indium localization, we examined the MOVPE growth of 130 nm thick InAlGaN layers on top of (0001) $Al_{0.5}Ga_{0.5}N$/AlN/sapphire pseudo-substrates with the goal of realizing UVB-LEDs with $In_xAl_yGa_{1-x-y}N$ quantum wells emitting near 310 nm. Growth studies involving variations of the temperature of the InAlGaN growth between 790°C and 930°C, the In-flux and the Al-flux were carried out. The composition of the InAlGaN layers was determined by wavelength dispersive X-ray spectroscopy, as well as the strain state by X-ray diffraction. It was found that the maximal In-incorporation of 14% could be achieved at a growth temperature of 790°C. The morphology of these layers was investigated by atomic force microscopy (AFM). As shown in Fig. 1, the surface deteriorates with decreasing temperature, due to not optimal temperature regime for AlGaN growth and partial relaxation of the layers.
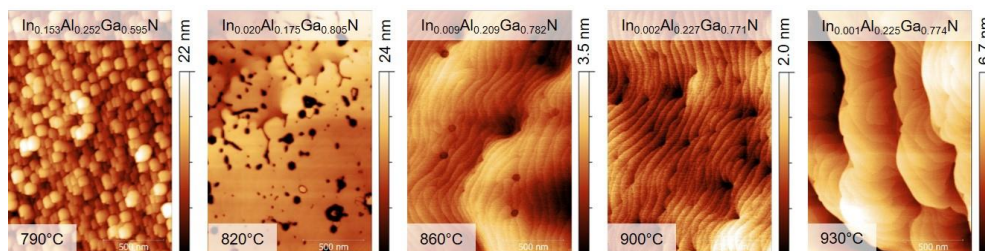
Figure 1: AFM images showing the surface morphology of 130 nm InAlGaN grown on an $Al_{0.5}Ga_{0.5}N$ pseudo-substrate at temperatures from 790°C to 930°C.

An investigation of the optical properties of InAlGaN layers by photoluminescence, cathodoluminescence and transmission spectroscopy indicates localization and a strong shift of the band edge even for low In-containing layers. In a next step, we will apply these findings to realize InAlGaN quantum well LEDs emitting in the UVB spectral region with increased radiative recombination efficiencies.

[1] M. Kneissl and J. Rass, III-Nitride Ultraviolet Emitters: Technology and Applications, Vol. 227 Springer, 2015
[2] H. Hirayama et al., Journal of Applied Physics **97**, 091101 (2005)
[3] S.F. Chichibu et al., Nature Materials **5**, 810 (2006)

Three Dimensional Simulation on the Transport and Quantum Efficiency of UVC-LEDs with Random Alloy Fluctuations

Hung-Hsiang Chen [1], Yuh-Renn Wu [1,2, *]

[1]*Graduate Institute of Photonics and Optoelectronics, National Taiwan University, Taipei, Taiwan, 10617*
[2] *Industrial Technology Research Institute, Hsinchu, Taiwan.*
[*]*yrwu@ntu.edu.tw*

As we know, random alloy fluctuations in nitride based Multiple Quantum Wells (MQWs) plays very important role in carrier transport and radiative efficiency in blue LEDs[1]. Moreover, for UVC-LEDs, besides the QWs, the EBL, QBs and n-type AlGaN injection layers are all random alloys. This makes carrier injection and confinement more complicated and could affect the UVC-LEDs device performance even more significantly. In this paper, we applied our 3D simulation programs [1] to model UVC-LEDs at 280 nm wavelength and 3D random alloy fluctuations are considered in all alloy layers. The devices structures are based on a common UVC-LEDs with a n-type AlGaN buffer layer, 5 pairs of MQW/QBs, 70% p-AlGaN EBL and a gradual p-type AlGaN injection layer with composition from 65% to 0%. The p-GaN layer is used for a better injection, where the light extraction might be poor. As shown in Figures, due to the potential fluctuation at the n-AlGaN buffer layer, QWs and QBs, the electron currents are percolating through the minimum potential before injecting into the QWs. The same behavior is observed for holes. By comparing with the case without considering random alloy fluctuation, the turn-on voltage is 0.2V smaller, which is expected due to more local percolation path. The fluctuation potential provides some routes with lower energy for hole to climb over high barrier given from electron blocking layer (EBL) and get into multi-quantum wells(MQWs) region. Due to the random alloy fluctuation, several behaviors are observed. (1) The IQE peak is larger due to carrier localization. (2) The droop is mainly due to poor hole injection and the droop is stronger due to weaker blocking ability of EBL caused by the fluctuated potential. (3) A gradual layer could help carrier injection, rising the hole density in MQWs, and suppress carrier overflow to an acceptable range[2]. (4) The carriers are not well confined in the QW but more extended into the QB due to potential fluctuation. As we know, holes in the QB with high Al compositions are mainly |Z>-state dominated. When the extended hole wave function penetrating into QB, it might lead to a strong TM emission, where the light extraction might be even more poor. Therefore, a thin and high Al confining layer on top of QW might be needed for a better hole confinement. This work was supported by MOST in Taiwan (105-2221-E-002 -098 -MY3)
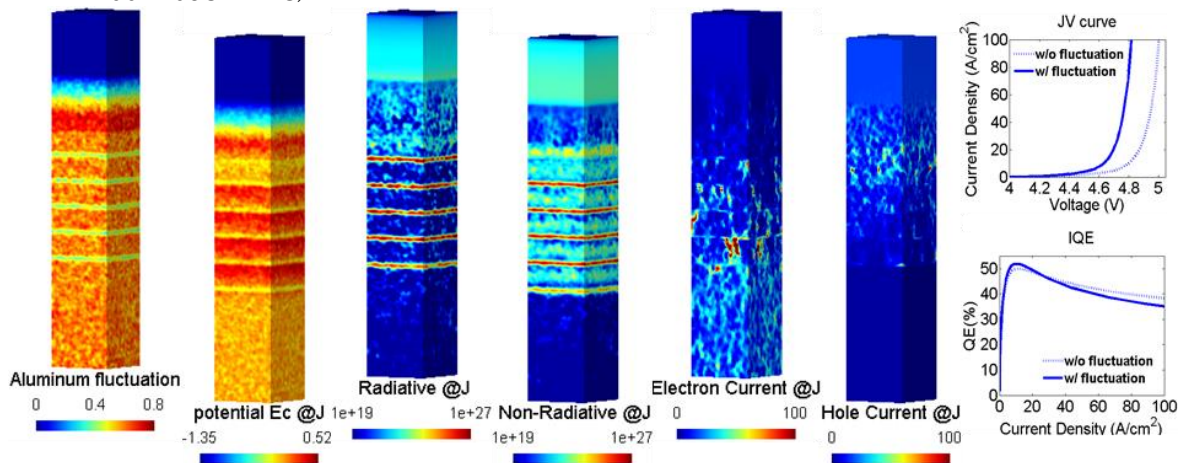
Fig. 1 Results for UVC-LED with alloy fluctuation model @J=(4.7V,20A/cm^2)

[1] M. Filoche, M. Piccardo, Y.-R. Wu, C.-K. Li, C. Weisbuch, S. Mayboroda, Phys. Rev. B 95, 144204-144206 (2017)
[2] H. Hirayama, N. Noguchi, S. Fujikawa, J. Norimatsu, T. Takano, K. Tsubaki, N. Kamata, Phys. Status Solidi A 206, 1176 (2009)

Invited lecture

Thermodynamics on HVPE of Group-III Nitrides

Yoshinao Kumagai [1,2]

[1] *Department of Applied Chemistry, Tokyo University of Agriculture and Technology, Koganei, Tokyo, Japan*
[2] *Institute of Global Innovation Research, Tokyo University of Agriculture and Technology, Koganei, Tokyo, Japan*

High speed and high temperature growth of quasi-bulk GaN by hydride vapor phase epitaxy has attracted much attention. High-purity GaN growth has also been investigated. In this study, thermodynamic analysis of GaN growth by halide vapor phase epitaxy (HVPE) using GaCl and tri-halide vapor phase epitaxy (THVPE) using $GaCl_3$ with increased number of related gaseous species is presented to explain growth behavior at high temperatures. Unintentional Si donor incorporation by the reduction of quartz glass reactor walls by H_2 is also presented.

Fig. 1 shows driving force of GaN deposition (ΔP_{Ga}) as a function of growth temperature calculated for different values of hydrogen mole fraction in the carrier gas (F°). Growth conditions of total pressure (ΣP_i) at 1.0 atm, input partial pressure of GaCl (P°_{GaCl}) or $GaCl_3$ (P°_{GaCl3}) of 1.0×10^{-3} atm, an input V/III ratio of 20, and the mole fraction of decomposed NH_3 (α) of 0.03 were selected. HVPE and THVPE with F° of 0.0 show nearly equal positive ΔP_{Ga}'s at high temperatures. On the other hand, HVPE with F° of 1.0 shows positive ΔP_{Ga} only below 1000°C, while ΔP_{Ga} becomes negative above 1000°C due to increase of equilibrium partial pressure of Ga. Therefore, growth is expected below 1000°C. In THVPE with F° of 1.0, positive ΔP_{Ga} cannot be obtained. Therefore, small values of F° are essential for GaN growth at high temperatures by HVPE and THVPE.

Fig. 2 shows equilibrium partial pressures of gaseous species over quartz glass reactor walls at 1100°C as a function of F°. H_2O, SiO and SiH_4 are generated when a small amount of H_2 is incorporated in the carrier gas. For example, at F° of 0.2, equilibrium partial pressure SiO reaches 2.3×10^{-6} atm, which is enough for unintentional Si doping of GaN. Therefore, growth zone free of quartz glass is needed to grow high-purity GaN by HVPE and THVPE.

GaN HVPE and THVPE
ΣP_i: 1.0 atm, P°_{GaCl} or $P^\circ_{GaCl_3}$: 1.0×10^{-3} atm, V/III: 20, α: 0.03
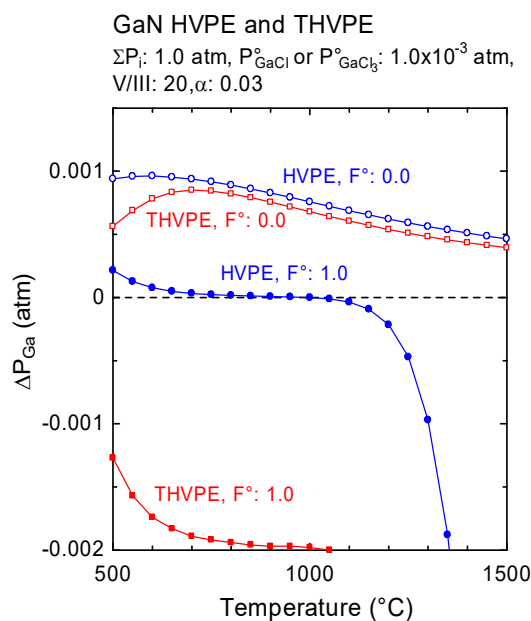
Fig. 1. Comparison of the driving force for GaN deposition by HVPE and THVPE under inert carrier gas ($F^\circ = 0.0$) and H_2 carrier gas ($F^\circ = 1.0$) conditions.

ΣP_i: 1.0 atm, Temp.: 1100°C
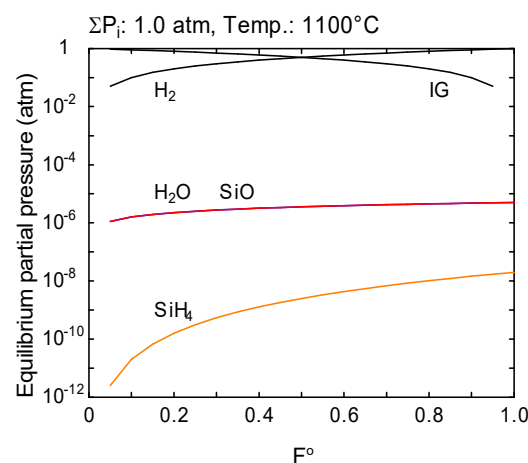
Fig. 2. Equilibrium partial pressures of gaseous species over quartz glass reactor walls at 1100°C as a function of hydrogen mole fraction in the carrier gas (F°).

Defect and stress engineering in GaN layers grown by high temperature vapor phase epitaxy

T. Schneider [1], **M. Förste** [1], **G. Lukin** [1], **M. Barchuk** [2], **C. Röder** [3], **C. Schimpf** [2], **E. Niederschlag** [1], **F. C. Beyer** [4], **O. Pätzold** [1], **D. Rafaja** [2], **and M. Stelter** [1]

[1] *Institute for Nonferrous Metallurgy and Purest Materials TU Bergakademie Freiberg, Leipziger Straße 34, 09599 Freiberg, Germany*
[2] *Institute of Materials Science, TU Bergakademie Freiberg, Gustav-Zeuner-Straße 5, 09599 Freiberg, Germany*
[3] *Institute of Theoretical Physics, TU Bergakademie Freiberg, Leipziger Straße 23, 09599 Freiberg, Germany*
[4] *Institute of Applied Physics, TU Bergakademie Freiberg, Leipziger Straße 23, 09599 Freiberg, Germany*

The high temperature vapor phase epitaxy (HTVPE) for the growth of GaN uses thermally evaporated, elemental gallium and ammonia as precursors. First 2D HTVPE GaN layers on sapphire substrates, so called HTVPE GaN templates, were presented in [1]. They were produced in a multi-step growth process, which consisted of the deposition of 3D nucleation islands to compensate the lattice mismatch between GaN and sapphire, and a subsequent coalescence of the islands followed by lateral overgrowth to form a closed 2D surface layer. The dislocation density and the stress level of the surface layer are known to depend mainly on the coalescence sub-process [2]. This approach can be used for a defect and stress engineering by a controlled coalescence of the nucleation layer.

In this contribution, the influence of a delayed coalescence of the nucleation layer on the dislocation density and the residual stress of HTVPE GaN templates is investigated. A controlled delay of the coalescence was achieved by decreasing the V/III ratio and increasing the H_2 flow in the total carrier gas flow of 3.0 slm. Fig. 1 shows nucleation layers deposited under different coalescence conditions. The morphology of the layers depends strongly on the degree of delay, which increases from coalescence process A (Fig. 1a) to process C (Fig. 1c). With increasing delay, the nucleation islands become larger and more facetted. The residual stress and the threading dislocation density of the related GaN templates were determined by confocal Raman spectroscopy and HRXRD, respectively. The layers are compressively stressed in the range of -1.03 GPa and -0.83 GPa, whereas the dislocation densities are found to be $8.1 \cdot 10^8$ cm^{-2} (process A), $5.8 \cdot 10^8$ cm^{-2} (process B), and $3.2 \cdot 10^8$ cm^{-2} (process C). The changes of the stress levels and the reduction of the dislocation densities are discussed.
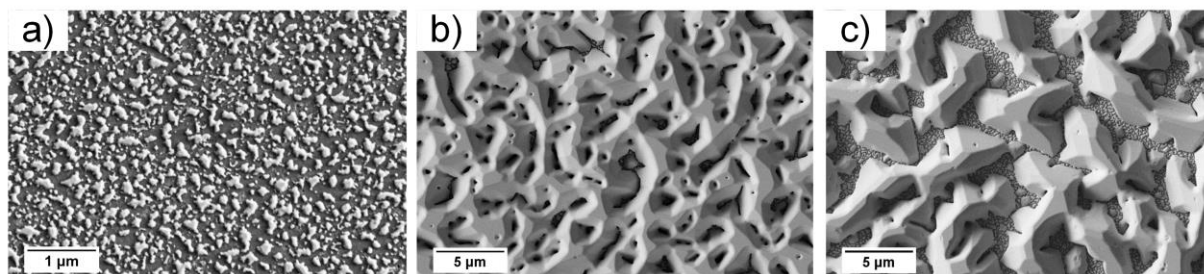
Fig. 1*: SEM images of the nucleation layers for the lateral overgrowth process, which were grown at a substrate temperature of 1100°C. 3D GaN nucleation islands grown a) by process A with a NH₃ flow of 0.2 slm and a H₂ flow of 0.6 slm, b) by process B with a NH₃ flow of 0.03 slm and a H₂ flow of 0.6 slm, and c) by process C with a NH₃ flow 0f 0.03 slm and a H₂ flow of 1.37 slm.*

[1] T. Schneider et al., *J. Cryst. Growth* **468**, 212 – 215 (2017).
[2] T. Böttcher et al., *Appl. Phys. Lett.* **78**, 1976 – 1978 (2001).

Excess Chlorine and Growth Temperature Effects of N-Polar GaN Growth via Tri-halide Vapor Phase Epitaxy and its Theoretical Study

Nao Takekawa[1]*, **Daisuke Oozeki**[1], **Akira Yamaguchi**[2],
Hisashi Murakami[1], **Yoshinao Kumagai**[1], **Koh Matsumoto**[2], **Akinori Koukitu**[1],

[1] *Department of Applied Chemistry, Tokyo University of Agriculture & Technology, Koganei, Tokyo 184-8588, Japan*
[2] *TAIYO NIPPON SANSO Corporation, 10 Ohkubo, Tsukuba, 300-2611 Japan*

GaN is widely used as a substrate for high-power white-light-emitting diodes and blue or green laser diodes, and applications to high-electron-mobility transistors and vertical power devices have also been extensively studied. In order to enable the widespread use of nitride-based devices, new approaches to reduce the cost of GaN substrates are necessary. Our group has proposed the GaN growth on N-polar surface via tri-halide vapor phase epitaxy (THVPE) using $GaCl_3$ as a group III precursor and demonstrated the diameter of the crystal to expands perpendicular to the growth direction [1]. In addition, THVPE-GaN growth has a surface orientation selectivity [2], which suppress the unintended growth mode in the peripheral edge area; example to wing growth mode in HVPE method, thus stress-free long-term growth of GaN is possible. In the HVPE method, it has demonstrated that additional HCl was effective for the control of growth rate [3]. In the THVPE method, Cl_2 is used instead of HCl for generating gallium precursor, and it is worth investigating the influence of additional Cl_2 gas on the growth of GaN via THVPE. In this study, we focused on the effect of free Cl_2 partial pressure and the growth temperature for high-speed and high-crystalline-quality GaN growth and its theoretical investigation.

A horizontal reactor with a resistance heater for the source zone and a RF inductive heating hot wall for the deposition zone was used. The source zone consists of two successive reaction zones, the first to form GaCl by the reaction of metallic-Ga and Cl_2, and the second to generate $GaCl_3$ precursor by the reaction of GaCl and Cl_2. At the second, stoichiometrically excessive Cl_2 was introduced to supply additional Cl_2 (called excess Cl_2 hereafter) to the growth zone. NH_3 was separately introduced and reacted with $GaCl_3$ to grow GaN on the substrate. The substrate used is a freestanding (000-1) GaN. In addition, to evaluate the influence of excess Cl_2 quantitatively, the equilibrium partial pressure of Cl radical was thermodynamically calculated and compared with the experimental results.

Figure 1 shows the dependence of growth rate on the excess Cl_2 ratio to partial pressure of $GaCl_3$ with constant partial pressures of $GaCl_3$ and NH_3; the growth temperature was varied from 1250°C to 1375°C and compering equilibrium partial pressure of Cl radical calculated thermochemically. The growth rate increased with increasing the excess Cl_2 and the required amount of Cl_2 for high growth rate decreased with increasing growth temperature. Calculated values of Cl radicals and experimental growth rate showed a very good correlation, indicating that Cl radicals play an important role in the system of THVPE growth of GaN.

Fig.1 Relation between the growth rate (square plots) and calculated value of the equilibrium partial pressure of Cl radical (solid line).

[1] H. Murakami J. Cryst. Growth. 456 (2016) 140.
[2] K. Iso Appl. Phys. Express 9 (2016) 105501.
[3] A. Trassoudaine Mat. Res. Soc. Symp. Proc. 639 (2001).

Carbon-doped GaN: Identification of tri-carbon defects formed at substantial fraction

I. Gamov[1], E. Nowak[1,2], G. Gärtner[3], F. Zimmermann[4], F. C. Beyer[4], E. Richter[5], M. Weyers[5], and K. Irmscher[1]

[1] *Leibniz-Institut für Kristallzüchtung, Max-Born-Strasse 2, 12489 Berlin, Germany*
[2] *Faculty of Technical Physics, Politechnika Poznanska, Piotrowo 3, 60-965 Poznan, Poland*
[3] *Institute of Experimental Physics, TU Bergakademie Freiberg, 09599 Freiberg, Germany*
[4] *Institute of Applied Physics, TU Bergakademie Freiberg, 09599 Freiberg, Germany*
[5] *Ferdinand-Braun-Institut, Leibniz-Institut für Höchstfrequenztechnik, Gustav-Kirchhoff-Str. 4, 12489 Berlin, Germany*

Carbon doping is widely used to render GaN crystals semi-insulating. Since in nominally undoped crystals *n*-type conductivity prevails, carbon doping must be accompanied by the formation of compensating acceptors. This is generally explained by the formation of isolated carbon substituting for nitrogen (C_N) as theory predicts C_N acting as acceptor and having the lowest formation energy among the considered carbon related defects (see e.g. [1]). In particular, defect complexes consisting of multiple carbon atoms are assumed to have too high formation energies to attain substantial equilibrium concentrations. Here we present strong evidence, that carbon doping of GaN leads to the formation of tri-carbon defects. Analogue defects were already identified in AlN using ^{13}C isotope doping [2]. In GaN they are more abundant and occur in two crystallographically inequivalent configurations.

For the investigations C-doped GaN layers were grown by hydride vapor phase epitaxy (HVPE) on (0001) sapphire. The samples cut from the self- separated layers have dimensions of about $10\times5\times0.5\text{-}1$ mm^3 and are polished on both sides. The carbon concentration [C] ranges from $< 10^{16}$ cm^{-3} to several 10^{19} cm^{-3} as determined by secondary ion mass spectrometry. The infrared absorption (FTIR) spectra of such samples (Fig. 1(a)) show two prominent local vibrational modes (LVMs) at 1717 cm^{-1} and 1680 cm^{-1} which are clearly correlated with [C]. The polarization dependence of these LVMs, obtained on a cross-sectional sample, is shown in Fig. 1(b). While the LVM at 1717 cm^{-1} follows the behavior of a tri-carbon defect in the *c*-bond configuration, the LVM at 1680 cm^{-1} belongs to the basal plane configuration of this defect as depicted in Fig. 1(c). We will present a detailed discussion of our FTIR measurements supplemented by UV-VIS absorption and photoluminescence results.
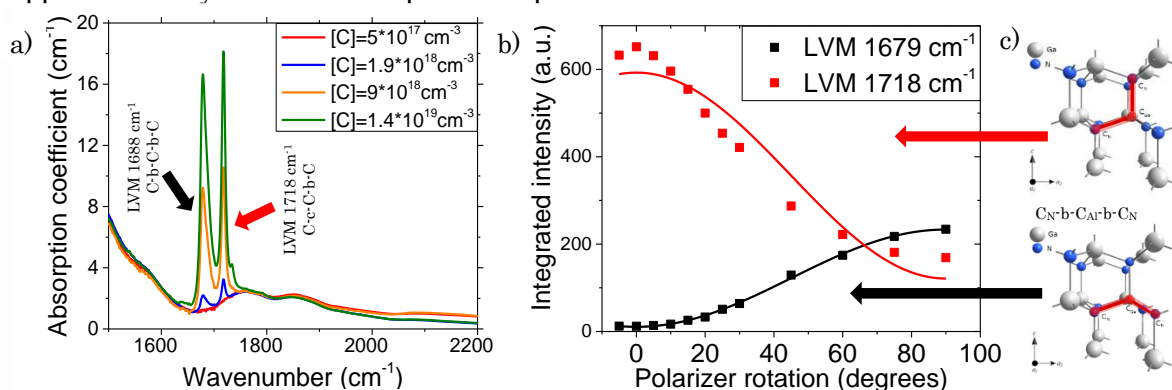
Fig. 1. (a) FTIR of C-related LVMs. (b) LVM polarization dependence. (c) Tri-carbon defect model for the two inequivalent configurations.

[1] J.L. Lyons, A. Janotti, and C.G. Van de Walle, Phys. Rev. B **89**, 35204 (2014).
[2] K. Irmscher et al., J. Appl. Phys. **114**, 123505 (2013).

Photoluminescence of Carbon-doped HVPE GaN layers

F. Zimmermann[1], G. Gärtner[2], K. Irmscher [3], I. Gamov [3], E. Nowak[3],
E. Richter[4], M. Weyers[4], J. Heitmann[1], and F. C. Beyer[1]

[1]*Institute of Applied Physics, TU Bergakademie Freiberg, Leipziger Straße 23, D-09599 Freiberg, Germany*

[2]*Institute of Experimental Physics, TU Bergakademie Freiberg, Leipziger Straße 23, D-09599 Freiberg, Germany*

[3]*Leibniz-Institut fur Kristallzüchtung, Max-Born-Straße 2, D-12489 Berlin, Germany*

[4]*Ferdinand-Braun-Institut, Gustav-Kirchhoff-Straße 4, D-12489 Berlin, Germany*

C-doped GaN layers grown by hydride vapour phase epitaxy (HVPE) on (0001) sapphire substrates were analysed by photoluminescence (PL) spectroscopy at 15 K. The carbon concentration [C] varied from $< 10^{16}$ cm^{-3} (undoped) to low 10^{19} cm^{-3} as determined by secondary ion mass spectrometry.Self-separated layers are polished on both sides and the sample surfaces were etched to get access to the bulk region since the excitation wavelength of the HeCd laser (325 nm) has a limited penetration depth of only 90 nm.

As reported in literature, different defect bands could be resolved, including a blue luminescence (BL2) [1] and a green luminescence band [2]. During UV excitation BL2 transformed into a yellow band (YL) as earlier reported by [1, 3]. Here, we investigated, the time constants of this reversible transformation in dependence on the carbon doping level and the excitation power. For the highest excitation level an aquamarine band (AL) [4] evolved, see figure 1a, whose origin is still under debate. Additionnally, YL started to decrease again after an initial exponential increase. The evolution of the PL bands was analysed using a double exponential decay in case of BL2 and a single exponential growth for the YL band [3]. τ_2(BL2) and τ(YL) show a clear dependence on the carbon concentration, while τ_1(BL2) stays independent as illustrated in figure 1b. Our results will be compared to discussions from FTIR and absorption measurements.
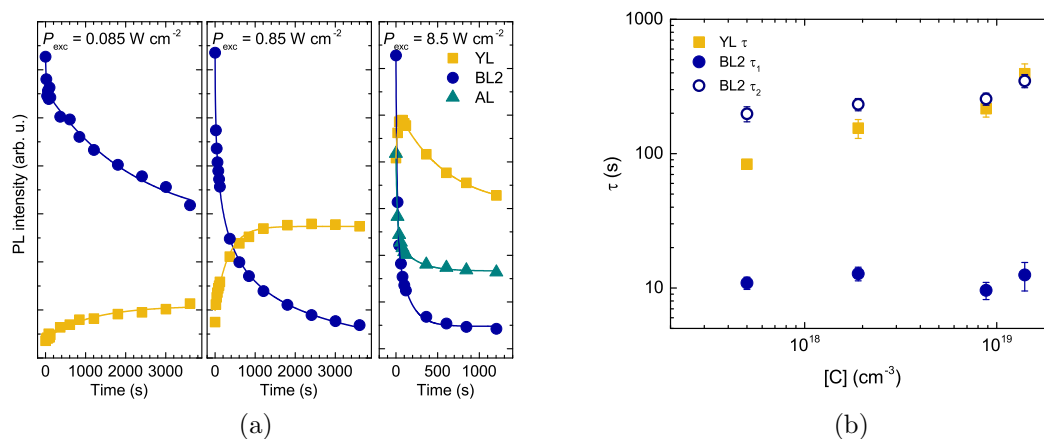
Figure 1: Time evolution of the PL intensity for a C-doped sample (8.8×10^{18} cm^{-3}) at varying excitation powers (a) and time constants depending on the C-doping level (b). BL2 is fitted with double exponential decay, YL with a single exponential growth.

[1] D. O. Demchenko et al., *J. Appl. Phys.* **119**, 035702 (2016).

[2] M. A. Reshchikov et al., *Phys. Rev. B* **90**, 235203 (2014).

[3] S. A. Brown et al., *Nanotechnology* **11**, 263 (2000).

[4] M. A. Reshchikov et al., *Mater. Res. Soc. Symp. Proc.* **831**, E9.8.1 (2005).

Invited lecture

A new method to achieve efficient iron doping of HVPE GaN substrates

J.A. Freitas, Jr. [1], J.C. Culbertson[1], E.R. Glaser[1],
E. Richter[2], M. Weyers[2], A.C. Oliveira[3], V.K. Garg[3]

[1]Naval Research Laboratory, 4555 Overlook Av. SW, Washington, USA 20375
[2]Ferdinand-Braun-Institute, Gustav-Kirchhoff-Str. 4, 12489 Berlin, Germany
[3]Institute of Physics, University of Brasilia, Asa Norte, 70919-970 Brasilia, DF, Brazil

HVPE GaN is intrinsically electrically conductive with room temperature net carrier concentrations typically between ~5×10^{16} to ~5×10^{18} cm^{-3}. This characteristic is convenient for the fabrication of light emitting devices, but it is inadequate for high-power/high-frequency devices application. SI HVPE GaN substrates have been successfully grown by adding C or Fe precursors to introduce compensating deep levels in the GaN bandgap [1,2]. High concentrations of shallow donors require higher concentrations of compensating impurities, which may degrade the intrinsic and structural material properties [3]. A new method to produce Fe-doped HVPE-GaN, with low shallow-donor concentrations, is reported.

A commercial vertical AIXTRON HVPE reactor was employed to deposit GaN films on 2 inch sapphire substrates with thickness of 1 mm. It was desired for spectroscopic investigations that the incorporated Fe ions exhibit nuclear transitions, which is the case for the Fe-57 isotope. The source material was Fe_2O_3 powder highly enriched with the Fe-57 isotope. The oxide was mounted in a small crucible between the group III gas inlet and the substrate holder. Before use, the oxide was reduced to metallic Fe in a hydrogen flow at a temperature of 850°C for one hour. The films were grown at 200 hPa at a growth rate of 400 µm/h; a 200 µm thick un-doped GaN buffer was grown at 990°C; an 800 µm thick Fe-doped GaN layer was subsequently grown at 1010°C. An extra flow of HCl was injected at the iron doping source to form $FeCl_2$ which dilutes in the group III flow. This leads to a constant Ga to Fe ratio across the wafer, i.e. uniform doping. The iron uptake was below the detection limit of SIMS in the UID GaN film. In the Fe-doped layers 4×10^{17} cm^{-3} and 4×10^{18} cm^{-3} Fe (dominantly Fe-57 with less than 5% Fe-56) were measured. Only low levels of C, Si, and O were detected. Full widths at half maximum of X-ray rocking curves for the (0002) and (30-32) reflections were below 90 arcsec and 80 arcsec for UID samples. Higher values were observed for the Fe-doped samples. It has been reported that high concentrations of Fe in GaN result in the formation of Fe-clusters [3]. Mössbauer spectroscopy measurements on the Fe-57 were carried out and only one line was observed in the spectra, which is consistent with the isolated Fe^{3+} paramagnetic ions positioned on Ga sites in the wurtzite structure. Electron paramagnetic resonance measurements confirmed these observations. Thus efficient substitutional Fe doping without indication of other incorporation sites or cluster formation was obtained.

High lateral and depth resolution Raman scattering measurements were carried out on the Ga-polar front face of all samples. The E_2^2 phonon frequency in a typical map yielded 567.45 ± 0.05 cm^{-1} Raman shift indicating stress-free GaN. Analysis of the $A_1(LO)$ phonon frequencies and the linewidths are consistent with low concentrations of free carriers in all samples. Low temperature PL measurements performed on UID and Fe-doped samples clearly show the compensation of the free-carriers, which is evident from the decrease of the exciton-bound-to-shallow-donor intensities (X_AO° and X_ASi°) relative to the increasing intensities of the free-exciton lines (FEA and FEB). The electrical properties of the substrates will be presented.

[1] M. Iwinska, R. Piotrzkowski, E. Litwin-Staszewska, T. Sochacki, M.j Amilusik, M. Fijalkowski, B. Lucznik, M. Bockowski , Appl. Phys. Express **10** (2017) 011003.
[2] D. Hanser, M. Tutor, E. Preble, M. Williams, X. Xu, D. Tsvetkov, L. Liu, J. Crystal Growth, **305** (2007) 372.
[3] G. Talut, H. Reuther, A. Mücklich, F. Eichhorn, K. Potzger, Appl. Phys. Lett., **89** (2006) 161909.

Invited lecture

Plasma-assisted molecular beam epitaxy of monolayer-thick GaN/AlN heterostructures for high efficient sub-250-nm UV emitters

V. N. Jmerik[1], D. V. Nechaev[1], A. A. Toropov[1], E. A. Evropeitsev[1], V. I. Kozlovsky[2], V. P. Martovitsky[2], S. Rouvimov[1,3], and S. V. Ivanov[1]

[1] *Ioffe Institute, Polytekhnicheskaya str. 26, St. Petersburg 194021, Russia*
[2] *Lebedev Physical Institute, Leninsky pr. 53, Moscow 119991, Russia*
[3] *University of Notre Dame, Notre Dame, Indiana 46556, USA*

Plasma-assisted MBE (PA MBE) gives a unique opportunity to grow the (Al,Ga)N heterostructures at the metal-rich conditions and extremely low growth temperatures down to 700°C. In combination with ultrafast control of growth fluxes, it allowed us to form the 2D-heterostructures with extremely abrupt interfaces. We demonstrate application of this technology for fabrication of the one-to-several-ML-thick GaN/AlN single and multiple QW structures emitting in the mid-UV range down to a wavelength of 235 nm under optical and electron-beam pumping. First, we discuss the most suitable design of PA MBE-setup and growth conditions for maintaining a controlled concentration of group-III atoms during growth of several-nm-thick AlN barrier layers and GaN QWs with a thickness of 0.5-4MLs. Combination of different pulsed PA MBE methods, such as metal-modulated and migration-enhanced epitaxy, were used to achieve 2D growth of AlN/GaN QW structures with the sharp and homogeneous interfaces at low T_S~700C and fast (<0.5s) altering the growth fluxes. The formation of plane QWs with abrupt symmetrical interfaces was confirmed by both scanning transmission electron microscopy and *x*-ray diffraction (XRD) analysis. Photoluminescence measurements in the single-QW structures revealed drastic enhancement of the emission efficiency in ultra-thin QWs with d_w~1.5 ML. Special attention is paid to the peculiarities of stress relaxation in the MQW structures using the data of multi-beam optical stress sensor. These measurements in combination with XRD analysis revealed the stress-free and coherent growth of the 1.5ML-GaN/AlN MQW structures with a number of wells up to 360, whereas the MQW-structures with a thicker wells (>4MLs) demonstrated the standard development of stress from compressive to tensile ones. The possible mechanism of elastic relaxation of GaN in-plane lattice parameter in the former is explained by the formation of ultra-thin spatially-separated platelets with a thickness very few MLs. The 150(28) mW output power at the wavelength 235 nm has been achieved at room temperature in the electron-beam pumped deep-UV emitters with a pulse-scanning (continuous-wave) excitation using an electron beam energy and current of 20(15) kV and 1(0.45) mA, respectively.
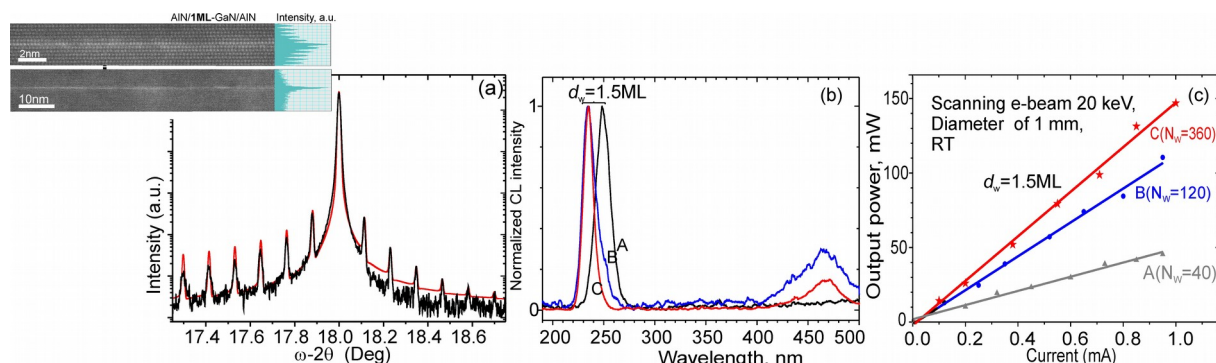
Fig.1 (a) XRD scans of 40×{AlN(39.5ML)/GaN(1.5ML) MQW structure. Inset shows HAADF STEM images of GaN(1ML)/AlN SQW. Normalized RT CL spectra (b) and output power vs exciting e-beam current (c) for the GaN(1.5ML)/AlN MQW structures with a varied number of QWs (A-N_w=40, B-N_w=120, C-N_w=360).

UVC LEDs on AlN/sapphire templates prepared by high-temperature annealing and regrowth process

Yuri Itokazu, Masafumi Jo, Satoshi Minami and Hideki Hirayama

RIKEN, 2-1 Hirosawa, Wako, Saitama 351-0198, Japan

AlGaN-based UV light-emitting diodes (LEDs) have been extensively studied for disinfection, water purification, and bio-medical applications. Many attempts have been made to increase the efficiency and light output power of the UV LEDs. In terms of the internal quantum efficiency, high-quality AlN templates on sapphire have recently been developed by using a high-temperature annealing (HTA) and regrowth process [1]. Recrystallization during the annealing greatly reduced the threading dislocation density, which is promising for improving the efficiency of UVC LEDs. However, only a few studies have been reported on the operation of LEDs on HTA AlN templates [2]. Here, we demonstrate UVC LEDs on HTA AlN templates operating at an equivalent level of a conventional LED.

LEDs were grown on a control AlN template (4 µm) and an HTA AlN template by metal-organic chemical vapor deposition (MOCVD). The HTA AlN template was fabricated as follows: a 300-nm AlN grown on sapphire by MOCVD, then annealed at 1700 °C for 1h under N_2 ambient, finally a 2-µm AlN regrown by MOCVD. Although the HTA AlN template was half the thickness of the control AlN, typical XRC FWHMs were comparable to or smaller than those of the control AlN: 190arcsec for the (002) reflection and 390arcsec for the (102) reflection. In addition, few cracks were observed for the HTA AlN. Figure 1 depicts the reciprocal space map of the AlGaN/HTA-AlN. The AlN was almost fully relaxed, and the AlGaN showed a narrow peak with small mosaicity of 0.1 degree, indicating a good crystalline quality of AlGaN. Figure 2 plots the efficiency of the two LEDs, with the corresponding EL spectra in the inset. As expected from the XRC analysis, the efficiency of the two LEDs was nearly equal. These results demonstrate that the HTA and regrowth process can be a reliable technique for realizing efficient UVC LEDs.
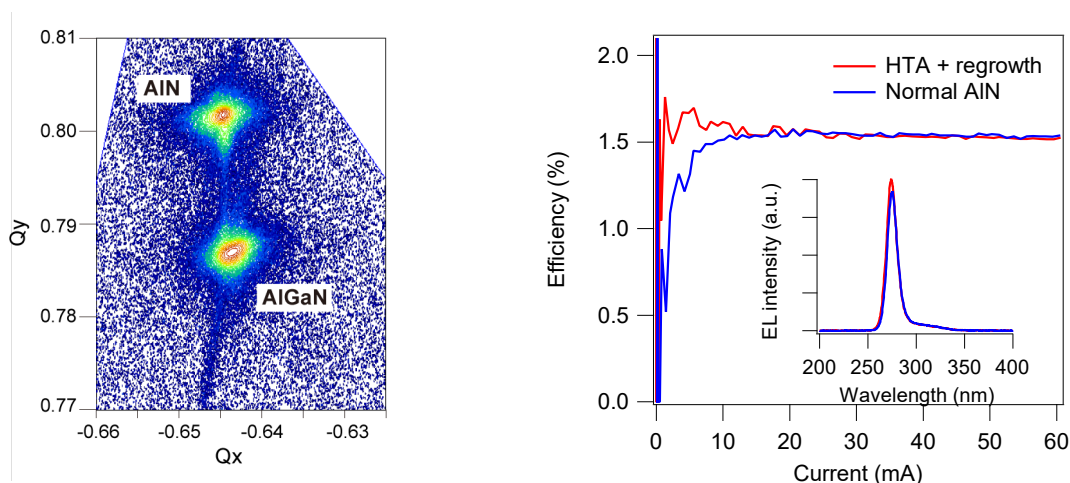
Figure 1 (-1-14) XRD reciprocal space map of AlGaN grown on an HTA AlN template.

Figure 2 Efficiency of the LEDs plotted as a function of current. The inset shows EL spectra of the LEDs.

[1] H. Miyake *et. al.*, Appl. Phys. Express, 9, 025501 (2016).
[2] N. Susilo *et. al.*, Appl. Phys. Lett., 112, 041110 (2018).

Investigation of the Thermal Droop in InGaN-based Layers and UVA LEDs

Carlo De Santi [1]**, Matteo Meneghini** [1]**, Desiree Monti** [1]**, Holger Koch**[2]**,**
Gaudenzio Meneghesso [1]**, and Enrico Zanoni** [1]

[1] *Dept. of Information Engineering, University of Padova, via Gradenigo 6/B, Padova, Italy*
[2] *OSRAM Opto Semiconductors GmbH, Leibnizstrasse 4, 93055 Regensburg, Germany*

The thermal droop, i.e. the temperature dependence of the efficiency of GaN-based LEDs, is a topic of growing interest for high power density and high temperature operation. The aim of this work is to investigate the role of the SRH recombination and of the thermionic escape in the thermal droop of GaN-based layers and LEDs.

To understand the thermal performance of the quantum well material, we analyzed the thermal droop of 120 nm thick InGaN layers with different indium content under optical excitation. As can be seen in Fig. 1, the decrease in PL intensity can be closely reproduced in a wide temperature range by means of the variation in non-radiative lifetime according to the SRH recombination model (equation in the inset). The inset confirms that the extrapolated activation energy of the deep level responsible for the decrease is close to the intrinsic Fermi level, where it behaves as a very efficient non-recombination center, and shows that its value has almost no dependence on the indium content. All these data suggest that the mechanism responsible for the PL decrease with temperature is a stronger SRH recombination, and that the deep level causing it is the same in every layer regardless of the indium content.

In some devices the SRH recombination may not be the only process causing the thermal droop. We measured a set of commercial devices with nominal emission wavelength 385, 395, 405 and 420 nm and GaN barriers, leading to a different barrier height for the carrier confinement into the quantum wells. When the barrier is very low, the energy of some carriers may be high enough to overcome it, leading to a thermionic emission process that is enhanced by the temperature. In order to analyze this effect, we developed a new semi-classical model of the carrier distribution in the quantum wells. The density of states is the one of a three-dimensional material, and given the high degeneracy of the quantum well in forward bias the Fermi-Dirac distribution is used instead of the easier Boltzmann distribution. The Fermi level is set at the lowest allowed energy level (E_1) in the quantum well, computed according to a 3 nm thickness. The density of states is shifted in order to start at E_1, since no carrier can be present below this level in the quantum well. The computed electron density distribution is plotted in Fig. 2 for all the temperatures under analysis, along with lines showing the barrier height for the various samples. As can be seen in Fig. 3 and its inset, the amount of thermal droop predicted by this model may be as high as 50% of the total experimental thermal droop (the remaining part likely originated by the SRH recombination), and its effect is more severe the lower the barrier. This confirms the importance of the AlInGaN material system in increasing the thermal performance of UV LEDs.
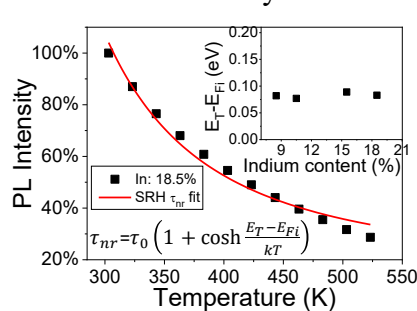
Fig. 1: PL droop of InGaN layers and its SRH model.
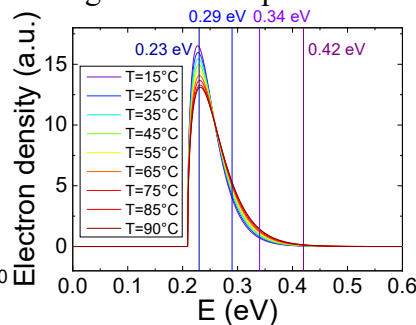
Fig. 2: Model of the electron density in the quantum wells.
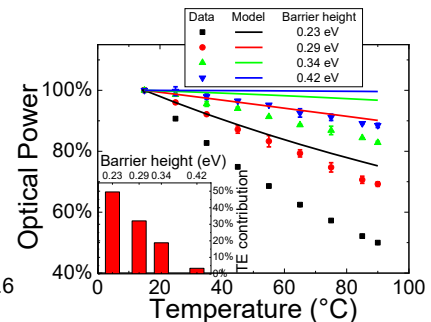
Fig. 3: Amount of thermal droop predicted by the model.

Investigation of crystallinity and current injection issue in 310nm-AlGaN UVB LED grown on AlN template in LP-MOVPE

M. Ajmal Khan[1,2], T. Matsumoto[1,3], N. Maeda[1,2], M. Jo[1,2], N. Kamata[3] and H. Hirayama[1,2]

[1] *RIKEN, 2-1 Hirosawa Wako, Saitama, 351-0198, Japan*
[2] *RIKEN Center for Advanced Photonics(RAP),2-1 Hirosawa, Wako, Saitama 351-0198, Japan*
[3] *Saitama University, Saitama 338-8570, Japan*

Smart, high-power UV LED light sources are needed for both medical and agricultural applications, including vitamin D3 production in human skin, immunotherapy (for the treatment of psoriasis), and enriching phytochemicals in plants, water sterilization, aid in the transportation of foods, making bank notes, biochemical agent detection, fluorescence detection, identification of protein, DNA, and bacteria etc [1-3]. Phytochemicals in the fruits and vegetables can be enriched by using upper bound (UB), UVB light with 310nm emission wavelength [2-3]. Torii et al., confirmed that 310nm UVB, induces the secretion of high-mobility group box-1 (HMGB1, nuclear protein) [4] without inducing the apoptosis (death of cells), but the 280nm UVB can induce both the secretion of HMGB1 as well as apoptosis at the same time. NB-UVB light sources were highly recommended for the treatment of psoriasis under the national guidelines of USA [2]. But NB-UVB light sources from safe, smart and low cost LED devices are still very rare. Kim et al., reported about AlGaN UVB LEDs grown on AlN template and achieved maximum output power about 2.7 mW with 305 nm emission wavelength [5]. Recently, Susilo et al., investigated the effect of GaN: Mg contact layer in AlGaN UVB LEDs on AlN template and achieved output power of 0.83mW at 20mA, with 302nm emission wavelength [6]. We also reported about AlGaN UVB LEDs grown on AlN template and the EQE 3.4 % at 20mA with maximum output power of 12.4 mW with 295nm emission wavelength using transparent p-AlGaN [7]. But these UVB LED devices confronted with current injection and light extraction efficiencies problems for wavelength longer than 300nm. Therefore, we attempted to further improve the performance of NB AlGaN UVB LEDs grown on AlN template with 310±2 nm emission.

To achieve this purpose we have developed a novel crystal growth technique, where we successfully grown high-quality graded stacks of AlGaN buffer layers and low TDDs 1×10^9 cm^{-2}, current spreading layer observed by TEM. Subsequently AlGaN based multi quantum wells (MQWs) with high IQEs, and highly transparent p-AlGaN contact layers were successfully fabricated on AlN template in the LP-MOVPE as shown in the device structure of Fig. 1(a). The output power around 11.2 milliwatt and EQE around 1.58 % were successfully achieved, as shown in Fig.1(c) and 1(b) respectively for the real world applications.
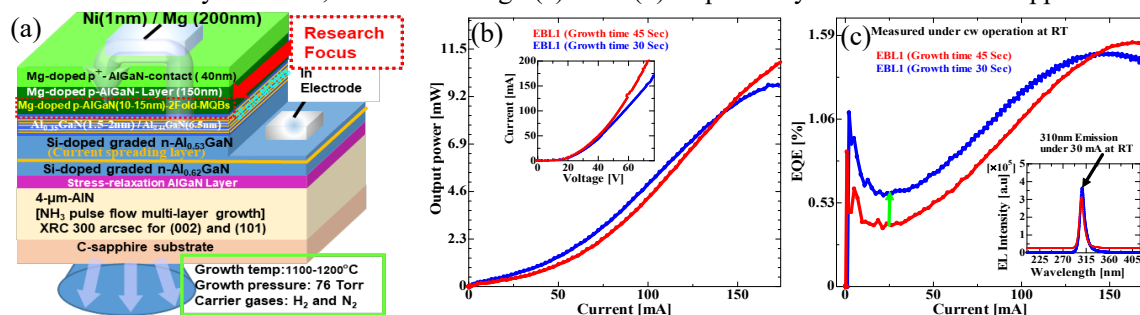
Figure 1(a) Schematic of AlGaN UB-UVB LED, (b) Current versus output power (I–L), and in the inset *I–V* characteristics, and (c) improved EQE (η_{ext}) characteristics, just on wafer of LB-UVB LED and in the inset EL emission under 20 mA dc driving current.

References

[1] Hirayama et al., Jpn. J. Appl. Phys 53, 100209 (2014).
[2] M. Kneissel and J. Rass (eds.), III-Nitride Ultraviolet Emitters, Springer Series in Material Science 227, Woodhead Publishing, ISSN 0933-033X. (2016).
[3] Kneissel et al., *Plenary Talk*, IWUMD-2017, Fukuoka, Japan (2017).
[4] Kan Torii and Akimichi Morita, Exp Dermatol. 25(9):741-2 (2016).
[5] Kim et al., Appl. Phys. Lett. 85, 4777(2004).
[6] N. Susilo, and M. Kneissl, Phys. Status Solidi A, 1700643(2017).
[7] Khan et al., Extended abstract of 06pE07O ISPlasma2018/IC-PLANTS2018 March 4-8, (2018).

UVC emission from (11-22) AlGaN quantum wells grown by metal-organic chemical vapor deposition

Masafumi Jo, Yuri Itokazu, and Hideki Hirayama

RIKEN, 2-1 Hirosawa, Wako, Saitama 351-0198, Japan

Semipolar nitride has been attracting much attention because the reduced polarization in the active layer can improve the device performance. Among them, AlGaN-based emitters operating in UVC range are important for the application of disinfection. However, because of the difficulties in obtaining high-quality semipolar AlGaN layers, there are few reports on the UVC emission from semipolar AlGaN quantum wells (QWs). Recently, we have developed high-quality AlN templates on sapphire by using high-temperature annealing technique [1]. Here, we report the fabrication of high-quality (11-22) AlGaN QWs emitting in UVC range, with their optical properties.

Samples were grown on m-plane (10-10) sapphire substrates by metal-organic chemical vapor deposition (MOCVD). High-quality AlN templates were fabricated using high-temperature annealing at 1700 °C combined with the AlN growth by MOCVD. Then, a 1.5-µm AlGaN buffer layer was grown on the AlN template, followed by an AlGaN multiple QW structure. The QW width varied from 2 to 6 nm. Figure 1 shows a cross-sectional TEM image of a 4-nm AlGaN QW. The QW interface showed an atomically smooth interface. No misfit dislocation was observed and the QWs are coherently grown on the AlGaN buffer layer. Figure 2(a) shows PL spectra from (11-22) QWs with different well widths. UVC emission from the QW was clearly observed at room temperature. The PL linewidth of 100 meV was small compared to that of a (0001) QW. As the well width increased, the PL peak shifted to longer wavelength while the PL intensity decreased. Figure 1(b) plots the PL peak energy as a function of the well width. The peak shift due to quantum confined Stark effect was greatly reduced for the (11-22) QW, which indicates the small polarization field in the QW.
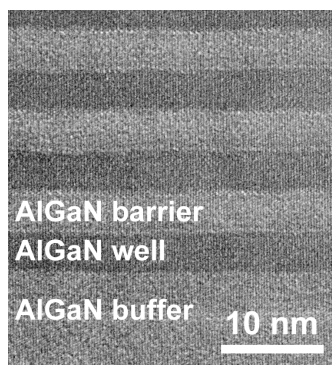
Figure 1 Cross-sectional TEM image of a (11-22) AlGaN QW along the [-1-123] zone axis.
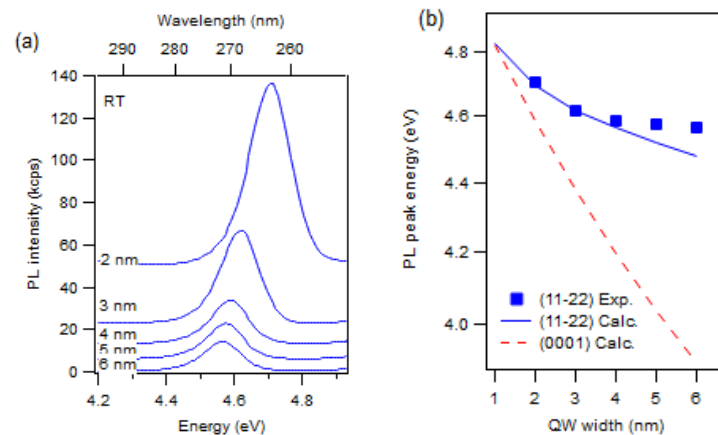
Figure 2 (a) PL spectra of (11-22) AlGaN QWs with different well widths. (b) PL peak energies plotted as a function of the well width. The blue solid line denotes the calculated emission energy for the (11-22) QW, while the red dashed line denotes the one for the (0001) QW.

[1] M. Jo *et. al*., submitted to J. Appl. Phys.

Oxygen-induced high diffusion rate of magnesium dopant in GaN/AlGaN based UV LED heterostructures

Paweł P. Michałowski,* Sebastian Złotnik, Jakub Sitek and Mariusz Rudziński

Institute of Electronic Materials Technology, Wólczyńska 133, 01-919 Warsaw, Poland

Further development of GaN/AlGaN based optoelectronic devices requires optimization of the *p*-type material growth process. In particular, an uncontrolled diffusion of Mg dopant may decrease the performance of a device thus it is meaningful to study in detail Mg behavior and origin of its diffusion. In this work we have employed Secondary Ion Mass Spectrometry to study the diffusion of magnesium in GaN/AlGaN structures. We show that magnesium has a strong tendency to form Mg-H complexes which immobilize Mg atoms and restrain their diffusion. However, these complexes are not present in samples post-growth annealed in oxygen atmosphere or Al-rich AlGaN structures which naturally have high oxygen concentration. In these samples more Mg atoms are free to diffuse and thus an average diffusion length is considerable larger than for a sample annealed in inert atmosphere.
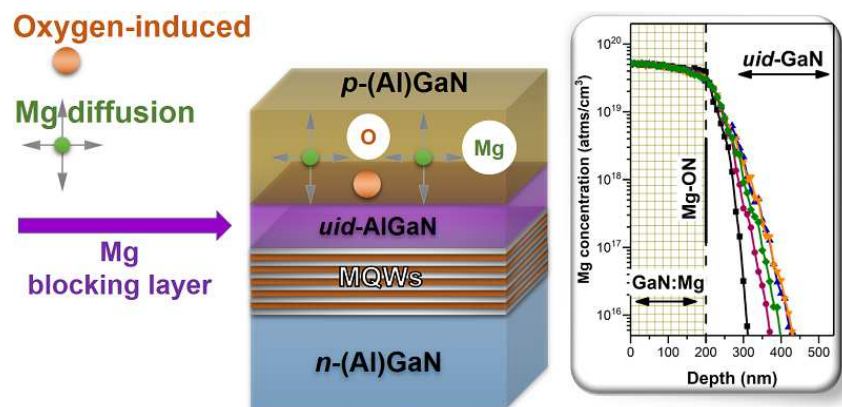
Figure 1: Oxygen breaks Mg-H complexes and induces high diffusion of Mg in GaN/AlGaN hetero-structures.

Invited lecture

Recent progress of in acidic ammonothermal growth of GaN crystals

S. F. Chichibu[1], **M. Saito**[1,2]**, Q. Bao**[1,3]**, D. Tomida**[1]**, K. Kurimoto**[1,3]**,
K. Shima**[1]**, K. Kojima**[1] **and T. Ishiguro**[1]

[1]IMRAM-Tohoku Univ., 2-2-1 Katahira, Aoba-ku, Sendai, Miyagi 980-8577, Japan
[2]Mitsubishi Chemical Corp., 1000 Higashimamiana, Ushiku, Ibaraki 300-1295, Japan
[3]The Japan Steel Works, Ltd., 11-1 Osaki 1-chome, Shinagawa-ku, Tokyo 141-0032, Japan

For realizing energy-saving power electronic devices, the fabrication of vertically current-flowing transistors is one of the promising ways. Especially, GaN-based power transistors switchable at high frequencies have several advantages for high-efficiency operating characteristics. As the areal size of such power devices is much larger than that of optical devices, large diameter GaN wafers of low dislocation density and quite a low wafer bowing are required. For this purpose, the ammonothermal (AT) method using acidic mineralizers is one of the promising routes for the mass production of large diameter GaN wafers. The research alliance among Tohoku Univ., Mitsubishi Chemical Corp., and The Japan Steel Works, Ltd. has been studying AT growth of GaN using ammonium halide acidic mineralizers [1-4]. At the symposium, our recent activities on the AT growth of GaN will be presented.

For preventing GaN crystals from possible contaminations due to the corrosion of the autoclave made of a Ni-based superalloy, the vessel has a lining using a precious metal. After charging polycrystalline GaN precursors and seed crystals, ammonium fluoride was added as a mineralizer. Then, filter-purified NH_3 gas was fed into the autoclave. The autoclave was heated using a two-zone vertical furnace to give a temperature gradient for the mass transport.

We studied the growth rate of AT-GaN as functions of temperature, temperature gradient, pressure, and orientations to obtain very high growth rate faster than 1000 µm/day under the optimum growth conditions. The full-width at half maximum values of the (0002) x-ray ω-rocking curves for most of the crystals were smaller than 30 arcsec. By using a newly developed *medium-scale* autoclave designed for the specific growth conditions shown in Fig.1, approximately 2-inches-long GaN crystals were routinely grown. The curvature radius of the best crystal shown in Fig. 2 was longer than 1,400 m. These results encourage to grow high-quality large-size GaN boules using the acidic AT method.

Fig.1 Medium-scale autoclave   Fig.2 *m*-plane crystal, radius of curvature: 1460m

[1] S. F. Chichibu *et al.*, *Appl. Phys. Express* **4**, 045501 (2011).
[2] D. Tomida, S. F. Chichibu *et al.*, *J. Cryst. Growth* **348**, 80 (2012).
[3] D. Tomida, S. F. Chichibu *et al.*, *J. Cryst. Growth* **353**, 59 (2012).
[4] Q. Bao, S. F. Chichibu *et al.*, *Cryst. Growth Design* **13**, 4158 (2013).

Invited lecture

Basic ammonothermal growth of GaN

**M. Zajac[1], R. Kucharski[1], K. Grabianska[1], A. Gwardys-Bak[1], A. Puchalski[1]
D. Wasik[2], E. Litwin-Staszewska[3], R. Piotrzkowski[3], J. Z. Domagala[4], and M. Bockowski[1,3]**

[1] *Ammono Lab, Institute of High Pressure Physics, Polish Academy of Sciences, Sokolowska 29/37, 01-142 Warsaw, Poland*
[2] *Faculty of Physics, University of Warsaw, Pasteura 5, 02-093, Warsaw, Poland*
[3] *Institute of High Pressure Physics Polish Academy of Sciences, Sokolowska 29/37, 01-142 Warsaw, Poland*
[4] *Institute of Physics, Polish Academy of Sciences, Aleja Lotników 32/46, 02-668 Warsaw, Poland*

Basic ammonothermal method uses supercritical ammonia for the dissolution of feedstock material and crystallization of GaN on native seeds due to convection-driven transport and supersaturation of the ammonia solution. The growth takes place in presence of basic mineralizers in form of alkali metals is characterized by negative solubility coefficient, having impact on arrangement of solubility and crystallization zones. The progress in the growth of truly bulk GaN crystals by basic ammonothermal method allows a production of 2-inch GaN substrates with different conductivity, including n-type conductivity of the tunable electron concentration 10^{18} - 10^{19} cm-3, p-type conductivity with the hole concentration of 10^{16} cm-3, as well as the semi-insulating material with the resistivity in the range of 10^6 - 10^{12} Ω cm. Wide range of electrical properties was achieved by controlling the oxygen and acceptor concentration. The optimization of the electrical properties will be discussed in terms of the point defects formation.

In this communication we will also show progress on overcoming the problem of limited yield of basic ammonothermal method, originating from stress generated on crystal edges, while growing in lateral a[110] and m[100] directions. Such stress was also reported for GaN crystals grown by HVPE [1] and is a serious problem in manufacturing of bulk GaN. The stress caused cracking and systematic reduce of the usable area needed for 2-inch substrate fabrication. Recent technological works lead to diminishing of this stress and further improvement on crystal yield and increase of seed multiplication efficiency. The results will be supported by X-ray diffraction and lattice parameters measurements. Moreover, successful growth of crystals of dimensions large enough to produce 3-inch crystals by lateral growth, will be shown.

[1] J. Z. Domagała, J. Smalc Koziorowska, M. Iwińska, T. Sochacki, M. Amilusik, B. Łucznik, M. Fijałkowski, G. Kamler, I. Grzegory, R. Kucharski, M. Zając, M. Boćkowski, Journal of Crystal Growth 456 (2016) 80.

Fabrication of GaN Crystals with Low Resistivity Grown with the Na-flux Point Seed Technique

K. Endo[1], T. Yamada[1], H. Kubo[1], K. Murakami[1], M. Imanishi[1], M. Yoshimura[1,2], and Y. Mori[1]

[1] *Grad. Sch. of Eng., Osaka Univ., 2-1, Yamada-oka, Suita, Osaka, 565-0871, Japan*
[2] *ILE, Osaka Univ., 2-1, Yamada-oka, Suita, Osaka, 565-0871, Japan*

GaN crystals with low threading dislocation density (TDD) as well as low resistivity are indispensable for development of power devices with low power consumption. As shown in Fig. 1 (a), we have succeeded in fabricating low-TDD GaN crystals using Na-flux point seed technique [1], and recent study suggests that resistivity of the GaN crystals in $\{10\bar{1}1\}$-growth sector is extremely low, in which donor impurity is on the order of 10^{20} cm^{-3} [2]. Therefore, GaN crystals grown with Thin-Flux-Growth method in Na-flux point seed technique [3] are expected to satisfy both low TDD and low resistivity because the GaN crystals grown with this method consist of $\{10\bar{1}1\}$-growth sector as shown in Fig. 1 (b). In this study, we fabricated GaN crystals grown with this method and investigated distribution of the TDD and electrical properties.

The optical image of the GaN crystal taken in the experiment is shown in Fig. 2 (b). Electrical properties and TDD in the crystal were evaluated by Hall measurement and etch-decoration technique, respectively. Table 1 shows the measurement results of electrical properties. Resistivity of the crystal was on the order of 10^{-4} Ωcm, which was much lower than that of high-doped GaN crystals grown by Hydride Vapor Phase Epitaxy (HVPE) method [4]. The distribution of the etch pit density of the sample is given in Fig. 3. As results, a few etch pits with a density of ~10^3 cm^{-2} occupied the greater portion of the crystal, excluding the region above the point seed. TDD in this region can be reduced by promoting pyramidal growth mode in the early stage of growth and gathering the TDD at the center of grains on a point seed [5]. These results suggest that GaN crystals with low TDD as well as low resistivity can be realized by using Thin-Flux-Growth method in Na-flux point seed technique.

[1] M. Imanishi *et al.*, Cryst. Growth. Des. **17**, 3806-3811 (2017).
[2] K. Endo *et al.,* 36th Electric Materials Symposium We2-**11** (2017).
[3] M. Hayashi *et al.,* J. Cryst. Growth **468,** 827-830 (2017).
[4] K. Motoki, SEI technical review **175,** 10-18 (2009).
[5] M. Imanishi *et al.*, J. Cryst. Growth. **427**, 87-93 (2015).
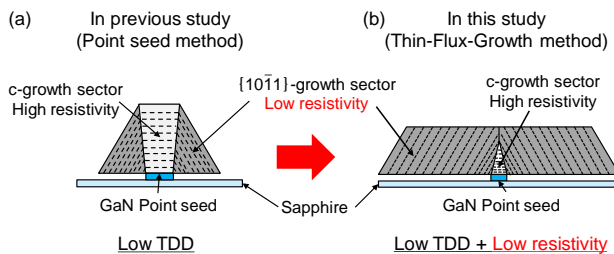
Fig. 1 Schematic drawing of the GaN crystal grown with (a) Point seed method, and (b) Thin-Flux-Growth method.
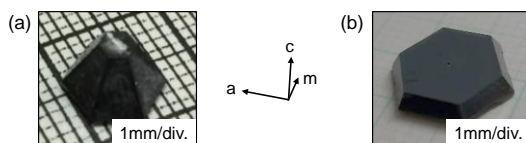
Fig. 2 Optical image of the GaN crystal grown with (a) Point seed method, and (b) Thin-Flux-Growth method.

Table 1 Electrical properties of the GaN crystal grown with Thin-Flux-Growth method and HVPE method.

Growth method	Carrier Concentration [cm^{-3}]	Resistivity [Ωcm]	Mobility [cm^2/Vs]
Thin-Flux-Growth	1×10^{20}	9.6×10^{-4}	65
HVPE[4]	5×10^{18}	8.5×10^{-3}	170
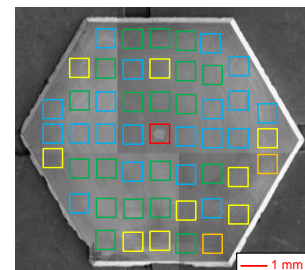
Fig. 3 Distribution of the etch pit density of the crystal.

Reduction of Li impurity in the Freestanding GaN Substrate Fabricated by the Na-Flux Sapphire Dissolution Technique

T. Yamada, M. Imanishi, K. Murakami, K. Nakamura, M. Yoshimura, and Y. Mori

Grad. Sch. of Eng., Osaka Univ.

Large-diameter GaN substrates are indispensable for the realization of low-cost GaN-based electronic devices. In a previous study, we succeeded in fabricating 1-in. GaN substrate using sapphire dissolution technique after GaN crystals were grown on c-GaN templates (GaN on sapphire) by the Na-flux method [1]. This technique is useful for avoiding stress due to the differences of thermal expansion coefficient between GaN and sapphire. However, in this method, Li impurity was incorporated in GaN crystals in the dissolution process. Li was used as a solvent for dissolving sapphire. Li impurity in GaN substrates may diffuse to epitaxial layers grown on the GaN substrates for manufacturing electronic devices, resulting in a decrease in device performance. Therefore, we need reduction of Li impurity in GaN crystals using sapphire dissolution technique. In this study, we investigated the diffusion of Li impurity in the crystals and tried to reduce Li impurity by regrowth of the crystals.

A freestanding GaN crystal was grown using the sapphire dissolution technique, as shown in Fig. 1(a). Li concentration was evaluated by Secondary Ion Mass Spectrometry (SIMS) at the thickness of 250, 500, and 750 µm. Figure 1(b) shows Li concentration in the grown crystal as a function of grown thickness. Li concentration is the order of 10^{15} atoms/cm^3 everywhere at the measurement point and lowest at thickness of 500 µm. Li concentration reduced with increasing in distance from the c-face and back-side surface of the crystal. This indicated that Li diffuse to inside from outside of the crystal during dissolution of sapphire after growth. GaN crystal was regrown on the crystal, which was grown using the sapphire dissolution technique. Figure 2(a) and (b) show the surface and cross-sectional optical images of the regrown crystal. As shown in Fig. 2(b), Li concentration was evaluated by SIMS at 250, 650, and 1050 µm from the backside of the crystal, named "D," "E," and "F," respectively. Figure 2(c) shows Li concentration in the regrown crystal as a function of distance from backside to D-F. Li concentration reduced with increasing in distance from the backside of the crystal, reaching less than 10^{14} atoms/cm^3 (detection limit) when the distance was 1050 µm. This result means that diffusion length of Li in GaN crystals during regrowth is less than 450 µm (seed thickness is 600 µm), which indicated that we can obtain Li-free GaN regrowth layer when regrown thickness was larger than diffusion length as shown in the schematic drawing of Fig. 2(d).
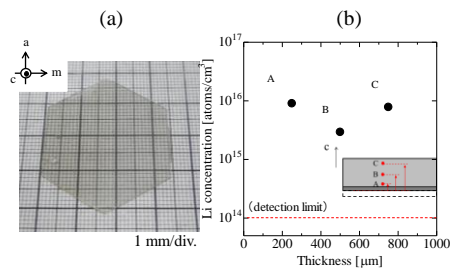
Fig. 1 (a)optical image of the crystal grown by sapphire dissolution technique and (b)Li concentration in the grown crystal as a function of grown thickness.
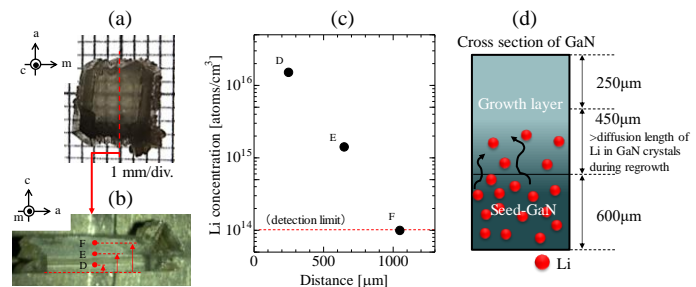
Fig. 2 (a)The surface and (b)cross-sectional optical images of the crystal regrown on the crystal grown by sapphire dissolution technique, (c)Li concentration in the regrown crystal as a function of distance from backside to measurement point, and (d)the schematic drawing of Li concentration distribution in the regrown crystal.

[1] T. Yamada *et al.*, The 37th Electronic Materials Symposium We2-10.

The effect of undissolved carbon on GaN crystal growth in Na flux method

N. Takeda, T. Yamada, K. Murakami, K. Kakinouchi, M. Imanishi, Y. Mori

Graduate School of Engineering, Osaka University, 2-1, Yamada-oka, Suita, Osaka, Japan

GaN crystal with low dislocation density is now strongly demanded for the fabrication of power devices. Na flux method is one of highly anticipated growth method to achieve GaN crystal with low dislocation density and we have been increasing efforts to overcome this challenge. We discovered that by adding the graphite directly into the Ga-Na flux, we could improve the crystal growth rate and suppress the generation of polycrystals [1]. However, it is also known from the previous study that further addition of graphite in the aim of suppressing further polycrystals could lead to the generation of pits on the crystal surface. The reason for the generation of pits, we hypothesized, is due to the undissolved carbon in the flux. Although graphite is considered to form CN ion in the flux condition [2], increase in the amount of graphite would require extra time for the graphite and nitrogen to react, which then creates undissolved carbon remained in the flux. To testify this surmise, we developed a new addition method, which enables to put CN ion directly into flux by NaCN, and succeeded in achieving crystal without polycrystals or pits. Yet this mechanism is elusive, in this work carbon dissolution time was introduced to elucidate the effect of undissolved carbon on GaN crystal.

We provided three different time conditions for crystal growth experiment, 24h, 48h, 72h, as a keeping time of seed crystal before dipping into the flux. We carried out crystal growth for 24h each and investigated how the extension of seed keeping time affects the area density of pits on the crystal surface after growth. For the crystal with the seed keeping time of 24h, pit area density was 8.2×10 cm^{-2} and void density at depth of 200 µm was 1.2×10^4 cm^{-2}. As for the crystal held 48h before dipping, the pit density decreased to 6.7 cm^{-2}, void density decreased to 1.9×10^2 cm^{-2}. On the other hand, for the crystal held 72h before dipping, neither pit nor void was observed. As shown in Figure 3, yellow luminescence at the bottom of the pit in photoluminescence image suggests carbon existence in the origin of pits.

By extending the seed keeping time before dipping into the flux from 24h to 72h, we managed to achieve crystal with no pit as a result of eliminating undissolved carbon remained in the flux before crystal growth. Considering this fact, carbon is preferred to be added into flux in NaCN rather than in graphite, as it becomes the origin of pits.
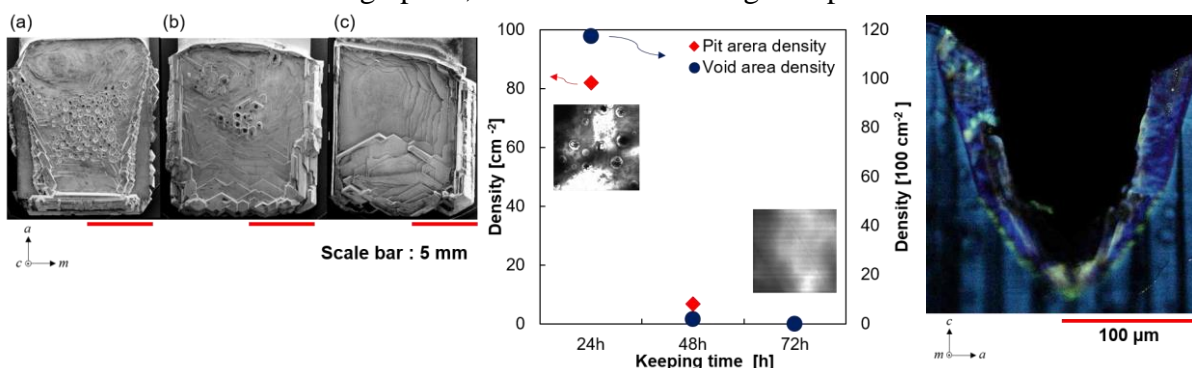
Figure 1. SEM images showing the morphology of GaN crystals by (a) 24h, (b) 48h, (c) 72h keeping time.

Figure 2. Differences in the pit and void area density for each keeping time with two typical sectional views at the depth of 200 µm.

Figure 3. Sectional view of PL image showing yellow luminescence at the bottom of the pit.

[1] F. Kawamura *et al*., J. Cryst. Growth **310** 3946 (2008).
[2] T. Kawamura *et al*., Appl. Phys. Express **9** (1) 015601 (2016).

Growth of GaN Single Crystal by Na Flux Method Adding Nitrogen-doped Carbon

Z. L. Liu [1], L. Shi [1], X. J. Su [1], G. Q. Ren [1,2], J. F. Wang [1,2] and K. Xu [1,2,*]

[1] *Suzhou Institute of Nano-tech and Nano-bionics, Chinese Academy of Sciences, Suzhou 215123, People's Republic of China*
[2] *Suzhou Nanowin Science and Technology Co., Ltd., Suzhou 215123, People's Republic of China*

The Na Flux method is one of the commercially potential bulk GaN production techniques, which can obtain large size, high quality and low cost GaN single crystals. It has many advantages to grow bulk GaN single crystal. However, it is difficult to grow large-size GaN crystals with a moderate growth rate because of the difficulty in controlling the spontaneously nucleation process. Moreover, the surface of GaN seed will be redissolved in the solution before the solution becomes saturated with nitrogen. This process would result in voids, inclusions and dislocation generation, which will cause the quality of the overgrowth GaN to reduce. To overcome such drawbacks, there are several attempts have being used.

In our study, it can more effectively suppress the polycrystals by adding carbon sources with graphitic N in the majority. Moreover, nitrogen-doped carbon additives can suppress the GaN seed redissolution and achieve a higher growth rate of LPE GaN single crystal. The growth interface is good by means of precisely controllable process. The threading dislocation is effectively restrain at the initial growth interface. The mechanism of GaN growth by Na Flux method adding nitrogen-doped carbon has been studied. And a high-quality 2-inch GaN single crystal has been obtained by such a above process.
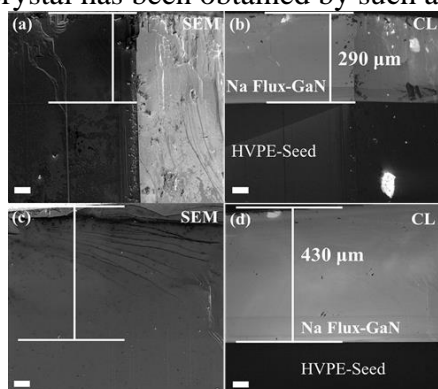
Figure 1. The panchromatic CL images of GaN cross-section growth with OMC (a, b) and N-OMC (c, d). Scale bar is 50 μm
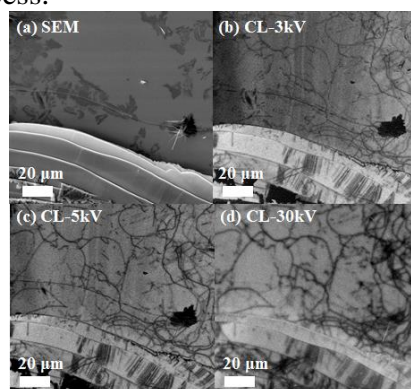
Figure 2. The panchromatic CL images of the threading dislocation restrained at the initial growth interface.
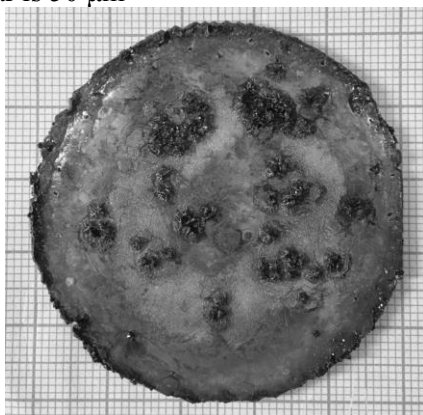
Figure 3. A 2-inch GaN grown by Na Flux method adding Nitrogen-doped Carbon. Without polishing.

Invited lecture

Tunnel Junctions for Next Generation III-Nitride Optoelectronics

Siddharth Rajan

Department of Electrical and Computer Engineering, The Ohio State University, Columbus, Ohio 43210, USA

This presentation will discuss evolution and current state-of-art in tunnel junction-based III-Nitride optoelectronic devices. I will begin with a discussion of the fundamental device engineering to realize high conductivity tunnel junctions in wide band gap semiconductors, including polarization engineering and heavy doping, and the applications of these tunnel junctions for III-Nitride optoelectronics. This will be followed by a discussion of experimental results that demonstrate the realization of Gallium Nitride-based tunnel junctions for visible wavelength single and multiple active region LEDs, and the observation of quantum phenomena such as negative differential resistance.

I will then discuss the use of tunnel junctions for ultra-violet light emitters. The low p-type conductivity and high contact resistance remain a critical problem in wide band gap AlGaN-based ultraviolet light emitters. We show that non-equilibrium hole injection through interband tunneling can overcome the fundamental material limitations and enable next-generation ultraviolet emitters. I will discuss experimental results showing how heterostructure engineering can enable efficient interband tunneling for hole injection in tunnel-injected UV LED devices with emission wavelength spanning from 330 nm down to 257 nm, and high on-wafer efficiencies comparable to state-of-the-art values. I will also discuss metal/semiconductor tunnel junction structures employing reflective Al-based metal stack that could enable excellent light extraction.

The progress in III-Nitride tunnel junctions in the last few years has enabled several new paradigms for design of visible and ultraviolet light emitting diodes and diode lasers. With continued progress and research, the use of tunneling injection will enable a new generation of highly efficient, high power density light sources ranging from the visible to the ultra-violet.

Invited lecture

Long-Living Laser Diodes Grown By Plasma Assisted Molecular Beam Epitaxy

Grzegorz Muziol

Institute of High Pressure Physics PAS, Sokolowska 29/37, 01-142 Warsaw, Poland

In this paper the recent development of III-nitride based optoelectronic devices grown by plasma assisted molecular beam epitaxy (PAMBE) will be presented. The increasing comprehension of the growth process resulted in a major improvement in the material quality of PAMBE grown layers [1]. As a result, laser diodes with extremely long lifetimes reaching 100 000 hours have been achieved.

Additionally, the development of high indium content InGaN allowed to incorporate it as waveguides in the LD design. This resulted in demonstrations of LDs without light leakage to the substrate [2] and aluminum-free LDs [3].

One of the key features of PAMBE is the lack of hydrogen incorporation into the p-doped III-nitride layers. On the other hand, the material grown by the commonly used metal organic vapour phase epitaxy suffers from incorporation of hydrogen which passivates the Mg dopant. The hydrogen can be removed post-growth by annealing to activate the Mg dopant and obtain p-type conductivity but it requires the p-doped layers to be on top of the heterostructure. This limits the spectrum of devices to those without buried p-type layers. The PAMBE technique does not suffer from such limitations. One of the applications of PAMBE in this regard is the growth of buried tunnel junctions [4].

In this paper the idea behind the growth of buried tunnel junctions and their application to the devices will be presented. New concepts of devices such as LED and LD stacks will be demonstrated. Furthermore, a demonstration of a distributed feedback nitride laser diode will be presented which benefits from the use of tunnel junction to obtain strong coupling between the optical mode and the grating.

[1] C. Skierbiszewski, H. Turski, G. Muziol, M. Siekacz, M. Sawicka, G. Cywiński, Z. R. Wasilewski and S. Porowski, *J. Phys.* D 47 (7), 073001 (2014).

[2] G. Muziol, H. Turski, M. Siekacz, S. Grzanka, P. Perlin and C. Skierbiszewski, *Appl. Phys. Express* 9 (9), 092103 (2016).

[3] G. Muziol, H. Turski, M. Siekacz, P. Wolny, J. Borysiuk, S. Grzanka, P. Perlin and C. Skierbiszewski, *Opt. Express* 25 (26), 33113-33121 (2017).

[4] C. Skierbiszewski, G. Muziol, K. Nowakowski-Szkudlarek, H. Turski, M. Siekacz, A. Feduniewicz-Zmuda, A. Nowakowska-Szkudlarek, M. Sawicka and P. Perlin, *Appl. Phys. Express 11* (3), 034103 (2018).

Structural Investigation Of InGaN/GaN Heterostructures Quantum Wells For Long Wavelength Emission

N. Chery[1], T. H. Ngo[2], M.P. Chauvat[1], B. Damilano[3], B. Gil[2], M. Morales[1], S. Kret[4] and P. Ruterana[1]

[1] *CIMAP, 6 boulevard du Marechal Juin, Université de Caen, Caen, France*
[2] *L2C, Bâtiment 21 Campus Triolet, Université de Montpellier, Montpellier, France*
[3] *CRHEA, Rue Bernard Gregory, Université Côte d'Azur, Valbonne, France*
[4] *Institute of Physics, Polish Academy of Sciences, al. Lotników 32/46, Warsaw, Poland*

Author corresponding: nicolas.chery@ensicaen.fr

InGaN/GaN multiple quantum wells (MQW) heterostructures are at the basis of highly efficient light-emitting diodes (LED) and laser diodes in the near UV to the green range [1]. However, bridging the green gap still remains an important challenge [2]. Different mechanisms have been reported in the literature in order to explain the decrease of emission efficiency when the indium composition is increased in order to reach longer wavelengths. One of them is the quantum confined Stark effect (QCSE) which introduces a large spatial separation between electrons and holes [3]. Others are the Auger effect which impacts the internal quantum efficiency (IQE) mainly under high excitation regime [4], and the non-radiative recombination centers which could be predominant for highest indium contents due to possible generation of high densities of defects [5]. In this alloy, reports have shown that there could be strain relaxation by generation of defects such as stacking faults, dislocations [6] or trenches which may constitute non-radiative recombination centers [7]. More recently, it was reported that the relaxation of the local strain through I_1 basal stacking faults (BSF) was at the origin of **a** type threading dislocations (TDs) from QW layers to the surface [8].

In this work, we investigate the local structure of such heterostructures produced by metalorganic chemical vapor deposition (MOCVD) using transmission electron microscopy (TEM). Our observations point out typical hexagonal defects that also give rise to the formation of **a** type threading dislocations. Interestingly, they become predominant when the nominal indium composition is beyond 20%. For these native defects, the measured displacement vector is also along <10-10> directions and it is very small, therefore, they do not correspond to the conventional stacking faults of the wurtzite structure.

[1] M. R. Krames, O. B. Shchekin, R. Mueller-Mach, G. O. Mueller, L. Zhou, G. Harbers, and M. G. Craford, *J. Disp. Technol.* **3**, 160 (2007).
[2] T. Mukai, M. Yamada, and S. Nakamura, *Jpn. J. Appl. Phys.* **38**, 3976 (1999).
[3] W. Liu, D. G. Zhao, D. S. Jiang, P. Chen, Z. S. Liu, J. J. Zhu, X. Li, F. Liang, J. P. Liu, S. M. Zhang, H. Yang, Y. T. Zhang, and G. T. Du, *Superlattices Microstruct.* **88**, 50 (2015).
[4] C. Weisbuch, M. Piccardo, L. Martinelli, J. Iveland, J. Peretti, and J. S. Speck, *Physica Status Solidi (A)* **212**, 899 (2015).
[5] T. Li, A. M. Fischer, Q. Y. Wei, F. A. Ponce, T. Detchprohm, and C. Wetzel, *Appl. Phys. Lett.* **96**, 031906 (2010).
[6] M. Zhu, S. You, T. Detchprohm, T. Paskova, E. A. Preble, D. Hanser, and C. Wetzel, *Phys. Rev. B* **81**, (2010).
[7] F. Wu, Y.-D. Lin, A. Chakraborty, H. Ohta, S. P. DenBaars, S. Nakamura, and J. S. Speck, *Appl. Phys. Lett.* **96**, 231912 (2010).
[8] J. Smalc-Koziorowska, C. Bazioti, M. Albrecht, and G. P. Dimitrakopulos, *Appl. Phys. Lett.* **108**, 051901 (2016).

AlInN/GaN DBRs for Long-wavelength GaN-based VCSELs

K. Hiraiwa[1], W. Muranaga[1], J. Ogimoto[1], T. Akagi[1],
T. Takeuchi[1], S. Kamiyama[1], M. Iwaya[1] and I. Akasaki[1,2]

[1] *Fac. Sci. & Eng., Meijo University, 1-501 shiogamaguchi, Tenpaku-ku, Nagoya, Japan*
[2]*Akasaki Research Center, Nagoya Univ., Furo-cho, Chikusa-ku, Nagoya, Japan*

While GaN-based green VCSELs with dielectric DBRs have been demonstrated[1], those with semiconductor-based bottom DBRs have not been reported yet. In fact, very few GaN-based DBRs showing a high reflectivity over 99% in the long-wavelength region have been reported. In this study, we successfully fabricated lattice-matched AlInN/GaN DBRs with target wavelengths from 410 nm to 570 nm, showing high reflectivity values of 99% and over.

We fabricated 40-pair lattice-matched AlInN/GaN DBRs with target wavelengths of 410 nm, 520 nm, and 570 nm on GaN substrates by MOVPE as shown in Fig. 1. Total designed thicknesses of the 40-pair DBRs were 3.44 µm (λ =410 nm), 4.56 µm (λ=520 nm), and 5.04 µm (λ=570 nm).

Fig. 2 shows measured and calculated (0002) 2θ-ω X-ray diffraction curves of the 570 nm DBR. Sharp high-order satellite peaks were observed and matched with the calculated ones. An RMS value from the inset AFM image of the DBR surface (GaN) was 0.1 nm. Not only the 570 nm DBR but also the 410 nm and 520 nm DBRs showed similar results. The result suggests that structural qualities of the DBRs were similarly high. Fig.3 shows measured and calculated reflectivity spectra of the DBRs. In the calculation, reported refractive index values [2, 3] were used. First, peak reflectivity values of 99 % and over were obtained in the wavelength regions from 410 nm to 570 nm. In addition, shapes of the stop band and the side lobe in measurement were in excellent agreement with the calculations. At the same time, we found that the measured peak reflectivity value became 0.4 % lower than the calculated one from the 570 nm DBRs. At this moment, the reason for the discrepancy is not clear. Assuming that this is caused by an internal absorption in the DBR, our calculation suggests that the internal loss of 48 cm^{-1} leads to the 0.4 % lower reflectivity value. Note that such an internal loss corresponds to a total internal loss of 20 cm^{-1} in our VCSEL structure in consideration with an optical confinement factor of the DBR, which must be suppressed towards high-performance long-wavelength VCSELs.
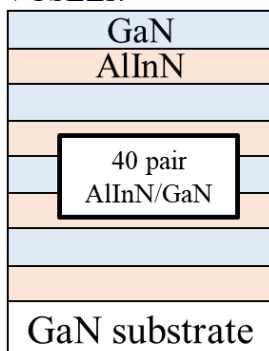
Fig. 1
Sample structure
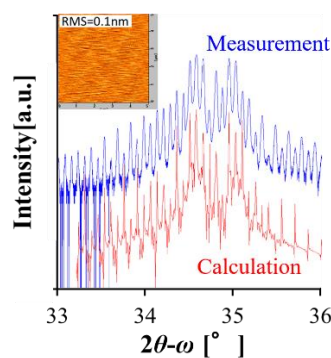
Fig. 2 (0002) 2θ-ω
X-ray diffraction curves
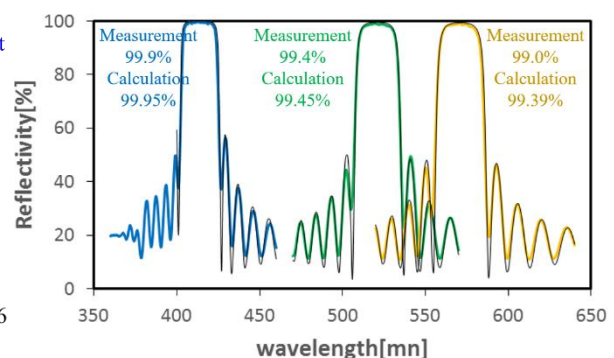
Fig. 3 Reflectivity spectra
(Measurement : Color-bold line,
Calculation : black-thin line)

[1] D. Kasahara et al., Appl. Phys. Express 4, 072103 (2011). [2] T. Aschenbrenner et al. J. Appl. Phys. 108, 063533 (2010). [3] M. Miyoshi et al., Appl. Phys. Express 11, 051001(2018).

Improvement of emission efficiency in green LEDs by sputtered AlN buffer layer

S. Ishimoto [1], D.P. Han [1], K. Yamamoto [1]
S. Kamiyama [1], T. Takeuchi [1], M. Iwaya [1], I. Akasaki [1,2]

[1] *Meijo Univ., 1-501, Shiogamaguchi, Tempaku-ku, Nagoya, Japan*
[2] *Akasaki Research Center, Nagoya Univ., Furou-cho, Chikusa-ku, Nagoya, Japan*

Nitride-based light-emitting diodes (LEDs) have a great potential for all visible wavelength light emission. However, large biaxial compressive strain in active region leads to decrease of radiative efficiency, in particular GaInN-based longer wavelength LEDs. So far, numerous approaches for this problem have been attempted. It was reported that radiative efficiency of green LEDs was improved by thinning a sapphire substrate to reduce thermal strain in epitaxial layer. [1] On the other hand, it is known that LEDs with a sputtered AlN (sp-AlN) buffer layer have lower curvature than those with a low-temperature-deposited GaN (LT-GaN) buffer layer. It means that LEDs with the sp-AlN buffer layer have less thermal strain in epitaxial layer, similar to the above report. Therefore, we expect the improvement of emission efficiency of green LEDs by using the sp-AlN buffer layer.

We prepared green LEDs with the sp-AlN and the LT-GaN buffer layers by MOVPE. As shown in Fig.1, enhancement of PL intensity was observed in the sample with sp-AlN buffer layer. The internal quantum efficiency (IQE) improvement was implied in EL measurement, due to the effect of the sp-AlN buffer layer. In order to clarify the reason why LEDs properties were improved, we compared 4 μm-thick GaN samples with each buffer layer, and they were characterized by X-Ray diffraction measurements. Table 1 summarizes the in-plane lattice constant a and the compressive strain of GaN epilayers with the LT-GaN and the sp-AlN buffer layers. As in the table, it is clearly that the GaN epitaxial layer with the sp-AlN buffer layer has lower compressive strain. As a result, the sp-AlN buffer layer is effective for the suppression of compressive strain in epitaxial layer, and it leads to the improvement of IQE in green LEDs.

[1] W. Z. Tawfik, S. J. Bae, S. B. Yang, *J. Appl. Phys.* **6**, 122103 (2013).
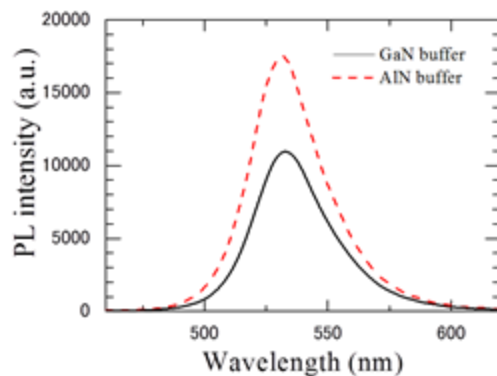
Fig 1 PL spectra of green LEDs

Table 1 Lattice constant a and compressive strain in GaN epitaxial layers

Buffer layer	Lattice constant a [Å]	Compressive strain [-]
LT-GaN	3.1822	2.1×10^{-3}
sp-AlN	3.1851	1.2×10^{-3}
bulk	3.189	

Kinetic Mechanisms of InGaN(0001) by RF-MBE in the entire composition range: Phenomenological Model and Impact on Epilayer Properties

E. Papadomanolaki [1], S.A. Kazazis [1], L. Lymperakis [2], and E. Iliopoulos [1,3,*]

[1] *Department of Physics, University of Crete, GR-70013, Heraklion, Greece*
[2] *Max-Planck-Institut für Eisenforschung, 40237 Düsseldorf, Germany*
[3] *Microelectronics Research Group, I.E.S.L.-FO.R.T.H., GR-71110, Heraklion, Greece*
[*] *E-mail: iliopoul@physics.uoc.gr*

Epitaxial growth of high quality InGaN alloy thin films and heterostructures with compositions spanning the entire composition range is essential for contemporary and future device applications [1]. Plasma assisted molecular beam epitaxy is particular suited for mid- and high InN mole fraction alloys growth due to its high indium incorporation efficiency and metastable growth mode. However, apart from inherent material challenges, the largely different growth conditions of the alloy system endpoints, GaN and InN, complicate the epitaxial growth control. In that aspect understanding and quantifying the kinetic mechanisms of growth is of particular importance.

In contrast to endpoints epitaxial kinetics, in the case of InGaN epilayers, two major processes are active concurrently: alloy decomposition and indium desorption, with their relative importance dictated by the growth temperature [2] and the incident elemental fluxes. In this work both mechanisms are studied in details. Indium desorption has been studied *in-situ* by RHEED and by *ab-initio* DFT calculations. The determined experimental activation energy values, for the different indium adlayer configurations, were in close agreement with the ones derived by the theoretical calculations. Furthermore, the non-Langmuir kinetic order of the process was identified. The kinetic decomposition mechanisms were investigated by growth of a large number of epilayers in different conditions and detailed *ex-situ* measurements. The dependence of decomposition on the effective surface stoichiometry was quantified.

In depth quantitative understanding of the basic kinetic mechanisms leads to the derivation of a universal phenomenological model that consistently describes the InGaN alloys' epitaxy in the entire growth parameter space. This permits accurate composition control, as well as, independent tuning of the growth mode characteristics. Regarding the latter, we will present its important consequences on the epilayers' structural, electronic and optical properties. Emphasis will be given to conditions leading to high quality non-clustered thick films growth on GaN(0001) in the entire composition range [3].

[1] J. Wu, *J. Appl. Phys.* **106**, 011101 (2009).
[2] E. Papadomanolaki et al, *J. Cryst. Growth* **437**, 20 (2016)
[3] S.A. Kazazis et al, *J. Appl. Phys.* **123**, 125101 (2018)

Invited lecture
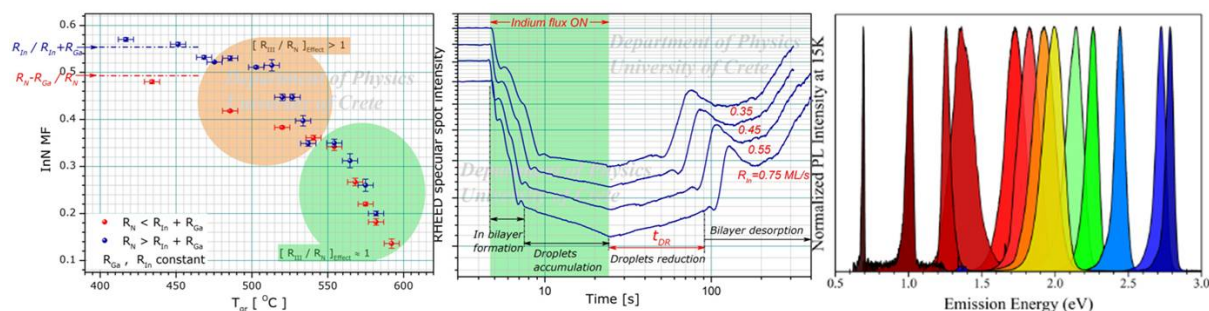
Growth of InN films with high electron mobility by MBE

X. Wang[1], H. Liu[1], X. Zheng[1], T. Wang[1], P. Wang[1], B. Sheng[1], X. Rong[1], X. Yang[1], F. Xu[1] and B. Shen[1]

[1]*State Key Laboratory of Artificial Microstructure and Mesoscopic Physics, School of Physics, Peking University, Beijing 100871, China*

InN has the narrowest direct bandgap of ~0.64 eV among III-nitrides, which extends wavelength range of group III-nitride alloys from deep ultraviolet to near infrared, and makes InGaN material the most promising candidate for fabricating high efficiency solar cells.[1] In addition, InN has attracted considerable attention for fabrication of high-speed electronic devices due to its smallest electron effective mass among III-nitrides. [2] Of course, those devices require high crystalline quality materials. Unfortunately, the epitaxy of InN and InGaN is quite difficult due to the low maximum epitaxial temperature and the large lattice mismatch of InN over common buffer layers and/or substrates (for example 11% with GaN and 25% with sapphire).[3-4] Thus, the experimentally detected electron mobility of InN is still far away from the theoretical prediction.[5]

We have proposed two growth methods to improve the electron mobility of InN. One is "boundary-temperature-controlled epitaxy",[6] and the other is "extremely In-rich growth technology"[7]. Both the two kind of samples are grown by molecular beam epitaxy. MOCVD-grown GaN layers with a thickness of around 4-5 um are usually used as templates. After the regrowth of GaN layer by MBE, the InN growth is directly started.

For boundary-temperature-controlled epitaxy, where the growth temperature of InN is controlled at its maximum one, InN film exhibits a directly-probed mobility of 3010 cm^2/Vs and a residual electron concentration of 1.77×10^{17} cm^{-3} at room temperature Hall-effect measurement, which corresponds to a mobility of 3280 cm^2/Vs and a residual electron concentration of 1.47×10^{17} cm^{-3} in InN bulk layer, taking into account of surface electron accumulation layer.

To further improve the electron mobility of InN and be compatible with existing processing technologies developed for Si integrated circuits, we studied the epitaxy of InN films grown under extremely In-rich condition on Si substrate. The electron mobility reached 3640 $cm^2V^{-1}s^{-1}$ with the residual electron concentration of 2.96×10^{17} cm^{-3} at room temperature, which corresponds to a mobility of 3970 $cm^2V^{-1}s^{-1}$ and an electron concentration of 2.45×10^{17} cm^{-3} in the InN bulk layer, taking into account of the electron accumulation layers with an electron density of 5.83×10^{13} cm^{-2} and a mobility of 429 cm^2/Vs.

[1] J. Wu, W. Walukiewicz, K. M. Yu, W. Shan, J. W. Ager, E. E. Haller, H. Lu, W. J. Schaff, W. K. Metzger, and S. Kurtz, J. Appl. Phys. 94, 6477 (2003).
[2] T. Itoh, A. Kobayashi, J. Ohta, and H. Fujioka, Appl. Phys. Lett. 109, 142104 (2016).
[3] Y. Saito, N. Terauchi, A. Suzuki, T. Araki, and Y. Nanishi, Jpn. J. Appl. Phys. 40, L91 (2001).
[4] V. Lebedev, V. Cimalla, T. Baumann, O. Ambacher, F. M. Morales, J. G. Lozano, and D. González, J. Appl. Phys. 100, 094903 (2006).
[5] V. M. Polyakov and F. Schwierz, Appl. Phys. Lett. 88, 032101 (2006).
[6] X.Wang, S. Liu, N. Ma. L, Feng, G. Chen, F. Xu, N. Tang, S. Huang, K. Chen, S. Zhou and B. Shen, Appl. Phys. Express 5, 015502 (2012).
[7] H. Liu, X.Wang, Z. Chen, X. Zheng, P. Wang, B. Sheng, T. Wang, X. Rong, M Li, J. Zhang, X. Yang, F. Xu, W. Ge and B. Shen, Appl. Phys. Lett. to be published.

Stacking-fault-free (20-2-1) GaN on 4" sapphire substrates: a pathway to commercialize semipolar optoelectronics

J. Song [1,2], J. W. Choi [2], and J. Han [1]

[1] *Department of Electrical Engineering, Yale University, New Haven, CT, USA*
[2] *Saphlux Inc, Branford, CT, USA*

Semipolar and nonplar orientations of gallium nitride (GaN) have the possibility to address long-standing problems in III-Nitride light emitting diodes (LEDs). They have drawn substantial attentions since 2000 [1]. In the past several years, high output power green and blue LEDs and laser diodes (LDs) have been demonstrated on (20-21), (20-2-1), and several other oriented GaN [2-5], respectively. However, all these high-brightness semipolar GaN devices have only been produced on bulk GaN substrates [2-5]. These bulk GaN substrates are produced by cross-slicing GaN crystals into tiny stripes and are not compatible with mass production. It is highly desirable to produce high quality semipolar GaN films of any orientation on large-diameter sapphire substrates without the need for bulk or high-rate crystal growth process.

We will present our recent work about eiminating the stacking faults in heteroepitaxy of semipolar GaN on large-area sapphire substrates. Focus will be given to the understanding and control of stacking faults in the semipolar GaN, which has been a most challenging issue due to the formation of nitrogen-polar (000-1) facet in heteroepitaxy. As an example, we will exhibit high quality stacking-fault-free semipolar (20-21) and (20-2-1) GaN grown on large size 4-inch sapphire substrates. We will also demonstrate the growth of blue and green LEDs on stacking-fault-free semipolar GaN/sapphire templates. The availability of high-quality stacking-fault-free semipolar GaN-on-sapphire templates will enable the manufacturable production of high-performance, next generation GaN LEDs with economic feasibility.

References
[1] P. Waltereit *et al.*, Nature, **406**, 865 (2000).
[2] Y. Zhao *et al.*, Applied Physics Express, **4**, 082104 (2011).
[3] C.C. Pan *et al.*, Applied Physics Express, **5**, 062103 (2012).
[4] S. Takagi *et al.*, Applied Physics Express, **5**, 82102 (2012).
[5] D.L. Becerra *et al.*, Applied Physics Letters, **105**, 171106 (2014).
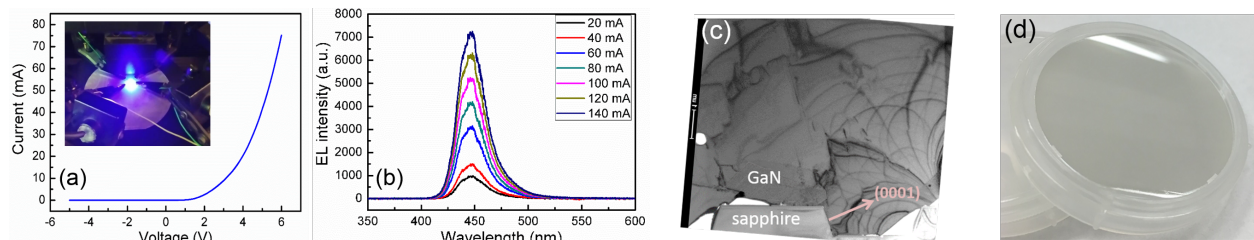
Figure 1. (a) I-V curve of a $(20\bar{2}1)$ LED die and inset shows a photo of a blue LED on a 4-inch $(20\bar{2}1)$ wafer. (b) Electronlumilescence spectra with different injection current, (c) Cross-sectional TEM image under two-beam condition taken along a diffraction vector of $g = <10\bar{1}0>$, confirming SF-free, and (d) a photo of a 4-inch, stacking-fault-free $(20\bar{2}1)$ GaN grown on sapphire.

MOVPE grown AlN on nano-patterned sapphire substrates with different offcut angles

S. Walde [1], **S. Hagedorn** [1], **P.-M. Coulon** [2], **P.A. Shields** [2], **G. Kusch** [3], **G. Naresh-Kumar** [3], **C. Trager-Cowan** [3], **A. Knauer** [1], **R.W. Martin** [3], and **M. Weyers** [1]

[1] *Ferdinand-Braun-Institut, Leibniz-Institut fuer Hoechstfrequenztechnik, Gustav-Kirchhoff-Straße 4, 12489 Berlin, Germany*
[2] *Centre of Nanoscience & Nanotechnology, University of Bath, Bath, BA2 7AY, UK, Department of Electronic and Electrical Engineering, University of Bath, Bath, BA2 7AY, UK*
[3] *Department of Physics, SUPA, University of Strathclyde, 107 Rottenrow East, Glasgow G4 0NG, UK*

Due to the lack of AlN bulk crystals of sufficient size at affordable cost AlN on sapphire is commonly used as the starting template for AlGaN-based ultraviolet light-emitting diodes (UV LEDs). However, from this approach two major problems arise: The heteroepitaxial growth leads to a high density of threading dislocations and the light extraction efficiency is reduced by total internal reflection at the planar AlN/sapphire interface. Growing on nano-patterned sapphire substrates (NPSS) is a promising technique for addressing these challenges by enabling an efficient defect reduction and an enhanced light extraction through the textured AlN/sapphire interface.

We will present MOVPE growth and characterization of AlN on 2-inch NPSS consisting of **c**-plane sapphire with hexagonally aligned patterns of nano-pillars. Those nano-pillars have a top diameter of 260 nm and a pitch of 1 μm and were prepared using Displacement Talbot Lithography combined with Inductively Coupled Plasma Etching. By selecting particular growth parameters it is possible to overgrow these patterns ending up with a fully coalesced surface [1]. However, for the typical sapphire offcut of 0.2 ° towards the *m* direction the surface shows step bunches with a height of 10 nm (Fig. 1 a), which is undesirable for further AlGaN growth. By changing the offcut to 0.1 ° towards *m* we were able to increase the smoothness of the surface by suppressing the formation of step bunches (Fig. 1 b). Combined with a threading dislocation density below 10^9 cm^{-2} estimated by ECCI, this represents a high quality UV LED template. So as the next step the growth of AlGaN layers on top of the NPSS will be targeted.
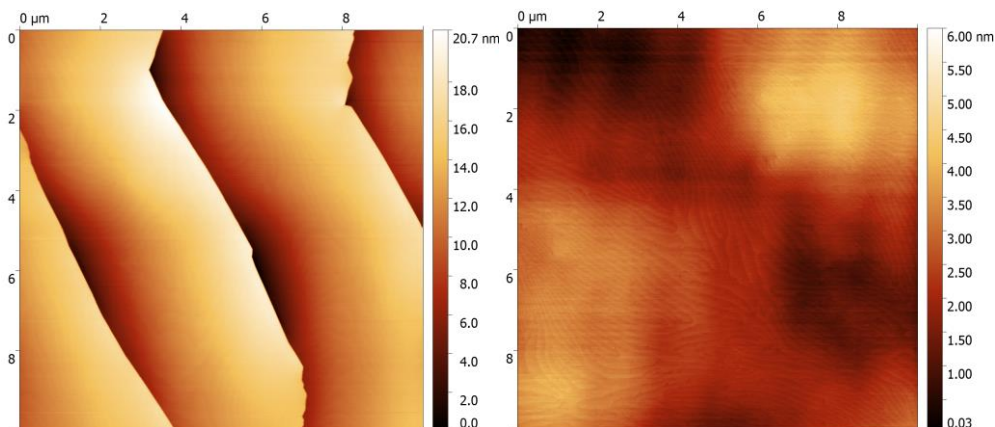
Figure 1: AFM images of the AlN surface of the overgrown patterns of nano-pillars on sapphire with 0.2° (a) and 0.1° (b) offcut towards the m direction.

[1] S. Hagedorn, A. Knauer, A. Mogilatenko, E. Richter, and M. Weyers, Phys. Status Solidi A **213**, No. 12, 3178-3185 (2016).

Semi polar (10-11) GaN growth on silicon-on-insulator substrates for defect reduction and melt back etching suppression

R. Mantach [1,2], G. Feuillet [2] P. Vennéguès [1], P. De Mierry[1], J. Zuniga Perez[1]

[1] *Université Côte d'Azur CNRS CRHEA, Rue Bernard Gregory, Valbonne, France*
[2] *Université Grenoble Alpes CEA-LETI, 17 rue des Martyrs, Grenoble, France*

Group III-nitride semiconductors (including GaN, AlN…) are essential materials for the optoelectronic devices, but they are mainly limited to polar GaN grown along c-axis. This orientation presents a number of fundamental issues such as the internal polarization field effect etc. In order to grow polarization-free III-nitride semiconductor, semi polar growth has been developed which drastically reduces the internal polarization effects. However semi-polar bulk substrates are still of small size and high cost, hence the need of a heteroexpitaxial growth i.e. GaN grown on foreign substrate. The later presents a huge dislocation density especially when it is grown on a planar substrate. Therefore, in order to reduce the defect density, GaN has been grown on a patterned foreign substrate, such as sapphire and silicon, where growth takes place on inclined facets. Growth on Si is yet to improve, regarding the presence of the so-called melt-back etching, a reaction between Si and Ga, and the defect density that can be reduced.

In this presentation we will illustrate a method to eliminate the melt-back etching and to reduce even more the defect density using an original patterned substrate: Silicon on insulator (SOI). The advantage that SOI gives us is the possibility to control the thickness of the Si top layer, therefore controlling the interaction surface between Ga and Si to eliminate the melt-back phenomenon and on the other hand reduce the dislocation density related to the area of the Si growth surface.

Pyramidal growth takes place on the Si facets and the pyramidal shape of GaN results in dislocation bending towards the surface in the inclined c-plane. We will show how reducing the size of the facet results in drastically reducing the width of the area where dislocations intersect the surface.

Growth is divided into two steps, the first one is to ensure a good GaN nucleation on the small Si facets (150 nm of thickness) and a very selective growth and the second step is to enhance the growth in the c-direction to make a completely coalesced layer.

Cathodoluminescence and photoluminescence measurements have been done to prove the reduction of dislocation density, X-ray diffraction measurements assesses the structural quality of the GaN layer. Scanning Electron Microscopy images proves that melt-back etching does not occur and evidences the evolution of the GaN pyramidal shape during growth.

Invited lecture

InGaN quantum structures on patterned substrates

Marcin Sarzyński[1,2], Grzegorz Targowski[1,2], Ewa Grzanka[1,2], Szymon Grzanka[1,2], Sławomir Sakowski[1]

[1] *Institute of High Pressure Physics PAS, Sokołowska 29/37, 01-142 Warsaw, Poland*
[2] *TopGaN Ltd., Sokołowska 29/37, 01-142 Warsaw, Poland*

III-N quantum structures with large indium composition (30-40%) have important potential applications, such as general lighting and solar cells. However, due to huge lattice mismatch between InN and the substrate GaN such structures are difficult to grow with high quality. One technique to increase indium composition is to grow InGaN/GaN quantum wells (QWs) on relatively thick (40-300 nm) InGaN buffer layer with low indium composition (3-5%), see Fig. 1a. To suppress defect creation in these structures we grew them on substrates with ridges (see Fig. 1b). Growth method was metalorganic vapor phase epitaxy (MOVPE). It was found that, photoluminescence wavelength in the studied structures strongly depends on the ridge width (Fig. 1c).

In the present work we study indium composition and layer thickness near the ridge. We found that both parameters vary substantially near the ridge walls on lateral scale of several micrometers. This scale increased with growth pressure and we suggest that they were due to gas phase diffusion. We regard the ridge wall as an additional sink for precursors during growth [1] and we perform diffusion simulations using ANSYS Fluent software. We suggest that the observed diffusion phenomena and elastic strain relaxation could be main reasons of the PL wavelength variations in QW structures.
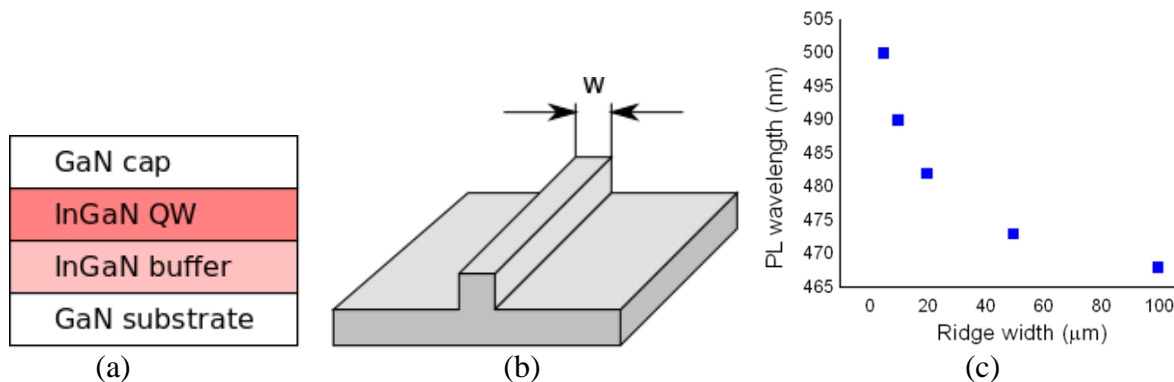
Fig. 1. a) Structure schematic of InGaN QW grown on GaN substrate with InGaN buffer, b) schematic of GaN substrate with ridge width **w**, c) photoluminescence wavelength of the InGaN QW structure as a function of **w**.

[1] H. Fang *et al.*, *J. Appl. Phys.* **103**, 014908 (2008).

Invited lecture

Vertical Power Devices based on Bulk GaN Substrates

Isik C. Kizilyalli

Advanced Research Project Agency – Energy, U.S. Department of Energy

Silicon (Si) has been the semiconductor material of choice for power devices for quite some time due to cost, ease of processing, and the vast amount of information available about its material properties. Si devices are, however, reaching their operational limits in blocking voltage capability, operation temperature, and switching frequency due to the intrinsic material properties of Si. Wide bandgap (WBG) power semiconductors, such as gallium nitride (GaN) and silicon carbide (SiC), are an attractive emerging alternative to Si in many applications. Power converters based on WBG devices can achieve both higher efficiency and higher gravimetric and volumetric power conversion densities than the equivalent Si based converters. The power figure of merit (PFOM), which captures the trade-off between the device specific resistance (Rsp) versus the device BV clearly illustrates the advantage of GaN over Si and SiC devices. This arises from the cubed dependence of the figure-of-merit on the critical electric field where the critical electric field for GaN is 10 times that of Si and 1.6 times that of SiC. To date, the majority of GaN power device development has been directed toward lateral architectures, such as high-electron mobility transistors (HEMTs), fabricated in thin layers of GaN grown on foreign substrates (including Si or SiC). Such lateral devices suffer from well-known issues such as current-collapse, dynamic on-resistance, inability to support avalanche breakdown, and inefficient thermal management. Many of these shortcomings arise from defects originating in the very large lattice and coefficient of thermal expansion (CTE) mismatch between GaN and the substrate. Furthermore, most power electronics semiconductor and diodes are vertical architectures. Fabricating vertical semiconductor device structures on lattice and CTE matched bulk GaN substrates possible to realize the material-limited potential of GaN including true avalanche-limited breakdown and more efficient thermal management, leading to large device currents (> 100A) without resorting to device parallelization, high breakdown voltages (1.2 to 5kV), and increased number of die on a wafer. Recent availability of both 2- and 4-inch bulk GaN substrates is enabling breakthroughs in GaN device performance with vertical diode structures. In this tutorial recent advances in bulk GaN substrates and vertical architecture GaN power electronic devices (diodes, transistors, and application circuits) is surveyed with emphasis on the ARPA-E (Department of Energy) funded projects in the SWITCHES and PNDIODES Programs along with recent significant advances made in Japan. The SWITCHES Program (launched 2013) aimed to catalyze the development of vertical GaN devices using innovations in materials and/or device architectures that drive the costs of the devices. The goal was to enable the development of high voltage (>1200V), high current (100A) single die power semiconductor devices that, upon ultimately reaching scale, would have the potential to reach functional cost parity with Si power transistors while also offering breakthrough relative circuit performance (low losses, high switching frequencies, and high temperature operation). The PNDIODES (Power Nitride Doping Innovation Offers Devices Enabling SWITCHES, launched 2017) Program funds transformational advances and mechanistic understanding in the process of selective area doping in the III-Nitride wide band gap (WBG) semiconductor material system and the demonstration of arbitrarily placed, reliable, contactable, and generally useable p-n junction regions that addresses a major obstacle, enables high-performance and reliable GaN vertical power electronic semiconductor devices.

Electrical characterization of homoepitaxial GaN layers for GaN vertical power devices

Jun Suda[1,2] and Masahiro Horita[2]

[1] *Nagoya University, Furo-cho, Chikusa-ku, Nagoya, Japan*
[2] *Kyoto University, Katsura, Nishikyo-ku, Kyoto, Japan*

Gallium nitride (GaN) is one of the most promising semiconductors for next-generation power devices due to its large breakdown electric field and high electron mobility. In particular, GaN vertical power devices fabricated on GaN substrates have attracted much attention for power devices with large blocking voltage and high current capability. To realize GaN vertical power devices, growth of low-doped thick GaN drift layer (voltage-blocking layer) is crucial. For 10 kV-class devices, doping concentration of low 10^{15} cm^{-3} and thickness of >50 μm are required.

To realize such a low doping, concentrations of residual impurities and native point defects should be much lower than the target doping concentration. Last two decades, growth technologies for GaN-based light-emitting diodes (LEDs), laser diodes (LDs) and high-electron-mobility transistors (HEMTs) have been extensively developed. However, these technologies are not directly applicable for the growth of the drift layer since the requirement for the growth is very different. Further development of growth technologies is required. For the development, it is very important to characterize grown layers to obtain good feedback for growth. In addition, detailed electrical properties of such low-doped n-GaN layers have not been understood yet. In this paper, we present electrical characterization of metal-organic-vapor-phase-epitaxy (MOVPE)-grown low-doped n-type GaN grown on hydride-vapor-phase-epitaxy (HVPE)-grown free-standing GaN substrates with threading dislocation density of 3×10^6 cm^{-2}.

Compensation mechanism

We investigated compensation mechanism in MOVPE-grown Si-doped homoepitaxial GaN layers [1]. By analyzing temperature-dependence of Hall-effect measurements, donor and compensating acceptor concentrations were extracted separately. For low-doped layers (< 5×10^{16} cm^{-3}), the acceptor concentration (2-4×10^{15} cm^{-3}) does not depend on Si doping, and it is close to carbon concentration (2-5×10^{15} cm^{-3}) in the grown layers, indicating that carbon acts as a deep acceptor (C_N) and a major source of compensation. Seeking a way of further reduction of carbon incorporation in MOVPE or other carbon-free growth methods is important. For high-doped layers, we found another compensating acceptor whose concentration is proportional (10-20%) to Si doping.

Wafer-level mapping

Suppression of spatial distribution of net donor concentration and thickness within the wafer is necessary towards mass production of power devices. We performed wafer-level electrical mapping by using matrix array of small Schottky contacts [2]. In addition to net donor concentration, distribution of trap concentration was measured. The trap distribution was different from the net donor distribution. Looking at both net donor and trap distributions is very important for optimization of growth conditions as well as reactor design.

[1] N. Sawada, T. Narita, M. Kanechika, T. Uesugi, T. Kachi, M. Horita, T. Kimoto and J. Suda, Applied Physics Express, **11**, 041001 (2018).
[2] M. Horita, T. Narita, T. Kachi, T. Uesugi, and J. Suda, IWN2016, D1.7.03.

Characterization of Shallower Level Traps in p-GaN Grown by MOVPE Using Low Frequency Capacitance DLTS

Y. Tokuda [1], T. Kogiso [1], T. Narita[2], K. Tomita[2] and T. Kachi [3]

[1] *Aichi Institute of Technology, Yakusa, Toyota, Japan*
[2] *Toyota Central R&D Laboratories Inc., Nagakute, Japan2*
[3] *Nagoya University, Chikusa-ku, Nagoya, Japan*

We have already observed hole traps in p-GaN grown by MOVPE using n^+p diodes by capacitance DLTS [1,2].   Then, capacitance measurements were made using the frequency at 1 MHz which is conventionally used for DLTS measurements.   However, the lower measurement temperature of 1 MHz capacitance DLTS for GaN n^+p diodes is restricted to around 200 K due to the unionization of Mg acceptors. This is due to the higher resistance of neutral p-GaN with decreasing temperatures. To extend the DLTS measurements to the lower temperatures, measurement frequencies of capacitance should be lowered to increase the reactance arising from depletion layer capacitance to neglect the resistance of the neutral region.   In this work, we used 1 kHz capacitance DLTS to detect shallower level traps in p-GaN of p^+pn^+ diodes consisting of 100-nm p^+([Mg]=8×10^{19} cm^{-3})/700-nm p([Mg]=2×10^{17} cm^{-3})/200-nm n^+([Si]=1×10^{19} cm^{-3}) on n-GaN substrate.

Fig.1 shows the already reported 1 MHz capacitance DLTS spectrum, where four hole traps labeled H_c (0.46 eV), H_d (0.88 eV), H_e (1.0 eV) and H_f (1.2 eV) are detected [1,2]. It is noted that another peak around 150 K is observed. However, as shown in Fig. 1, the 1 MHz capacitance decreases with decreasing temperatures due to the unionization of Mg acceptors around 150 K, which might affect the DLTS spectrum. Fig.2 shows the 1 kHz capacitance DLTS spectrum together with the temperature dependence of the 1 kHz capacitance, where two hole traps labeled H_a (0.29 eV) and H_b (0.33 eV) are clearly observed. H_a and H_b trap concentrations are obtained to be 8.1×10^{15} cm^{-3} and 4.0×10^{15} cm^{-3}, respectively.

In summary, we performed 1 kHz capacitance DLTS to study shallower level traps in p-GaN grown by MOVPE. Tow traps labeled H_a (0.29 eV) and H_b (0.33 eV) are detected in addition to H_c (0.46 eV), H_d (0.88 eV), H_e (1.0 eV) and H_f (1.2 eV) which have been observed in 1 MHz capacitance DLTS. The trap concentration of H_a is found to be comparable to that of H_d, the dominant hole trap in MOVPE p-GaN.

[1] Y. Tokuda, T. Kogiso, T. Narita, K. Tomita, and T. Kachi, EMRS 2017 Fall Meeting, P.7.3.
[2] T. Narita, Y. Tokuda, T. Kogiso, K. Tomita, and T. Kachi, to be published in *J. Appl. Phys.*
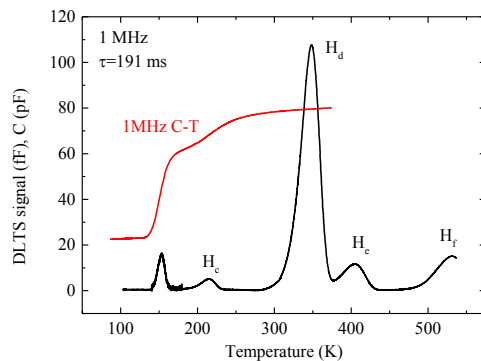
Fig.1 1 MHz capacitance DLTS spectrum.
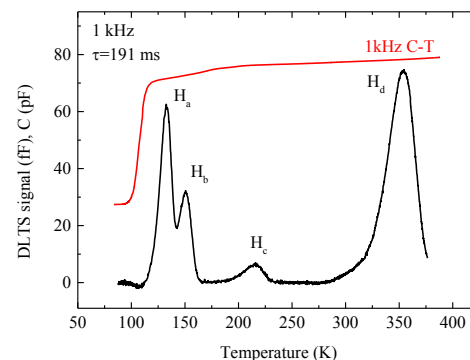
Fig.2 1 kHz capacitance DLTS spectrum.

Accurate estimation of H1 trap concentration in n-type GaN layers

K. Kanegae [1], **M. Horita** [1], **T. Kimoto** [1] **and J. Suda** [1, 2 ,3]

[1] *Kyoto Univ., Nishikyo, Kyoto City, Japan*
[2] *Nagoya Univ. IMaSS, Chikusa, Nagoya City, Japan*
[3] *Nagoya Univ., Chikusa, Nagoya City, Japan*

Reduction of deep traps in GaN epitaxial layers is one of the most important issues to realize high performance GaN devices. Previous studies have reported that E3 trap ($E_T = E_C - 0.59$ eV, the capture cross section: $\sigma_n = 3.2 \times 10^{-15}$ cm^2 [1]) and H1 trap ($E_T = E_V + 0.87$ eV, $\sigma_p = 1.0 \times 10^{-13}$ cm^2 [1,2]) in MOVPE-grown homoepitaxial n-type GaN layers are dominant electron and hole traps, respectively. Accurate estimation of trap concentrations is necessary to optimize growth parameters. Such estimation is easy for E3 trap (majority carrier trap), while it is difficult for H1 trap because of complicated processes during measurements. In this study, an analysis method for accurate estimation of the H1 trap concentrations in minority carrier transient spectroscopy (MCTS) is proposed. The analysis considers not only hole occupancy ratio during filling period but also a quick recombination process at the very initial stage of measurement period. The method was applied to a MOVPE-grown homoepitaxial n-type GaN layer.

Fig. 1 shows a schematic cross-section of a GaN p-n junction diode (PND) with SIMS results of the GaN epitaxial layer grown by MOVPE. The Si concentration is 3.0×10^{16} cm^{-3} in the n$^-$-type layer and the Mg concentration is 5×10^{19} cm^{-3} in the p$^+$-type layer. The doping concentrations are spatially uniform. In this study, a one-sided abrupt junction was assumed. Current injection isothermal capacitance transient spectroscopy (ICTS) was performed on the GaN PND at 300 K. The measurement bias voltage U_R ranges from 1 to –50 V.

Apparent H1 trap concentrations $\widetilde{N}_T$ in the n-type GaN layer obtained from the ICTS spectra are plotted in Fig. 2. $\widetilde{N}_T$ depends on the depletion layer width w, which changes with U_R. In the case of large w, there is the region where H1 traps are not filled with the holes because the holes cannot reach during the filling pulse in the depletion layer. Thus, the emission of holes from the H1 traps is decreased and $\widetilde{N}_T$ is underestimated compared to the true H1 trap concentration N_T. This underestimation can be well reproduced by using a model taking account of the hole diffusion and is indicated as a red dashed line in Fig. 2 (effect A). In the case of small w, the H1 traps at the edge of the depletion layer capture electrons very quickly at the very initial stage of measurement period, and these traps do not contribute to the peak in the ICTS spectrum which is determined from the thermal emission with time constant of ~30 s. Thus, even if the H1 traps are completely filled with the holes by the filling pulse, $\widetilde{N}_T$ is also underestimated. This underestimation can be well reproduced by using a model taking account of the electron capture near the edge of the depletion layer and is indicated as a blue dashed line in Fig. 2 (effect B). The experimental results fitted to these models and $N_T = 2.3 \times 10^{15}$ cm^{-3} was obtained. Most of previous studies seem to consider only effect A. Our results clearly show that accurate H1 trap concentration can be obtained by considering both effects.

[1] Y. Tokuda, ECS Transs. **75** (4), 39 (2016).
[2] A. Y. Polyakov, N. B. Smirnov, E. B. Yakimov, I. H. Lee and S. J. Pearton, J. Appl. Phys. **119**, 015103 (2016).
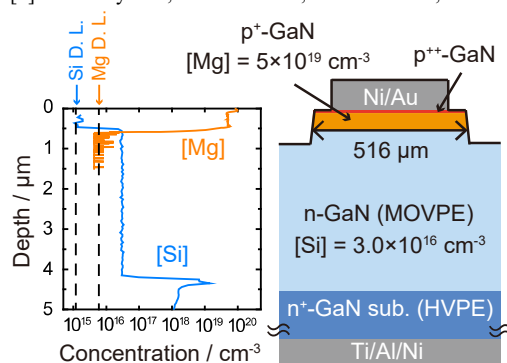
Fig. 1 Schematic cross-section of the GaN PND and the depth profiles of Si and Mg concentrations measured by SIMS.
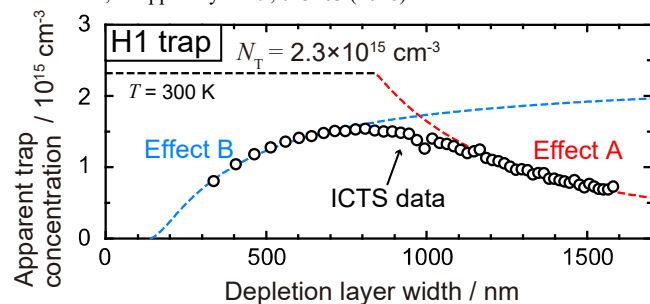
Fig. 2 Dependence of the apparent H1 trap concentration on the depletion layer width, which is varied by the measurement bias. The open circles are the experimental values. The red and blue dashed lines present fitting curves taking account of the effect A and B, respectively.

Invited lecture

Donor states of carbon in p-type GaN grown by MOVPE

T. Narita [1]**, K. Tomita** [1]**, Y. Tokuda** [2]**, T. Kogiso** [2]**, M. Horita** [3]**, and T. Kachi** [4]

[1] *Toyota Central R&D Labs., Inc., Yokomichi, Nagakute 480-1192, Japan*
[2] *Aichi Institute of Technology, Toyota 470-0392, Japan*
[3] *Kyoto University, Kyoto 615-8510, Japan*
[4] *Nagoya University, Nagoya 464-8601, Japan*

The well-controlled p-type GaN (p-GaN) layers are crucial for controlling threshold voltages of vertical GaN power devices. Although magnesium (Mg) is the only p-type dopant with shallow acceptor levels in GaN, the sources of hole compensation in the Mg-doped GaN are not clarified. In the case of n-GaN grown by metalorganic vapor phase epitaxy (MOVPE), the 0/-1 charge state of a carbon on nitrogen site (C_N) plays a key role as a compensation source [1]. We previously reported the formation of identical C_N state in p-GaN layer grown by MOVPE [2]. The first principle calculation predicted the +1/0 transition of C_N state at an energy of E_V +0.35 eV [3] but such donor states are not supported by experiments. In this paper, we experimentally reveal the donor states of C_N in MOVPE-grown p-GaN samples with different carbon concentrations [C] by using temperature-dependent Hall-effect analyses.

We prepared the p-GaN samples doped with Mg concentration [Mg] of 1×10^{17} cm^{-3} and doped with [C] of $(0.2\text{-}4.8)\times10^{16}$ cm^{-3} on n-GaN substrates by controlling the temperature and the pressure during MOVPE-growth. The p$^+$-GaN contact layers were formed on sample surfaces, and the p$^+$ layers other than under Ni/Au ohmic electrodes were removed by dry etching. Figure 1 shows the temperature-dependent hole concentrations (120-470 K). The curve fitting according to the charge-neutrality condition gave both acceptor and donor concentrations (N_a and N_d) for samples as shown in Table 1. The N_a values were in good agreement with [Mg], while the N_d values compensating holes increased with increasing [C]. The hole mobility μ was reduced by elevating [C], especially below 200 K. Table 1 also shows μ values at 160 K as a representative. The low-temperature mobility is limited by the charged-impurity concentration due to the ionized-impurity-scattering. Therefore, the lower mobility and the higher N_d for the higher [C] sample provide evidence of the positively-charged C_N donor state under the the Fermi level close to the valence band.

This work was supported by MEXT GaN R&D Project.

Fig.1. Temperature-dependent hole concentrations
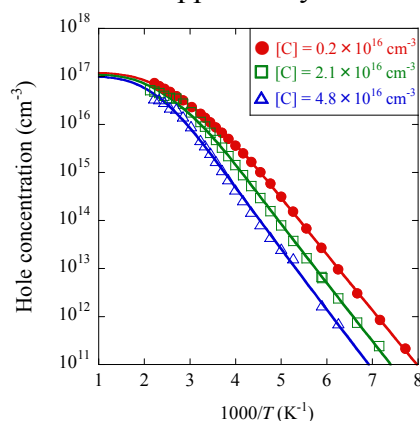
Table 1. Summary of N_d, N_a, [C] and μ for samples

Sample	N_a (cm^{-3})	N_d (cm^{-3})	[C] (cm^{-3})	μ (cm^{-3}) @160K
A ●	1.3×10^{17}	1.4×10^{16}	0.2×10^{16}	156
B □	1.4×10^{17}	2.7×10^{16}	2.1×10^{16}	96
C △	1.6×10^{17}	5.8×10^{16}	4.8×10^{16}	61

[1] N. Sawada, T. Narita, *et al.*, Appl. Phys. Express **11**, 041001 (2018).
[2] T. Narita, Y. Tokuda, T. Kogiso, K. Tomita, and T. Kachi, J. Appl. Phys. **123**, 161405 (2018).
[3] J.L. Lyons, A. Janotti, and C.G. Van de Walle, Phys. Rev. B **89**, 035204 (2014).

Invited lecture

On the preparation of AlN single crystal boules and substrates for AlGaN devices

Carsten Hartmann, **Juergen Wollweber**, **Andrea Dittmar**, **Klaus Irmscher**, **Matthias Bickermann**

Leibniz Institute for Crystal Growth, Max-Born-Str. 2, 12489 Berlin, Germany

Bulk AlN single crystals are highly interesting as substrates for UVC devices comprised of pseudomorphically strained $Al_xGa_{1-x}N$ layers (with x>0.6). The device characteristics and efficiency is greatly influenced by, (i) an epi-ready (chemo-mechanically polished) surface with high crystalline perfection (for low dislocation densities in the epilayers), (ii) specific off-cut orientations (for layer-by-layer growth to prevent compositional changes in the epilayers), and (iii) deep-UV optical transmittance (for light outcoupling). In this presentation the challenges to satisfy the above requirements and the routes to solve them are discussed. The focus is on the bulk AlN crystal growth technology employed at IKZ, i.e., physical vapor transport (PVT) of AlN in TaC crucibles at seed temperatures below 2100°C, with N-polar growth direction.

EPI-ready Al-polar c-AlN substrates are prepared by using a qualified chemo-mechanical polishing (CMP) process. Transmission and back-reflection topographs of the substrates reveal TDD $< 10^4$ cm^{-2} over the entire area of substrates. No residual polishing-induced subsurface damage is visible in the topographs. The accuracy of the wafer orientation reliable achieve miscuts $< 0.2°$ ensuring long terrace widths of the step flow when growing epi-layers.

Deep-UV transparent AlN crystals with $\alpha < 25$ cm^{-1} at 265 nm are grown with the above-mentioned technique when the concentrations of oxygen, silicon, and carbon impurities [O], [SI], and [C] satisfy the inequalities [1]:

$$3[C] < ([O] + [Si]) \text{ and}$$
$$([O] + [Si] + [C]) < 10^{19} \text{ cm}^{-3}.$$

These conditions can be reached using getter materials for carbon and oxygen. TaC has proven to be highly efficient by converting $Al_2O(g)$ to CO(g). Remaining volatile carbon species can be efficiently gettered by adding tungsten which reacts partially to W_2C during the growth. Best values of $\alpha(265nm) = 14$ cm^{-1} are achieved at [O] = 6.4×10^{18} cm^{-3} and [C] = 1.8×10^{18} cm^{-3}. Entire AlN wafers (Ø $\geq$ 10 mm) with $\alpha(265nm) < 25$ cm^{-1} can be grown in a reproducible manner.

[1] C. Hartmann, J. Wollweber, S. Sintonen, A. Dittmar, L. Kirste, S. Kollowa, K. Irmscher, M. Bickermann, CrystEngComm 18 (2016) 3488-3497

Invited lecture

Homoepitaxy of AlN on annealed AlN/sapphire template

H. Miyake[1,2], K. Shojiki[2], X. Liu[1], Y. Hayashi[1], X. Shiyu[1], K. Uesugi[3]

[1] *Graduate School of Regional Innovation Studies, Mie University, Tsu, Japan*
[2] *Graduate School of Engineering, Mie University, Tsu, Japan*
[3] *Organization for the Promotion of Regional Innovation, Mie University, Tsu, Japan*

AlN-based UV light-emitting devices have great potentials in a wide range of applications such as a water purification. AlN templates with a low density of threading dislocations (TDs) is essential for UV light-emitting devices. In the case of AlN/sapphire templates, a lower production cost with larger wafer diameter can be expected. Recently, we obtained high-crystal-quality sputter-deposited AlN/sapphire templates using face-to-face high-temperature annealing in N_2 atmosphere [1]. In this study, we investigated the growth condition of metal-organic vapor phase epitaxial (MOVPE) growth of AlN to realize the atomically flat surface.

The growth rate increases with increasing the NH_3 flow rates. When the growth rate is about 1.0 µm/hr, the atomically flat surface with atomic-step-and terrace structure was obtained with step height of about 0.29 nm. This height roughly agrees with the height (0.25 nm) of monolayer of AlN. Step bunching occurs when the growth rate is slower than 1.0 µm/hr. Spiral growth occurs when the growth rate is faster than about 1.0 µm/hr.

MOVPE-grown AlN film and annealed sputter-deposited AlN/sapphire template. The full-width at the half maximum (FWHM) values of the X-ray rocking curves (XRCs) for (0002)- and (10-12)-planes of the MOVPE-grown AlN film were about 31 and 236 arcsec. From these values, the screw- and edge-dislocation densities were calculated to be about 1.0×10^6 and 7.4×10^8 cm^{-2} by the technique reported by P. Gay *et al.*[2], respectively. Figure 1(a) shows cross-sectional bright field transmission electron microscopy (TEM) images of the MOVPE-grown AlN film with the MOVPE-growth rate of 1.0 µm/hr. Cross-sectional dark-field images under two-beam condition with g = 0002 and 1-100 are also shown in Fig. 1 (b) and (c), respectively. There are few screw and mix dislocations, while the density of edge dislocation is estimated to be 1×10^9 cm^{-2}. The TD densities calculated from XRC data are well agree with values obtained from the TEM observation.
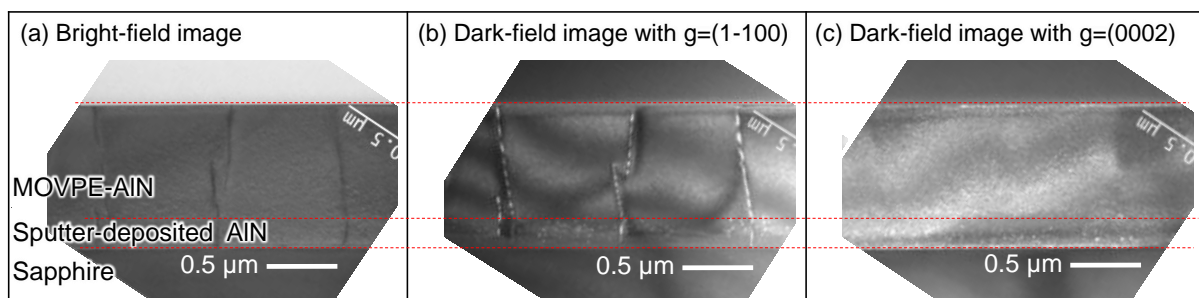
Fig. 1 Cross-sectional TEM images for the AlN film grown on annealed sputter-deposited AlN. (a) Bright-field image and (b) dark-field images under (b) *g=(1-100)* and (c) *(0002)* conditions.

[1] H. Miyake *et al.*: J. Cryst. Growth **456**, 155 (2016).
[2] P. Gay *et al.*: Acta Metallurgica **1**, 315 (1953).

Di-carbon defects in AlN bulk crystals grown by physical vapor transport

I. Gamov [1]**, C. Hartmann** [1]**, A. Dittmar** [1]**, J. Wollweber** [1]**, M. Bickermann** [1]**,
I. Kogut** [2]**, H. Fritze** [2]**, and K. Irmscher** [1]

[1] *Leibniz-Institut für Kristallzüchtung, Max-Born-Strasse 2, 12489 Berlin, Germany*
[2] *Institut für Energieforschung und Physikalische Technologien, Technische Universität Clausthal, Am Stollen 19B, 38640 Goslar, Germany*

AlN bulk crystals grown by physical vapor transport unintentionally contain high concentrations of oxygen, carbon (both $10^{18} – 10^{19}$ cm^{-3}), and silicon (~10^{17} cm^{-3}) impurities. These impurities are known to introduce energy states within the band gap of AlN, hence, they strongly influence the optical and electrical properties of the crystals. In particular, carbon related defects are responsible for the broad ultraviolet absorption band around 4.7 eV [1, 2]. This absorption may impair the use of the crystals as a substrate for UV emitters and must be suppressed [3]. Furthermore, AlN single crystals are a promising candidate for high-temperature piezoelectric sensing applications [4], where high electrical resistivity must be maintained at high operation temperatures (> 1000°C). For controlling both UV absorption and high-temperature resistivity, the concentration levels and carbon-to-oxygen ratios seem to play a key role [3, 4]. To achieve genuine control in this respect, detailed knowledge on the various impurity defect configurations and their associated deep levels is necessary.

Here we report on the identification of a di-carbon defect by Raman spectroscopy. The corresponding local vibration mode (LVM) at 1187 cm^{-1} can only be detected under the following conditions. (i) The exciting laser wavelength must be short enough. Our experiments show that for 325 nm the LVM can be excited, while for longer wavelengths (488 nm, 633 nm) not. (ii) The LVM intensity attains a maximum when the exciting light polarization is parallel to the *c*-axis, and it drops to zero for the corresponding perpendicular orientation. Therefore, the LVM is not observable if the exciting light shines perpendicular on a *c*-plane wafer. (iii) It seems that the appearance of the LVM is restricted to crystal regions of *m*-plane growth. These observations hint at (i) a resonance Raman effect due to the UV absorption transitions, (ii) a defect configuration polarizable along the *c*-axis, and (iii) a preferred incorporation of the defect on *m*-planes. The unambiguous identification as a di-carbon defect is based on the three-fold splitting of the LVM in ^{13}C isotope enriched AlN, as shown in Fig. 1. The most probable atomic model of a nearest-neighbor carbon pair $C_N – C_{Al}$ and anticipated electronic properties of the di-carbon defect will be discussed.
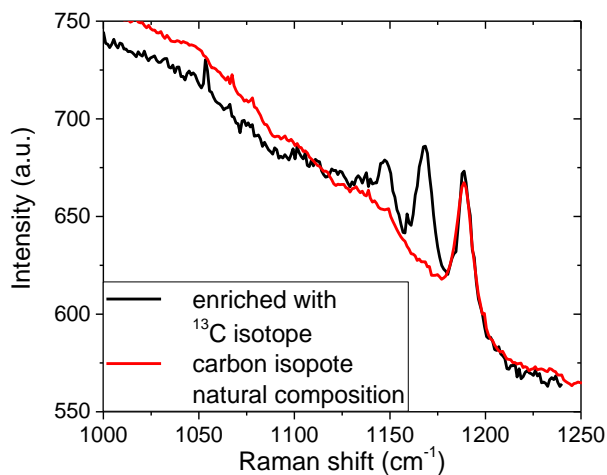
Fig. 1. Raman spectrum of the LVM at 1187 cm^{-1} in an AlN crystal containing the natural C isotope composition in comparison to the spectrum observed in a crystal enriched with ^{13}C.

[1] R. Collazo et al., Appl. Phys. Lett. **100**, 191914 (2012).
[2] K. Irmscher et al., J. Appl. Phys. **114**, 123505 (2013).
[3] C. Hartmann et al., CrystEngComm **18**, 3488 (2016).
[4] T. Kim et al., IEEE Trans. Ultrason. Ferroelectr. Freq. Control **62**, 1880 (2015).

Tuning the growth of AlN epilayers on Al$_2$O$_3$ via TMAl preflow by MOCVD

Haiding Sun[1], Young Jea Park[2], Kuang-Hui Li[1], Theeradetch Detchprohm[2], Russell D. Dupuis[2], Xiaohang Li[1]

[1] *King Abdullah University of Science and Technology (KAUST), Thuwal, 23955 Saudi Arabia*
[2] *School of Electrical and Computer Engineering, Georgia Institute of Technology, Atlanta, Georgia 30332, USA*

AlN and its alloys Al$_x$Ga$_{1-x}$N (0<x<1) have large and direct bandgaps, which are suitable for ultraviolet (UV) devices. However, due to the limited availability of large-scale bulk AlN substrates, most of the UV devices have been developed on AlN templates grown on (0001) sapphire by MOCVD. The growth of high quality AlN epitaxial films relies on precise control of the initial growth stages. In this work, we investigated the influence of trimethylaluminum (TMAl) pretreatment of sapphire substrates on the properties, impurity incorporation and growth mode change of AlN films grown by MOCVD. Prior to each growth, a flow of TMAl was introduced with preflow times of 0, 5, and 40 s (hereafter Sample 1, Sample 2, and Sample 3).[1] Without the pretreatment, no trace of carbon was found at AlN/sapphire interface and the residual oxygen resulted in N-polarity (Sample 1). With 5s pretreatments, carbon started to be incorporated, forming scattered carbon-rich zones due to the decomposition of TMAl. It was discovered that carbon attracted surrounding oxygen impurity atoms and consequently, suppressed the formation of N-polarity (Sample 2). With 40 s pretreatment, a significant presence of carbon clusters at the AlN/sapphire interface occurred, which attracted considerable co-existed oxygen. While preventing the N-polarity, the carbon clusters served as random masks to further induce a 3D growth mode, creating Al-polar AlN nanocolumns with different facets (Sample 3). [2]
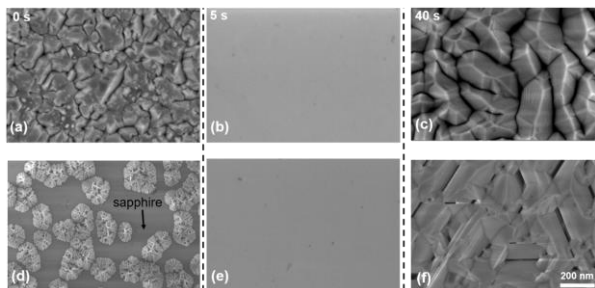
Figure 1. SEM plan-view images of morphological changes of Samples 1, 2 and 3, including (a)-(c) before and (d)-(f) after KOH etching.

Furthermore, a comprehensive investigation of the structural properties, including surface morphology, polarity, and crystal quality of AlN templates were carried out. The structural integrity were revealed and elemental distributions of Al, N, O, and C from the AlN-NL/sapphire interfaces was studied. In particular, we conducted a detailed analysis of the carbon and oxygen impurities at the AlN/sapphire interface where the AlN NL was grown. A correlation between the carbon clustering and the change in polarities and growth modes, is proposed, stressing the significance of appropriate preflow to achieve desirable AlN films.

Figure 2. Schematic of film polarity and growth mechanism with corresponding 3D AFM images of the Sample 1, 2 and 3. Carbon was also presented in the evolving the crystallinity during the nucleation process.

[1] H. Sun et al., Appl. Phys. Lett. **110,** 192106 (2017). [2]H. Sun et al., J. Phys. D: Appl. Phys. 50, 395101 (2017).

Controlling the growth mode and strain of AlN grown directly on 6H-SiC(0001) substrate by metal-organic chemical vapor deposition

Hisashi Yoshida and Shigeya Kimura

Corporate Research and Development Center, Toshiba Corporation, 1, Komukai-Toshiba-Cho, Saiwai-ku, Kawasaki 212-8582, Japan

We investigated the growth mode and strain of AlN grown directly on 6H-SiC(0001) substrate by metal-organic chemical vapor deposition using various V/III ratios. The growth temperature of AlN was fixed at 1200 °C, and V/III ratio of AlN was varied widely. Figure 1 shows atomic force microscopy (AFM) images of 500-nm-thick AlN on 6H-SiC(0001) substrates. The root mean square (RMS) roughness and V/III ratio are also shown in the figure. These results show that the growth mode of AlN was strongly depended on V/III ratio. The growth mode changed from two-dimensional to three-dimensional as the V/III ratio was increased [1], and obvious spiral growth appeared as indicated by dashed circles in Fig. 1. Although the RMS roughness tended to increase a higher degree of spiral growth, the flatness of the 500-nm-thick AlN was satisfactory. In addition, threading dislocation density improved as the V/III ratio was increased, according to AFM and X-ray diffraction measurements. Furthermore, cracks were observed even though the in-plane lattice constant of AlN is larger than that of 6H-SiC(0001) at a V/III ratio of 35. One reason for the cracks in AlN was difference in coefficient of thermal expansion between AlN and 6H-SiC [2]. However, in situ curvature measurement revealed another reason, namely, differences in strain accumulation and its relaxation during AlN growth depending on the V/III ratio. It was demonstrated that compressive strain accumulation was larger at low V/III ratios than at high V/III ratios in the initial growth stage of AlN. As the thickness of AlN increased, the compressive strain decreased dramatically and the tensile strain increased for low V/III growth. Therefore, low V/III growth is thought to lead to cracks in AlN. Note that there was no critical relaxation of compressive strain for high V/III ratio growth in the range of AlN thickness below 500 nm. In this presentation, we discuss the relationship between growth mode and strain of AlN grown directly on 6H-SiC(0001) substrate, and propose a mechanism for differences in strain according to growth mode.
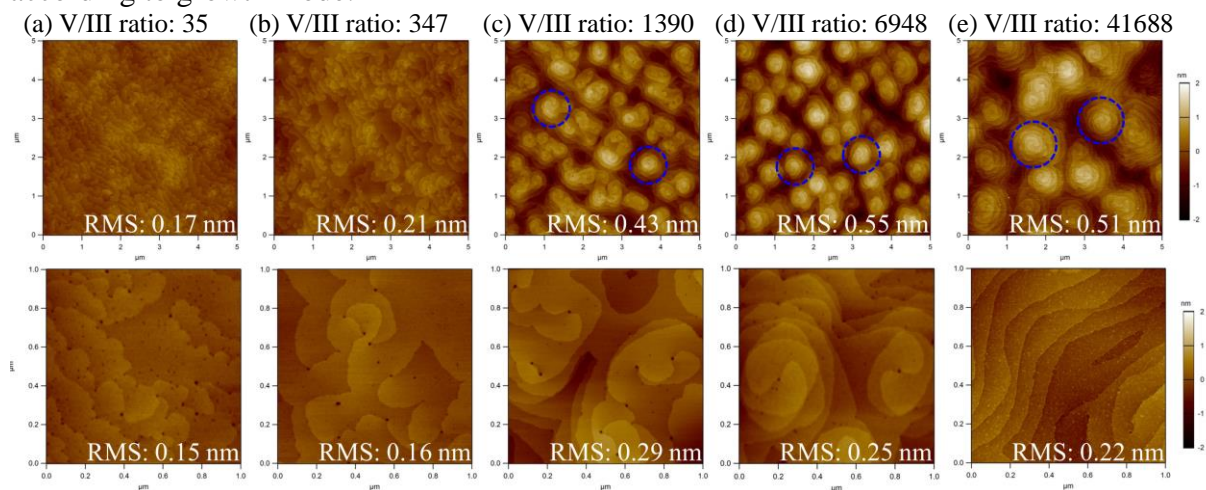
Fig. 1 AFM images of 500-nm-thick AlN grown directly on 6H-SiC(0001) substrate with V/III ratios of (a) 35, (b) 347, (c) 1390, (d) 6948, and (e) 41688.

[1] S. Kitagawa, H. Miyake, and K. Hiramatsu, *Jpn. J. Appl. Phys.* **53**, 05FL03 (2014).
[2] L. Liu and J. H. Edgar, *Mater. Sci. Eng. R* **37**, 61 (2002).

Hot-wall MOCVD growth of N-polar AlN nucleation layer on C-face vicinal and on-axis SiC substrates

Hengfang Zhang, Chih-Wei Hsu, Jr-Tai Chen, Pitsiri Sukkaew and Vanya Darakchieva

Department of Physics, Chemistry and Biology (IFM), Linköping University, SE 581 83 Linköping, Sweden

Group III-nitrides semiconductors have drawn much attention recently for radio frequency applications. For applications of III-nitride materials in high-electron mobility transistor (HEMT) structures, N-polar HEMT heterostructures have several advantages compared to metal-polar ones, including the feasibility to fabricate low ohmic contact, an enhanced carrier confinement with a natural back barrier as well as high device scalability [1,2].

Growth of N-polar layers are expected on C-face SiC substrates [3]. However, previous studies reported that metal(Al)-polarity layers can occur as a result of supplying a pre-flow of metal precursors trimethylaluminum (TMAl) or by keeping a low V/III(NH3/TMAl)-ratio flow [3,4]. This indicates that the initial AlN nucleation step is critical to the polarity control on SiC substrates. Much work has been focused on the growth of N-polar III-Nitride materials by MOCVD. Nevertheless, only cold-wall MOCVD epitaxy has been investigated. On the other hand, hot-wall MOCVD for highly efficient and uniform growth of AlN has also been reported [5]. In addition, hot-wall MOCVD-grown AlN nucleation layers (AlN-NLs) were shown to exhibit a superior structural quality [6], enabling a reducing of the NL thermal-boundary resistance (TBR) by as much as 25% compared to those grown using cold-wall MOCVD, as well as resulting in ~10% reduction of the operating temperature of AlGaN/GaN HEMTs [7].

In this work, we investigated surface morphology, crystalline quality, and polarity of AlN-NLs grown by hot-wall MOCVD on C-face 4H-SiC substrates, cut either on-axis or 4° misoriented towards <11$\bar{2}$0>, as a function of growth temperature. We characterized the AlN-NLs by scanning electron microscopy (SEM), atomic force microscopy (AFM) and high-resolution X-ray diffraction measurement (HR-XRD). The polarity of AlN-NLs was determined by the etching rate in potassium hydroxide solution (KOH) [8]. With decreasing the growth temperature from 1200°C to 850°C, we observed significant changes in the resulting surface morphology and crystalline quality of the N-polar AlN-NLs. The grain sizes of the N-polar AlN-NLs decreased for on-axis 4H-SiC substrates, while the surface step bunching reduced significantly for the 4° misoriented substrates. With decreasing growth temperature from 1200°C to 850°C, the root mean square roughness was reduced significantly from 8.2 nm to 0.7 nm. The full width at half maximum (FWHM) of symmetric (002) ω-scan corresponding to screw dislocation density was not affected by the temperature change. However, the FWHM of asymmetric (102) ω-scan related to edge dislocation density decreased significantly when growth temperature was reduced.

[1] Lemettinen, J., Okumura, H., Kim, … & Suihkonen, S. *J. Cryst. Growth.* (2018).
[2] Wong, M. H., Keller, S., ... & Chini, A. *Semicond. Sci. Technol.*, **28**(7), 074009 (2013).
[3] Keller, S., Fichtenbaum, N., … & Mishra, U. K. *Jpn. J. Appl. Phys.*, **45**(3L), L322 (2006).
[4] Fu, Y., Ni, X., ... & Choyke, W. J. *MRS OPLA*, 955 (2006).
[5] Kakanakova-Georgieva, Anelia, et al. *Cryst. Growth Des.* 9.2 (2008): 880-884.
[6] Chen Jr, -Tai, et al. (2015).
[7] Riedel, Gernot J., et al. *IEEE Electron Device Lett.* 30.2 (2009): 103-106.
[8] Guo, W., Kirste, R., Bryan, ... & Sitar, Z. *Appl. Phys. Lett.*, **106**(8), 082110 (2015).

Crystal quality improvement of sputter-deposited AlN films on SiC substrates by high temperature annealing

K. Uesugi[1], Y. Hayashi[2], K. Shojiki[3], S. Xiao[2], K. Nagamatsu[1], H. Yoshida[1], H. Miyake[2,3]

[1] *Organization for the Promotion of Regional Innovation, Mie University, Tsu, Japan*
[2] *Graduate School of Regional Innovation Studies, Mie University, Tsu, Japan*
[3] *Graduate School of Engineering, Mie University, Tsu, Japan*

For the realization of highly efficient deep ultraviolet (DUV) light-emitting devices, high quality AlN films are indispensable as the templates for MOVPE growth of AlGaN layers. Previously, we have reported the threading dislocation densities of sputtered AlN films on sapphire substrates can be reduced by high temperature face-to-face annealing (FFA) technique [1,2]. However, when the thickness of the AlN film is large, FFA introduces dense of cracks and wafer bowing. From the view point of thermal expansion and lattice constant mismatch, SiC can be more suitable material as the substrates for AlN growth. In this work, we fabricated AlN films on SiC substrates with sputtering and FFA, and characterized the crystal quality of the AlN films.

AlN films were deposited on (0001) on-axis Si-face 6H-SiC substrates by RF sputtering with polycrystalline AlN as the source target. N_2 and Ar were supplied as sputtering gases. Thickness of the AlN films were varied with 100, 200, 400, and 600 nm. During the AlN deposition, substrates temperature, chamber pressure, and RF power were fixed at 600 ºC, 0.2 Pa, and 700 W, respectively. After the deposition, high temperature annealing was performed in FFA configuration at 1700 ºC under N_2 ambient for 3 hrs. The crystal quality of the AlN films were characterized by X-ray diffraction (XRD) measurement.

Figure 1 shows the AlN film thickness dependence of the full width at half maximum (FWHM) values of XRC from AlN (0002) and (10-12) planes. After annealing, these values remarkably decreased compared to those of the samples before annealing. The samples with 100-nm-thick and 200-nm-thick AlN films have FWHM values of 50 and 158 arcsec for (0002), and 302 and 274 arcsec for (10-12) planes, respectively. Despite the room for optimization of thickness of AlN films or annealing conditions, these values are comparable to those of AlN films on sapphire substrates.

Figure 2 shows the c-axis lattice constants (c_{AlN}) of AlN films before and after annealing, Before the annealing, the AlN film with a 100-nm-thick is almost strain free. However, AlN films with thickness larger than 200 nm are tensely strained. even the in-plane lattice constant of AlN is larger than that of SiC. After annealing, c_{AlN} decreased for the sample with a 100-nm-thick AlN film. On the other hand, c_{AlN} increased for the samples with thicker AlN films. From these results, it can be said that the tensile strain accumulated in relatively thick AlN films is partially released by high temperature annealing. However, tensile strain is resided in the AlN films after annealing. Understanding and controlling of the strain relaxation introduced to AlN films during sputtering and annealing are important to realize high-quality AlN templates on SiC substrates and AlGaN layers grown on these templates.
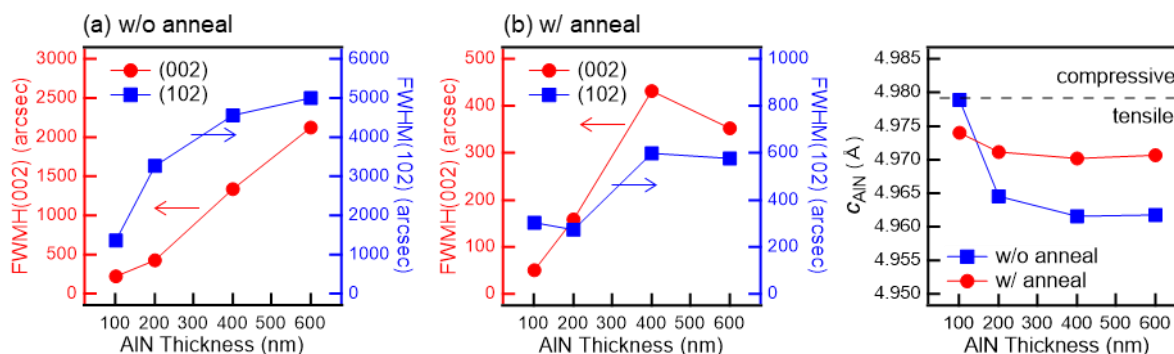
Figure 1. (left, center) AlN thickness dependence of the FWHM values of XRC from AlN (0002) and (10-12) planes (a) before annealing and (b) after annealing. **Figure 2**. (right) AlN thickness dependence of the c-axis lattice constants before and after annealing. Broken lines indicate the lattice constant of bulk AlN.

[1] H. Miyake *et al.*, J. Cryst. Growth **456**. 155 (2016).
[2] R. Yoshizawa, *et al.*, Jpn. J. Appl. Phys., **57**. 01AD05 (2017).

Growth of thick AlGaN layers by HVPE method on GaN seeds

Michal Fijalkowski, Tomasz Sochacki, Boleslaw Lucznik, Mikolaj Amilusik, Sławomir Sakowski, Małgorzata Iwinska, Izabella Grzegory, and Michal Bockowski

Institute of High Pressure Physics PAS, Sokolowska 29/37, 01-142 Warsaw, Poland

Among III-nitride wide-band gap semiconductors AlGaN alloys have attracted much attention due to their applications for high-power and high-frequency electronic devices and ultraviolet (UV) optoelectronic devices. [1,2]. The epitaxial growth of high quality AlGaN material plays an important role in preparation of AlGaN-based devices. Possibility of the fabrication of these devices on high quality AlGaN substrate (with aluminium contentup to 50%) seems to be beneficial [3]. Thus, growth of AlGaN crystals is required. However, crystallization of bulk AlGaN is a huge technological challenge.

In this study growth of the AlGaN ternary alloys on GaN substrates by hydride vapour phase epitaxy (HVPE) will be presented. Transport mechanism of Al to the crystal growth zone will be analyzed and discussed. Numerical simulation model of reactants flows in the growth zone will be created. The results of simulations will be applied for HVPE crystal growth experiments. Up to 100-µm-thick AlGaN layers will be deposited on (000-1) and (0001) planes of the GaN seeds. X-ray spectroscopy (XRD) as well as energy dispersive spectrometry (EDS) will be applied to determine aluminium content in the crystals. Morphology and structural properties of AlGaN layers, will be presented and discussed.

[1] Ban K., Yamamoto J.I., Takeda K., Ide K., Iwaya M., Takeuchi T., Kamiyama S., Akasaki I., Amano H., *Appl. Phys. Express* **4**, 052101 (2011).
[2] Imura M., Nakano K., Narita G., Fujimoto N., Okada N., Balakrishnan K., Iwaya M., Kamiyama S., Amano H., Akasaki I., *J. Cryst. Growth* **298**, 257–260 (2007).
[3] H.J. Kim, S. Choi, D.W. Yoo, J.H. Ryou, R.D. Dupuis, *J. Cryst. Growth* **310**, 4880–4884 (2008).

Invited lecture

Theoretical study: Impurity incorporation in GaN MOVPE

Yoshihiro Kangawa[1,2]**, Paweł Kempisty**[2,3]**,**
Stanisław Krukowski[3]**, and Kenji Shiraishi**[2]

[1] *RIAM, Kyushu University, Fukuoka 816-8580, Japan*
[2] *IMaSS, Nagoya University, Nagoya 464-8603, Japan*
[3] *IHPP, PAS, Sokolowska 29/37, 01-142 Warsaw, Poland*

Recently, researchers focus on the development of high voltage GaN power devices for hybrid vehicle and electric vehicle application. A vertical GaN power device with a blocking voltage of 1200V is required for high-power modules such as drive unit of main motors. To develop the required devices, it is indispensable to reduce carrier concentration in drift layer less than 1×10^{16} cm^{-3}. [1] That is, a high-purity GaN with few contamination is necessary to make a low-carrier-concentration and low-resistive-drift layer since carbon (oxygen) impurities act as acceptors (donors). It is known, however, that ~1×10^{16} cm^{-3} of carbon and oxygen exist in GaN grown by MOVPE. The unintentionally doped carbon mainly come from TMG, Ga source. The oxygen come from H_2O in NH_3 source gas, and so on. Reduction of impurities in GaN drift layer is a crucial issue to develop high voltage power devices. In the present work, we investigated the impurity incorporation mechanism during polar GaN MOVPE by an ab initio-based approach. [2] First, *p-T* surface phase diagrams for GaN(0001) and GaN(000-1) under typical MOVPE conditions are simulated to understand surface reconstructions appeared on growth surfaces. Next, relative energy changes in the system with substitutional carbon or oxygen in subsurface layers are analyzed. The calculation results suggest that in addition to the change of chemical potential of the gas phase, the next crucial factors for impurity incorporation are Fermi level pinning and accompanying surface band bending. This implies that these effects are responsible for hindering the incorporation of impurities. The influence of diluent gas species (hydrogen or nitrogen) on impurity incorporation is also discussed in the presentation.

References
[1] T. Kachi, *Jpn. J. Appl. Phys.* **53**, 100210 (2014).
[2] P. Kempisty, Y. Kangawa, A. Kusaba, K. Shiraishi, S. Krukowski, M. Boćkowski, K. Kakimoto, and H. Amano, *Appl. Phys. Lett.* **111**, 141602 (2017).

Invited lecture

Adsorption at nitride semiconductors surfaces - electronic aspects: surface states occupation, the equilibrium pressure, growth and doping

Stanisław Krukowski*, Paweł Strak, Paweł Kempisty and Konrad Sakowski

Institute of High Pressure Physics, Polish Academy of Sciences, Sokołowska 29/37, 01-142 Warsaw, Poland

Adsorption at semiconductor surfaces entails the change of their electronic properties, including the number of states, their energy and occupation. As an examples, the adsorption of hydrogen, ammonia, nitrogen, gallium and oxygen at GaN(0001) and AlN(0001) surfaces are presented. It is argued that during the process the electrons may be shifted between the states, either decreasing or increasing their energy which contributes to the energy balance, i.e. it affects the adsorption energy. For wide bandgap semiconductors the effect may change the adsorption energy by several electronvolts, i.e. it is substantial. The effect of electron transfer is possible for the Fermi energy pinned by specific, partially filled surface states. When the electron transfer is not possible, i.e. the surface states are fully empty of fully occupied, which occurs for specific coverage of the surface, the Fermi level is no longer pinned, that entails the sudden change of the adsorption energy. The formalism of determination of equilibrium pressure over the surface is also presented, including thermal contribution to enthalpy and entropy. The procedure allowing to avoid singular behavior of entropy of ideal gas at low temperatures is demonstrated. Using the data obtain by this procedure it is shown that the jump-like change of adsorption energy is associated by the variation of the equilibrium pressure by many orders of magnitude. The span is so large that the typical growth proceeds for the Fermi level not pinned, dependent on the position of Fermi level in the bulk, i.e. the bulk doping. The effect is universal, it occurs for majority of the growth processes of the nitrides. It is also shown that the electronic properties of the surfaces may be easily changed by the presence of other species at the surface, affecting the electric charge balance. Thus the effect may explain surfactant influence on the growth and doping of semiconductor crystals and layers.

A Simple Theoretical Approach to Growth Mode of III-Nitride Thin Films

Tomonori Ito, Toru Akiyama, Kohji Nakamura and Abdul-Muizz Pradipto

Department of Physics Engineering, Mie University, Tsu 514-8507, Japan

Semiconductor quantum dots (QDs) fabricated by heteroepitaxial growth have attracted significant interest for device applications. In III-nitride based semiconductors, the QDs are utilized not only as blue and ultraviolet light emitting devices but also as single photon sources. Most of the QDs are grown self-assembled on the substrates in the Stranski-Krastanov (SK) growth mode forming three dimensional (3D) islands. Despite the importance of the QDs, there have been very few theoretical studies of the growth mode incorporating atomistic data in III-nitride heteroepitaxial systems. In this study, the growth mode of GaN and InN on 3C-SiC(001) is systematically investigated using our macroscopic theory [1] with the aid of empirical potential calculations for dislocation energy and ab initio calculations for surface energy.

In our macroscopic theory, free energy F (eV/Å^2) for two-dimensional coherent (2D-coh), SK island formation (3D-coh) and 2D with misfit dislocation formation (2D-MD) growth modes is described as a function of layer thickness h as follows.

$$F = \gamma(1 + \beta) + \frac{1}{2}M(1 - \alpha)\varepsilon^2\left(1 - \frac{l_0}{l}\right)h + \frac{E_d}{l}, \qquad (1)$$

where γ, β, M, α, ε (= 0.037 for GaN and 0.142 for InN), l, l_0 (= 86.30 Å for GaN and 24.64 Å for InN), and E_d denote the surface energy, the effective increase in surface energy of the epitaxial layer due to 3D island formation, the effective elastic constant, the effective decrease in strain energy due to 3D island formation, the intrinsic strain of the system, the average MD spacing, the MD spacing at which strain is completely relaxed, and the formation energy of the MD, respectively.

Using eq. (1), the boundary between the 2D-MD and the 3D-coh is described as $\beta/\alpha = 1/(2\gamma)(E_d/l_0)$. Employing E_d = 295.4 meV/Å for GaN and 624.3 meV/Å for InN obtained in this study, the growth mode boundaries for GaN/SiC(001) (open triangle) and InN/SiC(001) (open circle) are shown in Fig. 1 as functions of β/α and γ. The stable region of the 3D-coh for GaN/SiC(001) is much smaller than that for InN/SiC(001) because of its smaller E_d and large l_0. Moreover, large surface energies γ = 104.7 (meV/Å^2) for GaN and 74.9 (meV/Å^2) for InN narrows the QD formation range of β/α < 0.016 for GaN/SiC(001) and β/α < 0.16 for InN/SiC(001). This is consistent with small β/α ~ 0.006 for GaN/SiC(001) system estimated from QD size and density observed in the experiments [2]. Furthermore, the versatility of our simple approach is shown by comparing with the prototypical results for InAs/GaAs(001) system. Consequently, the surface energy γ and the MD formation energy E_d are crucial factors for interpreting growth mode of the III-nitride thin films from atomistic and macroscopic viewpoints.
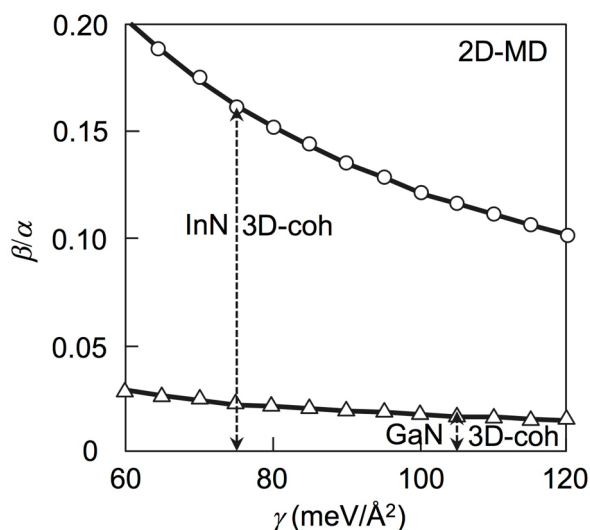
Fig.1. Calculated growth mode boundaries for GaN and InN on SiC(001).

[1] K. Shiraishi et al., *J. Cryst. Growth* **237-239**, 206 (2002).
[2] S. Tanaka, S. Iwai, and Y. Aoyagi, *Appl. Phys. Lett.* **69**, 4096 (1996).

AlGaN MOVPE Growth Simulation under 10-100 kPa Considering Polymer formation

Kazuhiro Ohkawa [1] **and Kenichi Nakamura** [2]

[1] *Electrical Engineering, King Abdullah University of Science and Technology (KAUST), Thuwal, Saudi Arabia*
[2] *Dept. Applied Physics, Tokyo University of Science, Tokyo, Japan*

MOVPE growth of AlGaN is usually under low pressure. At atmospheric pressure, its growth rate goes down significantly. In this paper, we will report on successful AlGaN growth simulation in the wide range of pressure, 10-100 kPa. Growth rates and compositions of AlGaN in the simulations are in good agreement with those in the experiments by considering proper polymer formation.

Temperature is a crucial point in chemical reactions. We included the optical properties of sapphire and quartz at high temperatures to calculate the temperature distribution [1]. Based on the realistic simulation of temperature distribution in the gas phase and surfaces of reactor wall and substrates, we have developed GaN and AlN growth simulations in $TMGa/NH_3/H_2$ and $TMAl/NH_3/H_2$ systems, respectively [2, 3]. The code for simulation is CFD-ACE+ using our original nitride MOVPE parameters. The parameters are available from Wave Front Ltd, Japan [4]. We used a Taiyo-Nippon Sanso MOVPE system for the experiments.

We cannot explain AlGaN growth by a simple sum of AlN and GaN simulations as shown in Fig.1. The simple sum (broken line) indicates a small pressure dependence in the growth rate. The large difference in growth rate from the experimental data implies that the adoption of independent polymer formations of Al-related and Ga-related molecules is not enough, and the consideration of additional polymer formation among these molecules is necessary. From the previous simulation of the independent Al and Ga reaction systems, we recognized that some reactive molecules exist in the same space on the heated substrate. Such molecules presumably form polymers. The solid line is the latest version including the additional polymer formation of $[MMAl-NH]_n-[Ga-N]_m$, $[MMAl-NH]_n-[Ga-N]_m-[Al-N]_k$, and $[Al-N]_n-[Ga-N]_m$ (k, m, and n are 1-6). Here, MM is a mono-methyl group. The pressure dependencies of growth rate and composition exhibit good agreements among the simulation and the experiment, eventually.

Also, the MOVPE growth of AlGaN is sensitive to temperature and the ratio of TMAl / (TMAl + TMGa). We will explain these dependencies at the conference.
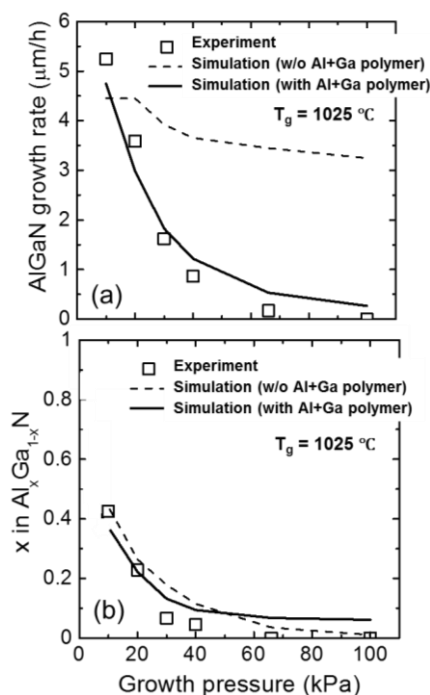
Fig.1 Simulated and experimental AlGaN growth rate and composition as functions of pressure. Data are from the center of a 2" wafer.

[1] A. Hirako, and K. Ohkawa, J. Cryst. Growth **276**, 57 (2005).
[2] A. Hirako, K. Kusakabe, and K. Ohkawa, Jpn. J. Appl. Phys. **44**, 874 (2005).
[3] T. Uchida, K. Kusakabe, and K. Ohkawa, J. Cryst. Growth **304**, 133 (2007).
[4] http://www.wavefront.co.jp/CAE/MOVPE-database/

Relationship between the CH$_4$ Adsorption Probability and the C Impurity Concentration in the Polar-GaN MOVPE System

A. Kusaba [1], **G. Li** [2], **M. R. von Spakovsky** [3], **P. Kempisty** [4] **and Y. Kangawa** [1,5,6]

[1] *Department of Aeronautics and Astronautics, Kyushu University,*
744 Motooka, Nishi-ku, Fukuoka 819-0395, Japan
[2] *Department of Engineering Science, University of Oxford,*
Parks Road, Oxford OX1 3PJ, UK
[3] *Center for Energy Systems Research, Mechanical Engineering Department, Virginia Tech,*
Blacksburg, VA 24061, USA
[4] *Institute of High Pressure Physics, Polish Academy of Sciences,*
Sokolowska 29/37, 01-142 Warsaw, Poland
[5] *Research Institute for Applied Mechanics, Kyushu University,*
6-1 Kasuga-koen, Kasuga, Fukuoka 816-8580, Japan
[6] *Institute of Materials and Systems for Sustainability, Nagoya University,*
Furo-cho, Chikusa-ku, Nagoya 464-8601, Japan

GaN is a promising material for the next generation of high power devices. Reduction of the C impurity concentration is essential for realizing such devices. In this research, the polarity-dependent (i.e., Ga-polar and N-polar) carbon incorporation is studied in terms of the CH$_4$ adsorption probability. First, the adsorption structures of CH$_4$ on GaN reconstructed surfaces during MOVPE [1] are determined based on the energetics of density functional theory (DFT). Second, the adsorption probabilities are found based on steepest-entropy-ascent quantum thermodynamics (SEAQT). SEAQT is a thermodynamic-ensemble based, first-principles framework that can predict the behavior of non-equilibrium processes, even those far from equilibrium [2,3]. In [4], the SEAQT framework is applied to modeling NH$_3$ chemical adsorption on GaN surfaces to obtain the NH$_3$ adsorption probability (see Fig. 1). The same approach is used here to obtain the CH$_4$ adsorption probability, while the formation energy of the C impurity substituting nitrogen, $E_f(C_N)$, is calculated at each layer from the surface to the bulk using DFT [5]. Assuming that the C impurity concentration at the surface is proportional to the CH$_4$ adsorption probability and applying a Boltzmann distribution to this $E_f(C_N)$ profile, the polarity-dependent C impurity concentration profile is obtained. Using this procedure, it is possible to determine if CH$_4$ adsorption is a critical factor in the polarity dependence of the C impurity concentration.

Reference
[1] Y. Kangawa *et al.*, *Materials* **6**, 3309-3360 (2013).
[2] G. Li and M. R. von Spakovsky, *Phys. Rev. E* **93**, 012137 (2016).
[3] M. R. von Spakovsky and J. Gemmer, *Entropy* **16**, 3434-3470 (2014).
[4] A. Kusaba *et al., Materials* **10** , 948 (2017).
[5] P. Kempisty *et al.*, *Appl. Phys. Lett.* **111**, 141602 (2017).
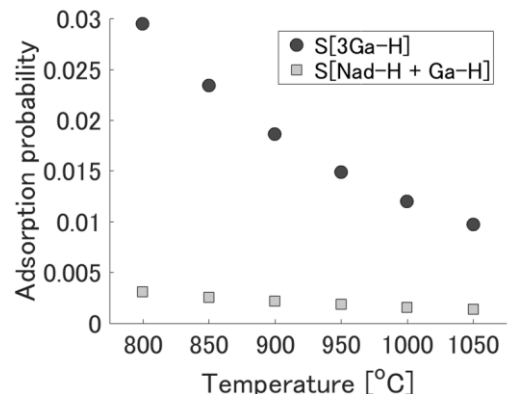
Figure 1. Adsorption probability of NH$_3$ on GaN reconstructed surfaces.

Contribution of first principles phonon calculations to thermodynamics analysis of GaN surfaces

Pawel Kempisty[1], Yoshihiro Kangawa[2,3], and Stanislaw Krukowski[1]

[1]*Institute of High Pressure Physics, Sokolowska 29/37, 01-142 Warsaw, Poland*
[2]*RIAM, Kyushu University, Fukuoka 816-8580, Japan*
[3]*IMaSS, Nagoya University, Nagoya 464-8603, Japan*

A good knowledge of surface physics can significantly help in overcoming further technological barriers in the growth of nitrides crystals, layers, structures, and devices. The difficulties in growth on different crystallographic orientations are well known, so developing theoretical models of growth of nitride semiconductors is still desirable, in particular regarding gas phase epitaxy. Molecular structure of the semiconductor surfaces can change in function of temperature, so making a reliable thermodynamic analysis is very important. In the literature there is a large number of surface phase diagrams for gallium nitride, based on first principles calculations. Unfortunately, they are commonly made with many simplifications. In particular, they rarely include the entropy term of solid phase assuming that it is low compared to the gas phase. Therefore, until now temperature dependencies have been taken into account mainly in the chemical potential of gas phase species.

In this work we present a revised, more accurate approach to model the true hot surface existing during growth processes. It included also dynamic and thermal properties of surfaces which were determined on the basis of first principles phonon calculations. We present changes of the specific heat, entropy, and free energy of several reconstructed GaN surfaces. Molecules adsorbed on the surface introduce to the phonon spectrum additional vibration modes, often very different in frequency from the vibrations of atoms in the bulk. In some temperature range, the corrections are fairly large, what should be included in the thermodynamic calculations. For very low temperature, the crucial factor is the zero-point vibration energy, whereas in the high temperature it is vibrational entropy. The example of hydrogen adsorption on the GaN(0001) surface was used to show that adding exact entropy and vibrational contributions can change the calculated equilibrium hydrogen pressure above the surface by several orders of magnitude [1].

[1] P. Kempisty, P. Strak, K. Sakowski, Y. Kangawa, and S. Krukowski, *Phys. Chem. Chem. Phys.* **19**, 29676 (2017).

Kinetic Monte Carlo simulation of MOVPE growth/sublimation of GaN on the vicinal GaN(0001) substrate

Jan Endres[1], Václav Holý[1], Stanislav Daniš[1], Marcin Sarzyński[2]

[1]*Faculty of Mathematics and Physics, Charles University, Ke Karlovu 3, 121 16 Prague, Czech Republic*

[2]*Institute of High Pressure Physics PAS, ul. Sokołowska 29/37, 01-142 Warsaw, Poland*

Our attempt is to simulate growth/sublimation of the GaN on the vicinal GaN(0001) substrate during deposition/annealing. We deal with growth and annealing in MOVPE reactor with ammonia rich conditions. Main growth parameters are growing temperature, fluxes of components, properties of the substrate (structural and chemical) and miscut. Two types of substrate steps have different properties due to the wurtzite structure.

Atomic scale model for the kinetic Monte Carlo (KMC) simulation was developed to study surface pattern evolution during growth [3,4,5] and high temperature annealing of GaN substrates [6,7]. Due to the ammonia rich conditions all available bonds are considered as saturated by N atoms and the model describes only evolution of the lattice of Ga atoms. The different properties of two step types was described by many body interaction between neighbouring Ga atoms connected by N. Even after simplifications the model is capable to describe experimental observations. It was demonstrated that by changing simulation parameters like temperature, diffusion barrier, Schwoebel barrier or deposition flux the step structure can vary between step bunching, step meandering, parallel wavy steps and molds creation.

We used model based on models from [3,4,5,6,7]. Atomic force microscopy (AFM) data for thermal sublimation for various miscut angles and growth/sublimation rates for different miscuts and temperatures will serve as reference results to determine optimal values of the simulation parameters of the GaN model. We were able to obtain results similar to observed double step structure after the annealing.

We are interested not only in the growth on the plain vicinal substrate but also in the growth on the top of the ridges oriented along miscut direction prepared by photolithography. In this case the main question is behaviour of atoms at the edge of the ridge. Another goal is to extend the simulation model by incorporating of the In atoms and compare the results with experimental AFM data for InGaN layer growth.

[1] N. Metropolis, S. Ulam, *J. Am. Stat. Assoc.* **44**, 335 (1949).

[2] K. A. Fichthorn, W. H. Weinberg, *J. Chem. Phys.* **95**, 1090 (1991).

[3] M. A. Załuska-Kotur, F. Krzyżewski, S. Krukowski, *J. Non. Cryst. Solids* **356**, 1935 (2010).

[4] M. A. Załuska-Kotur, F. Krzyżewski, S. Krukowski, *J. Appl. Phys.* **109**, 023515 (2011).

[5] M. A. Załuska-Kotur, F. Krzyżewski, S. Krukowski, *J. Cryst. Growth* **343**, 138 (2012).

[6] M. A. Załuska-Kotur, F. Krzyżewski, *J. Appl. Phys.* **111**, 114311 (2012).

[7] M. A. Załuska-Kotur, F. Krzyżewski, S. Krukowski, R. Czernecki, M. Leszczyński, *Cryst. Growth Des.* **13**, 1006 (2013).

[8] F. Krzyżewski, M. A. Załuska-Kotur, H. Turski, M. Sawicka, Czesław Skierbiszewski, *J. Cryst. Growth* **457**, 38 (2017).

Catalytic potential of AlN(0001) surface for N2 + H2 ammonia synthesis reaction

Pawel Strak, Konrad Sakowski, Pawel Kempisty, Izabella Grzegory, Stanislaw Krukowski

Institute of High Pressure Physics, Polish Academy of Sciences, Sokolowska 29/37, 01-142 Warsaw, Poland

Adsorption of molecular nitrogen and molecular hydrogen at Al-terminated AlN(0001) surface was investigated using ab initio simulation methods. It was shown that both species undergo dis-sociation during attachment to the surface, i.e. the adsorption is dissociative. Despite high bond-ing energies of both molecules, the dissociative adsorption is energetically highly favorable, and in addition, the process has negligibly small energy barriers. The adsorption sites were identified for both H and N adatoms. It is also shown that extended electron counting rule is obeyed, thus assuming that intra-surface electron transition contributes considerable energy to overall energy balance, which terminates at specified coverage equal to 1/4 and 3/4 for N and H, respectively. The adsorbed species potentially may react creating N-H radicals. Thus the adsorption processes provide strong indication that AlN(0001) is powerful catalyst for high pressure – high tempera-ture synthesis of ammonia, indicating that AlN may be candidate for industrial application in ammonia synthesis.

Williamson-Hall analysis on epilayers – A review on common practice

Lars Grieger [1] **and Joachim F. Woitok** [1]

[1] *Malvern Panalytical B.V., Lelyweg 1, Almelo, The Netherlands*

This paper discusses the practice to perform a Williamson-Hall (WH) analysis. It does not aim to damage the work of other authors, but highlights mistakes made during measurements with graphs from literature and the following wrong conclusions. We will provide a correct way of measurement and the difference it makes to the result. (Figure 1) The WH technique is a subgroup of the X-Ray diffraction methods employing the integral breadth (IB) as a figure of merit. In most cases, the IB in qx-direction is plotted in reciprocal space for multiple reflection orders in qz to distinguish between angular broadening (mosaicity) from the slope and size related broadening (lateral correlation length) from the y-intercept. These values are commonly accessed via rocking curves at different orders. For GaN investigated with Cu-kα radiation, (00L) reflections with L = (2,4,6) are accessible. The impact of the measurement geometry is commonly ignored and is key to a correct result. Reciprocal space maps offer another direct way to measure peak position and shape. Due to recent advances in data acquisition, they are available in similar timescales. The emphasis is on the rocking curve method but pitfalls and advantages of both methods are discussed.
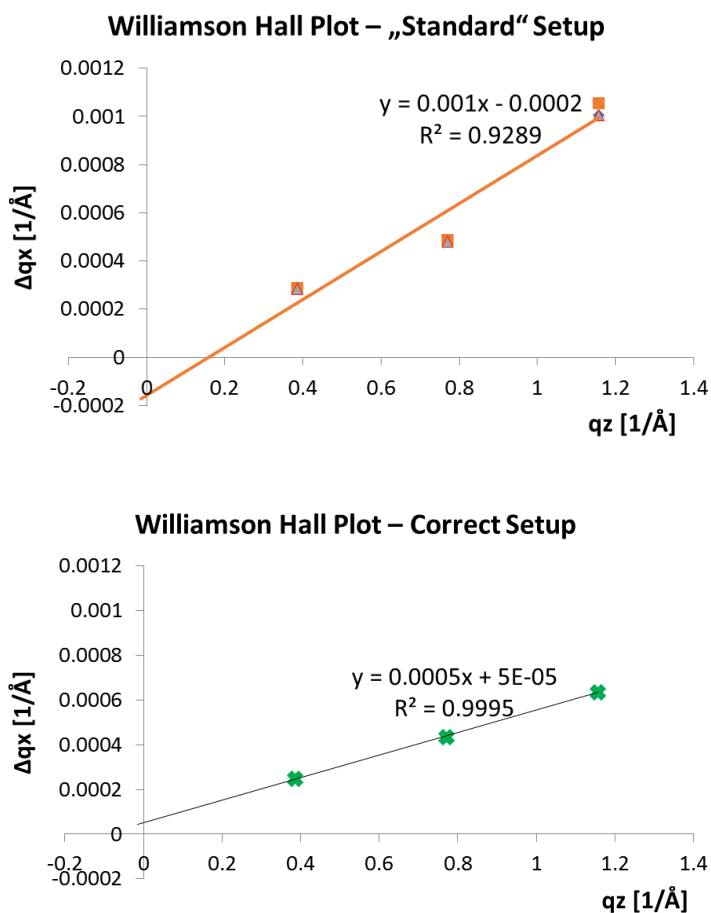
Figure 1 Williamson-Hall plot of the same sample done with wrong data acquisition settings (upper) and with the correct setup (lower). The instrumental influence on the 006 peak in the top graph is well visible. The correlation of points is greatly improved in the lower graph.

Invited lecture

X-ray Diffraction in Nitride Technology- most common mistakes and new opportunities

Mike Leszczynski [1,2]**, Ewa Grzanka** [1,2] **, Marcin Krysko**[1]**, Jarek Domagala**[3]**, Jana Stranska-Matejova**[4]**, Vaclav Holy**[4,5]

[1] *Institute of High Pressure Physics UNIPRESS, Sokolowska 29/37, 01 142 Warsaw, Poland,*
[2] *TopGaN, Sokolowska 29/37, 01 142 Warsaw, Poland*
[3] *Institute of Physics, Al. Lotnikow 32/46, 06-668 Warsaw, Poland*
[4] *Department of Condensed Matter Physics, Faculty of Mathematics and Physics, Charles University, Ke Karlovu 5,121 16 Praha, Czech Republic.*
[5] *CEITEC at Masaryk University,Kotlarska 2,611 37 Brno,Czech Republic*

X-ray Diffraction (XRD) is the most common tool for examinations of the bulk GaN substrates and AlGaInN epi wafers. The commercial X-ray diffractometers and their simulation software based on the dynamical theory of X-ray diffraction for perfect crystals (changes of lattice parameters are only in the direction perpendicular to the surface) offer an easy and quick way of characterization. In the presentation proposed, we will list a number of the most common misinterpretation of the experimental data, as well we will show how the more advanced XRD analysis can help not only to avoid those mistakes, but also to draw additional conclusions.

We will discuss examples of XRD analysis done for the following samples:

i) **Bulk GaN substrates**. For those samples, the XRD peaks are broadened by the presence of defects and by the sample bowing. The most common mistake of the GaN growers is evaluating the crystal quality by the half-width of the XRD rocking curves neglecting their intensity. This can be especially misleading when the line focus (the most popular) of the X-ray tube is used.

ii) **AlGaN layers on various GaN substrates**. To analyze thin films, it is necessary to fit not only the XRD peak positions, but also the peak intensities. For nitrides, it is a very complex problem because the GaN substrates and the AlGaN layers are far from being perfect and the commercial simulation software is only for the perfect epi-structures. It will be shown that only the samples having the dislocation density lower than 10^5 cm^{-2} can be analyzed using the commercial simulation software. For worse quality samples, the kinematical theory is more adequate, however, there is a number of ambiguities to be taken into account (for example, what should be the reference intensity- GaN peak, background, or the other?).

iii) **InGaN layers on various GaN substrates.** In this case, we deal not only with a poor crystallographic quality reproduced from the substrate, but also with indium fluctuations , V-pits, and new misfit and threading dislocations. We will show that an analysis of the reciprocal lattice maps and diffuse scattering can lead to much more reliable data for the InGaN quantum wells and layers.

iv) **Laser diode epi structures before and after InGaN decomposition.** When p-type in such structures is grown at temperature that is too high, the InGaN quantum wells get decomposed.

Raman Spectroscopic Study of GaN Grown on (111)Si Using an AlInN Intermediate Layer by MOVPE

T.Sugiura[1], S.Kawasaki[2], Y.Honda[3], T.Nonaka[1], D.Oikawa[1], T.Tsukamoto[1], H.Andoh[1] and H.Amano[3]

[1]*National Institute of Technology, Toyota College, 2-1 Eisei-cho, Toyota, Japan*
[2]*Department of Electronics, Nagoya University, Furo-cho Chikusa-ku, Nagoya, Japan*
[3]*Institute of Materials and Systems for Sustainability, Nagoya University, Nagoya, Japan*

Raman spectroscopic analysis of GaN grown on (111)Si using an AlInN intermediate layer was performed and investigated compositional dependence of In-content x for intermediate $Al_{1-x}In_xN$ alloy. The sample was made with selective MOVPE epitaxy with a grid mask pattern to avoid cracking in the GaN grown layer[1]. The AlInN layer were grown at 640-800[°C] and the thickness of layers were 20-120[nm]. The Indium composition of the AlInN intermediate layer was determined by XRD analysis. The layers are usually subject to strain or stress due to mismatches between the layer boundaries and the thermal expansion coefficients. It is often used to quantify the stress and to evaluate the degree of the size of microcrystals in the layer, because of the Raman spectra are sensitive to the strain. It was attributed to the relaxation of the momentum selection ($q=0$) rule in Raman scattering process because of the finite size of the crystal. The size of a region where we can find a meaningful amplitude of a phonon mode is expressed in a characteristic length which is given by a correlation length, which has similar meaning as the size of microcrystals. We have studied the asymmetric broadening of Raman spectra by use of the Spatial Correlation model[2].

In Fig.1, typical Raman spectra exhibited well-known several phonon peaks attributed to E_2 and A_1 modes of GaN layer. If the asymmetric broadening of the phonon mode is caused to the relaxation of momentum selection rule, it can be significantly affected in $E_2(low)$ frequency mode, which has smallest energy. Thus, we focus the $E_2(low)$ mode in GaN. In Fig.2, $E_2(low)$ mode is subjected to the obvious tensile stress (red-shift) compared with that of strain-free bulk GaN, respectively. The asymmetric broadening of $E_2(low)$ mode is also depend on the x of $Al_{1-x}In_xN$ intermediate layer, however, it is out of proportion to the increase of x. That is, it suggests that sample of $x=0.05$ is strongly subject to tensile strain than that of $x=0.104$. Especially, it is notable for the asymmetric broadening of $x=0.05$ and broken line fitted by theoretical model. As shown in Fig.3, ratio of upper and lower HWHMs(half-widths at half maximum) of $x=0.05$ shows the greater value compared with that of $x=0.104$, while that of $x=0.015$ is near unity, i.e., the broadening is almost symmetric. This finding might suggest that the residual strain of GaN using $x=0.104$ is reduced, because of the intermediate layer is close to the $Al_{0.83}In_{0.17}N$, which is possible to be lattice-matched to GaN. Moreover, the correlation lengths noted in right axis is on about 10nm at given In-content x. The size of the periodic pyramidal-like microcrystalline AlInN is in order of tens nm[1], in close agreement with the present results. In summary, it was found that the tensile strain of GaN using $Al_{0.9}In_{0.1}N$ intermediate layer on (111)Si was smaller than that of using layer decreased In-incorporation by half.

[1] M.Irie et al., *J. Cryst. Growth* **311** 2891 (2009). [2] T. Sugiura et al., *Jpn. J. Appl. Phys.* **40** 5955 (2001) .
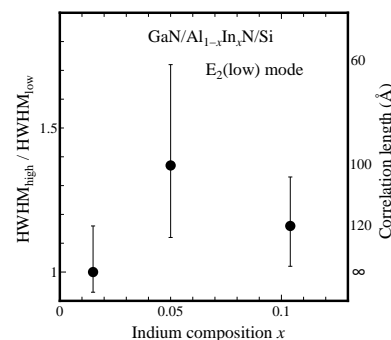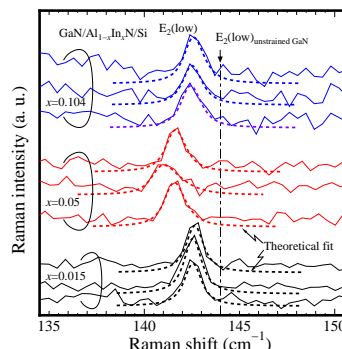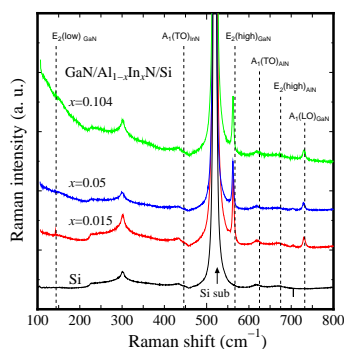
Fig.1 Typical Raman spectra of GaN/AlInN/Si,   Fig.2 $E_2(low)$ mode of GaN,   Fig.3 Ratios of HWHMs vs x

InGaN Band Gap Compositional Dependence Determined by Means of Photoacoustic Spectroscopy

R. Oliva,[1] **S. J. Zelewski,**[1] **Ł. Janicki,**[1] **K. R. Gwóźdź,**[2] **J. Serafińczuk,**[3]
M. Rudziński,[4] **E. Özbay**[5] **and R. Kudrawiec**[1]

[1] *Dept. of Experimental Physics, Faculty of Fundamental Problems of Technology, Wroclaw Univ. of Science and Technology, Wybrzeże Wyspiańskiego 27, 50-370 Wrocław, Poland*
[2] *Dept. of Quantum Technologies, Faculty of Fundamental Problems of Technology, Wroclaw University of Science and Technology, Wybrzeze Wyspianskiego 27, 50-370 Wrocław, Poland*
[3] *Faculty of Microsystem Electronics and Photonics, Wroclaw University of Science and Technology, Janiszewskiego 11/17, 50-372 Wrocław, Poland*
[4] *Institute of Electronic Materials Technology, Wólczyńska 133, 01-919 Warsaw, Poland*
[5] *Nanotechnology Research Center, Bilkent University, 06800 Bilkent, Turkey*

Since the establishment of the band gap of InN at 0.65 eV a great deal of research has been paid to the InGaN alloy system because its band gap extends up to the ultraviolet (3.4 eV for GaN), covering the whole visible spectral range. Such property can be exploited to design a great variety of optoelectronic devices including light-emitting devices or tandem solar cells.[1] Remarkably, the growth of inexpensive high-brightness blue LEDs with GaN and InGaN acting as active layer boosted the interest in this alloy system.

Despite its large technological interest, the compositional dependence of the band gap is not yet precisely established. It is well known that the compositional dependence of the InGaN band gap energy can be described by the formula $E(x) = 0.65 \cdot x + 3.4 \cdot (1-x) - b \cdot x \cdot (1-x)$, where b is the so called bowing parameter. In order to properly determine the bowing parameter of InGaN many different phenomena must be taken into account. In the first place, high-quality InGaN thin films typically exhibit large in-plane strain arising from the substrate or buffer layers that strongly blueshifts the band gap. Secondly, as grown indium-rich InGaN typically exhibits large residual electron densities which result in an increase of the optical band gap. Finally, Stokes shifts up to 500 meV have been reported for InGaN, which is mostly accounted by compositional inhomogeneity.[2] Hence, in order to determine the band gap of InGaN it is crucial to carefully select appropriate spectroscopic techniques to account for the Sotkes shift, and correct strain or electron density effects on the optical band gap.

Here we performed photoacoustic measurements on a series of $In_xGa_{1-x}N$ thin films ($x > 50\%$) and compared these results with other conventional techniques: photoluminescence, transmittance and contactless electro reflectance. Our results show that photoacoustic spectroscopy is a highly useful technique to determine the band gap of InGaN thin films. In order to determine the bowing parameter, we assessed the strain state of our samples by means of high-resolution X-ray diffraction and Raman scattering measurements. Owing to the large residual electron densities present in the thin films, we corrected the Burstein Moss shift and band gap renormalization effects on the optical band gap. Our measurements and subsequent analysis allowed us to validate a bowing parameter of $b = 1.43$ eV for intrinsic InGaN.[3]

[1] Wu, J. *J. Appl. Phys.* **106**, 011101 (2009).
[2] J. Wu, W. Walukiewicz, et al., *Appl. Phys. Lett.* **80**, 4741 (2002).
[3] R. Oliva, S. J. Zelewski, et al., *Semicond. Sci. Technol.* **33**, 035007 (2018).

TEM Investigations on High-Temperature Annealed epi-AlN on Sapphire

L.Cancellara[1], S.Hagedorn[2], S.Walde[2], D.Jaeger[3], M.Weyers[2], T.Markurt[1], M.Albrecht[1]

[1]*IKZ, Leibniz-Institute for Crystal Growth, Max-Born-Str. 2, Berlin, Germany*
[2]*Ferdinand-Braun-Institut, Gustav-Kirchhoff-Str. 4, Berlin, Germany*
[3]*Evatec AG, Hauptstr. 1a, Trübbach, Switzerland*

AlN and AlGaN are attractive materials for UV applications due to a large direct bandgap, and high thermal/chemical stability. Bulk AlN substrates with high structural quality and sizes up to 2" are available, but are still costly and not fully transparent in the UV. Therefore great efforts were made recently to optimize growth on sapphire. Sapphire, widely available and UV-transparent, exhibits however large lattice and thermal mismatch with AlN, resulting in a high threading dislocations density with conventional growth techniques such as metal-organic vapor phase epitaxy (TDD$>10^9$cm^{-2}) and sputter deposition (TDD$>10^{10}$cm^{-2}). This is detrimental for the efficiency of light-emitting devices. Recently, it was demonstrated by Miyake *et al.* that the threading dislocation density of as-grown AlN layers can be significantly reduced with a high-temperature face-to-face annealing at temperatures above 1600°C [1]. The mechanisms responsible for this reduction are however far from well understood.

In this paper we use high resolution (scanning) transmission electron microscopy (HR(S)TEM) to investigate the elementary mechanisms that lead to dislocation reduction upon annealing. AlN thin films on c-plane sapphire from both MOVPE and sputter deposition were annealed face-to-face at 1700°C for 3h in N_2 atmosphere. TEM contrast imaging before and after annealing shows a reduction in dislocation density of up to two orders of magnitude (TDD$\approx10^8$cm^{-2}). Moreover, the initial mixed polar MOVPE films become Al-polar and free of inversion domains. However, at the interface between Al_2O_3 and annealed AlN we observed, regardless of the growth method, a roughly 10nm-thin N-polar layer separated from the Al-polar film by an inversion boundary resembling the R27-$Al_9O_3N_7$ structure described by Mohn *et al.* [2]. On the surface of the sputtered film γ-AlON islands are found by HR(S)TEM. According to the AlN-Al_2O_3 phase diagram, oxygen-containing AlN will separate precisely above 1700°C into γ-AlON and AlN [3]. Our results thus hint at a sizeable material transport upon annealing. Following this, we discuss the mechanisms leading to the reduction in dislocation density in terms of dislocation climb promoted by a high density of mobile vacancies. We estimate the vacancy density based on the oxygen content found by secondary ion mass spectroscopy and the estimated Fermi level at N-rich conditions, present during annealing. Together with the improvement of the crystallinity, an increase in the compressive strain is measured by Raman spectroscopy and XRD in all samples after annealing. We show that this can be ascribed to the difference in thermal expansion of substrate and layer, assuming that the AlN layer is fully relaxed at the annealing temperature of 1700°C.

*STEM-HAADF images of sputter deposited AlN on sapphire, pre- and post-annealing (**a.** and **b.** respectively), and detail of the γ-AlON on top (image **c.**)).*
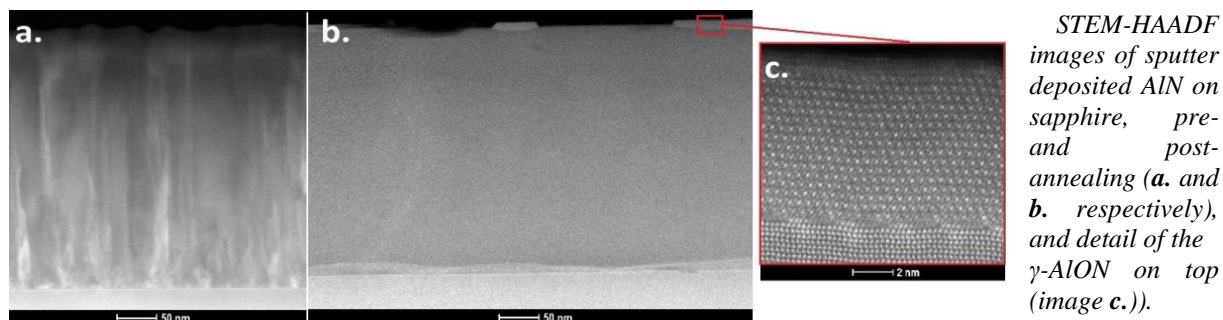
[1]   H. Miyake *et al.* "Preparation of high-quality AlN on sapphire by high-temperature face-to-face annealing", *J. Crystal Growth* 456, 2016, pp. 155-159.
[2]   S. Mohn *et al.* "Polarity Control in Group-III Nitrides beyond Pragmatism", *Phys. Rev. Applied* 5, 2016
[3]   McCauley J.W. and Corbin N.D., "High Temperature Reactions and Microstructures in the Al_2O_3-AlN System", in *Progress in Nitrogen Ceramics*, Springer, Dordrecht, 1983, pp. 111-118.

Diffusion and out-diffusion of Mn in gallium nitride.

Rafal Jakieła[1], Katarzyna Gas[1], Maciej Sawicki[1], Adam Barcz[1,2]

[1] *Institute of Physics, Polish Academy of Sciences, Lotników 32/46, Warsaw, Poland*
[2] *Institute of Electron Technology, Lotników 32/46, Warsaw, Poland)*

The aim of this work is to determine diffusion mechanisms of manganese in gallium nitride under different conditions. The diffusion was observed in two type of samples: Mn-implanted MOCVD (Metalorganic Vapour Phase Epitaxy) GaN layer deposited on a sapphire substrate or (Ga,Mn)N layers grown by PA-MBE (Plasma Assisted Molecular Beam Epitaxy) [1].

Implanted samples were annealed under 1 atm nitrogen pressure at 900–1200°C. MBE grown was executed at temperatures 600 – 700°C. Diffusion of Mn from implanted region and the out-diffusion of manganese atoms during the cooling of the as-grown sample was characterized.

The extent of diffusion of species in both types of samples was characterized using the SIMS (Secondary Ion Mass Spectrometry) technique. The resultant concentration profiles are characterized by two diffusion types: slow diffused Mn atoms at the low concentration described by substitutional migration in implanted samples and oxidation-driven out-diffusion at high concentration in MBE grown samples.

[1] Katarzyna Gas et al. – Journal of Alloys and Compounds 747 (2018) 946 – 959

Impact of Si doping in different GaN layers on luminescence properties of InGaN/GaN multiple quantum well structure

František Hájek, Markéta Zíková, Alice Hospodková, Tomáš Hubáček, Jiří Oswald

Institute of Physics, Czech Academy of Science, Cukrovarnická 10, Prague 6, Czech Republic

InGaN/GaN multiple quantum wells (MQW) structures seem to be perspective scintillator because high luminescence efficiency and spatial photoluminescence (PL) resolution [1]. In contrary to LEDs, there is no need for p-type doped layer. On the other hand, reduction of the internal electric field present in these structures is required to improve luminescence efficiency which can be done via Si doping. In this work a dependence of PL and cathodoluminescence (CL) on Si doping of different layers of MQW structure is discussed.

Structures were grown by MOVPE on c-oriented sapphire substrates. The MQW region consists of a pair of 5 InGaN/GaN quantum wells (QW) separated by 25 nm thick GaN. Details can be found in [1]. PL measurements were performed with 375nm excitation laser, grid monochromator and GaAs photomultiplier. Intensity oscillations are caused by Fabry-Perot resonance. Simulation was carried out in Nextnano software.

PL spectra of samples with Si doping under MQW area (A), over MQW area (B), under and over MQW area (C) and without Si doping (D) are depicted in Fig. 1a). The high energy band originates from QW levels recombination, the low energy one (DB) is probably recombination electron from QW level to deep acceptor state. Since deep acceptors are homogenously laid out among QWs (SIMS results not shown here), DB recombination can be used as reference for electron concentration in MQWs.
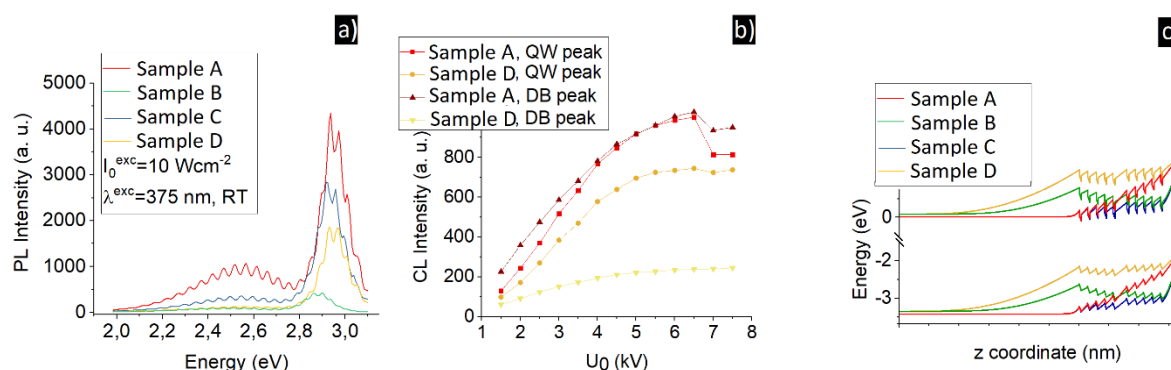
Fig. 1 a) PL spectra of samples with different Si doped layers, b) CL integral intensity of QW and DB peak of samples with Si under MQW and without Si, c) band structure for undoped structure and structure doped under MQW.

CL integral intensity of QW and DB peaks as a function of acceleration voltage U_0 is shown in Fig. 1b. Below U_0=7 kV, the cathodoluminescence signal originates from MQW region. The slope of the curves provides information about electron and holes layout. For structure A, the carriers are laid out homogenously, there is only small excess of holes near surface (slope QW vs DB peak). Holes in the structure D are much more localized at surface QWs (intensity saturation around 5 kV), the slope of DB intensity for this structure is smaller because worse localized electrons are pulled out from the MQW region by electric filed (see Fig. 1c).

Doping above MQW region enhances gradient of electric field as can be seen from 1c) which leads to charge carriers separation. Doping under and above MQW region combines above described effects.

[1] Hospodkova et al. Journal of Applied Physics 121, 214505 (2017).

Optical modulation spectroscopy of $Al_xGa_{1-x}N$ epilayers and $Al_xGa_{1-x}N$/GaN quantum wells in the UV spectral range

E. Zdanowicz[1,2*], W. Olszewski[1], S. Gorantla[1], K. Moszak[1,3], Ł. Janicki[2], D. Hommel[1,3,4] and R.Kudrawiec[1,2]

[1]*Wroclaw Research Center EIT+ Sp. z o.o., ul. Stabłowicka 147, 54-066 Wrocław, Poland*
[2]*Faculty of Fundamental Problems of Technology, Wroclaw University of Science and Technology, Wybrzeże Wyspiańskiego 27, 50-370 Wrocław, Poland*
[3]*Institute of Low Temperature and Structure Research, Polish Academy of Sciences W. Trzebiatowski Institute, ul. Okólna 2, 50-422 Wroclaw, Poland*
[4]*Faculty of Physics, University of Wroclaw, plac Maxa Borna 9, 50-204 Wroclaw, Poland*
*Email: ewelina.zdanowicz@eitplus.pl

Fabrication of efficient UV emitters is still a challenge. Not only the processing issues are under consideration, but also the design of the active region and its characterization but proper absorption-like methods are still under debate/studies.

Contactless electroreflectance (CER) is a tool of optical modulation spectroscopy which is a powerful technique allowing us to obtain optical spectra with sharp derivative-like features related to optical transitions between ground and excited states in the investigated samples. Moreover due to Franz-Keldysh effect it can be also applied to study the built-in electric field in semiconductor structures.

In this work we will present our recent progress in the application of CER spectroscopy to study AlGaN layers and AlGaN QWs dedicated for UV emitters. The samples were grown by MOVPE on sapphire substrates in a CSS reactor (Thomas Swan, Aixtron). The application of CER technique allows us to study not only the optical transitions between the ground and excited states in quantum wells and barriers but also the built-in electric field in these barriers. From comparison of photoluminescence and CER we obtain the Stokes shift which is an indication of sample quality and homogeneity. In this work obtained results will be presented in the context of polarization effects in III-nitrides and their screening by the intentional and unintentional doping. In addition the carrier localization phenomenon induced by alloy content fluctuations and QW width fluctuations will be discussed for proper interpretation of CER and PL data.

Excess Carrier Lifetime in Ammonothermal GaN Doped with Si, Mg, and Mn

Łukasz Janicki[1,*], Robert Kucharski[2], Marcin Zając[2], and Robert Kudrawiec[1]

[1] *Faculty of Fundamental Problems of Technology, Wrocław University of Science and Technology, Wybrzeże Wyspiańskiego 27, 50-370 Wrocław, Poland*
[2] *AMMONO S.A., Prusa 2, 00-493 Warsaw, Poland*

Microwave photoconductivity decay (µPCD) studies have been performed on ammonothermaly grown GaN to assess the impact of doping on the carrier lifetime. GaN was doped during growth with Si to obtain *n*-type conductivity, with Mg for *p*-type conductivity, or with Mn to make the material semi-insulating. Additionally, an effect of annealing was studied on a part of the samples. Generally, the carrier lifetime in Ammono-GaN is < 1 ns, that is below the resolution of the µPCD method. This is to be expected since Ammono-GaN has the point defect density on the order of $10^4 - 10^5$ cm^{-3} and is free of extended defects making carrier recombination fast. Introduction of Si does not degrade the material and no deep trapping centers are introduced. Therefore, the carrier lifetime is comparably low. Introduction of Mg or Mn, however, creates trap levels at which carriers can reside for a prolonged time. Decay times on the order of several microseconds are observed. Annealing extends the decoy time to several tens of microseconds.

Influence of Depletion Layer on Spatial Distribution of Cathodoluminescence Intensity in GaN Nanowires

B. Adamowicz [1], M. Matys [2]

[1] *Institute of Physics - CND, Silesian University of Technology, Konarskiego 22B, 44 -100 Gliwice, Poland*
[2] *Research Center for Integrated Quantum Electronics, Hokkaido University, Kita-13 Nishi-8, Kita-ku, 060-8628 Sapporo, Japan*

Spatially resolved cathodoluminescence (CL) spectroscopy is the key tool extensively applied to investigate the defects in GaN nanowires, which are important for future electrical and optoelectronic devices. A typical CL spectrum of GaN nanowires often consists of a near band edge (NBE) emission band in the ultraviolet range and a controversial deep-level emission (DLE) band in the spectrum visible part [1]. It is widely accepted that the distribution of DLE and NBE CL intensity along/across a nanowire corresponds to the spatial distribution of defects, which are responsible for DLE.

However, in this work, we show using three-dimensional (3D) theoretical analysis that in the case of GaN nanowires, which exhibit the surface band banding related to a depletion layer, the spatial distribution of NBE and DLE CL intensity may not correlate with the distribution of the DLE defect concentration but reflects the strength of the depletion layer electric field in a nanowire. For this analysis, we developed a model based on the numerical solution of 3D Poisson's equation, current continuity equations and generation - recombination rate equations using a finite element method and COMSOL Multiphysics simulation software. In the simulations, we assumed the oxygen-related shallow donors, deep acceptors, non-radiative centers and U-shaped surface state continuum responsible for surface recombination of excess carriers in terms of the Shockley-Read-Hall statistics [2]. The surface states also induce the depletion layer where the excited carriers are separated by the electric field, i.e., photo-holes are strongly attracted towards the nanowire surface whereas electrons are repelled into the bulk. In addition, some photo-holes can be captured by donor-like surface states and cause reduction of the negative surface charge. Our calculations showed that all these processes result in the lowering of the surface band bending and strong accumulation of photo-holes in the depletion region. As a consequence, the DLE CL intensity is the highest in the areas where the electric field is the strongest (near the surface) and the lowest were the electric field is absent (in the bulk). The opposite relationships were found for NBE CL, i.e., the strongest signal is in the bulk and weakest near the surface, both for the uniform and non-uniform spatial distribution of DLE defects. We explained these results in terms of the strong impact of the depletion layer electric field on the spatial distribution of radiative recombination rates.

In conclusion, our findings indicate that the commonly observed spatially inhomogeneous CL intensity distribution in GaN nanowires can be the result of the presence of depletion layer fields but not widely accepted non uniform defect distribution.

[1] Qiming Li, George T. Wang, *Nano Lett.*, **10**, 1554 (2010)
[2] M. Matys, B. Adamowicz, *J. Appl. Phys.* **121**, 065104 (2017).

Influence of Macrosteps on Deep-ultraviolet Emission from AlGaN/AlGaN Multiple Quantum wells

K. Kataoka [1], K. Horibuchi [1], Y. Saito [2], H. Makino[2], K. Nagata[2], and Y. Kimoto [1]

[1] *Toyota Central R&D Labs., Inc., Nagakute, Aichi 480-1192, Japan*
[2] *TS Opto Co. Ltd., Ichihara, Chiba 290-0067, Japan*

The light emitting diodes (LEDs) operating in the deep-ultraviolet (DUV) range are expected for various applications. AlGaN is a candidate material for DUV-LEDs [1]. For familiarizing the AlGaN-based DUV LEDs, improvement of the external quantum efficiency is one of the most important issues [1]. In this study, the AlGaN/AlGaN multiple quantum wells (MQWs) were analyzed using cathodoluminescence (CL) and transmission electron microscope (TEM) to investigate the spatial distribution of luminescent.

The MQWs(AlGaN/AlGaN)/nAlGaN/AlN structure was grown on *c*-plane sapphire substrate by metal-organic vapor phase epitaxy. The spatial distribution of DUV emission from the MQWs was measured by SEM-CL equipment. The cross-section of the sample was analyzed by TEM and TEM-energy dispersive x-ray spectroscopy (EDX).

CL spectra showed DUV emission from AlGaN MQWs around 267 nm. Figure 1 shows results of CL spectral mapping. The CL intensity mapping (Fig. 1 (a)) indicated high intensity lines corresponding to macrosteps on MQW surface. Furthermore, the high intensity regions exhibited longer peak wavelength as shown in Fig. 1(b). From the cross-sectional TEM-EDX analysis, the lower Al composition in the AlGaN/AlGaN MQWs was observed along the propagating macrosteps. The correlation between the macrosteps and the lower Al composition were consistent with the previous reports [2-4]. The longer peak wavelength near the macrosteps comes from the lower Al composition, and the higher luminescence intensity was probably caused by the carrier localization in the energetic minima at the lower Al regions. TEM analysis revealed that the macrosteps emerged during the growth of the underlying AlN layer. We suggest that avoiding the bunched step formation during the epitaxial growth is important for the homogeneous MQWs emission.
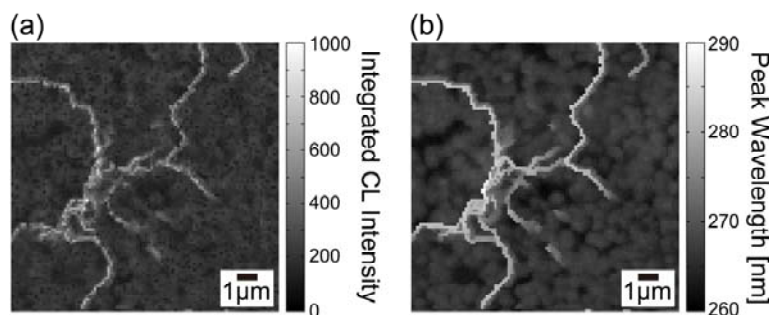
Figure 1 Analysis results of CL spectral mapping. (a) The CL intensity mapping and (b) the peak wavelength mapping for the MQW emission.

[1] H. Hirayama, N. Maeda, S. Fujisawa, S. Toyoda, and N. Kamata, *Jpn. J. Appl. Phys.* **53**, 100209 (2014).
[2] A. Mogilatenko, A. Knauer, U. Zeimer, and M. Weyers, *Semicond. Sci. Technol.* **31**, 025007 (2016).
[3] M. Hou, Z. Qin, L. Zhang, T. Han, M. Wang, F. Xu, X. Wang, T. Yu, Z. Fang, and B. Shen, *Superlattices and Microstructures* **104**, 397 (2017).
[4] K. Kataoka, M . Funato, and Y. Kawakami, *Appl. Phys. Express* **10**, 031001 (2017).

Growth of InGaN Films by Reactive Sputtering

Qixin Guo, Katsuhiko Saito, and Tooru Tanaka

Synchrotron Light Application Center, Department of Electrical and Electronic Engineering, Saga University, Saga 840-8502, Japan

III-V nitride semiconductors have been extensively investigated owing to their applications in light-emitting diodes, laser diodes, photodetectors, and high-power and high-speed electronic devices. With its wide band gap energy variation, ternary InGaN has received considerable attention as an excellent candidate for high-efficiency photovoltaic devices. However, the growth of these InGaN films is performed by metalorganic chemical vapor deposition (MOCVD) and the substrate temperature during the growth is high, which results in a high cost of fabricating InGaN films in the photovoltaic industry. Moreover, MOCVD faces technological challenges in the epitaxial growth of a high-indium-content InGaN film due to the low thermal stability of InN. We have shown that reactive sputtering technique has the advantage of using simple apparatus and low growth temperature for obtaining III-V nitrides [1-4]. In this study, we report on the growth and structural properties of InGaN films by the reactive sputtering.

InGaN films were grown on (0001) sapphire substrates by reactive radio-frequency (rf) magnetron sputtering in nitrogen ambient. The indium and GaAs were separately mounted onto the targets and were simultaneously sputtered at different rf powers, while the substrate holder was rotated. After the growth, film thickness was determined by a surface step profile analyzer. The chemical compositions of the films were determined from energy-dispersive X-ray spectra by quantitative analysis after calibration using a cobalt standard specimen. Optical transmission spectra of these InGaN films were measured at room temperature using a dual-beam spectrophotometer. We found that Ga, In, As, and N atoms adsorb on the substrate and react with each other to form InGaNAs film at substrate temperatures lower than 500°C. However, with increasing the substrate temperature up to 550°C, the active nitrogen atoms had sufficient surface mobility to replace the arsenic atoms and bond to the gallium or indium completely, forming the InGaN film. It was shown that the In composition in the InGaN films can be controlled by varying the ratio of the applied rf power of the indium target to that of the GaAs target. The optical results revealed that the InGaN films exhibit a direct band transition. The absorption edges clearly shifted toward a longer wavelength with the increase of In composition, indicating InGaN with the desired In composition can be obtained by varying the ratio of the rf power of the indium target to that of the GaAs target. The results suggest that InGaN multilayers with different In compositions can be fabricated sequentially in the same growth chamber, which is a promising process for growing InGaN-based solar cells with high conversion efficiency at a low cost.

References
[1] Q.X.Guo, H.Ogawa, H.Yamano, and A.Yoshida, Appl. Phys. Lett. 66, 715 (1995).
[2] Q.X. Guo, M. Nishio, H. Ogawa, and A.Yoshida, Phys. Rev. B 55, R15987 (1997).
[3] Q.X. Guo, J. Ding, T. Tanaka, M. Nishio, and H. Ogawa, Appl. Phys. Lett. 86, 111911 (2005).
[4] Q.X. Guo, H. Senda, K. Saito, T. Tanaka, M. Nishio, J. Ding, T.X. Fan, D. Zhang, X.Q. Wang, S.T. Liu, B. Shen, and R. Ohtani, Appl. Phys. Lett. 98, 181901 (2011).

High temperature vapor phase epitaxy for the growth of GaN layers on sapphire substrates

M. Förste[1], T. Schneider[1], G. Lukin[1], M. Barchuk[2], C. Schimpf[2], C. Röder[3], E. Niederschlag[1], O. Pätzold[1], F. C. Beyer[4], D. Rafaja[2], and M. Stelter[1]

[1] Institute for Nonferrous Metallurgy and Purest Materials, TU Bergakademie Freiberg, 09599 Freiberg (Germany)
[2] Institute of Materials Science, TU Bergakademie Freiberg, 09599 Freiberg (Germany)
[3] Institute of Theoretical Physics, TU Bergakademie Freiberg, 09599 Freiberg (Germany)
[4] Institute of Applied Physics, TU Bergakademie Freiberg, 09599 Freiberg (Germany)

Recent progress in high temperature vapor phase epitaxy (HTVPE) [1, 2] and halogen-free vapor phase epitaxy (HF-VPE) [3] has shown the potential of physical vapor transport-type techniques for the growth of GaN. In this contribution, the growth of GaN layers on sapphire substrates by HTVPE is investigated. The layers were deposited in a growth reactor with a newly developed gallium evaporation cell (Fig. 1) by a two-step process, which is composed of an initial deposition of an 3D nucleation layer followed by lateral overgrowth to form a closed 2D surface layer.

The properties of GaN layers with different thicknesses between 3,8 and 43 µm were analyzed by SEM, DIC, XRD, CL, Raman, and GDMS. The typical FWHMs of the (002) XRD reflex are about 254 arcsec, and the densities of edge dislocations are $2\text{-}5 \cdot 10^8$ cm^{-2}. At room temperature, the layers are compressively stressed in the range of $-831 - 35$ MPa depending on the thickness of the surface layer. The main impurities in the layers are found to be silicon, oxygen, aluminum, boron, and iron with concentrations of $1 \cdot 10^{16}\text{-}1 \cdot 10^{17}$ cm^{-3}.
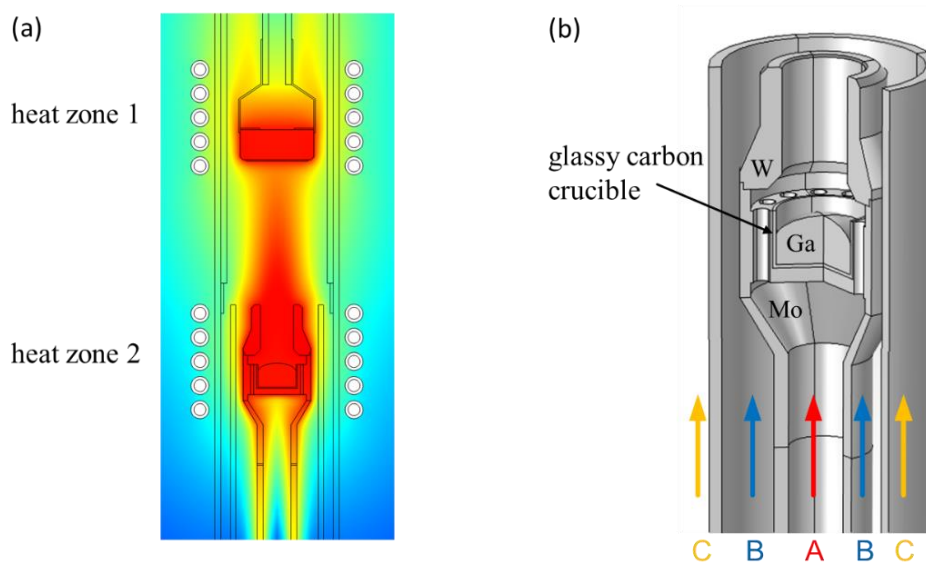
Fig. 1: (a) Scheme of the HTVPE reactor. (b) Details of the gallium evaporation cell. The arrows indicate the gas flows in the reactor: A – central Ar/H$_2$ carrier gas flow, B - separation flow, C - outer gas flow containing NH$_3$.

[1] T. Schneider et al., *J. Cryst. Growth* **468**, 212 – 215 (2017).
[2] G. Lukin et al., *Phys. Status Solidi A* **214**, 1600753 (2017).
[3] D. Nakamura, T. Kimura, *Appl. Phys. Express* **10**, 095503 (2017).

Study of Indium Incorporation in OMVPE Grown 200-nm Thick $In_xAl_{1-x}N$ Layers

Stanislav Hasenöhrl [1], **Prerna Chauhan** [1], **Edmund Dobročka** [1], **Roman Stoklas** [1], **Ľubomír Vančo** [2], **and Ján Kuzmík** [1]

[1] *Institute of Electrical Engineering, Slovak Academy of Sciences, Dúbravská cesta 9, 841 04 Bratislava, Slovak Republic*
[2] *Slovak University of Technology, University Science Park Bratislava Centre, Vazovova 5, 812 43 Bratislava, Slovak Republic*

$In_xAl_{1-x}N$ alloys have received much attention in structures for high electron mobility (HEMT) transistors. The replacement of $Al_xGa_{1-x}N$ barrier material with $In_{0.17}Al_{0.83}N$ was proposed and realized in HEMT transistors also in our group. It is not easy to prepare this material in sufficient device quality. The unintentional incorporation of gallium into the growing layers is a source of significant variations in material properties, because gallium incorporates into the growing layer not only from the underlying GaN buffer layer but also from the all surfaces inside the growth chamber [1]. The next difficulty occurring during the $In_xAl_{1-x}N$ growth is its compositional instability resulting from the large differences in the In to N and Al to N interatomic bonds. The further proposed application of the $In_xAl_{1-x}N$ is to use it as a buffer layer in the strained In-channel HEMT for high-frequency applications [2]. For this purpose we need to prepare the $In_xAl_{1-x}N$ thick layer with the molar ratio of InN (x_{In}) higher than 0.7 with fully relaxed strain.

In our contribution we will show that the indium incorporation into the $In_xAl_{1-x}N$ growing layer is extremely sensitive to the growth conditions and the overall structure design. Layers grown on Al_2O_3 substrate with GaN buffer layer deposited in the same growth run usually contain significant amount of Ga atoms (quaternary $In_xAl_yGa_{1-x-y}N$ is formed) and incline to form a few solid phases of different composition. Two $In_xAl_{1-x}N$ layers grown at almost the same growth conditions can differ in x_{In} for about 0.19. It happens when one growth is performed in the N_2 carrier gas but with TMAl line purged with H_2 and the other one uses the pure N_2. The content of 2.4 % of H_2 in the carrier gas decreases the x_{In} from 0.37 (pure N_2) to 0.18. Values of x_{In} were determined from simulations of X-ray diffraction scans so the potential presence of Ga in the layer can cause their inaccuracy. The Auger microprobe with Schottky emitter was used for accurate measurement of the compositional depth profiles. It was found that the layer grown with H_2 in the TMAl source line is completely quaternary $In_xAl_yGa_{1-x-y}N$. However, the layer grown with N_2 carrier gas is almost ternary $In_{0.37}Al_{0.63}N$ except ~50 nm layer, which was grown after GaN buffer and unintentionally form quaternary $In_xAl_yGa_{(1-x-y)}N$ with decreasing Ga and increasing In-molar fraction towards surface.

To ensure the defined initial state of the reactor and to avoid the Ga incorporation into the grown layer we defined the "Ga-free reactor state" which was then utilized for the $In_xAl_{1-x}N$ growth runs. The Al_2O_3 wafer (c-plane (0001) orientation) with pregrown 2.1 µm GaN layer was used as the growth substrate. Provided that the $In_xAl_{1-x}N$ lattice parameters adhere to Vegard`s law the misfit $\Delta a/a = (a_L-a_S)/a_S$ can vary from -2.4% (AlN) to 11.3% (InN) for the growth on GaN template. The 200 nm thick $In_xAl_{1-x}N$ layers grown on GaN template were partly relaxed and their composition $x_{In} \sim 0.3$-0.33 was stable through the large interval of reactor pressures and NH_3 molar flows. The reason why the composition is stabilized at $x_{In} \sim 0.3$ and how to increase the indium content in the layers is still under investigation.

[1] H. Ben Ammar et.all., *Phys. Status Solidi A* **214**, 1600441 (2017).
[2] J. Kuzmík, *Semicond. Sci. Technol.* **17**, 540 (2002).

Structure of AlN films formed by nitriding the aluminum metal layers on the (0001) sapphire substrates

A. V. Butashin, A. E. Muslimov, V. M. Kanevsky

Federal Research Center "Crystallography and Photonics", RAS,
59 Leninskii av., Moscow, 119333, Russia
amuslimov@mail.ru

The structure of films obtained by annealing in the nitrogen of previously deposited layers of metallic aluminum on (0001) surface of sapphire plates was studied by electron diffraction, electron and x-ray diffraction. Films of aluminum nitride on sapphire substrates grow in accordance with the orientation ratio $(0001)<10\bar{1}0>\text{AlN} \parallel (0001)<11\bar{2}0>\text{Al}_2\text{O}_3$. The best results were obtained with nitriding of aluminum films on sapphire in the heating mode up to a temperature of 1200 ° C (with a heating rate of ~ 100 ° C / h) and holding for 1 hour.

AlN layers grown by Ga-Al liquid phase epitaxy on nitrided r-plane sapphire substrate

Naoki Kanno, Masayoshi Adachi and Hiroyuki Fukuyama

Institute of Multidisciplinary Research for Advanced Materials, Tohoku University, Sendai 980-8577, Japan

AlN is a promising material for AlGaN-based deep-ultraviolet light emitting diodes (DUV-LEDs), because of high ultraviolet transmittance, high thermal conductivity and small lattice mismatch with AlGaN. C- and a-plane sapphire substrates have been widely used for growth of c-plane AlN film. A large internal electric field is generated along the vertical direction in c-plane AlGaN-based DUV-LEDs through the spontaneous and piezoelectric polarization. The internal electric field obstructs radiative recombination in the LEDs; therefore, the emission efficiency of the devices is degraded [1,2]. A non-polar crystal plane such as an a-plane AlN film has no internal electric field along the normal direction of the film. Therefore, a-plane AlN growth on r-plan (1-102) sapphire is necessary to realize high-efficiency DUV-LEDs. We previously succeeded fabrication of a-plane AlN thin films by thermal nitridation at 1603 K and 1623 K on r-plane sapphire substrates and homoepitaxial growth of a-plane AlN layer on the thin films by Ga-Al liquid phase epitaxy [3]. In this study, we attempted to obtain high quality a-plane AlN thin films by thermal nitridation of r-plane sapphire substrates at higher temperature than 1623 K. Moreover, we attempted to grow AlN layer on the substrates by Ga-Al liquid phase epitaxy.

R-plane sapphire substrates with / without off-cut angle of 1° toward [11-20] direction were used. These substrates were thermally nitrided as follows [4]. The r-plane sapphire substrate was set at a homogeneous temperature region in a graphite furnace. The substrate was heated to 973 K under vacuum condition. Subsequently, a N_2-2vol.%CO gas mixture was introduced into the chamber and the temperature was increased to 1703 K. The substrate was kept for 3 h under a N_2-2vol.%CO gas stream at a flow rate of 2 slm at 1703 K. The experimental details of the LPE technique are as follows. The Ga-40mol.%Al flux was set at a homogeneous temperature region in the reaction tube. After evacuating the reaction tube, the reaction tube was filled with N_2 gas. The nitrided r-plane sapphire substrates were immersed in the flux at 1073 K. Subsequently, N_2 gas was injected into the flux at a flow rate of 20 sccm. AlN layers grew on the nitrided r-plane sapphire substrate at 1573 K for 5 h.

Slightly tilted a-plane AlN thin films were fabricated on the r-plane sapphire substrate and r-plane sapphire substrate with an off-cut angle of 1° by the thermal nitridation. Moreover, single domain AlN formed on the r-plane sapphire substrate with an off-cut angle of 1°. The a-axis of the single domain AlN was tilted by 5° from the normal direction of the substrate. We attempted to grow the a-plane AlN using the Ga-Al liquid phase epitaxy on the substrates. As a result, the a-axis of the AlN layer grown by the liquid phase epitaxy was tilted by 67° from the vertical direction of the substrate, indicating that an AlN (11-27) plane grew on the nitrided r-plane sapphire substrates by Ga-Al liquid phase epitaxy.

[1] T. M. Al Tahtamouni, A. Sedhain, J. Y. Lin, H. X. Jiang, Appl. Phys. Lett. 2007, 90, 221105.
[2] R. G. Banal, M. Funato, Y. Kawakami, Phys. Rev. B 2009, 79, 121308(R).
[3] M. Adachi, H. Fukuyama, Phys. Stat. Sol. B, published online, doi:10.1002/pssb.201700478.
[4] H. Fukuyama, K. Nakamura, T. Aikawa, H. Kobatake, A. Hakomori, K. Takada, and K. Hiraga, J. Appl. Phys., 107 (2010) 043502.

HVPE Growth Method for Thick AlN Epilayer

Kyoung Hwa Kim [1,2]**, Hyeon Min Kim** [1]**, Ah Reum Park** [1]**, Injun Jeon** [3]**, Min Yang** [1]**,
Sam Nyung Yi** [1]**, Jae Hak Lee** [1]**, Hyung Soo Ahn**[1,2]***, Chae-Ryong Cho** [3]**,
Suck-Whan Kim** [4]*** and Nobuhiko Sawaki** [5]

[1]*Department of Electronic Materials Engineering, Korea Maritime and Ocean University,
Busan 49112, Korea*
[2]*Compound Semiconductor Fabrication Technology Center, Korea Maritime and Ocean
University, Busan 49112, Korea*
[3]*Department of Nano Fusion Technology, Pusan National University, Busan 46241, Korea*
[4]*Department of Physics, Andong National University, Andong 36729, Korea*
[5]*Department of Electrical and Electronics Engineering, AIT, Aichi 470-0392, Japan*
*e-mail: ahnhs@kmou.ac.kr, swkim@anu.ac.kr

In growing the Al-containing semiconductor such as AlGaN and AlN epilayers by the mixed-source HVPE method, the reactant HCl gas flowed over the Al mixed-source in the source zone formed the chemical compounds $(Al)Cl_n$, and after synthesizing with the source gas (NH_3), the AlN and the AlGaN epilayers were grown in growth zone. Mainly $AlCl_3$ at 850 ℃ and AlCl at 1000 ℃ of the chemical compounds $(Al)Cl_n$ react intensely with qualtz.

It is, therefore, desirable to minimize the reaction between quartz and $AlCl_n$ vapor species to increase the growth thickness of the AlN and the AlGaN epilayers. In this study, a thick AlN epilayer was grown on sapphire substrate at around 1150 ℃ using Al+Ga sources with the proper ratio of Al versus Ga, respectively, in a simplified reactor overlapping source and growth zones by the mixed source HVPE method. In the growth of AlN epilayer, the simplified reactor was designed to minimize the reaction between quartz and AlCl vapor species with high partial pressure of volatile $AlCl_x$ species at around 1150 ℃ from the synthesis between HCl reactive gas and Al material. The AlN epilayers were grown by coalescence between NH_3 and both AlCl and GaCl vapor species with high partial pressure at around 1150 ℃ from the synthesis between HCl reactive gas and Al+Ga mixed material. The growth of thick AlN epilayers with 1 mm thickness, seem to be due to the very high growth rate (>500 μm/h) from the minimization of the reaction between quartz and AlCl vapor species and the response distance for much quantity of coalescence between both AlCl and GaCl vapor species and NH_3 reactive gases at just above the substrate by overlapping the source zone edge upon a substrate in growth zone. The x-ray diffraction peaks and cross-sectional SEM image for AlN epilayers indicate that these epilayers had crystallized successfully.
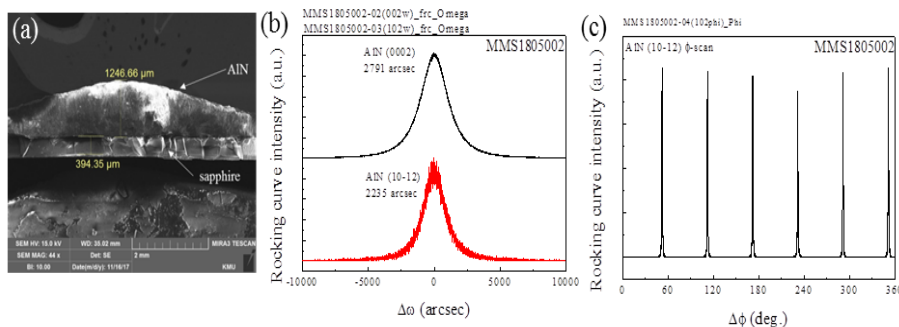
Fig.1 (a) cross-sectional FE-SEM image of the AlN epilayer grown by mixed-source HVPE method. (b) and (c) XRD rocking curve results of AlN grown, respectively.

Mg-doped AlN Epilayer Grown by Mixed Source HVPE Method

Sang Woo Kim [1]**, Kyoung Hwa Kim** [1, 2]**, Ki Beom Park** [1]**, Injun Jeon** [3]**, Jae Hak Lee** [1]**,
Min Yang** [1]**, Sam Nyung Yi** [1]**, Hyung Soo Ahn** [1, 2]***, Chae-Ryong Cho** [3]**,
Suck-Whan Kim** [4]*** and Nobuhiko Sawaki** [5]

[1]*Department of Electronic Materials Engineering, Korea Maritime and Ocean University,
Busan 49112, Korea*
[2]*Compound Semiconductor Fabrication Technology Center, Korea Maritime and Ocean
University, Busan 49112, Korea*
[3]*Department of Nano Fusion Technology, Pusan National University, Busan 46241, Korea*
[4]*Department of Physics, Andong National University, Andong 36729, Korea*
[5]*Department of Electrical and Electronics Engineering, AIT, Aichi 470-0392, Japan*
*e-mail: ahnhs@kmou.ac.kr, swkim@anu.ac.kr

AlN epilayers have been applied in many fields such as a detector in solid-state ultraviolet (UV), UV light-emitting diodes (LEDs), and high-performance III-nitride optoelectronic device. The AlN epilayer with a direct energy gap of 6.2 eV has diverse characters including high thermal conductivity, good chemical and physical stability. For a manufacturing an AlN-based applications, the growth of a p-type AlN epilayer with high conductivity is important. For a long time, Mg has been used as a dopant material for growing a p-type III-nitride epilayer. But, the growth of Mg-doped AlN (AlN:Mg) epilayer with high p-type conductivity is difficult due to the large activation energy of Mg in the AlN and the generation of compensating centers and defects during the crystal growth. In this study, AlN:Mg epilayers with various Mg composition were grown by a mixed-source HVPE. The mixed-source HVPE instruments consists of the reactor combining both a source zone with a RF heating coil and a growth zone with three furnaces for the growth of AlN:Mg epilayer. Metallic Al and Mg were filled in a well of graphite boat as source materials for the growth of AlN:Mg epilayer. Mg composition in the AlN:Mg epilayers was controlled by modulating the quantity of Mg source in the mixed-source. Surface morphology and crystalline structure of AlN:Mg epilayers with different Mg compositions were characterized by FE-SEM and HR-XRD. XPS was carried out to identify the chemical binding energy and confirm the Mg elements in the AlN:Mg epilayer. XPS spectra of the AlN:Mg epilayers indicate the presence of Mg^{2+} in the epilayer, which can be demonstrated that Mg was doped successfully into the AlN epilayer.
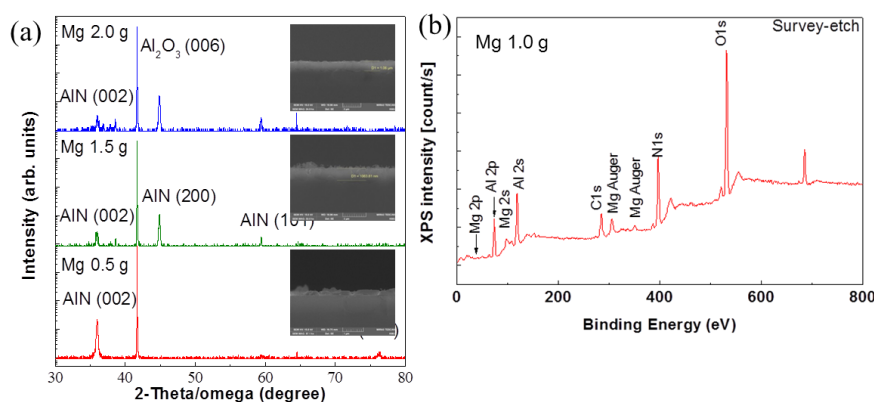
Fig.1 (a) XRD 2theta/omega scan results with varying Mg composition and cross-sectional FE-SEM images of the AlN:Mg epilayer (inset) (b) XPS survey spectrum of Mg doped AlN epilayers.

The Growth of High Al Composition $Al_xGa_{1-x}N$ Epilayers

Jin Seok Yu [1], **Kyoung Hwa Kim** [1,2], **Sang Woo Kim** [1], **Injun Jeon** [3], **Min Yang** [1], **Sam Nyung Yi** [1], **Jae Hak Lee** [1], **Hyung Soo Ahn** [1,2]*, **Chae-Ryong Cho** [3], **Suck-Whan Kim** [4]* **and Nobuhiko Sawaki** [5]

[1]*Department of Electronic Materials Engineering, Korea Maritime and Ocean University, Busan 49112, Korea*
[2]*Compound Semiconductor Fabrication Technology Center, Korea Maritime and Ocean University, Busan 49112, Korea*
[3]*Department of Nano Fusion Technology, Pusan National University, Busan 46241, Korea*
[4]*Department of Physics, Andong National University, Andong 36729, Korea*
[5]*Department of Electrical and Electronics Engineering, AIT, Aichi 470-0392, Japan*
*e-mail: ahnhs@kmou.ac.kr, swkim@anu.ac.kr

The $Al_xGa_{1-x}N$ alloys with high Al composition as epilayers grown on sapphire substrates have been employed in their applications as a detection with a biological agent in solid-state ultraviolet (UV) as well as optoelectronic performance for III-nitrides device. The energy band gap at room temperature for the Al composition of $Al_xGa_{1-x}N$ alloys is known from 3.44 eV for GaN at x=0 to 6.05 eV for AlN at x=1 varying linearly with Al fraction. In this study, the $Al_xGa_{1-x}N$ epilayer was grown on c-plane sapphire substrate by using a mixed-source hydride vapor phase epitaxy (HVPE) methods. In order to grow $Al_xGa_{1-x}N$ epilayer with high Al composition, metallic Al, Ga, and NH_3 gas was used as the precursor with N_2 carrier gas. HR-XRD results of $Al_xGa_{1-x}N$ layer grown for various Ga/Al ratio and source temperature shows a large main peak from $Al_xGa_{1-x}N$ (0002), and a broad shoulder due to the gradually changed Al composition, and the FWHM value of $Al_xGa_{1-x}N$ (0002) is wide. TEM and EDS image of the $Al_xGa_{1-x}N$ epilayer show the change of Al and Ga mole fraction versus the thickness of epilayer. The change of Al composition in the $Al_xGa_{1-x}N$ epilayer was controlled by changing of mixing ratio in Ga and Al mixed-source. The $Al_xGa_{1-x}N$ epilayer with Al composition above 85% or AlN epilayer were grown by decreasing the source zone temperature. From the results, high Al composition $Al_xGa_{1-x}N$ epilayer and AlN epilayer can be grown by mixed-source HVPE method, Al composition was controlled simply by changing of mixing ratio in Ga and Al mixed-source and source zone temperature.
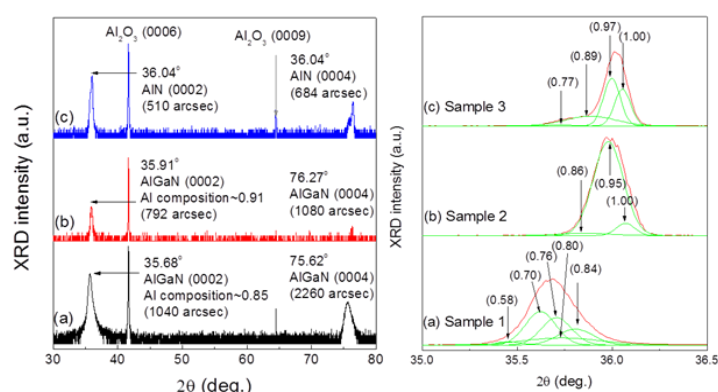
Fig. 1 XRD spectra and Gaussian fitting results as a function of 2-theta for different degrees of the samples, 1(a), 2(b), and 3(c) - $Al_xGa_{1-x}N$ epilayers.

Characteristics of Epilayers in Light Emitting Diode Grown by HVPE Method

Jae Hak Lee [1], Ki Beom Park [1], Jin Seok Yu [1], Kyoung Hwa Kim [1,2]*, Injun Jeon [3], Min Yang [1], Sam Nyung Yi [1], Hyung Soo Ahn[1,2]*, Chae-Ryong Cho [3], Suck-Whan Kim [4]* and Nobuhiko Sawaki [5]

[1]*Department of Electronic Materials Engineering, Korea Maritime and Ocean University, Busan 49112, Korea*
[2]*Compound Semiconductor Fabrication Technology Center, Korea Maritime and Ocean University, Busan 49112, Korea*
[3]*Department of Nano Fusion Technology, Pusan National University, Busan 46241, Korea*
[4]*Department of Physics, Andong National University, Andong 36729, Korea*
[5]*Department of Electrical and Electronics Engineering, AIT, Aichi 470-0392, Japan*
*e-mail: kimkh@kmou.ac.kr, ahnhs@kmou.ac.kr, swkim@anu.ac.kr

High-quality epilayers for lateral-type LEDs are typically grown by metal–organic chemical vapor deposition (MOCVD) known as a technique growing epilayers with fewer defects. However, the growth of high-quality epilayers by MOCVD still faces problems such as the need of a buffer layer and the expensive cost of organic–metal precursors. Meanwhile, it has been hoped that hydride vapor-phase epitaxy (HVPE) as a high-growth-rate technique can be used to grow buffer layers with low defect density, high thickness, and large area. In this study, we prepared two epilayers, of an AlGaN/GaN DH and a thick GaN:Si layer on a sapphire substrate grown by a previously developed method based on mixed-source HVPE method. These two epilayers were used to fabricate a vertical blue LED without a traditional substrate. Additionally, the thick GaN:Si layer was grown like a bulk material to minimize the effect of dislocations formed during the epilayer growth. The dislocation density in the thick GaN:Si layer was investigated at four positions in the bare chip by using field-emission scanning electron microscopy (FE-SEM), high-resolution X-ray diffraction (HR-XRD), and transmission electron microscopy (TEM). Furthermore, the bulk-like thick GaN:Si layer served as both a buffer layer and a new substrate for the vertical blue LED.
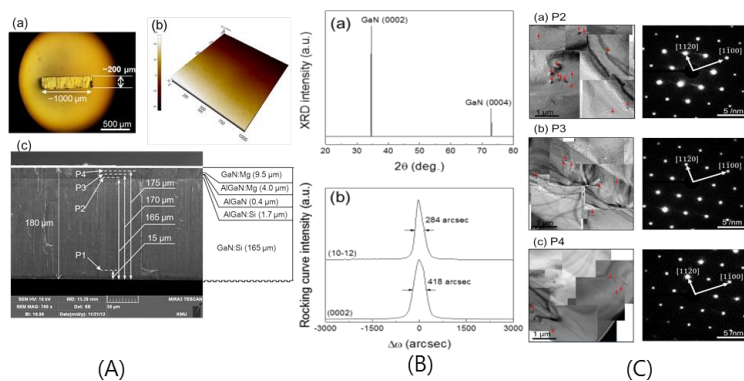
Fig. 1. (A) (a) Cross-sectional optical microscope image of a bare-chip. (b) AFM image (1×1 μm^2) of the top surface of a bare chip. (c) Cross-sectional FE-SEM image of a bare chip and schematic drawing of the epilayers; the dotted lines indicate the positions P1, P2, P3, and P4 at which TEM specimens were obtained; scale bar: 50 μm. (B) (a) XRD spectrum as a function of 2-theta from 20 to 80 degrees for the bare chip. (b) X-ray rocking curve of the GaN (0002) and GaN (10-12) as a function of omega (arcsec) for the bare chip. (C) Planar-view TEM images and SAED patterns at (a) position P2, (b) position P3, and (c) position P4. Scale bars in SAED patterns: 5 nm^{-1}.

Characteristics of aluminum nitride films on hexagonal boron nitride buffer layers using various growth methods through metal organic chemical vapor deposition

Min Han[1], Beo Deul Ryu[1], Kang Bok Ko[1], Chang Hee Jo[1], Tran Viet Cuong[1,2] and Chang-Hee Hong[1*]

[1]*School of Semiconductor and Chemical Engineering, Chonbuk National University, Jeonju, 561-756, South Korea*
[2]*NTT Hi-Tech Institute, Nguyen Tat Thanh University, 298-300 A Nguyen Tat Thanh Street, Ho Chi Minh City, Vietnam*

Hexagonal boron nitride (hBN) fused with III-nitride materials is attracting increasing attention for widening the applications of III-nitride materials. hBN was reported to have unique properties such as a wide band gap, negative electron affinity and high thermal conductivity. Due to its wide bandgap, h-BN has a significant potential for deep ultraviolet (DUV) photonic device applications [1-3]. Additionally, there is a possibility that the high thermal conductivity of h-BN can be applied to improve the heat dissipation of the UV-LED [4]. This application is the same application that graphene inserted in blue LED has heat dissipation effect. In order to realize these applications, it is necessary to directly grow AlN onto the h-BN using MOCVD. In this study, three methods were used to grow the hBN buffer layer: a 2-step (low and high temperature), a 1-step (high temperature), and a pre-TEB surface treatment method. The optical properties of the hBN buffer layers were determined through Raman spectroscopy and absorbance measurements to characterize the fusion between the III-nitride material (AlN) and hBN. The crystal quality of the AlN film grown under the same conditions on the three hBN buffer layers was investigated by X-ray diffraction (XRD). XRD data established that the surface roughness of the hBN layer and density of the AlN nuclei are important factors for crystal quality of III-nitride material. The surface roughness of the hBN layers varied for the different growth methods, while the V/III ratio for each method remained unchanged. This difference in the surface roughness was confirmed to be related to the bonding configuration within the hBN layer, and was further confirmed by X-ray photoelectron spectroscopy (XPS) to be due to the strong interactions between BN with the substrate (B1 peak) [5]. In addition, the strongly interacting BN bond, which is dependent on the method used for the growth of the buffer layer, resulted in a peel-off of the AlN layer. This phenomenon did not occur at the hBN/sapphire interface, but occurred at the AlN/hBN interface, confirming that the strong interaction bonding between BN and the substrate weakens adhesion at the AlN/hBN interface.

[1] M. Snurea, G. Siegel, D.C. Looka, and Q. Paduanoa, J. Cryst. Growth 464, 168 (2017).
[2] Y. Hattori, T. Taniguchi, K. Watanabe, and K. Nagashio, Appl. Phys. Lett. 109, 253111(2016).
[3] Y. Alaskar, S. Arafin, I.M. Velis, and K L. Two-dimensional Materials - Synthesis, Characterization and Potential Applications chapter 3 first ed., InTech, pp.44-57 (2016).
[4] R. Bourrellier, S. Meuret, A. Tararan, O. Stéphan, M. Kociak, L.H.G. Tizei, and A. Zobelli, Nano Lett. 16, 4317 (2016).

[5] A.B. Preobrajenski, M.A. Nesterov, M.L. Ng, A.S. Vinogradov, and N. Ma˚rtensson, Chem. Phys. Lett. 446, 119 (2007).

Synchrotron radiation x-ray topography and defect selective etching analysis of threading dislocations in HVPE-GaN.

J.L. Weyher[1], T. Sochacki[1], S. Sintonen[2], M. Bockowski[1]
[1] Institute of High Pressure Physics PAS, Warsaw, Poland
[2] IQE Cardiff, UK

Synchrotron radiation x-ray topography (SR-XRT) is a convenient and non-destructive characterization method suited for materials with threading dislocation densities (TDD) below 10^5 cm^{-2}. Due to the continuous wavelength distribution and very small divergence of synchrotron radiation, SR-XRT is extremely sensitive to strain and local lattice distortion around dislocations. The contrast associated with strain around dislocations can be used for imaging dislocation and the high intensity of synchrotron radiation allows quick mapping of defects over large areas.

In turn, defect selective etching (DSE) is one of the most popular and rapid? method for evaluation and characterization of etch pit density in a given area of crystalline material. The etch pits can be correlated with the type of threading dislocations due to the difference of size and depth on screw, mixed and edge type defects [1]. Analyze of threading dislocations by SR-XRT in ammonothermally grown gallium nitride (GaN) crystals, as well as GaN grown from vapor phase by hydride vapor phase epitaxy (HVPE) method was performed by Sintonen et al. [2] and Kirste et al. [3], respectively. In both cases, only two types of dislocation contrasts were observed. They were correlated with screw and mixed threading dislocations. No threading edge dislocations (TEDs) were found. The authors concluded, thus, that the TED density in ammonothermal and HVPE GaN should be extremely low. It is in opposite to the results of DSE of ammonothermal and HVPE GaN [4]. Three types of pits, in terms of their size, were distinguished on the c-plane of GaN: large, medium and small. Following the results presented in ref. [1], they were correlated to screw, mixed and edge dislocations with densities 10^0, 1-2x10^4, and 5x10^4 cm^{-2}, respectively.

In this paper, free standing HVPE-GaN, sliced from HVPE-GaN grown on ammonothermal GaN is analysed by SR-XRT and DSE methods. Back reflection SR-XRT image contrasts of threading dislocations performed for the c-plane of HVPE-GaN are compared with images after DSE. Correlation between contrast of the SR-XRT spots and size of the etched pits are examined, determined and described. It is shown that all three kinds of threading dislocations: screw, mixed as well as edges can be detected by the SR-XRT method. Additionally, these defects are correlated one to one with etched pits revealed by the DSE. It will be shown that the pronounced difference in size of pits on different types of dislocations occurs only when optimized etching conditions (time and temperature) are employed.

References
[1] J.L. Weyher et al., J. Crystal Growth, 305, 384 (2007);
[2] S. Sintonen et al. J Appl. Phys. 116, 083504 (2014) ;
[3] L. Kirste et al. ECS Journal of Solid State Science and Technology, 4 (8) P324 (2015);
[4] T. Sochacki et al. PSS B, 1–8 (2014).

Crystallization of Thin GaN Layers by HVPE Method on Native and Foreign Substrates

M. Oklej[1, 2]**, T. Sochacki**[2]**, M. Amilusik**[2]**, M. Fijalkowski**[2]**, M. Iwinska**[2]**, B. Lucznik**[2] **and M. Bockowski**[2]

[1] *Chemical Scientific Club of UKSW*
Cardinal Stefan Wyszynski University. Mathematics and Natural Sciences Department
School of Exact Sciences. ul. Woycickiego 1/3, 01-938 Warszawa, Poland
[2] *Institute of High Pressure Physics PAS. ul. Sokołowska 29/37,*
01-142 Warszawa, Poland

Possibility of using gallium nitride (GaN) for high-power vertical electronic devices (like Schottky diodes) determines the need to obtain 50-100-µm-thick, slightly conductive and with controlled level of impurities drift layers of GaN deposited on n-type bulk GaN substrates. Hydride vapor phase epitaxy (HVPE) seems to be the most promising technology for such approach. It is one of the best methods for fabrication of free-standing n-type GaN crystals and then substrates as well as to grow thick, up to 100 µm, high purity as well as high structural quality GaN layers [1,2]. It should be remarked that thickness of GaN layers deposited by MOCVD or MBE techniques does not exceed 10-15 µm.

In this work results of crystallization of thin layers (up to 100 µm) of GaN by HVPE method on native n-type ammonothermally grown GaN substrates, n-type HVPE-GaN, and foreign sapphire substrates will be presented. Examination of growth conditions and their influence on the properties of the deposited layers will be discussed. Results of characterization of obtained layers by DIC microscopy (growth morphology), XRD measurements (structural quality), defect selective etching (etch pit density), and SIMS measurements (concentration of impurities) will be presented. Additionally, photo-enhanced chemical (PEC) etching will be used for showing the structural quality of the interfaces between HVPE-GaN layer and seed.

[1] J. A. Freitas, Jr., J. C. Culbertson, N. A. Mahadik, T. Sochacki, M. Bockowski, and M. Iwinska, Cryst. Growth Des., 2015, 15 (10), pp 4837–4842
[2] M. Bockowski, M. Iwinska, M. Amilusik, M. Fijalkowski, B. Lucznik, T. Sochacki, Semicond. Sci. Technol. 2016, 31, 093002.

Highly resistive HVPE-GaN grown on native seeds – investigation and comparison of different dopants

Malgorzata Iwinska, Tomasz Sochacki, Boleslaw Lucznik, Michal Fijalkowski, Mikolaj Amilusik, Elzbieta Litwin-Staszewska, Ryszard Piotrzkowski, and Michal Bockowski

Institute of High Pressure Physics Polish Academy of Sciences, Sokolowska 29/37, 01-142 Warsaw, Poland

Results of doping of HVPE-GaN with different acceptors will be presented. Motivation was to increase the resistivity of crystallized material but also investigate different dopants in GaN and their influence on the properties of grown crystals.

Gallium nitride of the highest purity can be grown by HVPE method. In general, HVPE-GaN without doping is n-type with free carrier concentration at the level of $2\text{-}5\times10^{16}$ cm^{-3}. Main unintentionally incorporated donors are silicon and oxygen. The purity can be increased even further when no quartz parts are present in the growth apparatus [1]. Such material is highly resistive. In case of n-type HVPE-GaN, however, intentional incorporation of acceptors is required when the goal is to compensate residual donors. This should lead to semi-insulating properties of crystallized material. Manganese seems to be an ideal acceptor due to its energy level close to the middle of the bandgap (activation energy of 1.7-1.8 eV). The second transition metal commonly used as dopant in HVPE is iron (activation energy of 0.6-0.7 eV). Choosing the source (precursor) of iron is essential in order to remain a low level of unintentionally incorporated chemical elements which influence the electrical properties of obtained crystals. The last investigated dopant was carbon. Energy level connected to carbon in GaN is situated at about 1 eV above the valence band maximum. This leads to strong yellow luminescence observed in the PL spectra. Advantages and challenges connected to the three dopants (Mn, Fe, and C) used in HVPE crystallization will be described. GaN crystals and their structural, electrical and optical properties will be presented.
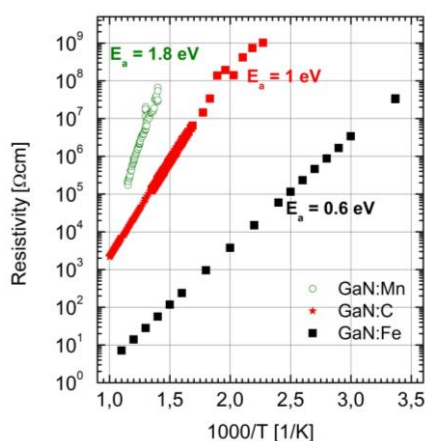
Fig. 1 Results of resistivity vs inverse temperature for HVPE-GaN samples doped with Mn, C, and Fe.

[1] H. Fujikura, T. Konno, T. Yoshida, and F. Horikiri, *Jpn. J. Appl. Phys.* **56**, 085503 (2017).

Highly conductive HVPE-GaN grown on native seeds – investigation and comparison of different dopants

Boleslaw Lucznik[1], Malgorzata Iwinska[1], Tomasz Sochacki[1], Michal Fijalkowski[1], Mikolaj Amilusik[1], Henryk Teisseyre[2], and Michal Bockowski[1]

[1]Institute of High Pressure Physics Polish Academy of Sciences, Sokolowska 29/37, 01-142 Warsaw, Poland
[2]Insititute of Physics, Polish Academy of Sciences, Al. Lotnikow 32/46, 02-668 Warsaw, Poland

Currently available commercial grade GaN substrates are prepared from crystals grown by HVPE. This method involves crystallization from the gas phase and has two advantages – fast growth and high purity of HVPE-GaN. Without intentional doping, the material is n-type with the free carrier concentration of the order of 10^{16} cm^{-3}. However, controllable doping of HVPE-GaN to prepare substrates of specific parameters is still a challenge. In this work, the influence of two different donor dopants, Ge and Si, on structural, optical, and electrical properties of GaN is presented. Silicon or germanium with dichlorosilane ($SiCl_2H_2$) and germanium tetrachloride ($GeCl_4$) as precursors, respectively, were introduced to the growth zone of the HVPE reactor in order to obtain highly conductive n-type material. Advantages and disadvantages of doping with Si and Ge will be presented and two types of highly conductive n-type HVPE-GaN will be compared.

When the material is intentionally doped with Si the YL peak increases with Si content. According to SIMS, Raman, and Hall measurements, the concentration of Si is always higher than the free carrier concentration in GaN:Si. This shows that part of Si donors is compensated by an acceptor state. The strong YL suggests that this deep acceptor is V_{Ga} or its complexes. The gradient of Si and free carrier concentration is also observed in the (0001) direction in GaN:Si.

When Ge is incorporated into HVPE-GaN, no YL is observed and there is no significant difference between the concentration of Ge and the free carrier concentration. It may suggest that in this case the V_{Ga} are not formed. Additionally, no changes in free carrier concentration and Ge concentration were observed in the in-depth profile ((0001) direction).

Vacancy defects in Si and Ge doped HVPE-GaN investigated by positron annihilation spectroscopy

I. Prozheev[1], F. Tuomisto[1], M. Iwinska[2] and M. Bockowski[2]

[1]Department of Applied Physics, Aalto University, Finland
[2]Institute of High Pressure Physics, Polish Academy of Sciences, Warsaw, Poland

Silicon and germanium impurities can be used for n-type doping of GaN. In-grown gallium vacancy defects (V_{Ga}) are known to act as compensating acceptors in n-type GaN and are often complexed with an impurity donor atom [1]. Such defects can be identified with the use of positron annihilation spectroscopy. It is a characterization method suitable to identify native vacancy defects in III-nitrides. In semiconductors thermalized positrons can be trapped at neutral and negative vacancy defects as well as negatively charged non-open volume defects. Changes in the positron-electron annihilation radiation evidence the event of positron trapping at these defects [2].

We have applied positron annihilation spectroscopy to study in-grown vacancy defects in a GaN crystals grown by hydride vapor phase epitaxy (HVPE) and doped with Si or Ge [3,4]. Preliminary results obtained at room temperature indicate that the Si-doped GaN samples contain poor concentrations of vacancy-type defects while the Si donors appear to be highly compensated. In comparison, there are significant concentration of vacancy defects in Ge-doped GaN samples without efficient compensation of the Ge donors. Both findings are in contrast to what is expected. Further temperature-dependent positron experiments need to be performed to shed light on this controversy.

[1] F. Tuomisto et al., Journal of Crystal Growth **350**, 93 (2012).
[2] F. Tuomisto and I. Makkonen, Reviews of Modern Physics **85**, 1583 (2013).
[3] M. Iwinska et al., Journal of Crystal Growth **456**, 91 (2016)
[4] M. Iwinska et al., Journal of Crystal Growth **480**, 102 (2017).

Growth of 2-inch HVPE-GaN doped with Si – numerical simulations and experiments

S. Sakowski , T. Sochacki , M. Amilusik , P. Kempisty , M. Fijałkowski, B. Lucznik, M. Iwinska, and M. Bockowski

Institute of High Pressure Physics Polish Academy of Sciences, Sokolowska 29/37, 01-142 Warsaw, Poland

Crystal growth of GaN by HVPE method was examined. Configuration and reactant flows for doping with Si in an HVPE reactor were scaled up from 1 inch to 2 inches. Numerical simulations and growth experiments were performed in parallel. The goal was to obtain a uniform incorporation of Si on the c-plane of grown crystal and maintain high crystallographic quality of the material.

Simulation model of the growth zone in HVPE reactor was created with commercially available Ansys software. First, CFD calculations were applied to establish concentrations of reactants on the surface of a 1-inch seed. Numerical simulations allowed to reproduce growth conditions of HVPE-GaN:Si that had been developed earlier [1]. The acquired concentrations were used as a point of reference in the next series of numerical experiments. The goal was to reproduce concentrations of reactants on the surface of a 1-inch seed on a 2-inch one. In these theoretical experiments the model was fixed and only flows of input reactants were changed. Results of such calculations are presented in Fig. 1. As a next step the results of simulations were successfully applied for HVPE crystal growth experiments. Thick, up to a few hundred micrometers, silicon doped ($[Si]\sim10^{19}$ cm^{-3}) GaN layers were grown on a 2-inch seed. Value of free carrier concentration was investigated with Raman spectroscopy. The electron concentration was at the level of 10^{18} cm^{-3} and uniform on the c-plane surface.
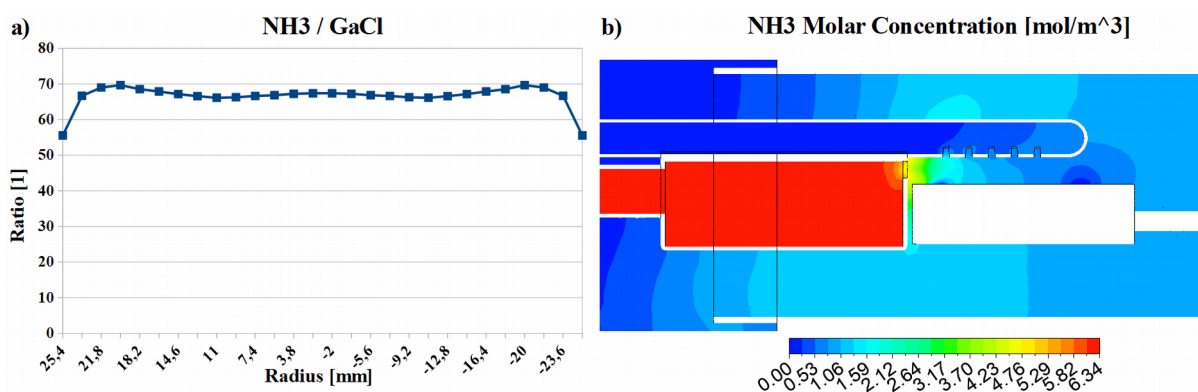
Fig. 1: Calculations performed for 2-inch GaN; a) ratio of NH3 to GaCl on crystal surface b)NH3 molar concentration in reactor's growth zone cross-section

[1] M. Iwinska, T. Sochacki, M. Amilusik, P. Kempisty, B. Lucznik, M. Fijalkowski, E. Litwin-Staszewska, J. Smalc-Koziorowska, A. Khapuridze, G. Staszczak, I. Grzegory, M. Bockowski, *J. Cryst. Growth* **456,** 91 (2016)

Homoepitaxial Semi Polar Growth of GaN on Ammono Seeds by HVPE

Mikolaj Amilusik*, Tomasz Sochacki, Michal Fijalkowski, Boleslaw Lucznik, Malgorzata Iwinska, Izabella Grzegory, and Michal Bockowski

Institute of High Pressure Physics PAS, Sokolowska 29/37,01-142 Warsaw, Poland
*E-mail: amilusik@unipress.waw.pl

Hydride Vapor Phase Epitaxy (HVPE) method is the most common approach for manufacturing gallium nitride substrates. Main advantages of this technique are relatively high growth rate and possibility to obtain high-purity material. HVPE-GaN crystals are mainly grown in the c-direction. Unfortunately, during crystallization runs in the c-direction the growth in lateral directions appears. This phenomenon leads to reduction in diameter of the c-plane and formation of semi polar {10-11}, {10-12}, and {11-22} facets on the growing crystal sides [1]. In order to understand the influence of lateral GaN growth on growth in the c-direction, crystallization in these naturally occurring semi polar directions should be investigated .

In this paper crystallization processes on listed above semi polar surfaces of Ammono GaN seeds will be described in detail. All seeds and obtained GaN layers will be examined by optical microscope with Nomarsky's contrast, X-ray diffraction, Raman spectroscopy, secondary ion mass spectroscopy, and defect selective etching. Influence of growth direction on growth rate and properties (morphology, structural quality, impurities and free carrier concentrations) of obtained crystals will be demonstrated and discussed. Contamination with some unintentional impurities will be detected. As mentioned, all these results will be analyzed in terms of growth in the c-direction.

[1] K. Fujito, S. Kubo, H. Nagaoka, T. Mochizuki, H. Namita, S. Nagao, *Journal of Crystal Growth* **311**, 3011–3014 (2009).

GaN crystallization from iron based solution at 1 and 6 GPa pressures – investigation of critical points of this experimental approach

B. Sadovyi[1], I. Petrusha[2], P. Sadovyi[1], S. Porowski[1], V. Turkevich[2], A. Nikolenko[3], B. Tsykaniuk[3], V. Strelchuk[3] and I. Grzegory[1]

[1] *Institute of High Pressure Physics, Polish Academy of Sciences, 29/37, Sokolowska str., 01-142 Warsaw, Poland*
[2] *V. Bakul Institute for Superhard Materials of the National Academy of Sciences of Ukraine, 2, Avtozavodska str., 04074 Kyiv, Ukraine*
[3] *V. Lashkaryov Institute of Semiconductor Physics, National Academy of Sciences of Ukraine, 45, prospekt Nauky, 03028 Kyiv, Ukraine*

The available data indicate that solubility of nitrogen in the liquid iron at high temperatures and at high pressures attains high values. For instance, at p_{N_2} = 1.5 GPa and T = 1400°C N solubility in Fe is higher than 10 at.% [1], which is significantly above N solubility in liquid gallium at typical conditions of high pressure solution growth of GaN (p_{N_2} = 1.0 GPa, T = 1400 °C) [2]. Therefore, at pressures required for GaN stability at high temperatures (T > 1300 °C) one can expect N solubility in Fe on the level of 10-15 at.% which is extremely promising for the growth of GaN from liquid solution.

Possibilities of GaN growing from solution of Ga and N in liquid Fe at pressures 1 and 6 GPa which are typical for high pressure – high temperature solution growth methods of GaN and diamond, respectively, were investigated. To prove the viability of the approach, the following "proof – of – concept" experiments were carried out: i) Fe-Ga-N system was explored in high pressure gas systems of high volume (1.0 GPa, 1500 °C, 1-5 dcm^3) used previously for crystal growth of GaN at the Institute of High Pressure Physics PAS; ii) Fe-Ga-N system was studied in the toroid high pressure (8.0 GPa, 2500 °C) systems for bulk growth of diamond at the Institute of Superhard Materials in Kyiv. The results of the studies of melting of Fe and Fe-Ga alloys in contact with nitrogen by DTA, dissolution of nitrogen from gas and solid (GaN) sources as well as physical properties of GaN crystals grown in Fe-Ga-N system will be reported.

[1] A. A. Kadik, N. A. Kurovskaya, Yu. A. Ignat'ev, N. N. Kononkova, V. V. Koltashev and V. G. Plotnichenko, *Geochem. Int.* **49**, 429 (2011).
[2] I. Grzegory, M. Bockowski, S. Porowski, GaN Bulk Substrates Grown under Pressure from Solution in Gallium, in: P. Capper (Ed.) *Bulk Crystal Growth of Electronic, Optical and Optoelectronic Materials*, Wiley&Sons, Chichester, 2005, 173-208.

Influence of electron concentration on chemo-mechanical polishing rate of gallium nitride wafers

G. Kamler, , G. Nowak, T. Sochacki, M. Amilusik, I. Dzięcielewski, I. Grzegory, and M. Bockowski

Institute of High Pressure Physics, Polish Academy of Sciences, ul. Sokołowska 29/37, 01-142 Warsaw, Poland

Chemo- mechanical polishing (CMP) was applied for preparation of the GaN wafers to the epi-ready state. 2-inch, 1-inch and 1 cm^2 ammonothermal and hydride vapor phase epitaxy (HVPE) samples were polished with colloidal silica containing slurries. The root mean square (RMS) roughness determined by atomic force microscopy (AFM) of the polished surfaces was less than 0,2 nm over 4 x 4 μm^2 area. It was observed that at the same conditions (slurry composition, applied pressure, polishing time and a rotation velocity of the polishing pad) the CMP removal rate was variable and depended on the free carrier concentration in the sample. Higher material removal rate was observed for the wafers with higher electron concentration. Local inhomogeneities- overgrown pits (pinholes) were found in some samples. In pinholes areas the polishing rate also varied with the local electron concentration. These regions were photoetched and examined by the Kelvin Probe Force Microscopy, Raman spectroscopy, and SIMS in order to investigate the correlation between the electron concentration and the CMP removal rate. To explain this correlation a simple model based on the difference in lattice parameters in the areas with different free carrier concentration will be proposed.

Growth of low Threading Dislocation Density GaN single crystal during the Na-flux Point Seed Method at low supersaturation

Yuki Sawada[1], Takumi Yamada[1], Kosuke Murakami[1], Keisuke Kakinouchi[1],

Kosuke Nakamura[1], Kanako Okumura[1], Tomoko Kitamura[1],

Masayuki Imanishi[1], Masashi Yoshimura[2], Yusuke Mori[1]

1. Grad. Sch. of Eng., Osaka Univ., 2. ILE, Osaka Univ.

Yamadaoka 2-1, Suita, Osaka 565-0871, Japan

The great potential of GaN substrates has been limited in many applications by high threading dislocations density (TDD). Recently, we succeeded in fabricating GaN crystal with extremely low TDD using Na-flux point seed technique by decreasing nitrogen pressure [1]. In this work, we focused on the amount of carbon additions that is another method to control of supersaturation, and investigated the relationship between threading dislocations (TDs) and a size of *c*-growth sector.

As presented in Fig. 1(a), point seed was established by mounting a sapphire plate with a small hole (0.5 mm in diameter) arbitrarily on a GaN template, which is a (0001) GaN film grown on a (0001) sapphire substrate. Point seed, Ga, Na and carbon (0.15, 0.3, 0.5 mol%) were placed in a crucible. Growth proceeded with nitrogen dissolution into a Ga-Na melt at 870°C under nitrogen pressure (4.0, 3.5, 3.0 MPa) for 96 h. We controlled the area of *c*-growth sector during growth by changing the supersaturation. In order to investigate TDD in *c*-growth sector of each crystal, we grinded the crystals at the height of 1.0 mm above mask surface to evaluate TDD at the same growth thickness as shown in Fig. 1(b). Evaluation of TDD was performed using etch-decoration technique on the surface.

The area of the *c*-growth sector got smaller by decreasing nitrogen pressure and the amount of carbon additions, resulted in reduction of the number of TDs in *c*-growth sector as shown in Fig. 2. The mechanism is reported in the previous study [2]. We revealed that decreasing of nitrogen dissolution in the flux, that is, low supersaturation enables to decrease the area of *c*-growth sector, and it is suitable for control of low supersaturation to decrease not only nitrogen pressure but also the amount of carbon additions.
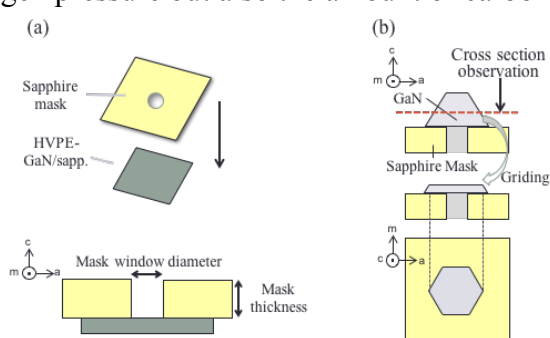
Fig. 1 Schematic drawing of (a) setup for a mask point seed growth, and (b) the grinding of grown crystal to investigate the TDD.
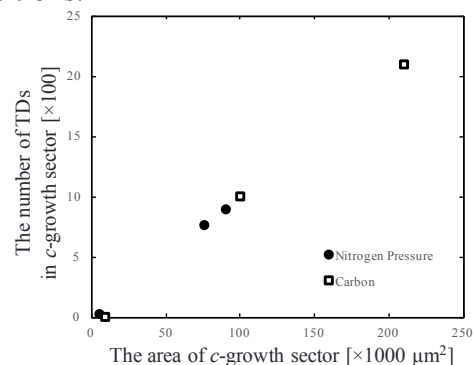
Fig. 2 Relationship between the area of *c*-growth sector and TDs in *c*-growth sector

[1] Y. Sawada *et al.*, International Conference on LEDIA'17 LEDp2-33

[2] M. Imanishi *et al.*, J. Cryst. Growth **427** (2015) 87-93

Effect of AlN Cap Protection on the Decomposition of High-Temperature Annealed GaN

M. Masłyk [1], E. Kamińska [1], O. Dyczewska [2], R. Jakieła [2], E. Dynowska [2], M. Wzorek [1] and K. Gołaszewska-Malec [1]

[1] *Institute of Electron Technology, al. Lotników 32/46, 02-668 Warsaw, Poland*
[2] *Institute of Physics, Polish Academy of Sciences, al. Lotników 32/46, 02-668 Warsaw, Poland*

High temperature treatment of GaN thin films is an important processing step in the fabrication of GaN-based devices. Thermal treatment causes the modification of surface morphology and crystalline structure as well as influences the defect density and enhances the activation of ion implanted dopants in GaN thin films, improving the device performance [1]. Temperatures applied for such processes are in the range from several hundred to about 1400-1500°C, which could lead to the deterioration of the subsurface region stoichiometry i.e. outdiffusion of nitrogen atoms from the GaN. As a result, the GaN surface can be severely damaged, significantly weakening the device performance. To reduce these phenomena a protective capping layer is required. Within materials applied for this role gallium oxide and aluminum nitride are the most promising ones [2,3].

Decomposition kinetics and mechanism of cap-annealed GaN depend on the annealing conditions as well as on the properties of capping layer itself. Investigations of these phenomena are focused mainly on the GaN surface analysis. However, decomposition of the subsurface region plays a crucial role in GaN-based electronic devices such as HEMTs. In this field only few studies were carried out [1,4].

In this work we concentrate on the analysis of both surface and subsurface regions of GaN affected by high temperature annealing and particularly focus on stoichiometry of the AlN cap/GaN interface and GaN subsurface region. GaN films with AlN(30 nm)/SiO_2 and AlN(200 nm)/SiO_2 capping bilayers annealed at 1000°C and 1150°C in a N_2 flow for 1 minute have been analyzed. AlN thin films were deposited by reactive magnetron sputtering in DC mode at room temperature followed by plasma enhanced chemical vapor deposition of 200 nm SiO_2 layers at 300°C. Properties of the AlN/GaN interface as well as the AlN and GaN films are discussed based on the results of structural (HRXRD, HRTEM, SEM, AFM) and chemical (SIMS/RBS) measurements.

[1] H. Bouazizi, M. Bouzidi, N. Chaaben, Y. El Gmili, J.P. Salvestrini and A. Bchetnia, *Mater. Sci. Eng., B* **227**, 16 (2018).
[2] H. Kim, N.-M. Park, J.-S. Jang, S.-J. Park and H. Hwang, *Electrochem. Solid-State Lett.* **4**, G104 (2001).
[3] G. El-Zammar, W. Khalfaoui, T. Oheix, A. Yvon, E. Collard, F. Collard, F. Cayrel and D. Alquier, *Appl. Surf. Sci.* **355**, 1044 (2015).
[4] H. Bouazizi, N. Chaaben, Y. El Gmili, A. Bchetnia, J.P. Salvestrini and B. El Jani, *J. Cryst. Growth* **434**, 72 (2016).

Increasing scintillator active region thickness by InGaN/GaN QW number

T. Vaněk [1,2], A. Hospodková [2], T. Hubáček [1,2], K. Kuldová [2], J. Oswald [2],
J. Pangrác [2], F. Dominec [2], M. Zíková [2], A. Vetushka [2]

[1] *Technical University of Liberec, Studentská 2, CZ-46117, Liberec, Czech Republic*
[2] *Institute of Physics CAS, v.v.i., Cukrovarnická 10, Prague 6 162 00, Czech Republic*

Luminescence results of InGaN/GaN multiple quantum well (QW) structures with number of QWs from 10 to 60 are studied in this work. The aim is to optimize a thickness of active region for maximization of the intensity of faster blue QW emission and suppression of the slower QW defect band luminescence, which is undesired for fast scintillator application [1]. The best excitonic/defect band intensity ratio was achieved for higher number of QWs, see Fig.1. The maximum of excitonic peak photoluminescence (PL) is saturated from 40 QWs for excitation wavelength of 325 nm (100 nm penetration depth) while the defect band is already suppressed for 20 QWs, see Fig. 1(a). It suggests that the defect band originates mainly from the several deepest QWs, which is supported by almost constant maximum of the defect band for 375 nm excitation wavelength that excites all QWs in the structure, see Fig. 1(b). For a more general view to the excitation by different wavelengths the excitation and emission maps for all samples were also measured.
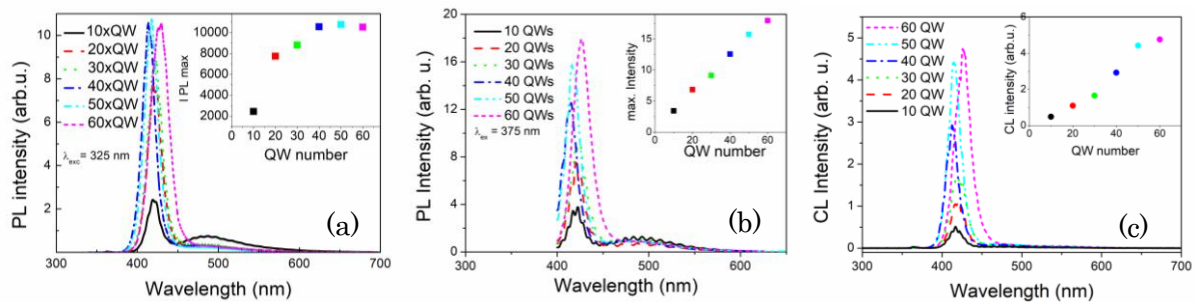
Fig.1. PL results of structures with different QW numbers for excitation at (a) 325 nm, (b) 375 nm and (c) CL spectra with acceleration voltage 20 kV.

The cathodoluminescence (CL) measurements from Fig. 1(c). show weak saturation of excitonic maximum for sample with 60 QWs but our X-ray diffraction measurement did not detect any sign of strain relaxation. The explanation could be a bigger size of V-pits (Fig.2.) which decrease effective luminescent area. This explanation also supports an increasing surface PL nonuniformity of 60 QWs. The decay time by TR soft X-ray radioluminescence was also measured in this work.
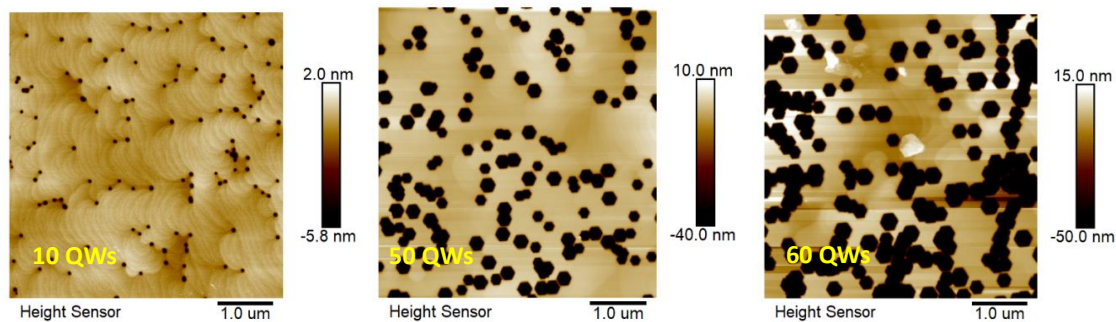
Fig.2. AFM images of surfaces with different QW number

[1] A. Hospodková, T. Hubáček, J. Oswald, J. Pangrác, K. Kuldová, M. Hývl, F. Dominec, G. Ledoux, and Ch. Dujardin, Phys. Status Solidi B **254**, 1700464 (2017).

Effect of dust contamination on GaN/InGaN multiple quantum well growth morphology

Karla Kuldová [1], **Tereza Kretková** [1], **Radek Novotný** [1], **Filip Dominec** [1], **František Hájek** [1], **Jiří Pangrác** [1] **and Alice Hospodková** [1]

[1] *Institute of Physics, Czech Academy of Sciences v.v.i., Cukrovarnická 10, 16200 Praha 6, Czech Republic*

We report about macroscopic defects from InGaN/GaN multiple quantum well (MQW) structures caused by unintended contamination of dust particles during the metalorganic vapour phase epitaxy. These structures are developed for use as fast scintillators and detectors of ionizing radiation [1], where extremely low intensity of excitation should be expected, and thus high demands on cleanliness must be required. On some of our samples, we found defects hundreds of μm in size with different types of changes in their epitaxial morphology and with different modifications in their physical properties (photoluminescence (PL) efficiency, strain in the structure). Using EDX in an electron microscope, particles of different elemental composition (e.g. Fe, Cr, Ni, Ca, Si) have been identified in the centre of the defects. We will present cathodoluminescence, PL and Raman spectra in surroundings of different defects and discuss the influence of the contamination.

In Fig. 1 is presented the defect with Fe particle in the middle and the map of PL of MQW band in the vicinity of the defect. Although the defect radius is ~500 μm, full PL intensity of undamaged surface (~10 arb.u.) is reached only after 3-4 mm.
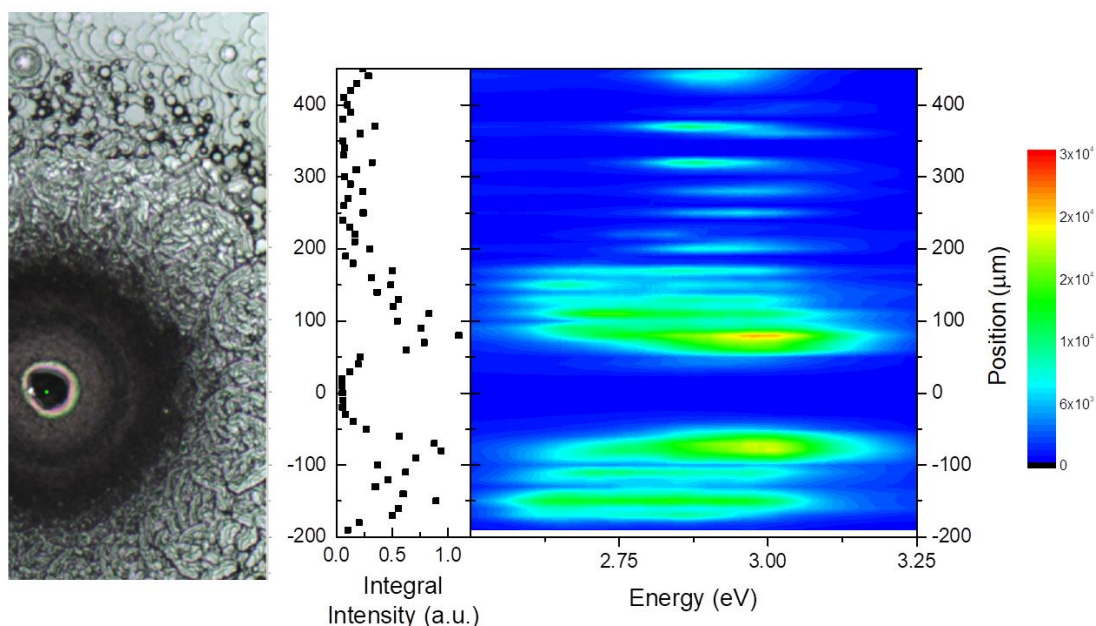
Fig. 1. Left: Optical reflection microscopy of the Fe defect. Right: Integral MQW PL intensity as function of distance from defect and color map of this PL intensity.

Understanding of the influence of macroscopic contaminants has allowed us to find and remove this elements present in much smaller concentrations in undamaged samples [2].

[1] A. Hospodková, J. Oswald, M. Zíková, J. Pangrác, K. Kuldová, K. Blažek, G. Ledoux, C. Dujardin, and M. Nikl, *J. Appl. Phys.* **121**, 214505 (2017).
[2] M. Zíková et al., this conference

Inhomogeneous Luminescence of InGaN/GaN Quantum Wells: Effect of Growth Temperature, Carrier Gas and the Buffer Layer Growth

Filip Dominec, Karla Kuldová, Markéta Zíková, Jiří Pangrác and Alice Hospodková

*Institute of Physics, Czech Academy of Sciences,
Cukrovarnická 10,165 00 Prague 6, Czech Republic*

Scintillators based on InGaN/GaN multiple quantum well (MQW) structures [1] promise high detection efficiency at the low portion of the energetic spectrum of ionizing radiation, as well as excellent temporal and spatial resolution. Using our Aixtron 3x2 CCS system, we have grown 5 μm GaN buffer on 2" sapphire substrates, covered with 10 $In_{0.06}Ga_{0.94}N$ quantum wells separated by low-temperature GaN barriers. Whereas the buffer is grown in the hydrogen carrier gas at roughly 1050 ºC, the InGaN quantum well layers require switching to nitrogen carrier gas and lower temperatures between 700 and 900 ºC. Unfortunately, such conditions are known to compromise the homogeneity of the surface through clusters of hexagonal v-pits, trench defects and other surface corrugations; moreover, we conjecture that contaminating elements embed preferentially into the MQW structure, causing unwanted defect-band luminescence with excessive decay time.
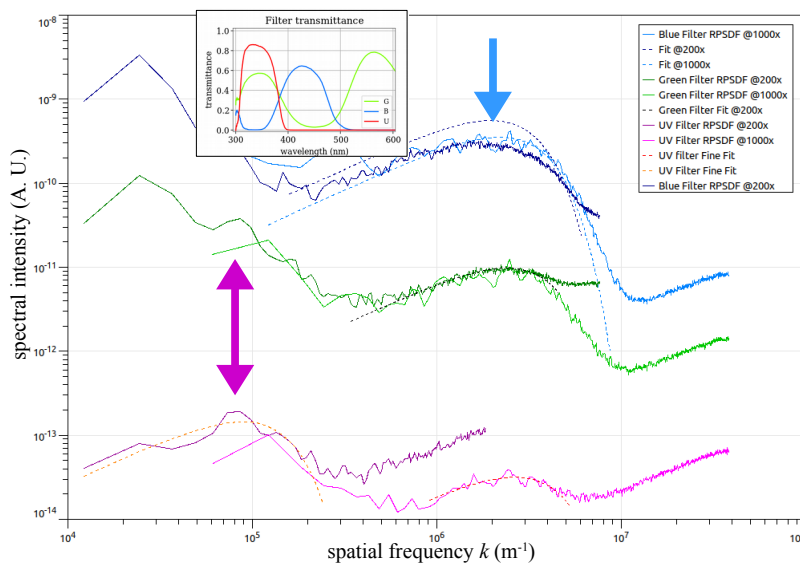
Fig. 1: Logarithmic RPSDF functions of MQW samples for three different filters (see inset), prominent spatial-frequency peaks fitted with Gaussian distribution.
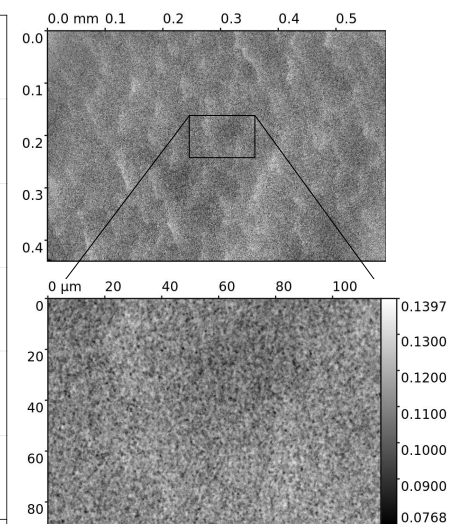
Fig. 2: Cathodoluminescence images at two magnifications taken with the green filter.

The homogeneity of our samples was evaluated using spatially resolved cathodoluminescence at 10 keV (see Fig. 2), showing three distinct emission bands in spectrum corresponding to the exciton in GaN (UV), exciton in the MQW structure (blue) and the defect band (green/yellow). We separated them using color filters (see inset of Fig. 1) and with each filter, we acquired CL images at different magnifications and converted them using 2D Fourier transform into radial power spectral density function (RPSDF). We observed coarse wave-like structures with spatial frequency $k \approx 10^5\,m^{-1}$, as well as fine grain with $k \approx 3\times10^6\,m^{-1}$. Since the former are more apparent with the UV and green filters (pink arrow in Fig. 1), we believe they arise from uneven buffer/MQW thickness, while the grain most prominent with blue filter (blue arrow in Fig. 1) may come from v-pits or clusters thereof protruding the MQW structure.

[1] Hospodková *et al.*, J. Appl. Phys. **121**, 214505 (2017)

Effects of Nitrogen Radical Irradiation on InN Growth by RF-MBE

**Faizulsalihin B. Abas, Ryoichi Fujita, Shinichiro Mouri,
Yasushi Nanishi, and Tsutomu Araki**

Ritsumeikan University, 1-1-1 Noji-higashi, Kusatsu, Japan

The interesting properties of InN such as the small bandgap, the small effective mass, and the high mobility make it suitable for numerous applications including near infrared optoelectronic devices and high-speed electronic devices. In the growth of III-nitrides, the MBE reactor is equipped with an RF plasma generator to supply active nitrogen radical as a nitrogen source. Besides, there are several other applications of N radical irradiation that have been reported such as to remove the oxide layer on the surface of GaN film [1] and for nucleation of self-induced InGaN nanocolumn [2]. Recently, we reported achieving a reduction of threading dislocation density in InN by employing the N radical irradiation to modify the surface morphology of the InN template in-situ before growing InN film on the template [3]. However, the InN template surface modification by the N radical beam irradiation has not been studied in detail. In this letter, we examined the mechanism of the template surface modification by N radical irradiation to further understand the effects on threading dislocation behavior in the regrown InN film.

All InN templates in this study were grown on MOCVD-grown (0001) GaN/sapphire substrates in a conventional RF-MBE system (EpiQuest RC2100NR) equipped with a nitrogen plasma source (SVT Associates 6.03). The details of these InN templates growth have been described elsewhere [3]. The templates were then irradiated with N radical beam in the MBE chamber with a plasma power of 200 W under different substrate temperatures (330-435 ℃). The surface morphological changes before and after the N radical irradiation were monitored in situ with RHEED and the results are as shown in Fig. 1. The RHEED patterns indicated that the InN template surfaces changed from atomically flat surfaces to three dimensional rough surfaces after the N radical irradiation and it is even more remarkable at a higher substrate temperature which is 435 ℃. It was argued that the surface morphology changes might be due to the annealing at high temperature and not related to the N radical irradiation. However, when compared with the samples annealed at 435 ℃ (without N radical irradiation) for 60 min, it shows not only the surface changes but also thermal decomposition of the InN template as the peak of In appears in XRD (Fig. 2). These results suggest that the N radical irradiation on the InN template not only able to modify the surface morphology of the template but also suppress the InN thermal decomposition. Furthermore, the N radial irradiation effects with a different plasma power, irradiation time and electrical properties of the irradiated InN template will also be discussed in detail in the presentation.

[1] S. Gangopadhyay *et al.*, *J. Vac. Sci. Technol.*, **A 32**, 051401 (2014).
[2] J. Xue *et al.*, *Appl. Surf. Sci.* **423**, 219 (2017).
[3] F. B. Abas *et al.*, *Jpn. J. Appl. Phys.* **57**, 035502 (2018).
[4] B. Loitsch *et al.*, *Appl. Phys. Lett.* **102**, 051916 (2013).
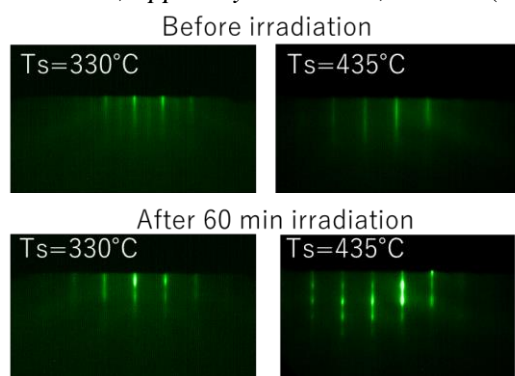
Fig. 1 RHEED patterns of InN template before and after N plasma irradiation.
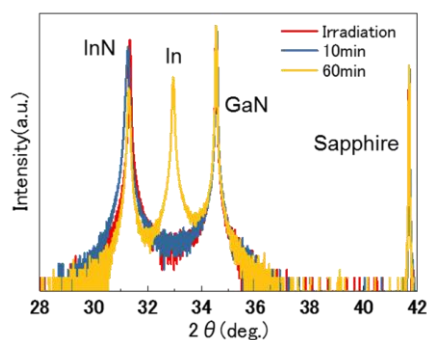
Fig. 2 XRD profiles of InN template after annealing with and without N plasma irradiation.

Influence of Different InGaN/(In)GaN Growth Modes on Indium Incorporation and Quality of Layers

Tomáš Hubáček [1,2]**, Alice Hospodková** [2]**, Jiří Pangrác** [2]**, Markéta Zíková** [2]**, Jiří Oswald** [2]**, Karla Kuldová** [2] **and Eduard Hulicius** [2]

[1] *Faculty of Mechatronics, Informatics and Interdisciplinary Studies, Technical University of Liberec, Studentská 2, CZ-46117, Liberec, Czech Republic*
[2] *Institute of Physics, CAS, v.v.i., Cukrovarnická 10, CZ-16200, Prague 6, Czech Republic*

Growth of InGaN/GaN heterostructures by MOVPE with high indium content in InGaN quantum wells (QW) is a quite difficult task. One of the possible ways how to reach it would be decreasing the QW growth temperature. On the other hand, higher temperature is necessary to have sufficient decomposition of ammonia to suppress nitrogen vacancies in InGaN layers and to get good crystallographic quality of the layers. Even the temperature profile during the increase for the barrier growth plays significant role on the quality of the whole heterostructure. General assumption is that In atoms are desorbed from the QW surface during the temperature rise for the barrier growth. The influence of different layers capping InGaN QWs was studied by other groups [1]. They observed that an increase of the temperature after the InGaN QW growth, without any GaN capping, is necessary to obtain homogeneous and highly efficient luminescence. Generally, we can say that different growth modes of InGaN/GaN heterostructures have big influence on the properties of InGaN quantum wells.

In our work we will show how to significantly increase the In content in QWs without lowering the QW growth temperature. We have studied different growth modes of InGaN/(In)GaN heterostructure while the QW growth parameters (temperature, pressure, flow, etc.) were kept constant. We have only changed parameters during the temperature rise to the barrier growth and parameters during the barrier growth. We have introduced a small TMIn flow immediately after the QW growth and observed not only increased concentration of In in the structure (in both, QW and barrier) but also strong increase of the growth rate (confirmed

Fig. 1: SIMS profile of In content for structures grown with and without TMIn flow during the growth of barriers. The QW growth conditions were identical.

by secondary ion mass spectrometry, see Fig. 1, and X-ray diffraction measurements). We explain this phenomenon by suppression of In desorption during the initial phase of the barrier growth. Photoluminescence spectra of samples with different combinations of (In)GaN QW capping and (In)GaN barriers will be shown and discussed. Luminescent homogeneity of these samples was characterized by PL intensity maps.

[1] M. J. Wallace, P. R. Edwards, M. J. Kappers, M. A. Hopkins, F. Oehler, S. Sivaraya, R. A. Oliver, C. J. Humphreys, D. W. E. Allsopp and R. W. Martin, *Journal of Applied Physics* **117**, 115705 (2015).

Use of Low Temperature Buffer Layer to Suppress the Contamination of InGaN/GaN Quantum Wells

Markéta Zíková, Alice Hospodková, Jiří Pangrác, Tomáš Hubáček, Filip Dominec, Jiří Oswald, Karla Kuldová and Eduard Hulicius

Institute of Physics, Czech Academy of Sciences, Cukrovarnická 10, 162 00 Prague 6, Czech Republic

Nowadays nitride semiconductors have many applications from blue LEDs, high electron mobility transistors, detectors to UV light sources. In our laboratory we are preparing InGaN/GaN quantum wells (QWs) that are planned to be used in scintillating structures. Such structures should have fast and strong luminescence response with short decay time. For this purpose we prepare InGaN/GaN multiple QWs. Unfortunately, in their photoluminescence (PL) spectrum there is also a broad defect band at around 470 nm besides the excitonic peak at around 420 nm. From the time resolved PL we know that this broad defect band is much slower than the excitonic peak which is detrimental for our planned structure application.

According to the measurement of samples with different number of QWs and theoretical simulations we assume that the main contribution comes from the five lowest QWs that face the transition from the higher growth temperature of GaN buffer layer to the lower growth temperature of InGaN QWs. SIMS data of selected samples prove the contamination under the lowest QWs, see an example of Fe contamination in Fig. 1. SIMS results for elements like Si, Ca or Zn show that some elements are contaminating not only a thin region beneath QWs, but also the QWs themselves. We expect that the contamination is due to lowering the temperature, which is a well-known phenomenon [1], and thus we introduced a low temperature (LT) buffer layer under QWs to incorporate the impurities further from the QWs where it does not affect them. In Fig. 2 there are PL spectra of two samples differing only in the presence of LT buffer and we can see that the sample with LT buffer has more intense excitonic peak and partly suppressed the defect band. PL and AFM results for different parameters of LT buffer will be compared. The influence of sample morphology on PL properties will be discussed.
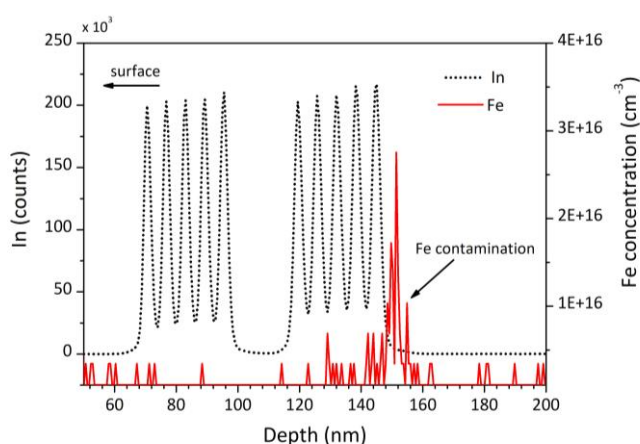
Fig. 1: SIMS results of Fe contamination for a sample with 10 InGaN/GaN QWs
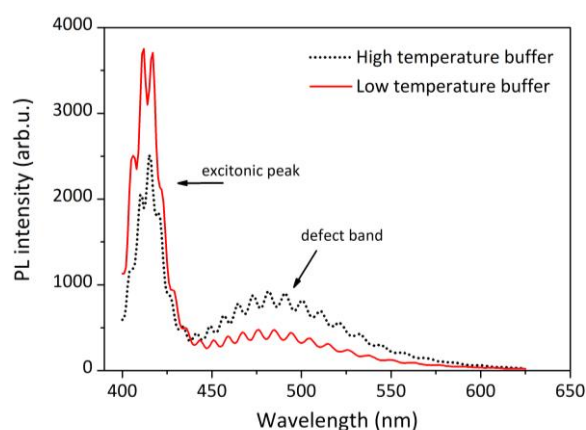
Fig. 2: PL spectra of samples with/without LT buffer

[1] Z. Lin, J. Zhang, R. Cao, W. Ha, S. Zhang, X. Chen, J. Yan, S. Xu, Y. Zhao, L. Li and Y. Hao, *J. Cryst. Growth* **384**, 96 (2013).

UV Emitting Defects in Hexagonal Boron Nitride

K. P. Korona[1], T. Korona[2], A.M. Witowski[1], M. Chojecki[2], A. K. Dąbrowska[1], K. Pakuła[1], J. Borysiuk[1], A. Wysmołek[1], R. Stępniewski[1]

1. Institute of Experimental Physics, Faculty of Physics, University of Warsaw, ul. Pasteura 5, 02-093 Warsaw, Poland
2. Quantum Chemistry Laboratory, Faculty of Chemistry, University of Warsaw, ul. Pasteura 1, 02-093 Warsaw, Poland

Boron nitride (BN) is a wide band-gap semiconductor with energy gap about 6 eV. In spite of lately observed wide interest in BN properties, there are still many discrepancies in reports on its photoluminescence (PL) spectra. In the present work we aim to elucidate some of the intriguing features of the PL of h-BN by means of a joint experimental and theoretical study.

In the theoretical part the defects of h-BN were simulated by the BN flakes capped with hydrogen atoms and modified with various point defects in the center of the flake. Their electronic spectra were calculated by time-dependent (TD) density-functional theory (DFT) with the CAM-B3LYP functional and jun-cc-pVDZ basis set. For the perfect BN flake these calculations gave the lowest excitation energy 6.2 eV, while the introduced defects usually gave rise to several electronic excitations of lower energies. Among considered defects, carbon impurities with various placements of carbon atoms were assumed (e.g. two separated or two neighboring carbon atoms - denoted as C101 and C2; two or three such pairs - C22, C222; four, six, of ten adjacent carbons - C4, C6, C10). The obtained lowest excitation energies were, for example, 4.8 eV for the C2, 3.6 eV for C101 and 3.7 eV for C10 configuration. The analysis of the character of the lowest excitations for such carbon-doped BN flakes reveals that they are localized (intra-defect) excitations. Additionally, within the harmonic vibrational modes one can find several vibrations localized on carbon defects, among which at least one stretching C-C node of frequency in the range 1550 - 1600 cm^{-1}, depending on the defect type, has a high intensity.

The experimental part was performed mostly on the boron nitride layers grown on sapphire substrates using the MOVPE equipment. We also measured some industrial-grade samples (in the powder form) for a comparison. The photoluminescence was excited with the 215 nm (5.8 eV) light generated as fourth harmonic of the Ti:Sapphire laser line. Micro-PL spectroscopy was performed with the mirror objective. Time-resolved PL (TRPL) was measured with a streak camera and with quartz optics. Infrared reflection and absorption measurements were performed at room temperature, using a Fourier transform spectrometer Bruker IFS 113 V.

In the photoluminescence a donor-acceptor (or DX) emission at 5.3 - 5.4 eV was observed (in addition to resonant emission at about 5.7 - 5.8 eV). Moreover, some sharp lines at range of 300 nm (4.1 eV) and 380 nm (3.2 eV) were measured. The 5.7-eV line had lifetime of about 20 ps, what in other materials is characteristic for free excitons. The 4.1-eV and 3.2-eV bands consisted of few sharp lines with nearly identical lifetimes (about 0.7 ns). The detailed analysis reveals two zero-phonon transitions followed by a series of phonon replicas. Based on the theoretical results we postulate that the 4.1-eV and 3.2-eV lines can be assigned to C2 and C101 defects, respectively.

Infrared reflection revealed that E_{1u} line of BN at 1370 cm^{-1} as well as few lines in the range 1500 - 1600 cm^{-1} that can be related to the local vibrations related to the discussed defects.

MOVPE Growth and Surface Morphology Investigation of High Quality GaN, $Al_{0.14}Ga_{0.86}N$ Epilayers and $Al_{0.14}Ga_{0.86}N$/GaN Superlattice

W. Olszewski[1*], S. Gorantla[1], K. Moszak[1,3], J. Stoever[4], R. Szukiewicz[1,2] and D. Hommel[1,2]

[1]*Wroclaw Research Center EIT+ Sp. z o.o., ul. Stablowicka 147, 54-066 Wroclaw, Poland*
[2]*Faculty of Physics, University of Wroclaw, plac Maxa Borna 9, 50-204 Wroclaw, Poland*
[3]*Institute of Low Temperature and Structure Research, Polish Academy of Sciences W. Trzebiatowski Institute, ul. Okolna 2, 50-422 Wroclaw, Poland*
[4]*Leibniz Institute for Crystal Growth, Max-Born-Str. 2, D-12489 Berlin, Germany*
Email:wojciech.olszewski@eitplus.pl

One of the main difficulties in the crystal growth of gallium nitride (GaN) is keeping the threading dislocation density (TDD) as low as possible. Those dislocations significantly reduce the efficiency of optoelectronic devices by acting as non-radiative recombination centres. Sophisticated methods like epitaxial lateral overgrowth (ELOG) or interlayer manage (SiN_x) are used to reduce TDD down to $10^5 – 10^6 \, cm^{-2}$. Surprisingly we have obtained similar TDD in GaN and $Al_{0.14}Ga_{0.86}N$ epilayers by standard MOVPE.

In this study we present the growth conditions optimization of GaN, $Al_{0.14}Ga_{0.86}N$ epilayers and $Al_{0.14}Ga_{0.86}N$/GaN superlattices on sapphire substrates by MOVPE, in a CSS reactor (Thomas Swan, Aixtron), and their morphology studies. TEM and XRD investigation reveal an etch pit density around $2x10^6 \, cm^{-2}$ in our 2 µm thick GaN buffer.

We have also obtained high quality $Al_{0.14}Ga_{0.86}N$/GaN heterostructures. Interestingly SEM images show that most of etch pits in 0.7 µm thick $Al_{0.14}Ga_{0.86}N$ top layer are located inside the area of crack channels (Fig. 1). The $Al_{0.14}Ga_{0.86}N$ layer exhibits areas free of cracks and etch pits as large as $0.2 \, mm^2$. The linear dislocation density in cracks has been estimated after wet-chemical etching to be about $2x10^3$ (which corresponds to an area density of the order of $10^6 – 10^7 \, cm^{-2}$). The etched surface morphology of the samples observed by atomic force microscopy (AFM) will be discussed as well.

High-angle annular dark field (HAADF) STEM images of $Al_{0.14}Ga_{0.86}N$/GaN superlattice structures show sharp interfaces between AlGaN and GaN layers (Fig.2). EPD of superlattice are found to be in the same order of magnitude as those of pure GaN template. Hall effect measurements reveal that the background electron concentration is as low as $\sim 8x10^{14} \, cm^{-3}$, which is really low for an uncompensated layer. This again confirms the high quality of our structure. The successful growth of such high quality structures by so easily transferable to industry is expected to dramatically increase the efficiency of GaN-based optoelectronic devices and will be applied for the fabrication of high efficiency UV emitter.
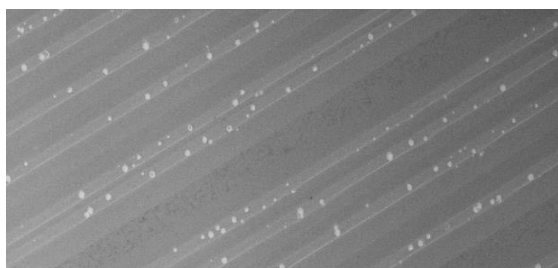
Fig. 1. Plane-view SEM image of etched surface of $Al_{0.14}Ga_{0.86}N$ layer
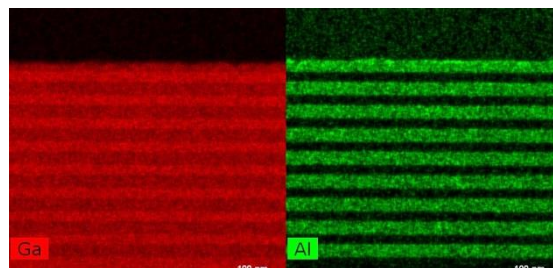
Fig. 2. EDS image of $Al_{0.14}Ga_{0.86}N$/GaN superlattice

Plasma-assisted MBE and structural properties of AlGaN nanorods selectively grown on μ-cone patterned c-sapphire substrates

A.N. Semenov, D.V. Nechaev, D.A. Kirilenko, S.I. Troshkov, V. N. Jmerik, and S.V. Ivanov

[1] *Ioffe Institute of RAS, Polytekhnicheskaya 26, St. Petersburg 194021, Russia*

The regular arrays of group-III nitrides nanorods (NRs) are of great interest in the field of nano-optoelectonic devices for quantum information processing and communications. The emission of single photons above room-temperature have been demonstrated in AlGaN NRs containing InGaN quantum dots, grown by selective area MOCVD on a dielectric SiO_2 nanomask formed by electron beam lithography [1]. Earlier we have reported an original approach to the selective area growth (SAG) of GaN NRs by plasma-assisted MBE (PA MBE) on μ-cone patterned sapphire substrates (μ-CPSSs) without any nanolithography techniques [2]. This paper describes the development of this method for growing the regular arrays of AlGaN/GaN NRs on the μ-CPSSs. A three-stage PA MBE fabrication process of AlGaN NRs has been developed, starting with a growth of GaN nucleation layer at high temperature of T_S=760-770°C and metal-rich conditions. Then (100-300) nm-thick GaN NRs were grown at strongly N-rich conditions (III/N~0.2) exactly on the cone tips at the same T_S. Finally, the AlGaN NRs with a height up to 1 mm were grown at the N-rich conditions and higher T_S varied in range of 760-830°C. During the latter stage, the pulsed mode of PA MBE was used with a growth interruption for 10-30 s every one minute. Structural properties of the AlGaN NRs were investigated using scanning electron (SEM) and high-angle annular dark-field scanning transmission electron (HAADF-STEM) microscopies.
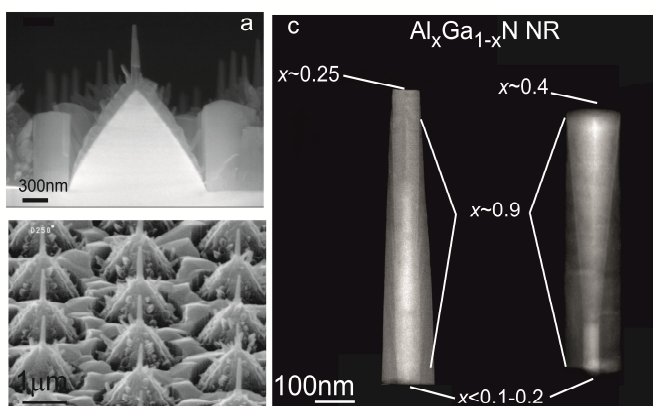
Fig. 1 SEM images of AlGaN NRs grown on m-CPSS at a substrate temperature of 810°C (a and b). (c) HAADF STEM images of AlGaN NRs grown with a duration of growth interruption of 10s (left), 20s (right).

Fig. 1a and b demonstrate the AlGaN NRs selectively grown at T_S~810°C which has been found to be optimal. The lower temperatures result in the worse growth selectivity, when parasitic growth of AlGaN NRs on the microcone slopes occurs. Higher T_S leads to the drastically decreased NR growth rate. While the growth selectivity of NR is governed by T_S, the Al distribution inside the NRs depends on the duration of growth interruptions. This is illustrated in Fig.1c showing the HAADF STEM images of the AlGaN NRs formed at the same temperature but the varied duration of growth interruptions: 10s (left) and 20s (right). The complex distribution of Al in AlGaN NRs in radial and longitudinal directions, quantified by the energy dispersive x-ray spectroscopy, as well as the shape of NRs are discussed in terms of (1) competition between incorporation of Ga and Al adatoms possessing the strongly different desorption rates and (2) different surface mobilities of Ga and Al adatoms, resulting from their different vertical surface diffusion rates and incorporation probabilities into the AlGaN NRs. In addition, the spontaneous formation of AlGaN/GaN superlattice with a period of several MLs along the NR core has been also observed. The work was supported by RSF (#14-22-00107).

[1] M.J. Holmes, K. Choi, S. Kako et al, Nano Lett. **14**, 982 (2014)
[2] V.N. Jmerik, N.V. Kuznetsova, D.V. Nechaev et al, J. Cryst. Growth **477**, 207 (2017).

Morphology and Electrical Properties of InGaN:Mg/InGaN:Si Tunnel Junctions Grown by Plasma-assisted Molecular Beam Epitaxy

M. Żak [1,2]**, M. Siekacz** [1]**, K. Nowakowski-Szkudlarek** [1]**, A. Feduniewicz-Żmuda** [1] **and C. Skierbiszewski** [1,3]

[1] *Institute of High Pressure Physics Polish Academy of Sciences,*
ul. Sokołowska 29/37, 01-142 Warsaw, Poland
[2] *Gdańsk Uniwersity of Technology, ul. Gabriela Narutowicza 11/12, 80-233 Gdańsk, Poland*
[3] *TopGaN Ltd, ul. Sokołowska 29/37, 01-142 Warsaw, Poland*

Discovered in 1958 by L. Esaki tunneling effect in high doped germanium p-n junction was breakthrough for electronic devices. In this systems carriers are tunneling through a thin triangular barrier, between degenerated valence and conduction bands. It is well known, that for the wide energy gap semiconductors the depletion region of p-n junction is larger. Therefore for gallium nitride homojunctions is hard to achieve high tunneling probability, due to high energy gap about 3,4 eV. It is shown by S. Krishnamoorthy et al., [1] that by adding a InGaN quantum well between heavily doped p-type and n-type GaN it is possible to increase tunneling by orders of magnitude. This effect is caused by strong polarization field inside GaN:Mg/InGaN/GaN:Si tunnel junction (TJ).

Application of tunnel junction to nitride based structures opened new possibilities for novel devices such as vertically integrated cascade multicolor LEDs and LDs [2]. However, to demonstrate efficient devices with TJ by Metal-Organic Vapor Phase Epitaxy (MOVPE) is very problematic. Presence of the n-type GaN:Si above GaN:Mg prevents activation of Mg doped bottom layer due to the fact that diffusion of hydrogen through n-type GaN:Si layer is completely blocked. In case of Plasma Assisted Molecular Beam Epitaxy (PAMBE) system we do not need to activate p-type layers, so there are possibilities to apply tunnel junctions inside the device structure.

In this work we study the influence of doping by Si donors and Mg acceptors of GaN/InGaN/GaN heterostructures grown by PAMBE on the morphology of p-n TJ and its electrical properties. We found that the tunneling currents strongly depend on the Si doping of the n-type region. We demonstrate that the lowest resistance of p-n TJ can be achieved for very high Si doping (at the level of $2 \times 10^{21} \text{cm}^{-3}$). However when we increased the Si doping level above 10^{20} cm^{-3}, the gradual deterioration of surface morphology is observed. We will discuss the optimum grow conditions, which give us as low as possible series resistance and smooth morphology of the devices.

[1] S. Krishnamoorthy, F. Akyol, P. S. Park and S. Rajan, *Appl. Phys. Lett.* **102**, 113503 (2013)
[2] C. Skierbiszewski, G. Muzioł, K. Nowakowski-Szkudlarek, H. Turski, M. Siekacz, A. Fedunewicz-Żmuda, A. Nowakowska-Szkudlarek, M. Sawicka and P. Perlin, *APEX* **11,** 034103 (2018)

Influence of Mg-doped Layers on Internal Optical Losses in InGaN Laser Diodes

M. Hajdel [1,2], G. Muzioł [1], K. Nowakowski-Szkudlarek [1], M. Siekacz [1], A. Feduniewicz-Żmuda [1], P. Wolny [1] and C. Skierbiszewski [1,3]

[1] *Institute of High Pressure Physics Polish Academy of Sciences, ul. Sokołowska 29/37, 01-142 Warsaw, Poland*
[2] *Gdańsk University of Technology, ul. Gabriela Narutowicza 11/12, 80-233 Gdańsk, Poland*
[3] *TopGaN Ltd, ul. Sokołowska 29/37, 01-142 Warsaw, Poland*

Internal optical losses (α_i) are one of the major factors which influence the external laser diode (LD) parameters such as threshold current density and differential efficiency. To develop high performance LDs it is necessary to gain a comprehensive understanding of the mechanisms causing optical losses in the laser cavity. Total internal optical losses in lasers can be shown in general as a sum of products of absorption coefficient (α_{layer}) and confinement factor (Γ_{layer}) of each layer of the device structure. Previous works indicate that the major component of α_i in GaN-based laser diodes is caused by p-type layers [1,2,3] due to the high absorption coefficient [4]. Knowledge of the absorption coefficient of Mg doped layers becomes the key to designing efficient high power LDs.

The most highly Mg doped layer in the III-nitride LDs is the electron blocking layer (EBL). It is placed right after the active region to ensure high carrier injection efficiency (η_i). The high doping level in EBL, needed to provide high η_i, is the cause of high α_i.

In this work the influence of Mg doping level on optical losses of the LDs was studied using different designs of electron blocking layer (EBL).Samples were grown by plasma-assisted molecular beam epitaxy (PAMBE). The EBL thickness varied from 5 to 20nm and Mg doping concentration in the EBL was varied from $7 \cdot 10^{18}$ to $6 \cdot 10^{19}$ cm^{-3}.

A strong influence of Mg doping concentration and EBL thickness on slope efficiency and threshold current of grown LDs was found. Moreover, it was observed that the external LD parameters are the result of interplay between η_i and α_i. This implies an existence of optimum Mg doping level in EBL. Experimental data were compared with theoretical calculation using SiLENSe simulation and our distribution model of optical mode inside laser cavity [5]. A model of η_i, α_i, absorption coefficient of Mg-doped layers and their impact on properties of LDs is proposed.

[1] S. Uchida, M. Takeya, S. Ikeda, T. Mizuno, T. Fujimoto, O. Matsumoto, S. Goto, T. Tojyo, and M. Ikeda, *IEEE J. Sel. Topics Quantum Electron*. **9** (5), 1252-1259 (2003).
[2] G. Muziol, H. Turski, M. Siekacz, P. Wolny, S. Grzanka, E. Grzaka, P. Perlin and C. Skierbiszewski, *APEX* **8**, 032103 (2015).
[3] E. Kioupakis, P. Rinke and C. G. Van de Walle, *APEX* **3**, 082101 (2010) .
[4] M. Kuramoto, M. Sasaoka, C. Futagawa, N. Nido, and M. Yamaguchi, *Phys. Stat. Sol. (a)* **192** (2), 329–334 (2002).
[5] G. Muziol, H. Turski, M. Siekacz, S. Grzanka, P. Perlin and C. Skierbiszewski, *APEX* **9,** 092103 (2016).

Comparison between MBE-grown InGaN/GaN Blue LEDs with Standard p-contact and Tunnel Junction p-contact

Shyam Bharadwaj[1], Kevin Lee[1], Henryk Turski[2], Huili (Grace) Xing[1], and Debdeep Jena[1]

[1] *Cornell University, Ithaca, USA*
[2] *Institute of High Pressure Physics, Warsaw, Poland*

Visible LEDs composed of III-Nitrides suffer from high p-contact resistances due to the large activation energy of Mg dopants in GaN. To address this issue, we investigate the use of a GaN tunnel-junction (TJ) above the p-type cladding layer, allowing the hole-injection contact to be made to n-GaN. Such geometry avoids the use of a resistive p-contact, and the enhanced conductivity of the top n-GaN layer allows for superior current spreading even without the use of a current-spreading metal layer, as observed by many groups [1-3].

The heterostructures in this study are grown by Plasma-assisted (PA) MBE on lumilog bulk GaN substrates. Standard geometry LEDs were processed into mesas with the top-contact composed of a Ni/Au current spreader followed by a thick Ti/Au pad for probing, while the TJ LED (structure shown in Fig. 1) top contacts simply consisted of the Ti/Au pad. IV, TLM, and EL measurements were performed to compare the performance of the TJ LEDs to the standard ones. Extracted contact resistances for the TJ LEDs are $\sim 7 \times 10^{-5}$ Ωcm^2, representing an improvement of 60x over the standard geometry LEDs (Fig. 2). The extracted on-resistance of the TJ LED (from Fig. 3) is $\sim 2 \times 10^{-2}$ Ωcm^2, comparable to others' results at the same wavelengths [3]. Optimization of the tunnel junction region will lead to enhanced on currents, allowing for highly efficient LEDs.

Fig. 1: Schematic structure of a blue TJ LED
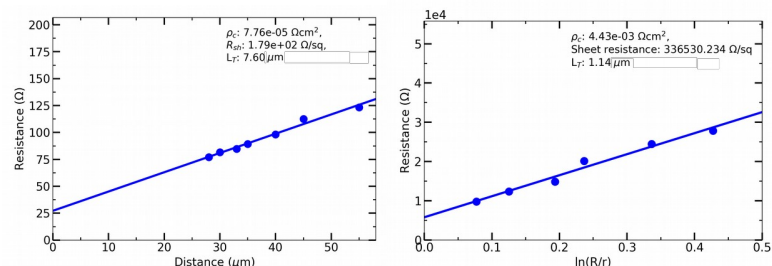
Fig. 2: TLM measurements for top contact of the TJ LED (left) and standard LED (right). The TJ LED top contact resistance is ~60x lower than that of the standard LED.
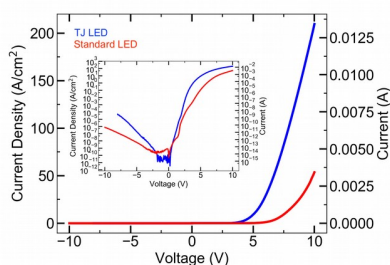
Fig. 3: Linear IV characteristic and log IV (inset) for standard and TJ LEDs
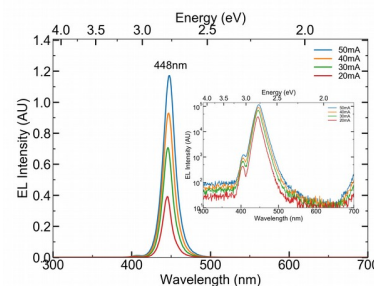
Fig. 4: linear EL spectrum and log EL (inset) for TJ LED at various bias levels

[1] S. R. Jeon, Y. H. Song, H. J. Jang et al., *Appl. Phys. Lett.* **78**, 21 (2001).
[2] Jae-Hoon Lee and Jung-Hee Lee, *IEEE Trans. Electron Devices* **58**, 9 (2011).
[3] S. Krishnamoorthy, F. Akyol, and S. Rajan, *Appl. Phys. Lett.* **105**, 141104 (2014).

Kelvin probe force microscopy study of High electron mobility transistors

A. Minj [1]**, M. P. Chauvat** [1]**, O. Patard**[2]**, P. Gamarra** [2]**, C. Lacam** [2]**, C. Dua** [2]**, S. L. Delage** [2]**, and P. Ruterana** [1]

[1] *CIMAP, UMR 6252, CNRS-ENSICAEN-CEA-UCBN, 6, Bd Maréchal Juin, 14050 Caen, France*
[2] *III-V Lab, 1 Avenue Augustine Fresnel, Campus Polytechnique, 91767 Palaiseau, France*

High electron mobility transistors (HEMT) based on AlGaN/GaN, InAlN/GaN and InAlGaN/GaN heterostructures are expected to play a major role in delivering high-output power at high-frequencies for multiple key applications in telecommunications, radars, military warfare etc. Recently, Fujitsu demonstrated InAlGaN/GaN-HEMT power amplifier with record high output power density of 4.5 watts/mm of gate-width in the W-band [1]. Despite promising results, there are serious reliability concerns that hinder their market growth. Highly-strained AlGaN/GaN heterostructures primarily suffer from inverse-piezoelectric effect that leads to formation of pits and/or craters near the gate-edge under reverse bias-condition. For In-based heterostructures such as in InAlN/GaN and InAlGaN/GaN, there is no scientific consensus on the origin of degradation. Device characterization and reliability study often includes optical techniques (emission microscopy or cathodoluminescence), whose resolution is limited by the diffraction-limit and sensitive to only vis-IR emission. Here, Kelvin probe force microscopy (KPFM) and surface photovoltage (SPV) microscopy is proposed which allows probing of electrical properties of surface, interfaces, junctions and defects. KPFM is performed on SiNx passivated HEMTs (AlGaN/AlN/GaN on SiC) under dark and under illumination (200 nm- 1200 nm). The analysis is understood in terms of effective surface photovoltage generation induced by photo-absorption at the interfaces and junctions, and deterioration of SPV at defects due to recombination. The study eventually reveals inhomogeneity of Ti/Al/Ni/Au alloy for ohmic contacts, effectiveness of ion implantation in device isolation, and identification of defects generated after reverse bias near the gate edge. KPFM results are in accordance with the contrasts in Emission microscopy.

Acknowledgements

References

1. Advanced HEMTs and MMICs Technologies for Next Generation Millimeter-wave Amplifiers, Symposium C (Electronic devices) July 24, 12th International Conference on Nitride Semiconductors (ICNS-12), Strasbourg, France (July 24-July28 2017)

Probing piezoelectric polarization and hole trapping induced surface band bending at interface dislocations in InGaN/GaN heterostructures

A. Minj[1], M. A. Fazio[2], D. Cavalcoli[2], M. P. Chauvat[1], Q. T. Li[1], N. Garro[3], A. Cros[3], and P. Ruterana[1]

[1] *CIMAP, UMR 6252, CNRS-ENSICAEN-CEA-UCBN, 6, Bd Maréchal Juin, 14050 Caen, France*
[2] *Department of Physics and Astronomy, University of Bologna, Viale Berti Pichat 6/2, 40127 Bologna, Italy*
[3] *Institute of Materials Science (ICMUV), Universidad de Valencia, P.O. Box 22085, E-46071 Valencia, Spain*

Strain relaxation of InGaN/GaN single and multi-heterostructures via generation of basal-plane interface dislocations has strong implications in optoelectronic applications that include light-emitting diodes and solar cells. In such hexagonal systems, where basal plane and prismatic slip systems are inactive, several pyramidal slip systems offer net shear strain required for dislocation glide. The most prominent slip systems include 1/3<11-23>{11-22} and 1/3<11-23>{1-101}, and, corresponding to the former, misfit dislocations along <10-10> have been reported [1]. Though it is apparent that edge-type misfit dislocations relieve the interface strain, the role of partial dislocations (with edge-, screw- or mix-character) cannot be neglected either. In fact, stacking fault/partial dislocation systems are commonly occurring defects in nitride family. Assessing their electronic and optical properties at the interface, whether they are perfect ($a+c$) and/or partial (Frank-Shockley partial dislocations 1/6<2-203>), is of critical importance due to their strong influence on piezoelectricity and on optical properties due to possible active defect levels formation. In this work, first the formation mechanism of interface dislocations dislocations in quasi-fully strained InGaN(50 nm)/GaN heterostructures ($0.18<x<0.20$) has been understood. Second, opto-electrical properties of such have been studied by photo-assisted Kelvin probe force microscopy and surface photovoltage spectroscopy. Through assessment of the change in surface band bending and surface barrier, both strong reduction of piezoelectric polarization charge due to local strain relaxation at these dislocations and their hole-trapping behaviour under steady-state illumination conditions has been deduced. Under below-bandgap illumination, a band close to 2.6 eV below the conduction band minimum, corresponding to the electronic transition from a defect level to the conduction band, is observed at these dislocations.

References

1. J. A. Floro, D. M. Follstaedt, P. Provencio, S. J. Hearne, and S. R. Lee, J. Appl. Phys. 96, 7087 (2004)

Stress and surface defects control for optimization of AlGaN/GaN/Si(111) HEMT-type structures properties

T. Szymanski [1]**, M. Wosko** [1]**, B. Paszkiewicz** [1] **and R. Paszkiewicz**[1]

[1]*Faculty of Microsystem Electronics and Photonic, Wroclaw University of Science and Technology, Janiszewskiego 11/17, 50-372 Wroclaw, Poland*

For almost two decades, research groups from around the world have investigated various *in situ* and *ex situ* methodologies in order to decrease the stress induced due to large lattice mismatch and to achieve crack-free AlGaN/GaN/Si heterostructures with micrometers thick GaN buffer. Multiple sources of stress induced in the GaN layer have to be taken into account when designing MetalOrganic Vapor Phase Epitaxy (MOVPE) process for fabrication of heterostructures with required layer scheme and composition. However, some of imperfections formed on the surface during the (Al)GaN growth can be utilized to alter final state of stress. Namely, trench defects and hexagonal micropits. Despite the presence of these imperfection 2DEG with very good electrical properties can be formed at the heterointerface of AlGaN barrier and GaN buffer, exhibiting sheet carrier concentration at the level of 1E13 $1/cm^{-2}$ and electron mobility in range of $1500 – 2000$ $cm^2V^{-1}s^{-1}$.

In the presented work the strain engineering methods will be presented and discussed including, low temperature AlN interlayer, SiN nanomasking layer and AlGaN gradient layer, application of which lead to various surface defects and GaN stresses imposing different electrical properties of AlGaN/GaN HEMT-type structures. Despite many published investigations of the aforementioned influence, it is still unclear if crystal quality and stress present in the deposited layers may be considered as a factor influencing 2DEG sheet resistance. In the presented work it will be shown that some of the defects can be beneficial from the point of view of AlGaN/GaN HEMT-type structures electrical properties.

The stress in the grown structures was altered via deposition of in situ SiN nanomask and LT-AlN interlayers, as well as the change of V/III ratio during the grown of HT-GaN layer. The trade-off between heterostructures electrical properties, biaxial stress, crystal and structural properties will be presented and discussed. Authors main focus was optimization of sheet resistance and determining the factors that mostly influenced its value.

On-chip near-ultraviolet multicomponent system toward the internet of things

Yuan Jiang, Jialei Yuan, Chuan Qin and Yongjin Wang

Peter Grünberg Research Centre, Nanjing University of Posts and Telecommunications, Nanjing, 210003, China
Email: jy@njupt.edu.cn

Nitride semiconductor materials inherently have the intriguing functionalities of simultaneous emission, transmission and photodetection. In particular, GaN-based multiple-quantum-well (MQW) diodes exhibit a simultaneous light-emitting light-detecting function, whereby MQW-based transmitter and receiver within a single chip can be produced with identical MQW active region by using same fabrication procedure. A multicomponent system, which integrates different III-nitride photonic components into a multicomponent system, can impart multiple, enhanced functionalities toward the internet of things (IoT). We propose, fabricate and characterize on-chip near-ultraviolet multicomponent system on an III-nitride-on-silicon platform using a wafer-level procedure. The AlN/AlGaN buffer layers are used to manage the lattice mismatch between GaN and silicon. Backside III-nitride film thinning is then conducted to decrease membrane thickness with improved performance of the device. A 2-µm-thick, 0.8-mm-in-diameter suspended multifunctional InGaN/AlGaN MQW-diode is fabricated with the dominant emission around 386 nm. The MQW-diode can realize light emission and detection at the same time. Monolithic near-ultraviolet photonic circuit, which consists of transmitter, waveguide and receiver, is mechanically transferred from silicon to foreign substrates. The transferred chip is wire-bonded to a test pad, and the in-plane light communication among transmitter, waveguide and receiver works. These transferrable near-ultraviolet multicomponent systems are promising for the development of multifunctional III-nitride photonic devices toward IoT applications from light communication to on-chip power monitor, optical sensor and intelligent displays.

[1] Yongchao Yang, Bingcheng Zhu, Zheng Shi, Jinyuan Wang, Xin Li, Xumin Gao, Jialei Yuan, Yuanhang Li, Yan Jiang, and Yongjin Wang, "Multi-dimensional spatial light communication made with on-chip InGaN photonic integration," Opt. Mater. **66**, 659-663 (2017).

[2] Yongjin Wang , Yin Xu , Yongchao Yang , Xumin Gao , Bingcheng Zhu , Wei Cai , Jialei Yuan, Rong Zhang and Hongbo Zhu. "Simultaneous light emission and detection of InGaN/GaN multiple quantum well diodes for in-plane visible light communication on a chip," Opt. Commun. **387**, 440-445(2017).

Monte Carlo simulation of carbon incorporation in GaN MOVPE

S. Yamamoto[1], Y. Inatomi[1], A. Kusaba[1], P. Kempisty[2, 3], and Y. Kangawa[1, 2, 4]

[1] *Department of Aeronautics and Astronautics, Kyushu University, Fukuoka 819-0395, Japan*
[2] *IMaSS, Nagoya University, Nagoya 464-8603, Japan*
[3] *IHPP, PAS, Sokolowska 29/37, 01-142 Warsaw, Poland*
[4] *RIAM, Kyushu University, Kasuga, Fukuoka 816-8580, Japan*

To develop GaN power devices, it is indispensable to obtain high purity crystals whose impurity concentration is less than 1.0×10^{16} cm^{-3}. [1] It is known that carbon atoms are strongly incorporated in GaN crystals during conventional metalorganic vapor phase epitaxy (MOVPE) process. To reduce the impurity concentration in the crystals, we studied carbon incorporation mechanisms in case of polar GaN MOVPE by Monte Carlo (MC) simulation.

In the MC simulation, 1 monolayer (ML) of adsorption process (Step I), and 5 ML of site exchanging process (Step II) were considered. In (Step I), a Ga−N layer including 1.0×10^{18}cm^{-3} of carbon was attached on the GaN film. Here, GaN(0001)Ga$_{ad}$ (T4) and GaN(000−1)3N-H surface reconstructions were considered. [2] Using formation energy of carbon substituting nitrogen in each layer/site [3], a site exchanging probability was calculated in (Step II). Then, equilibrium atomic arrangement in GaN:C layers were simulated.

Figure 1 shows depth dependence of carbon concentration in (a) GaN(0001)Ga$_{ad}$(T4), and (b) GaN(000−1)3N−H. Here, analyzing conditions are as follows: growth temperature T = 1000℃, MC step MCS = 5000. In case of GaN(0001)Ga$_{ad}$(T4), carbon concentration in the bulk is higher than that near the surface. This result implies that the adsorbed carbon prefers to migrate into the crystal. On the other hand, in case of GaN(000−1)3N−H, carbon concentration near the surface is higher than that in the bulk. The calculation results suggests that surface segregation of carbon occurs during growth. The relationship between growth orientation and carbon concentration in the bulk agree with experimental results. [4] By the present MC simulations, carbon incorporation mechanisms in case of polar GaN MOVPE was clarified.
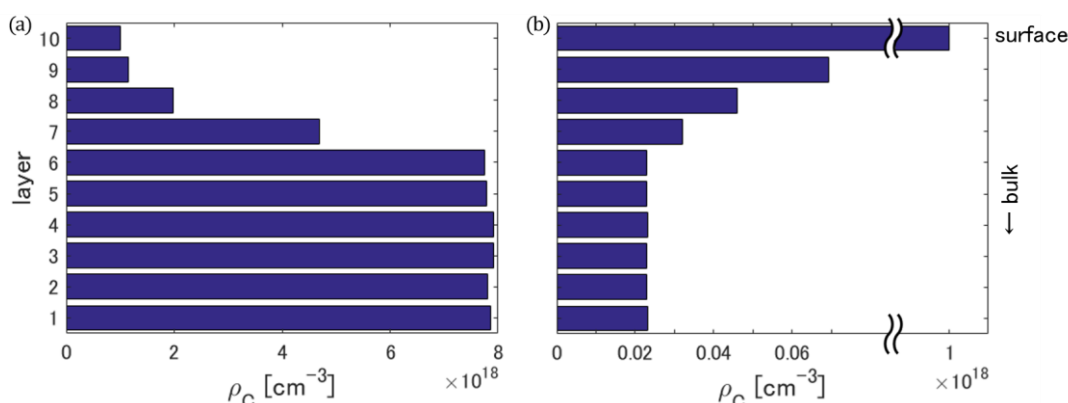
Fig. 1. Distribution of carbon concentration along growth orientation: (a) [0001] direction (Ga$_{ad}$(T4) surface), and (b) [000−1] direction (3N−H surface). Vertical axis shows layer number; upper side is surface and lower side is bulk.

References [1] T. Kachi, Jpn. J. Appl. Phys., **53**, 100210 (2014), [2] A. Kusaba et al., Jpn. J. Appl. Phys., **56**, 070304 (2017), [3] P. Kempisty et al., Appl. Phys. Lett. **111**, 141602 (2017), [4] N. A. Fichtenbaum et al., J. Cryst. Growth **310**, 1124 (2008).

Migration Energy of a N Atom around Ga Vacancy in GaN

Masato Oda

Department of Applied Physics, Wakayama University, Japan.

GaN is one of the most important materials in light-emitting diodes and laser diodes. There is a wide variety of research studies on GaN-related semiconductors covering from basic properties to commercial applications. Although many studies have been carried out on the mechanism of light emission, the mechanism of device degradation remains unclear. It is necessary to clarify the mechanism of degradation to guarantee a device lifetime. The degradation is related to dislocations observed in the dark region of an emitting layer in the device. Ueda proposed an origin of the growth of dislocations where point defects in the active layer are gathered via defect reactions to grow dislocation loops[1]. But the mechanism of the defect reaction is also unclear. We have to clarify the mechanism of the defect reaction in GaN.

In the previous work, we have investigated electronic structures, phonon modes, and their coupling at a Ga vacancy in GaN[2]. It has been shown that a Ga vacancy can act as a nonradiative recombination center and may trigger defect reactions in GaN-based devices[3]. Most promising step in the early stage of the defect reaction is one of the four N atoms around the vacancy moves toward to the V_{Ga}. In this study, we investigate adiabatic potentials of N atom from the stable position of V_{Ga} point defect system (fig. 1(a)) to N_{Ga}-V_N complex defect system (fig. 1(b)) under both neutral and positively charged states by DFT calculation.

Fig. 1. schematic picture of (a)V_{Ga} and (b)N_{Ga}-V_N systems.

Figure 2 shows calculated adiabatic potentials. We define x=0.0 (=1.0) as c-axis coordination of a circled N atom circled in fig. 1 in V_{Ga} point defect system (N_{Ga}-V_N complex defect system). It is shown that under the neutral system, migration barrier of the N atom towards V_{Ga} is about 2.25 eV and N_{Ga}-V_N complex is unstable. On the other hands, under the positively charged system, the migration barrier is about 1.65eV and N_{Ga}-V_N complex is stable than V_{Ga}. These results indicate that the defect reaction is likely to be occurring in the positively charged condition.

[1]O. Ueda, Jpn. J. Appl. Phys. **49** 090001 (2010).
[2]T. Tsujio, M. Oda, and Y. Shinozuka, Jpn. J. Appl. Phys. **56** 091001 (2017).
[3]Y. Shinozuka, M. Wakita, and K. Suzuki, Jpn. J. Appl. Phys. **51** 11PC03 (2012).

Fig. 2. adiabatic potentials

Compositional Dependence of Band Gaps in III-Nitride Semiconductor Superlattices

Takahiro Kawamura [1]**, Toru Akiyama** [1] **and Yoshihiro Kangawa** [2]

[1] *Graduate School of Engineering, Mie University, 1577 Kurimamachiya-cho, Tsu, Japan*
[2] *Research Institute for Applied Mechanics, Kyushu University, 6-1 Kasuga-koen, Kasuga, Fukuoka, Japan*

Band gap energies of GaN, AlN, InN are about 3.5, 6.2, and 0.7 eV [1]. Their alloys and superlattices (SLs) are expected to realize optoelectronic devices operating in wide wavelength range from infrared to deep UV region. It is well known that band gaps of III-nitride semiconductor alloys and SLs change depending on compositions and SL period thickness [2]. Therefore it is important to understand possible combinations of compositions and SL thickness to produce III-nitride epilayers with desirable band gap energy. In this study, we investigate compositional dependence of band gaps in III-nitride alloys and superlattices using first-principles calculations.

We use the QUANTUM ESPRESSO code [3], which is based on density function theory, plane-wave basis set, and pseudopotentials. First we optimize lattice vectors and atomic positions. Subsequently we calculate band structures with the pseudopotential self-interaction correction (pSIC) method [4,5]. The calculated band gap values of GaN, AlN, and InN are 2.82, 5.46, and 0.63 eV, respectively. These values are smaller than those of experimental values; however, it is enough to investigate the dependence of composition and SL thickness on band gaps.

We will discuss the compositional dependence of band gap energies of InGaN and AlInN SLs in the symposium.

[1] Junqiao Wu, J. Appl. Phys. **106**, 011101 (2009).
[2] I. Gorczyca et al., Phys. Rev. B **93**, 165302 (2016).
[3] P. Giannozzi et al., J. Phys. Condens. Matter **21**, 395502 (2009).
[4] A. Filippetti et al., Phys. Rev. B **67**, 125109 (2003).
[5] M. Wierzbowska et al., Phys. Rev. B **84**, 245129 (2011).

Electronic and Thermodynamic Properties of the AlN/diamond Interfaces – a DFT Studies

R. Hrytsak [1,2], **P. Kempisty** [1]**, S. Krukowski** [1] **and M. Sznajder** [2]

[1] *Institute of High Pressure Physics, Polish Academy of Sciences, Sokołowska 29/37, 01-142 Warsaw, Poland*
[2] *Faculty of Mathematics and Natural Sciences, University of Rzeszów, Pigonia 1, 35-959 Rzeszów, Poland*

The growth of thin AlN layers with improved crystalline quality on the oxygenated or hydrogenated diamond substrate is an experimental problem reported by Imura *et al*. in the last years [1,2]. A high quality single-crystal AlN/diamond heterojunction suitable for FET has been demonstrated in the case when AlN has been grown on H-diamond(111) surface [3], and the performance of AlN/diamond HFET fabricated on O-diamond(111) is significantly improved [4].

Recently, in the framework of DFT, we have modelled the early stages of AlN growth process on the O-diamond(111) surface and showed, in analogy to experiment [1], a formation of two competitive AlN structures with different morphologies as well as two essential charge carrier redistributions occurring in the diamond substrate [5].

Herein, in order to analyse the stability of the obtained AlN structures in experimental conditions, we find their temperature properties based on first principles phonon calculations. In particular, we present changes of the specific heat, entropy, and Gibb's free energy. Additionally, we determined several electronic properties of systems such as spatial profiles of the electrostatic potential and charge density distribution. We examine mechanisms of electron charge transfer occurring at the interface layers of the diamond/AlN system, including also the case where the wz-AlN plays the role of substrate, while the adsorbate are carbon atoms.

[1] M. Imura, K. Nakajima, M. Liao *et al*., *J. Cryst. Growth* **312**, 1325 (2010).
[2] M. Imura, R.G. Banal, M. Liao *et al*., *J. Appl. Phys*. **121**, 025702 (2017).
[3] M. Imura, R. Hayakawa, E. Watanabe *et al*., *Phys. Status Solidi PRL* **5**, 125 (2011).
[4] M. Imura, R. Hayakawa, H. Ohsato *et al*., *Diamond Relat. Mater*. **24**, 206 (2012).
[5] M. Sznajder, R. Hrytsak, *Diamond Relat. Mater*. **83**, 94 (2018).

On determination of the dominant recombination mechanisms from time resolved photoluminescence in nitride semiconductor heterostructures

Konrad Sakowski[1], Pawel Strak[1], Kamil Koroński[2], Kamil Sobczak[3], Jolanta Borysiuk[4], Krzysztof P. Korona[4], Andrzej Suchocki[2], Eva Monroy[5], Agata Kaminska[2,6], Stanislaw Krukowski[1]

[1] *Institute of High Pressure Physics, Polish Academy of Sciences, Sokolowska 29/37, 01-142 Warsaw, Poland*
[2] *Institute of Physics, Polish Academy of Sciences, Al. Lotników 32/46, 01-142 Warsaw, Poland*
[3] *Faculty of Chemistry, Biological and Chemical Research Centre, University of Warsaw*
[4] *Faculty of Physics, University of Warsaw, Pasteura 5, 02-093 Warsaw, Poland*
[5] *Université Grenoble-Alpes, CEA, INAC-Pheliqs, 17 av. des Martyrs, 38000 Grenoble, France*
[6] *Cardinal Stefan Wyszynski University, College of Science, Department of Mathematics and Natural Sciences, Dewajtis 5, 01-815 Warsaw, Poland*

A method for the determination of the recombination modes in optically excited matter is presented. This method operates on measurements made by standard time-resolved photoluminescence (TRPL) instruments. The considered phenomena include monomolecular, bi-molecular and tri-molecular recombination mechanisms. It allows to determine the dominant optical emission mode and also approximate values of ABC parameters in fundamental time evolution equation of optically excited samples measured by TRPL [1,2]. Therefore, it can detect non-radiative Shockley-Read-Hall (SRH) recombination, radiative recombination and Auger recombination modes. It is shown that this method can be applied to variety of semiconductor heterostructures, like quantum wells, LEDs and other systems investigated optically. However, our analysis requires a low noise measurement of the dependence of the photoluminescence versus time, as well as its derivative. In particular, to determine impact of the monomolecular recombination, it is important to obtain a good signal-to-noise ratio for the whole experiment period, which is not always possible when the signal becomes small, as time goes on after the excitation pulse. Under such conditions, recovering of the reliable approximation of the derivative is particularly problematic. Therefore the method of the signal smoothing is also presented. The numerical code used for the simulation was implemented by the authors and is available on the open source basis [3]. It is based on the least-squares problem and thus it does not rely on any particular solution of the ABC equation. Examples are provided to demonstrate the results of both introduced methods.

[1] R.N. Hall, *Phys. Rev.* **83**, 228 (1951).
[2] W. Shockley, W. T. Read, *Phys. Rev.* **87**, 835 (1952).
[3] https://github.com/ghkonrad/logpli

Effective approach for calculating absolute surface energies of polar and semipolar planes for group-III nitrides under MOVPE conditions

Toru Akiyama, Yuki Seta, Kohji Nakamura, and Tomonori Ito

Department of Physics Engineering, Mie University, 1577 Kurima-Machiya, Tsu 514-8507, Japan

The morphology and equilibrium growth rate during crystal growth are determined by the relative stability among different crystal planes. In the case of epitaxial growth of group-III nitrides, various surface orientations such as polar and nonpolar planes are used, and nonpolar and semipolar facets are sometimes formed depending on the growth conditions of selective area growth (SAG) [1]. Therefore, absolute surface energies are key properties to understand the epitaxial growth of group-III nitrides. However, polar surfaces for low-symmetry crystalline materials cannot be individually treated in conventional slab geometries and therefore absolute surface energies of polar and semipolar planes are fundamentally ill defined. To overcome this difficulty, a direct approach using wedge-shape geometries has recently been proposed for absolute surface energies of wurtzite (WZ) structured GaN polar planes [2]. Although this approach has been successfully applied for polar surfaces and interfaces of various group-III nitrides [2-6], the similarity between the polar $(0001)/(000\bar{1})$ surface with hexagonal symmetry and the $(111)/(\bar{1}\bar{1}\bar{1})$ surface in cubic structure is assumed. In this work, we propose an effective approach for simultaneously calculating absolute surface energies of polar and semipolar planes without invoking the similarity between hexagonal and cubic structures. Our approach is based on the calculations of total energy differences between two identical wedge-shape geometries with ideal surfaces using density functional calculations in conjunction with the evaluations of surface dangling bonds for various orientations.

Figure 1 shows the calculated absolute surfaces energies of polar, nonpolar, and semipolar planes of GaN under MOVPE conditions as a function of Ga chemical potential μ_{Ga}. The calculated absolute surface energy of GaN(0001) with H-terminated N adatom is ranging from 0.12 to 0.15 eV/Å^2 and that of GaN(0001) without H atom is ~0.16 eV/Å^2, which agree well with those in previous calculations [6]. It should be noted the absolute surface energy of semipolar GaN$(11\bar{2}2)$ under high H$_2$ pressure condition becomes lower than the energy of nonpolar GaN$(11\bar{2}0)$ surface. The lower absolute surface energy on the GaN$(11\bar{2}2)$ compared with the GaN$(11\bar{2}0)$ surface implies that semipolar GaN$(11\bar{2}2)$ surface is preferentially formed for high H$_2$ pressures during the MOVPE. This finding is reasonably consistent with the results of SAG in GaN, where different facet orientations have been observed depending on the MOVPE growth condition [1].

FIG. 1: Calculated absolute surface energies of polar, nonpolar, and semipolar planes of GaN as a function of Ga chemical potential μ_{Ga}. The values of hydrogen chemical potential $\mu_H - \mu_{H_2} = $ -0.75 and -1.1 eV, which correspond to high and low H$_2$ pressure (p_{H_2}) at 1270 K (μ_{H_2} is the chemical potential of single H$_2$ molecule at 0 K) are considered. Solid (dashed) lines correspond to surface energies for high (low) p_{H_2}.

The calculated results thus suggest that all of phenomena related to the stability of polar and semipolar surfaces of group-III nitrides would benefit from accurate values of surface energies.

[1] K. Hiramatsu *et al.*, *J. Cryst. Growth* **221**, 316 (2000).
[2] C. E. Dreyer, A. Janotti, and C. G. Van de Walle, *Phys. Rev. B* **89**, 081305(R) (2014).
[3] A. Kusaba *et al.*, *Appl. Phys. Express* **9**, 125601 (2016).
[4] A. Kusaba *et al.*, *Jpn. J. Appl. Phys.* **56**, 070304 (2017).
[5] T. Akiyama, H. Nakane, K. Nakamura, and T. Ito, *Phys. Rev. B* **94**, 115302 (2016).
[6] T. Akiyama *et al.*, *Phys. Status Solidi B*, pssb.201700329 (2018).

Plenary lecture

Recent Progress of GaN Growth by Na-flux Method

Yusuke Mori, Masayuki Imanishi, Masashi Yoshimura

Graduate School of Engineering, Osaka University, 2-1, Yamada-oka, Suita, Osaka, Japan

Na flux method developed by Yamane can grow GaN crystal in a Ga-Na mixed solution at relatively low pressure of nitrogen atmosphere (<5MPa) and at temperature range of 750~900 deg.C [1]. The big advantage of Na flux method is that the high quality GaN crystal can be grown on poor quality seed GaN substrate, especially better for the smaller seed. This feature of Na flux method can make possible to fabricate large-diameter (> 4 inch) GaN wafer with low TDD (102 ~ 105 cm-2) on multi-point seeds (MPS) [2]. However, if we just grow GaN crystal on MPS in a Ga-Na mixed solution normally, the lattice constants become different between the c-plane growth area and the {10-11}-plane growth area [3]. Although TDD would be reduced during forming region "A" as shown in Fig.1, oxygen impurities are likely to be incorporated only in {10-11}-plane growth sectors, resulting in increasing lattice constants.

In order to overcome this problem, we have invented the advanced MPS technique by the introduction of flux film coating (FFC) technique [4], so we named "FFC-MPS technique". In this method, thin Na-Ga flux is kept only in V-shaped valley between {10-11} facets of GaN crystals, which induces the growth only along lateral direction. By alternately repeating solution supply and lateral growth in the valleys, GaN growth surface is fully composed by the c-plane, indicated as region "B" in Fig. 1. Then it becomes possible to grow c-GaN crystal, indicated as region "C". This region "C" shows high transparency as dipicted in Fig. 2. GaN grown by present FFC-MPS technique showed relatively low dislocation density of 103 ~ 105 cm-2 (distribution of TDD: 15% area ~103 cm-2, 75% area ~104 cm-2, 10% area ~105 cm-2) and relatively large radius of lattice curvature (>30 m). We believe that the quality and size of GaN crystal are expected to improve more and more by optimizing FFC-MPS technique.
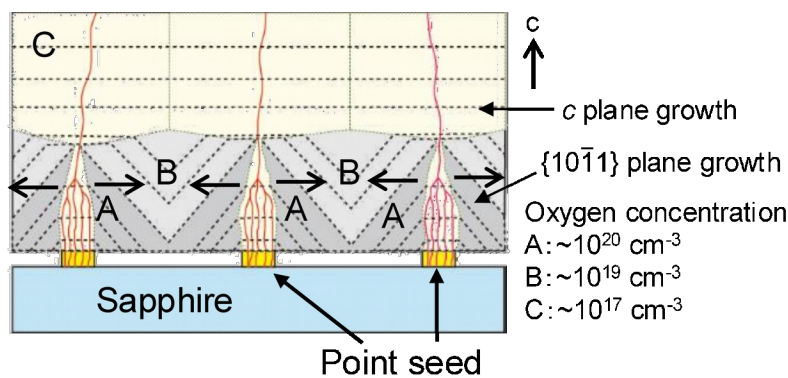
Fig. 1 Schematic drawing of the Na-flux growth with FFC –MPS technique
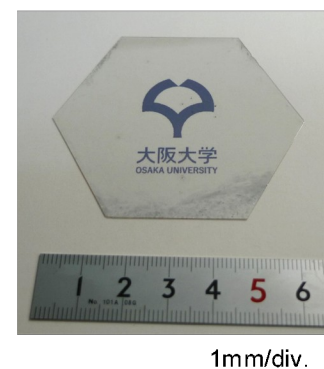
Fig. 2 2-inch GaN wafer grown with FFC-MPS technique

[1] H. Yamane, M. Shimada, T. Sekiguchi, F.J. Disalvo, Chem. Mater. 9, 413 (1997).
[2] M. Imade, et al., Appl. Phys Express 7 (2014) 035503-1-4.
[3] M. Imanishi, et al., Cryst. Growth & Design 17 (2017) 3806-3811.
[4] F. Kawamura, et al., Jpn. J. Appl. Phys 42 (2003) L879-L881.

Plenary lecture

Acceptors in Nitrides:
Doping, Compensation, and Impact on Device Performance

Chris G. Van de Walle

Materials Department, University of California, Santa Barbara, USA

p-type doping is notoriously difficult in nitrides. Mg is the only acceptor that provides adequate hole concentrations in GaN, but it is intrinsically a "deep level" [1]. There were hopes that Be might be shallow, but its ionization energy is 0.55 eV [2], and it has been shown to be a source of yellow luminescence [3]. p-type doping becomes even harder in wider-band-gap material, though there is some hope that Be could be suitable in the case of ultra-wide-band-gap BN [4].

Unintentionally introduced acceptor impurities, such as C, Ca, or Fe can lead to compensation of n-type material, but also to undesired recombination: C is a source of yellow luminescence [5], while Ca [6] and Fe [7] cause strong Shockey-Read-Hall (SRH) nonradiative recombination.

Native point defects [8] can of course also act as acceptors. Cation vacancies are likely to occur, though mostly in the form of complexes with unintentional impurities such as hydrogen or oxygen [5]. These complexes can be a strong source of SRH recombination [9], sometimes through involvement of excited states [10]. Our recent progress in calculating such defect-assisted recombination enables us to assess the impact on device efficiency, and point out avenues for suppressing loss mechanisms.

[1] J. L. Lyons, A. Janotti, and C. G. Van de Walle, Phys. Rev. Lett. 108, 156403 (2012).

[2] J. L. Lyons, A. Janotti, and C. G. Van de Walle, J. Appl. Phys. 115, 012014 (2014).

[3] H. Teisseyre, J. L. Lyons, A. Kaminska, D. Jankowski, D. Jarosz, M. Boćkowski, A. Suchocki and C. G. Van de Walle, J. Phys. D: Appl. Phys. 50, 22LT03 (2017).

[4] L. Weston, D. Wickramaratne, and C. G. Van de Walle, Phys. Rev. B 96, 100102(R) (2017).

[5] J. L. Lyons, A. Alkauskas, A. Janotti, and C. G. Van de Walle, Phys. Stat. Sol. B 252, 900 (2015).

[6] J.-X Shen, D. Wickramaratne, C. E. Dreyer, A. Alkauskas, E. Young, J. S. Speck, C. G. Van de Walle, Appl. Phys. Express 10, 021001 (2017).

[7] D. Wickramaratne, J.-X. Shen, C. E. Dreyer, M. Engel, M. Marsman, G. Kresse, S. Marcinkevičius, A. Alkauskas, C. G. Van de Walle, Appl. Phys. Lett. 109, 162107 (2016).

[8] J. L. Lyons and C. G. Van de Walle, NPJ Comput. Mater. 3, 12 (2017).

[9] C. E. Dreyer, A. Alkauskas, J. L. Lyons, J. S. Speck, and C. G. Van de Walle, Appl. Phys. Lett. 108, 141101 (2016).

[10] A. Alkauskas, C. E. Dreyer, J. L. Lyons, and C. G. Van de Walle, Phys. Rev. B 93, 201304(R) (2016).

Invited lecture

Defect Structure Analysis of GaN Substrates by Synchrotron X-Ray Diffraction Techniques

Lutz Kirste [1]**, Thu Nhi Tran Thi** [2]**, Andreas N. Danilewsky** [3]**, Tomasz Sochacki** [4]**, Michal Boćkowski** [4]**, José Baruchel** [2]

[1] *Fraunhofer Institute for Applied Solid State Physics (IAF), Freiburg, Germany*
[2] *European Synchrotron Radiation Facility (ESRF), Grenoble, France*
[3] *Crystallography, Albert-Ludwigs University, Freiburg, Germany*
[4] *Institute of High Pressure Physics PAS, Warsaw, Poland*

For demanding GaN-based high frequency or high power electronic devices like high mobility transistors (HEMTs) or Schottky diodes there is a need for material with low defect densities, since e.g. defects such as threading dislocations increase the leakage current, reduce the room temperature mobility and thereby limit the efficiency, performance and lifetime of these devices. The basic prerequisite for the realization of devices with outstanding performance is the homoepitaxial growth of these structures on free-standing GaN substrates with low defect density. Essentially, two techniques have been established in recent years which make it possible to produce GaN substrates with sufficient size and low defect density, namely hydride vapor-phase epitaxy (HVPE) and the ammonothermal growth method. A main advantage of the HVPE method is the low incorporation of unintentionally impurities. On the other side, for HVPE material typically grown on foreign seeds, threading dislocation densities in a range below 10^7 cm^{-2} have been demonstrated, which is still a too high number. Using the ammonothermal growth method threading dislocation densities as low as $5 \cdot 10^3$ cm^{-2} can be achieved. But here, the incorporation of impurities such as oxygen, hydrogen and traces of so-called mineralizer is high. It was shown that by combining the two growth techniques, growing HVPE-GaN with low impurities on low threading dislocation density ammonothermal GaN substrates, HVPE GaN can be made with almost the same dislocation density as ammonothermal GaN [1].

In this work we present a detailed analysis of defect structures of GaN (0001) crystals grown by HVPE on foreign seeds, the ammonothermal method and HVPE crystals grown on ammonthermal GaN seeds. Both, semi-insulating GaN substrates for lateral HEMT devices as well as n-type GaN substrates for vertical Schottky diodes were investigated. Different synchrotron X-ray diffraction techniques were used for this study: Synchrotron white-beam X-ray topography (SWXRT), which is a fast method to identify extended defects such as dislocations, growth sectors, grain boundaries, etc.) within a crystal. Additional, synchrotron X-ray monochromatic rocking curve imaging (RCI) was employed. RCI enables the local determination of the effective misorientation, which results from lattice parameter variation and the local lattice tilt, and the local Bragg position. Maps of the integrated intensity, the FWHM and the peak position angle of the diffracted intensity, calculated from the ensemble of rocking curve images, provide quantitative values related to the local distortion of the crystal lattice [2]. The results from the synchrotron X-ray diffraction techniques are compared to the standard laboratory X-ray diffraction methods like high resolution X-ray diffraction (HRXRD) and Lang X-ray topography. With the combination of the results from the different X-ray diffraction techniques models for the diverse defect structures of the GaN samples grown by HVPE, ammonothermal method and HVPE on ammonothermal GaN are discussed.

[1] L. Kirste et al., *ECS Journal of Solid State Science and Technology, 4 (8), 324-330 (2015)*
[2] T. N. Tran Thi et al., *J. Appl. Cryst., 50, 561–569 (2017).*

Invited lecture

Multi-microscopy of defects in nitride semiconductors

Thomas J. O'Hanlon [1], **Fabien C.-P. Massabuau** [1], **Menno J. Kappers** [1] **and Rachel A. Oliver** [1]

[1] *Department of Materials Science and Metallurgy, University of Cambridge, 27 Charles Babbage Road, Cambridge, CB3 0FS*

Multi-microscopy is an approach to the nanoscale analysis of the structure and properties of materials in which different microscopy techniques are brought to bear on exactly the same nanoscale structure, revealing more about its characteristics than any individual technique could achieve alone. Here, we focus on the application of scanning probe microscopy (SPM), cathodoluminescence (CL) in the scanning electron microscope (SEM) and transmission electron microscopy (TEM), and the information their coordinated application can provide concerning defects in nitride semiconductors. In order to effectively bring these diverse microscopies to bear on exactly the same nanoscale defect specific protocols and specialist sample preparation techniques have been developed.

One key example of this approach is the application of multi-microscopy to the so-called "trench defect" in InGaN/GaN multiple quantum well structures. The trench defect consists of a basal-plane stacking fault (BSF) located in the QW stack with a vertical stacking mismatch boundary (SMB) which opens up as a hexagonal pit whenever the boundary changes its direction [1]. The hexagonal pits coalesce to form the eponymous trench. Here, SPM is used principally to quantitatively address the morphology of the trench, CL reveals the change in the wavelength and intensity of the emission of the material enclosed by the trench compared to its undefected surroundings and TEM reveals the changes in composition and thickness of the quantum wells between the enclosed and undefected material. The same trenches were studied in all imaging modalities. Wider trench defects are shown to originate from BSFs forming in the lower part of the quantum well stack, and these trenches enclose regions with elevated indium content, leading to a redshift of emission.

Whilst in the example above, an adapted version of a standard focused ion beam (FIB) sample preparation method could be used to create the TEM lamella, in our second example, a new approach to sample preparation had to be developed. Here, the SPM experiments including scanning capacitance microscopy (SCM) studies on cross-sections. However, cross-sectional SCM in GaN is only successfully carried out on cleaved surfaces [2] and reveals details less than 20 nm beneath the cleaved surface. Hence, to look at the same region in TEM, it was necessary to develop a FIB protocol which could be used on a sample with a cleaved surface and in which no material was removed from that cleaved surface, but rather the FIB milling was restricted to the material behind the cleaved surface. This approach was used to address the formation of coalescence boundaries in GaN growth, where three dimensional islands coalesce to form a two-dimensional film. Samples with doped markers layers grown at regular intervals throughout the coalescence process were studied in SCM to reveal the position of the coalescence boundaries. These coalescence boundaries were then studied in CL and TEM, revealing that whilst the early stages of coalescence do not result in dislocation formation, boundaries forming late in the coalescence process do lead to the introduction of new dislocations into the film.

Overall, we show that multi-microscopy can reveal detailed links between the structure and properties of defects in nitrides which are difficult to understand by other processes, and that it can also provide insights into the growth mechanisms by which these structures form.

[1] Massabuau, F. C.-P. *et al.* (2012) *Appl. Phys. Lett.*, **101**, 212107.
[2] Sumner, J. *et al.* (2007) *phys. stat. sol. c*, **4**, 2576.

We1.3

Invited lecture

Spontaneous formation of quantum wells, ordering and composition fluctuations in ($11\bar{2}2$) semipolar AlGaN/GaN heterostructures grown by plasma enhanced MBE

Huaping Lei[1], Marie Pierre Chauvat[2], Slawomir Kret[3], Eva Monroy[4], and Pierre Ruterana[2]

[1] *Key Laboratory of Materials Physics, Institute of Solid State Physics, Chinese Academy of Sciences, Hefei 230031, China*
[2] *CIMAP, 6 boulevard du Marechal Juin, Université de Caen, Caen, France*
[3] *Institute of Physics, Polish Academy of Sciences, al. Lotników 32/46, Warsaw, Poland*
[4] *CEA Grenoble, INAC/SP2M, 25 Rue des Martyrs 38042, Grenoble Cedex 9, France*

In addition to their physical properties, which have driven important developments for the production of many devices, the nitride semiconductors still present many issues which still constitute bottlenecks for the optimization of their quality and performance of the devices. Their most striking property is the very large extension of the direct band gap covering from the deep ultraviolet (AlN: 6.2 eV) to the near infrared (InN: 0.65 eV). Unfortunately this goes along with differences in lattice parameters (AlN-GaN: 2.5%; InN-GaN: 11%; AlN-InN: 13%), growth temperatures, atomic mobility, etc. Due to these intrinsic properties, the growth of alloys and heterostructures which constitute the active parts of the devices is not always easy to optimize. As was shown experimentally the phase separation may take place in InGaN [1] and InAlN [2], in agreement with the theoretical predictions [3], whereas a long range atomic ordering, during AlGaN and InGaN epitaxy, can take place along the conventional [0001] growth direction in the basal plane [4, 5] as well as in pyramidal planes [6], and this was mainly explained by growth kinetics mediated by the surface atomic steps [7]. However, in AlGaN grown also along the [0001] direction, multiple [8], as well as incommensurate [9] types of ordering have also been reported, which are difficult to explain through the simple role of the different atomic steps which can be available for the growth along a particular direction. Up to now, the reported results have been obtained in layers grown by molecular beam epitaxy (MBE) or metalorganic vapour phase epitaxy along the [0001] direction.

In this work, we have used high resolution transmission electron microscopy to investigated MBE grown ($11\bar{2}2$) AlGaN/GaN heterostructures on m-sapphire; by changing the Al composition from 10 to 50%, it came out that the layer structure and chemistry are dominated by internal surface effects. When the AlGaN thickness is below 5 nm, the composition fluctuations take place inside the layer with no notable roughness build up. By 10 nm of AlGaN, interesting features become predominant. Along the main growth direction, perpendicular to the ($11\bar{2}2$) surface, normal sections are terminated by two to three atomic steps which are oriented along the two visible $\{10\bar{1}1\}$ lattice planes. In these areas, the composition fluctuations are quite random but along these two planes as one or two atomic layers which are either rich or poor in Al. Adjacent to such areas, long sections limited by $\{10\bar{1}1\}$ facets form spontaneous quantum wells of 1 to three alternating monolayers Ga (rich)N/Al(rich)N which give rise to unintentional quantum wells. The underlying mechanism and physical properties are also investigated using density functional theory techniques.

1. D. Doppalapudi et al. J. Appl. Phys.84, 1389(1998)
2. J. Palisaitis et al. Scientific Reports 7, 4490(2017)
3. I. Ho and G. B. Stringfellow, Appl. Phys. Lett. 69, 2701(1996).
4. D. Korakakis et al. Appl. Phys. Lett. 71, 72(1997).
5. P. Ruterana et al. Appl. Phys. Lett. 72, 1742(1998)
6. M. Benamara et al. Appl. Phys. Lett. 82, 547 (2003)
7. P. Venezuela et al. Nature 397, 678 (1999)
8. P. Ruterana et al. Appl. Phys. Lett. 78, 344(2001)

Observation of Dislocations in AlN Single Crystal by Using Synchrotron X-Ray Topography, Etch Pit Method and Transmission Electron Microscope

Y. Yao [1], **Y. Sugawara** [1], **Y. Ishikawa** [1], **D. Yokoe** [1], **N. Okada** [2],
R. Inomoto [2], **K. Tadatomo** [2], **Y. Takahashi** [3] and **K. Hirano** [4]

[1] *Japan Fine Ceramics Center (JFCC), 2-4-1 Mutsuno, Atsuta, Nagoya, Japan*
[2] *Yamaguchi Univ., 2-16-1 Tokiwadai, Ube, Yamaguchi, Japan*
[3] *Nihon Univ., 7-24-1 Narashinodai, Funabashi, Japan*
[4] *High Energy Accelerator Research Organization (KEK), 1-1 Ooho, Tsukuba, Japan*

1. Overview. Dislocations in high-quality AlN single crystal substrate were studied by using synchrotron X-ray topography (XRT), etch pit method and transmission electron microscope (TEM). They are categorized into edge-, screw- and mixed-type according to their Burgers vectors (b) revealed by XRT. Dislocation behavior was discussed based on these results.

2. Experimental details. Commercially available AlN substrate (ϕ35mm, chemical-mechanical polishing treated surface) was used. Synchrotron XRT was observed using monochromatic beam at energy of 9.7 keV. g-vectors of six equivalent asymmetric 11-26 diffractions and a symmetric 0006 diffraction were applied, to evaluate the edge- and screw- component included in the Burgers vectors of dislocations. Chemical etching was carried out using molten KOH solution with Na_2O_2 additive. Hexagonal etch pits at several size levels were formed at the surface termination point of threading dislocations that are parallel to the c-axis. Cross-sectional TEM specimens were picked up from under the etch pits by using focused ion beam (FIB). TEM observation was performed at g/3g weak-beam condition.

3. Results and discussion. Spot-like and arc-like contrasts were observed in the XRT images, and they are considered to be originated from threading dislocations (TDs) and basal plane dislocations, respectively. TDs can be further grouped into edge-type (b=ma), screw-type (b=nc) and mixed-type (b=ma+nc) as follows. According to the $g \cdot b$=0 invisibility criterion, all three types of dislocations are on contrast in XRT images at g=11-26, while edge-type dislocations are out of contrast at g=0006. In addition, six equivalent g=11-26 were carried out in order to judge the direction of a-component for mixed-type TDs. As shown in Fig. 1, the same mixed-type TD changes its contrast (bright or dark) among the six XRT images when the g-vector varies, similar to the case in SiC [1] and GaN [2]. Finally, etch pit method and TEM analysis were performed, and an example showing the observation of an edge-type dislocation was shown in Fig. 2.
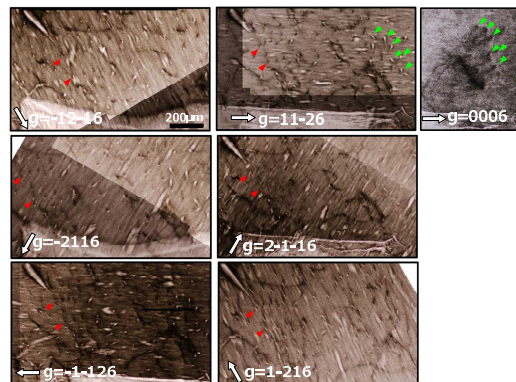
Fig.1 XRT images observed at g-vectors of six 11-26 and a 0006.
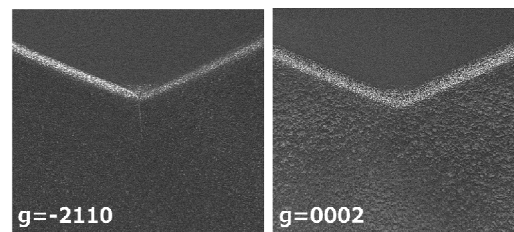
Fig.2 TEM g/3g weak beam dark field images observed from under a medium-sized etch pit, at g=-2110 and g=0002.

[1] I. Kamata, M. Nagano, et al., Mater. Sci. Forum, 600-603 (2009) 305.
[2] Y. Yao, Y. Ishikawa, et al., J. of Electron. Mater., in press (2018)

Investigation of Stacking Faults in Zincblende GaN Grown on 3C-SiC on Si templates with TEM and XRD

Lok Yi Lee[1], Petr Vacek[1], Martin Frentrup[1], Menno J. Kappers[1], Rachel A. Oliver[1], and D.J. Wallis[1, 2]

[1] *Department of Materials Science and Metallurgy, University of Cambridge, 27 Charles Babbage Rd, Cambridge, CB3 0FS, United Kingdom*
[2] *Centre for High Frequency Engineering, University of Cardiff, 5 The Parade, Newport Road, Cardiff, CF24 3AA, United Kingdom*

GaN in the metastable zincblende phase suffers from a high density of stacking faults (SFs), which are the dominate defect and may negatively impact the optical and electronic properties of the material. We have studied the alignment (Fig. 1) and density of the different SFs in a ~380 nm thick predominantly zincblende GaN thin film by cross-sectional bright-field transmission electron microscopy (BF-TEM) and X-ray diffraction (XRD). The sample was grown by metal organic vapor phase epitaxy on a (001)-oriented 3C-SiC on Si templates with a 4° miscut towards the [110] in-plane direction, under growth conditions which suppress the formation of the thermodynamically more stable wurtzite phase.

The use of miscut of the 3C-SiC on Si templates suppresses the formation of antiphase domains in the SiC, which would otherwise affect the GaN growth, but the impact of the miscut on the SFs requires examination. In the direction parallel to the miscut, [110], we observed an anisotropy in the SF alignment, with a range of $3 - 28$ times more (111) SFs than (-1-11) SFs measured across several regions of the sample. In the direction perpendicular to the miscut, [-110], the ratio of (-111) to (1-11) SFs measured varied from 12 to 0.2, suggesting that while there may be local anisotropy in the SF orientation, the global anisotropy seen parallel to the miscut is absent. The SF density measured close to the surface of the ~380 nm epilayer was higher along [110] than [-110], with averaged values of (5.9 ± 0.8) x 10^5 cm $^{-1}$ and (2.3 ± 0.1) x 10^5 cm $^{-1}$, respectively. This is probably because the anisotropy of the SF orientation makes it less likely the SFs will meet and annihilate.

The findings from the TEM analysis were also supported by XRD measurements, where diffuse scattering on SFs results in a characteristic streaking perpendicular to planes containing the SFs. Reciprocal space maps of the on-axis 002 GaN reflection measured perpendicular to the miscut along [-110] show a symmetric streak running along [-111] and [1-11] with similar intensities, which indicates similar (-111) and (1-11) SF densities. However, when measured parallel to the miscut along [110], the scattering pattern around the reflection has an asymmetric shape with a strong SF streak caused by (111) SFs, which shows a higher density of (111) SFs compared with (-1-11) SFs.

In summary, both BF-TEM and XRD suggested that there is an anisotropy in the SF alignment parallel and antiparallel to the miscut, but not perpendicular to the miscut. The overall SF density was higher parallel to the miscut than perpendicular to the miscut, which could imply that miscut controls the anisotropy of types of SFs generated, the subsequent annihilation of SFs, and hence reduction of SF density with layer thickness.
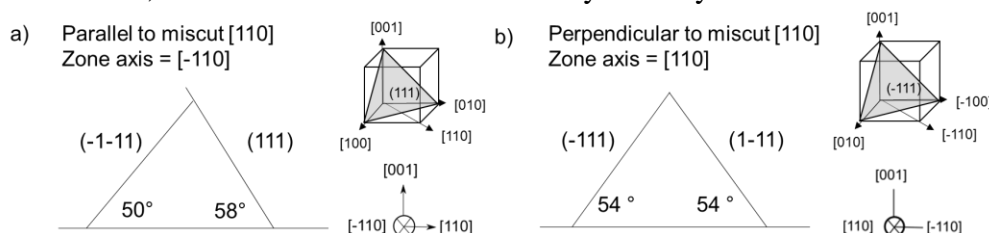
Fig. 1 Schematic of cross-section BF-TEM showing alignment of SFs along [110] and [-110].

Nanobeam X-ray Diffraction Analysis of Local Lattice Distortions in the Growth Direction of a Modified Na-Flux GaN Bulk Crystal

K. Shida [1], **S. Takeuchi** [1], **T. Tohei** [1], **M. Imanishi** [2], **M. Imade** [2], **Y. Mori** [2], **K. Sumitani** [3], **Y. Imai** [3], **S. Kimura** [3], **and A. Sakai** [1]

[1] *Graduate School of Engineering Science, Osaka University, 1-3 Machikaneyama-cho, Toyonaka, Osaka, Japan*
[2] *Graduate School of Engineering, Osaka University, 2-1 Yamadaoka, Suita, Osaka, Japan*
[3] *Japan Synchrotron Radiation Research Institute (JASRI), 1-1-1 Koto, Sayo, Hyogo, Japan*

High-quality GaN bulk single crystals fabricated by the Na-flux method combined with a multipoint-seed-GaN (MPS-GaN) technique [1] are now expected as seed materials for homoepitaxial GaN growth to produce free-standing GaN wafers. In this growth technique, one of remaining issues is the inhomogeneity of lattice constant in the Na-flux GaN crystal due to the local variation of oxygen impurity incorporation depending on the growth sectors, such as a c-plane growth sector (cGS) and a faceted-growth sector (FGS). This often generates the crack formation of hydride vapor phase epitaxy GaN subsequently grown on it [2]. To avoid this, we have newly developed a modified Na-flux GaN growth method. Here, the Na-flux GaN crystals are composed entirely of the cGS on the Na-flux GaN/MPS-GaN template. The key to improving the crystalline quality is to control the structures of homoepitaxial interfaces and coalescence boundaries in the templates. In this study, we have quantitatively elucidated lattice plane microstructure around such structures using nanobeam X-ray diffraction (nanoXRD).

A Na-flux GaN composed entirely of the cGS was grown on a Na-flux GaN/MPS-GaN template as illustrated in Fig. 1(a). Figure 1(b) shows a typical cross-sectional scanning electron microscope (SEM) image around the homoepitaxial interface and the coalescence boundary in the sample. Position-dependent nanoXRD was performed for the area surrounded by the dotted box in Fig. 1(b). The projection of the incident X-ray nanobeam with the size of 940 nm (c-direction) × 200 nm (a-direction) was set to be parallel to the c-axis of the GaN.

Figure 2 shows two-dimensional distribution maps of ω, 2θ, $\Delta\omega$ and $\Delta 2\theta$ for a symmetric GaN 2-200 Bragg reflection, where their values correspond to lattice plane tilting, spacing, and those fluctuations, respectively. In comparison with corresponding area shown in Fig. 1(b), it is clearly found that inhomogeneous distributions of ω and 2θ in FGSs are uniformized in cGS, while large $\Delta\omega$ and $\Delta 2\theta$ are seen around the coalescence boundary and abruptly decreases at the homoepitaxial interface. This result

Fig. 1 (a) Schematic of a modified Na-flux GaN sample and (b) cross-sectional SEM image showing an area measured by nanoXRD.
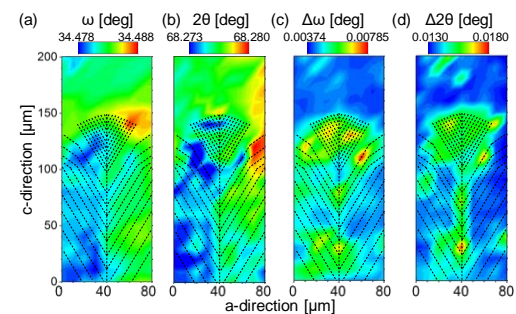
Fig. 2 2D-distribution maps of (a) ω, (b) 2θ, (c) $\Delta\omega$ and (d) $\Delta 2\theta$ in the dotted box area shown in Fig. 1(b). Dotted lines show contrasts observed in the SEM image.

indicates that the degradation of crystalline quality at that zone promotes strain relaxation and thus lead to homogenizations of lattice plane microstructure in the upper area.

References: [1] M. Imade *et al.*, APEX **7**, 035503 (2014). [2] M. Imanishi *et al.*, CGD **17**, 3806 (2017).

Strain relaxation in InGaN/GaN epilayers by formation of V-pit defects: XRD experiments and numerical simulations

Jana Stránská Matějová[1], Lukáš Horák [1], Peter Minárik[1], Václav Holý[1], Alice Hospodková[2], Ewa Grzanka[3], Jarosław Domagała[4], and Michał Leszczyński[3]

[1]*Faculty of Mathematics and Physics, Charles University, Ke Karlovu 5, 121 16 Prague, Czech Republic*
[2]*Institute of Physics, Czech Academy of Sciences, Cukrovarnická 10/112, 162 00 Prague, Czech Republic*
[3]*Institute of High Pressure Physics, Polish Academy of Sciences, Sokołowska 29/37, 01-142 Warsaw, Poland*
[4] *Institute of Physics,Polish Academy of Sciences, Al. Lotnikow 32/46, Warsaw, Poland*

Formation of V-pit defects is a commonly observed phenomenon in InGaN epilayers.[1] However, the exact mechanism of V-pit formation remains unclear in some aspects. TEM images from numerous studies show, that the V-pits emerge from the point, where a threading dislocation from GaN substrate intersects the boundary between the substrate and the layer. Nevertheless, it was not confirmed, that all the V-pits and all the threading dislocations at interface act in this way.[2] Moreover, X-ray diffraction (XRD) experimental data exhibit very low degree of plastic relaxation of InGaN layers, and it is still matter of controversy, if the V-pits creation can relieve elastic energy sufficient for the strain relaxation.[3, 4]

We present results of numerical simulations of elastic strain fields and X-ray reciprocal space maps (RSM) in comparison with XRD and AFM experimental data yielded from a series of MOVPE-grown samples. We used samples with InGaN layer thickness of 10 - 135 nm and 10-20% In content, for which high-resolution XRD reciprocal space maps were measured. These experimental RSMs were compared with simulations based on kinematic XRD theory and on strain field model, considering linear elastic behavior of materials. The results were verified by analysis of AFM images taken from the surface of the samples.

Our study provides an evidence, that the V-pits have major influence on strain relaxation in InGaN/GaN.

[1] Y. Chen, T. Takeuchi, H. Amano, I. Akasaki, N. Yamada, Y. Kaneko, and S.Y. Wang, *Applied Physics Letters*, **72**, 6 (1998).
[2] Z.Y. Gao, X. W. Xue, J.J. Li, X. Wang, Y.H. Xing, Cui BF, and D. S. Zou, *Chinese Physics B,* **25** (2016).
[3] S. L. Rhode, W. Y. Fu, M. A. Moram, F. P. Massabuau, M. J. Kappers, C. McAleese, and S. L. Sahonta, *Journal of Applied Physics*, **116**, 10, (2014).
[4] T. L. Song, *Journal of Applied Physics,* **98**, 8 (2005).

Invited lecture

Optical Properties of 1 ML GaN in AlN: What Happens Beyond the Envelope Function Approach

A. A. Toropov [1], **E. A. Evropeitsev** [1], **M. O. Nestoklon** [1], **D. S. Smirnov** [1],
V. N. Jmerik [1], **D. V. Nechaev** [1], **S. Rouvimov** [2], **T. V. Shubina** [1], **B. Gil** [1,3],
and S. V. Ivanov [1]

[1] *Ioffe Institute, Politekhnicheskaya 26, 194021 St Petersburg, Russia*
[2] *University of Notre Dame, Notre Dame, 46556 Indiana, USA*
[3] *Université Montpellier 2, L2C, UMR 5221, 34095 Montpellier Cedex 5, France*

Ultrathin GaN insertions in AlN are promising structures for efficient electron-beam pumped light sources [1] and light emitting diodes [2] emitting in middle- and deep-UV ranges. Nevertheless, despite the ~6 eV direct band-gap of AlN, quantum efficiencies for the light emission below ~240 nm remain impractically low. Among other issues, a detailed knowledge of the electronic band structure and excitonic spectrum is crucial since the optical properties strongly depend on whether the lowest-energy electron-hole transitions are optically allowed (bright) or forbidden (dark). Elucidation of this fundamental issue in 1-ML-thick GaN insertions emitting at the shortest wavelengths possible has been hampered by both technological challenges and inability of the conventional envelope-function approach to describe electronic states in the ultrathin structures. In this work, we systematically investigate peculiarities of electronic band structure of the GaN/AlN insertions in the thickness range of 1-4 MLs and present both experimental and theoretical evidence for the existence in the 1-2 ML thick structures of the optically dark excitonic state lying noticeably below the optically bright state.

Experimentally, we studied the temperature-dependent time-resolved photoluminescence (PL) in MBE grown GaN/AlN structures of varied thicknesses. It was found that the kinetics of low-temperature excitonic PL changes drastically, when the GaN thickness approaches 1 ML. In the thicker insertions, the PL signal homogeneously decays on the scale of a few hundreds of picoseconds, whereas in the 1-2 ML structures, the PL dynamics is characterized by two regimes with very different decay times. First, the PL intensity drastically drops within a picosecond range. Then, a thermalized exciton population is established yielding much longer decay in the nanosecond range. This behavior is consistent with the dark excitonic ground state and the dark-bright exciton splitting of 20-50 meV, as estimated from analysis of the temperature-dependent time-resolved PL measurements. Theoretically, this conclusion is confirmed by the density functional theory calculations of AlN with some atomic layers of Al substituted with Ga. The calculations show significant localization of both types of carriers even in the structure with 1 atomic layer of Ga. Estimations of the short range exchange interaction between electron and hole indicate that the splitting between bright and dark states is about a few meV in the 3 ML thick insertion and reaches a few tens of meV in the 1 ML thick QW that is in good agreement with experimental findings. Understanding of this issue is important since the dark nature of the split-off lowest-energy exciton may be the ultimate factor limiting the shortest wavelength that can be achieved in the GaN/AlN-based ultraviolet light emitters.

[1] X. Rong, X. Wang, S.V. Ivanov, et al., *Adv. Mater.* **28**, 7978 (2016).

[2] S.M. Islam, K. Lee, J. Verma, V. Protasenko, S. Rouvimov, H. (Grace) Xing, and D. Jena, *Appl. Phys. Lett.* **110**, 041108 (2017).

Invited lecture

First Principles and Thermodynamic Studies on GaN MOVPE Processes

Yuto Okawachi[1], Kazuki Sekiguchi[1], Kenta Chokawa [1], Masaaki Araidai[2], Mitsuo Shoji[3], Yasuteru Shigeta[3], Yoshihiro Kangawa[4,2], Koichi Kakimoto[4], and Kenji Shiraishi[2,1]

[1] *Graduate School of Engineering, Nagoya University, Furo-cho, Chikusa-ku, Nagoya 464-8603, Japan*
[2] *Institute of Materials and Systems for Sustainability, Nagoya University, Furo-cho, Chikusa-ku, Nagoya 464-8603, Japan*
[3] *Center for Computational Sciences, University of Tsukuba, 1-1-1 Tennodai, Tsukuba 305-8577, Japan*
[4] *Research Institute for Applied Mechanics, Kyushu University, 6-1 Kasuga-koen, Kasuga, 816-8580, Japan*

GaN is expected as materials for semiconductor power devices in the next generation and it can be achieved superior performance of devices and energy conservation by practical use of GaN devices. MOVPE is generally used for the fabrication of GaN devices. In case of GaN-MOVPE, trimethylgallium (TMG) and NH_3 are used for gallium and nitrogen source, respectively. The main problem in GaN-MOVPE is carbon contamination during growth procedure and MOVPE growth of high quality, carbon free, GaN is indispensable. For carbon free GaN growth, thermal desorption of all methyl group from TMG is crucial. In this study, we analyzed decomposition process of TMG during MOVPE growth based on first principles calculations and thermodynamic analysis.

To suppress the incorporation of carbon impurities during GaN-MOVPE, TMG should decompose into Ga(gas). In our past study, we concluded H_2 is indispensable for TMG decomposition and TMG with H_2 decomposes into $Ga(CH_3)$ under the total pressure of 1 atm [1]. In this study, we investigated the decomposition process of TMG to consider reaction with NH_3 by the first principles calculations and thermodynamical analysis. We considered following four possible reactions.

$$(a)\ Ga(CH_3)_3 + H_2 \rightarrow Ga(CH_3) + 2CH_4$$
$$(b)\ Ga(CH_3)_3 + 3/2H_2 \rightarrow Ga(gas) + 3CH_4$$
$$(c)\ Ga(CH_3)_3 + 2H_2 \rightarrow GaH(gas) + 3CH_4$$
$$(d)\ Ga(CH_3)_3 + NH_3 \rightarrow (CH_3)_2GaNH_2 + CH_4$$
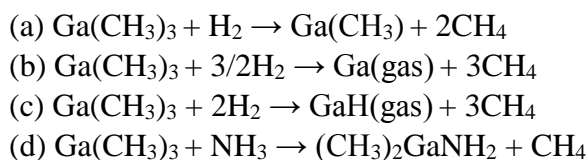
We calculated Gibbs free energies of each molecules as a function of temperature. We interpreted the reaction occurs when Gibbs free energies of the molecules after reaction lowbecomes minus. In the calculations, each partial pressure of inflow gases is that of TMG is 10^{-4} atm, that of NH_3 is 10^{-1} atm and that of carrier gases is the other in the total pressure. H_2 is 1 percent inside the carrier gases. The calculated results of reaction (d) indicated Gibbs free energy of $((CH_3)_2GaNH_2 + CH_4)$ is always lower than that of $(Ga(CH_3)_3 + NH_3)$. Therefore, reaction (c) occurs. Compared with the reactions (a), (b), and (c) however, reaction (d) only occurs when temperature is lower than 40 K. This result clearly shows TMG hardly reacts with NH_3 under the actual growth conditions with H_2 carrier gas, indicating the failure of the $(CH_3)_2GaNH_2$ adduct formation concept [2]. We also found that reaction (c) $(Ga(CH_3)_3 + 2H_2 \rightarrow GaH(gas) + 3CH_4)$ is most stable and GaH(gas) is the most probable final product.

[1] K. Sekiguchi *et al.*, J. Crystal Growth, **468**, 950 (2017).
[2] A. Thon and T. F. Kuech, Appl. Phys. Lett. **69**, 55 (1996).

Invited lecture

Compensation in Si-doped AlN: Mechanisms and opportunities

Douglas L. Irving[1], Joshua S. Harris[1], Jonathon N. Baker[1], Shun Washiyama[1], M. Hayden Breckenridge[1], Pramod Reddy[2], Ramón Collazo[1], and Zlatko Sitar[1,2]

[1]*Department of Materials Science and Engineering, North Carolina State University, Raleigh, NC, USA*
[2]*Adroit Materials, Cary, NC, USA*

The substantial Baliga figure of merit together with the wide direct bandgap have made AlN, and its alloys, desirable candidates for next generation power devices and optoelectronics. While significant strides have been made in the production of high quality bulk materials which, in turn, have enabled the creation of low defect density heterostructures, controlled doping of AlN remains a significant obstacle. Silicon, a common shallow donor dopant in GaN, exhibits a deeper ionization level in AlN due to its propensity to form a DX center for Fermi levels near the conduction band minimum. Further complicating doping of AlN is compensation by other deep acceptor defects. In the low doing regime, where controlled doping is important for the drift layer in power electronics, unintentional impurities and unintentional impurity complexes are often the source of free carrier compensation. In the higher doping limit, relevant to doping levels in optoelectronics, vacancy-dopant complexes have recently been identified as important contributors [1,2] as proposed earlier [3]. In this paper, we will explore the mechanisms for compensation in Si-doped AlN and also explore possible solutions. We have implemented first principles density functional theory calculations with screened hybrid exchange-correlation functionals to determine the properties of individual defects in AlN. The formation energies of each defect are used within a grand canonical equilibrium model to identify the predominant defects as a function of growth conditions. This approach has been extended to explore the defect energy landscape important to dopant implantation and we will also address how defect properties change in strained epitaxial films. Results from these methods are compared with complementary experimental data that includes below band gap optical absorption and photoluminescence, electrical measurements, dopant implantation, and available SIMS measurements.

[1] J. S. Harris, J. N. Baker, B. E. Gaddy, I. Bryan, Z. Bryan, K. J. Mirrielees, P. R. R. Collazo, Z. Sitar, and D. Irving, *Appl. Phys. Lett.* **112**, 152101 (2018).

[2] I. Bryan, Z. Bryan, S. Washiyama, P. Reddy, B. Gaddy, B. Sarkar, M. H. Breckenridge, Q. Guo, M. Bobea, J. Tweedie, S. Mita, D. Irving, R. Collazo, and Z. Sitar, *Appl. Phys. Lett.* **112**, 062102 (2018).

[3] S. Chichibu, H. Miyake, Y. Ishikawa, M. Tashiro, T. Ohtomo, K. Furusawa, K. Hazu, K. Hiramatsu, and A. Uedono,, *J. Appl. Phys.* **113**, 213506 (2013).

A theoretical model for carbon incorporation during step-flow growth of GaN by MOVPE

Y. Inatomi [1], and **Y. Kangawa** [1,2,3]

[1]*Department of Aeronautics and Astronautics, Kyushu University, Fukuoka 812-0395, Japan*

[2] *RIAM, Kyushu University, Fukuoka 816-8580, Japan*

[3] *IMaSS, Nagoya University, Nagoya 464-8601, Japan*

In recent years, high voltage / high current vertical GaN power devices for use in electric vehicles and the like has been intensively developed. These electric devices require low carrier concentration and low resistive GaN drift layer with low contamination [1]. Major considerable unintentional impurity during metalorganic vapor phase epitaxy (MOVPE) is carbon (C) from trimethylgallium (TMG) which compensates carriers, and makes the layer high resistive. Therefore, it is necessary to develop growth technique of low C concentration GaN by MOVPE.

In this study, we newly proposed an impurity incorporation model during crystal growth from vapor phase, and applied the model to GaN(0001) MOVPE to investigate the relationship between growth conditions and C concentration. This model considers kinetic behavior of adsorbed atoms on the crystal surface during step flow growth, and can quantitatively calculates C concentration as a function of partial pressure of gas phase near the surface assuming equilibrium between the gas phase and adsorbed phase. Figure 1 shows the change in C concentration when growth conditions (input TMG, input NH_3 and total pressure) are varied. The result indicates that increasing NH_3, decreasing TMG, increasing total pressure is effective to reduce C concentration. This theoretical tendency agrees well with experimental results. [2] Furthermore, in Fig. 1 (right), we can see that C concentration is kept almost constant under the condition of constant V/III ratio, which tendency corresponds to experimental results [3]. The theoretical model seems to be useful for optimizing growth condition to obtain GaN with low C concentration.
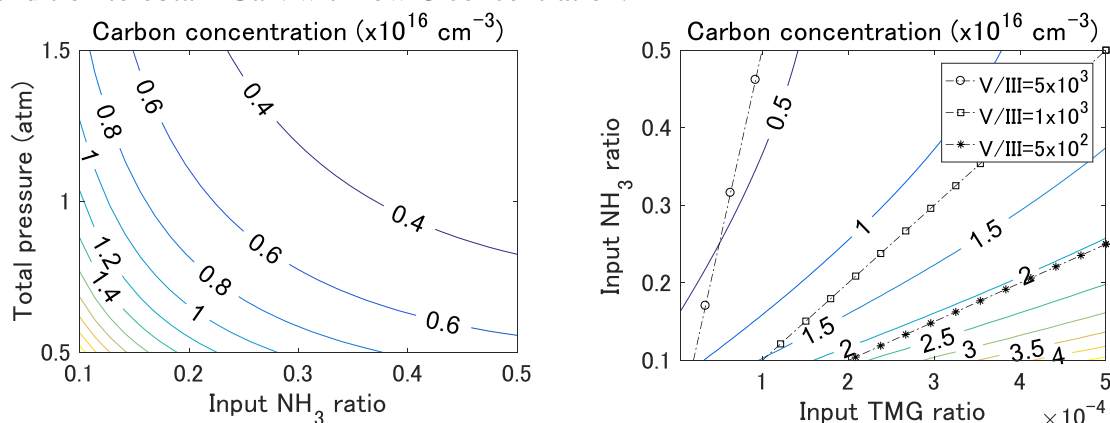
Fig. 1. Contour of C concentration. $T = 1000$ °C and N_2 carrier gas were considered. (Left) Input NH_3 molar ratio vs. total pressure. Input TMG molar ratio is 1.0×10^{-4}. (Right) Input TMG ratio vs. input NH_3 molar ratio. Total pressure is 0.8 atm.

References [1] T. Kachi, *Jpn. J. Appl. Phys.* **53**, 100210 (2014). [2] N. A. Fichtenbaum et al., *J. Cryst. Growth* **310**, 1124 (2008). [3] G. Piao et al., *J. Cryst. Growh* **456**, 137 (2016).

Perovskite Solar Cells with n-type GaN Electrodes

M. Wierzbowska [1]**, M. Sarzyński** [1]**, I. Dzięcielewski** [1]**, J. Weyher**[1]**, B.-E. Cohen**[2] **and L. Etgar** [2]

[1] *Institute of High Pressure Physics, Polish Academy of Sciences, Sokołowska 29/37, 01-142 Warsaw, Poland*
[2] *Institute of Chemistry, The Center for Nanoscience and Nanotechnology, The Casali Center for Applied Chemistry, The Hebrew University of Jerusalem, Israel*

The organic lead halide perovskite solar cells combine high photovoltaic conversion efficiency and high open circuit voltage with low cost fabrication. The perovskite layer could be of p-type or intrinsic due to the methylammonium vacancies and the solar structure. The n-type electrode is usually a transparent metal oxide. The most popular n-type substrate is TiO_2. For the reasons of the elastic properties in the composites with polymers, the junctions of perovskites with ZnO are also widely investigated. They achieve superior electronic properties with respect to those with the titanium oxide. On the other hand, the stability under elevated temperatures and moisture resistance are much poorer in the case of the zinc oxide junctions with perovskites.

As an alternative to the above mentioned oxides, the nitrides have very good hydrophobic properties which might be advantageous. GaN high quality crystals are widely used in the optoelectronic devices, combining good electronic transport parameters with high transparency. The n-type character is realized by doping them with silicon. The band gap of GaN is 3.4 eV, which value is much larger than the band gap of 1.5-1.7 eV of perovskites – necessary condition for the light absorption to occur at the perovskite. The conduction band minimum energy levels alignments of these materials also fit the necessary conditions for the electron injection from the perovskite to the GaN electrode. However, the electronic properties of the interfaces with the defects and various crystal directions differ much. The interface atomic-layer metalization and the midgap states were theoretically found and will be discussed. The electronic, transport and optical properties of pure and defected interfaces, obtained with *the first-principles* simulations, will be presented. Additionally, the interface co-doping with the elements possessing the valency matching the unsaturated surface bonds of GaN are investigated.

The preparation of the perovskite solar cells at the GaN crystals is as follows: The laser-beam lithography (Microtech LW 405B, precision 1 µm) will be used to fabricate a suitable stripe-shaped pattern in a 5 µm thick photoresist layer. Then, a typical ion etching procedure (Oxford Plasma Lab 100 with Cl/Ar chemistry) will be applied to transfer the pattern to GaN/sapphire template. For nano-structuring of the top GaN surface etching in 0.02 M $K_2S_2O_8$ + 0.02 M KOH solution (designated KSO-D) under a 300 W UV-enhanced Xe lamp (Oriel) illumination will be used, both in electroless and in galvanic mode.
For the perovskite deposition: two-dimensional perovskite solutions are dropped on the GaN substrate and spin-coated at 1000 rpm for 10 seconds followed by an additional spin 5000 rpm for 60 seconds; during the second spin 40 µL of toluene are dropwise added into the substrate. The films are annealed at 100˚C for 1 hour. Following the perovskite deposition a hole transport material layer is deposited also by spin coating. Then metal contact electrode is thermally evaporated on the film under a vacuum of $\sim 10^{-7}$ Torr.

Invited lecture

Morphology and Electronic Structure of Carbon Doped Hexagonal Boron Nitride

Agnieszka Jamróz and Jacek A. Majewski

Faculty of Physics, University of Warsaw, ul. Pasteura 5, 02-093 Warszawa

Hexagonal atomically thick boron nitride (h-BN) has become recently very important for functional devices based on two-dimensional materials. This insulator is employed in lateral and vertical heterostructures together with graphene and to insulate two conducting layers. Typically the h-BN layers are obtained through the exfoliation from the bulk material. However, the importance of the material for numerous applications has lead to attempts of h-BN growth employing the industrial growth techniques such as chemical vapor deposition (CVD). However, the usage of certain precursors in the CVD growth process leads to large induces large content of carbon in h-BN, which can modify the properties of pristine h-BN.

In the present communication we present extensive studies of C doped h-BN, considering the details of material morphology, distribution of dopants, elastic properties, and finally the electronic structure of doped material. We pay particular attention to the native structural defects in h-BN, such as vacancies, anti-sites, and grain boundaries and how these defects influence the distribution of carbon atoms in h-BN, and further modify material's properties.

Our studies are based on the Monte Carlo method in NVT ensemble with valence force field like potentials accounting for interaction between atoms. The use of empirical, reactive, bond-order potentials allows for investigations of large (up to tens thousands of atoms) systems. The electronic structure is obtained employing the empirical tight-binding Hamiltonian for the atomic positions obtained with the Monte Carlo study. The large systems we can treat within the Monte Carlo procedure guarantee that the obtained properties of C doped h-BN correspond to the thermo-dynamical equilibrium and additionally are free from large properties fluctuations observed in computational scheme based on sampling only particular realizations of the dopant density (mostly employing the super-cell geometry).

In our previous studies [1], employing the analogous methodology, it has been shown that boron and nitrogen doped graphene layers in honeycomb structure exhibit short-range order and deviate strongly from the random alloys. In the case of C doped h-BN we observe also the similar trend, i.e., deviation from the random distribution of carbons on the h-BN lattice and the pronounced short-range correlation in carbon distribution. Our calculations indicate that the defects do influence the distribution of the carbon atoms and typically there is access of carbon atoms around the structural defects in comparison to the average concentration of the dopant. With the C atoms incorporated mostly into B sites the system has tendency to be n-type at elevated temperatures. We establish the clear relation between the morphology of the C doped h-BN and the resulting electronic structure.

.

[1] A. Jamroz and J. A. Majewski, *Computational Materials Science* **147** (2018) 115–123.

Invited lecture

GaN Nanostructures
(or how to Take Transistor Linearity to new Levels)

Sameer Joglekar, Ujwal Radhakrishna, Qingyun Xie, and Tomás Palacios

Massachusetts Institute of Technology 77 Massachusetts Ave., Bldg. 39-567, Cambridge

State-of-the-art communication systems require very linear amplifiers to be able to support a large number of simultaneous communication channels and bandwidth. Traditionally, this linearity was made possible either by the use of highly linear bipolar transistors and/or of pre-distortion systems that would adapt the signal at the input to account for the non-linearities of the amplifier and generate an overall linear amplified output. Although this approach has worked well in the past, it is not enough to fulfill the linearity requirements of future 5G communication systems operating at Ka bands and beyond. Therefore, current research on RF GaN amplifiers has shifted from a focus on improving power density and efficiency, to a new emphasis on increasing the amplifier linearity at the device level.

This talk will review the origins of non-linearities in GaN-based amplifiers and propose device-level solutions to improve linearity. First, we will discuss how the drop in transconductance (gm) at high current levels observed in GaN transistors can be mitigated with either self-aligned or finFET-like structures [1-2]. This is due to the higher current-driving capability of the source access region on these devices. The second cause of device nonlinearity has been linked to the large second derivative of the transconductance with respect to gate-source voltage (Vgs) (gm"). This can be overcome by using a new generation of engineered finFET transistors where the width of each fin is optimized for minimizing gm" (Figure 1) [3]. In addition, the non-linear behavior of the device capacitances with operating voltage also plays a very important role in device non-linearities. In this case too, nanostructures can be used to improve device performance. Finally, memory effects due to surface and buffer traps also contribute to non-linearities in amplifiers, and they can also be overcome though the use of nanostructures.

The talk will conclude with an outlook of the future of GaN-based electronics, a field that is quickly evolving and growing, and that it is about to be transformed by new industrial players with a strong background on silicon-based electronics.
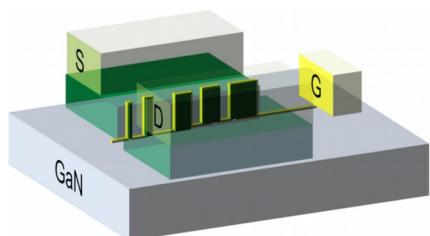
Figure 1: Diagram of an engineered Fin-FETdevice where the width of each fin isoptimized for improving device linearity.

References.-
[1] T. Palacios, et al, IEEE Trans. On Electron Devices, vol. 53, pp. 562-565, 2006.
[2] D.S. Lee, et al, IEEE Elect. Dev. Lett., vol. 34, no. 8, pp. 969–971, Aug. 2013.
[3] S. Joglekar, et al., 2017 International Electron Devices Meeting (IEDM 2017), 9.2, Dec 2017.

Invited lecture

Growth, Physics, and Applications of Tunneling Nitride Structures

Debdeep Jena[1]**, Jimy Encomendero**[1]**, Samuel Bader**[1], **Alex Chaney**[1],
Henryk Turski[1]**, Yongjin Cho**[1]**,** and **Grace Huili Xing**[1]

[1]*Cornell University, Ithaca, USA*

Ever since the discovery of the quantum mechanical tunneling of electrons through classical potential barriers in semiconductor crystals by Esaki [1] in 1958, the phenomenon has fascinated several generations of researchers. The scientific curiosity has led to significant technological use of tunneling in semiconductors, superconductors, and in metals and insulators. This is because tunneling currents give a glimpse of the inner quantum nature of crystals, and are the most sensitive measurements of bandgaps, band offsets, effective masses, and built in electric fields. Because the probability of tunneling of electrons across the bandgap barrier is given by $T_{WKB} \sim \exp[-\sqrt{m^*}E_g^{3/2}/qF\hbar]$, where E_g is the bandgap, m_c^* the effective mass, and F the electric field, this phenomenon is expected to be very weak in the wide bandgap Gallium Nitride family of semiconductors. The adjacent Figure shows a comparison of the calculated interband tunneling current densities possible in various *ideal* semiconductor pn junction diodes as a function of the peak junction electric field, and the device technologies that these tunneling currents can impact.
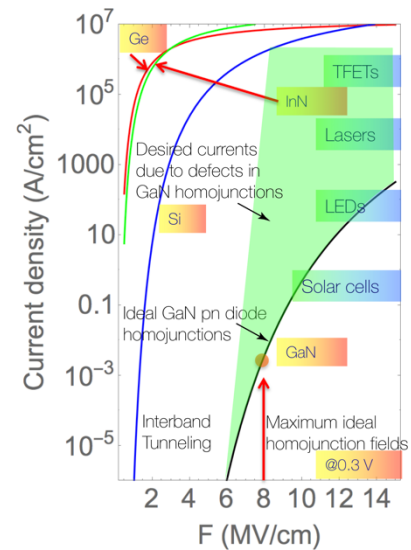
With typical doping levels, *ideal* homojunction GaN pn tunnel diodes cannot achieve the current densities necessary for LEDs, Lasers, or tunneling FETs (TFETs). This is however possible by *defect-assisted tunneling*, and in spike-doped homojunctions [2]. Because LEDs and Lasers are two-terminal devices, achieving interband tunneling through defect-assisted tunneling can be tolerated, and have enabled the first buried-tunnel junction GaN LEDs [3]. But for three-terminal GaN tunneling transistors [4], defect assisted tunneling prevents the basic operation of the device by making it impossible to turn the device off. To that end, polarization-induced interband tunnel junctions have been demonstrated [5], and recently employed to experimentally demonstrate the first GaN based TFETs [6]. Because TFETs also need the highest current densities as seen in the Figure above, it is the most stringent test for our understanding, control, and use of tunneling in the GaN material family. Unlike interband tunneling, *intraband* resonant tunneling has been successfully used for microwave oscillators for the first time in GaN/AlN double barrier structures [7]. These structures enable the direct measurement of the built-in polarization fields, and exhibit asymmetries not seen in non-polar III-V semiconductors.

[1] L. Esaki, "Long Journey into Tunneling", *Nobel Lectures* (1973).
[2] S. Bader et. al., IEEE DRC Tech. Digest (2016).
[3] H. Turski et al., U. S. Provisional Patent # 62/625,502 (2018).
[4] W. Li et al., IEEE J. Exploratory Devices and Circuits, 1, 28 (2015).
[5] J. Simon et al., Physical Review Letters, 103 026801 (2009).
[6] A Chaney et al., IEEE DRC, to be presented (2018).
[7] J. Encomendero et al., Phys. Rev. X 7, 041017 (2017).

High Reliability and Frequency Performances of InAlN/GaN HFETs

Z. H. Feng，Y. J. Lv, Y. L. Fang, Y. G. Wang, X. B. Song, and S. J. Cai

National Key Laboratory of ASIC, Hebei Semiconductor Research Institute, Shijiazhuang, China

Compared to the traditional AlGaN/GaN heterostrcture field-effect transistors (HFETs), InAlN/GaN HFETs have attracted considerable interests for its natural advantages such as lattice-match and strong spontaneous polarization. Particularly, the high two-dimensional electron gas (2DEG) density due to the strong spontaneous polarization in InAlN/GaN heterostrctures make the ultrathin barrier HFETs promising candidates for higher output power and higher working frequency applications [1]. However, the InAlN/GaN HFETs still are not used in practical applications due to large leakage current and poor stability [2]. The component inhomogeneity is a severe issue in InAlN epilayer, as clusters due to the phase separation is usual.

In this work, an ultrathin $In_{0.17}Al_{0.83}N/GaN$ heterostructure was grown on 3 inch 4H-SiC substrate by MOCVD. Field-effect transistors were fabricated on high crystalline quality InAlN/GaN heterostructures [3]. The reliability of InAlN/GaN HFETs was measured for the first time. The MTTF of the manufactured InAlN/GaN HFETs was estimated to be 8.9×10^6 hours at junction temperature of 150 ℃. The effective critical electric field reaches 0.8 MV/cm, which is a record value in the reported InAlN/GaN. Meanwhile，the record maximum frequency (fmax) of the fabricated HFETs with a 50nm T-shaped gate reaches 405 GHz.
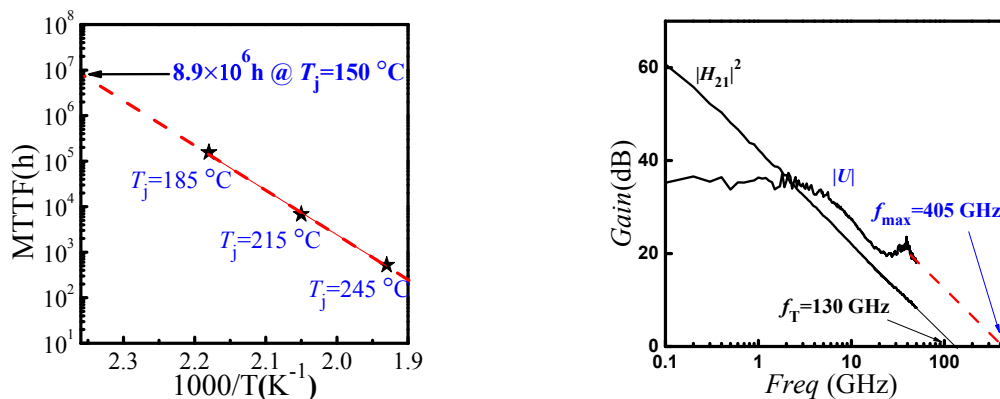
Fig. 1. MTTF and small signal characteristics of InAlN/GaN HFETs

[1] A. Crespo, M. M. Bellot, K. D. Chabak, J. K. Gillespie, G. H. Jessen, et al., *IEEE Electron Device Lett.* **3**, 2 (2010).
[2] L. Lugani, M. A. Py, J.-F. Carlin, and N. Grandjean, *J. Appl. Phys.* **115**, 074506-1 (2014).
[3] Y. L. Fang, Z. H. Feng, J. Y. Yin, Z. R. Zhang, Y. J. Lv, S. B. Dun, B. Liu, C. M. Li, and S. J. Cai, *Phys. Status Solidi B* **252**, 1006 (2015).

Demonstration of GaN vertical double implanted MOSFET

Ryo Tanaka [1], Shinya Takashima [1], Katsunori Ueno [1], Hideaki Matsuyama [1], Masaharu Edo [1], and Kiyokazu Nakagawa [2]

[1] *Fuji Electric Co., Ltd., 1, Fuji-machi, Hino-city, Tokyo 191-8502, Japan*
[2] *Univ. of Yamanashi, 7-32, Miyamae-cho, Kofu, Yamanashi 400-8511, Japan*

Vertical Gallium nitride (GaN) transistors are expected as next generation low loss power switching devices. For high voltage and large current power application, normally-off drive by insulated gate is strongly desired. Furthermore, for realizing a vertical MOSFET, The p-type layer is preferably formed by ion implantation (I/I). We have reported about the normally off operation of the lateral MOSFETs formed on the Mg implanted GaN layer [1]. In this paper, we present characteristics of GaN vertical double implanted MOSFETs (VDIMOSFET).

Fig. 1 shows a schematic cross section of the fabricated VDIMOSFETs by Mg and Si I/I process. Firstly, the Mg I/I into the p-well regions was carried out selectively on 10 μm-thick n-type GaN layers grown on the n-GaN (0001) substrates. The Mg-ions were implanted to create a 500 nm BOX profile with Mg concentration of 1×10^{18} cm^{-3}. Secondly, Si ions were implanted into the source regions selectively. For Mg and Si activation, the wafers were annealed at 1300 °C with AlN encapsulation cap to prevent dissociation of GaN during high temperature annealing. After the activation annealing, 100-nm-thick SiO$_2$ layers were deposited by using a remote plasma-CVD apparatus with TEOS gas. Ti/Al was used for a gate metal, source contact metal, and also a drain contact metal. The body contact metal was Ni. Finally, we performed a forming gas annealing. The designed channel length (L_{ch}) on photomask was 1, 2, and 4 μm. The gate length (L_g) was 3, 6, and 9 μm. The gate width (W_g) was 100 μm.

Fig. 2 shows the I_d-V_d output characteristics of fabricated GaN-VDIMOSFET (L_{ch} =4 μm, L_g = 9 μm). Normally-off MOSFET operation with a threshold voltage of about 5 V was confirmed. Fig. 3 shows L_{ch} dependence of the on-resistance (R_{on}, the differential resistance at V_d = 1 V and V_g = 30 V). R_{on} is proportional to L_{ch}, so it was confirmed that the device characteristics can be controlled by design dimensions. The breakdown voltage of pn-junction was still low because the activation of Mg implanted region was insufficient, so improvement of the Mg activation ratio is the most priority work.

[1] S. Takashima *et al*., Extended Abstracts of the 2017 International Conference on Solid State Devices and Materials (2017) 1075.
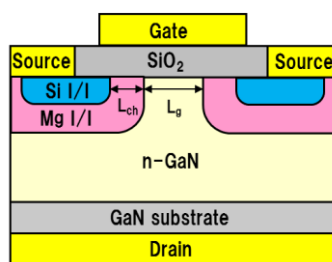
Fig.1. Fabricated GaN-VDIMOSFETs by Mg and Si double implantation.
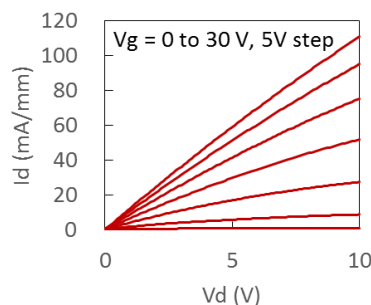
Fig.2. I_d-V_d characteristics of fabricated VDIMOSFET
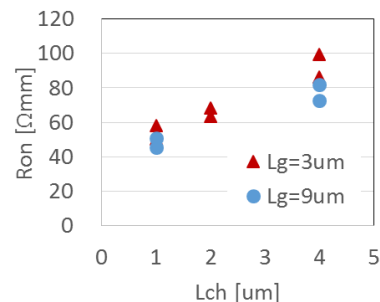
Fig. 3. R_{on}-L_{ch} characteristics of fabricated VDIMOSFETs

Optimized Ohmic Contacts For InAlGaN/GaN HEMTs

Farah F. Bouazzaoui[1], Marie-Pierre M-P. Chauvat[1], Malek M. Zegaoui[2], Farid F. Medjdoub[2], Piero P. Gamarra[3], Slawomir S. Kret[4] and Pierre P. Ruterana[1]

[1] *CIMAP, 6 boulevard du Marechal Juin, Université de Caen, Caen, France*
[2] *Institute of Electronics, Microelectronics and Nanotechnology (IEMN), Av. Poincaré,Villeneuve d'Ascq, France;*
[3] *III-V Lab, 1 Avenue Augustin Fresnel, Campus Polytechnique, Palaiseau, France*
[4] *Institute of Physics, Polish Academy of Sciences, al. Lotników 32/46, Warsaw, Poland*

During the last years, the most significant improvement of the contact resistance for InAlN/GaN high electron mobility has been the use of a highly doped n+ GaN layer grown by molecular beam epitaxy for the source and drain terminals. In a first report [1], the ohmic contact processing was carried out as follows, first the device surface was passivated using a SiN layer and then protected by SiO_2. Then the contact windows were opened through the protection and the InAlN(5.6 nm) /GaN heterostructures was then etched out to a depth of 12 nm followed by a regrowth of a 40 nm thick n+ doped GaN layer by MBE. After removal of the residual polycrystalline GaN from the SiO_2 surface, a Ti/Al/Ni/Au metal stack was deposited by electron-beam evaporation and annealed at 850°C for 30s in N_2 which resulted in an improved contact resistance of 0.40 Ohm.mm. In a more recent work using an identical procedure [2], the same authors deposited, a different metallic stack based on Mo/Au and measured a lower contact resistance of 0.16 Ohm.mm. In this work, the Ohmic contact is fabricated in a more conventional way by first removing the passivation layers through an optimized surface chemical cleaning procedure in ohmic region, and next using a Ti/Al/Ni/Au metallic stack is deposited by electron-beam evaporation. Finally, the sample is submitted to rapid thermal annealing at 875°C for 30 seconds. In our report, we shall discuss the results measured on two samples; S1 was processed using standard surface cleaning procedure which leads routinely to a reproducible contact resistance of about 0.5-0.6 Ohm.mm. For S2, we carefully optimized the InAlGaN barrier surface preparation prior to the metal stack deposition; the resulting in contact resistances as low as 0.15-0.16 Ohm.mm. Through a detailed analysis by transmission electron microscopy, it is shown that, for both samples the metallic stack is transformed into a multiphase alloy, although in a different way. In S1, there is an extensive phase separation with two dominant alloys, one AuAl rich, and the second NiAl rich. In S2, the metallic reaction leads to a homogeneous alloy of the four starting metals. Moreover, at the interface with the barrier extended epitaxial relationships are present with the metallic particles. 3. Although a diffusion of Ti, Ni, and Au can be seen along screw or mixed type dislocation, the surface layer of the barrier presents extended reaction with the metals. All this combination is probably at the origin of the measure low contact resistance, which become comparable to the case where the localized MBE growth of n+GaN has been used.

[1] J.Guo, Y.Cao, C.Lian, T.Zimmermann, G. Li, J.Verma, X.Gao, S.Guo, P.Saunier, M.Wistey, D.Jena, and H.Xing. Metal-face InAlN/AlN/GaN high electron mobility transistors with regrown ohmic contacts by molecular beam epitaxy. Physica Status Solidi A 208, No. 7, 1617–1619 (2011) / DOI 10.1002/pssa.201001177.

[2] J.Guo, G.Li, F.Faria, Y.Cao, R.Wang, J.Verma, X.Gao, A.Ketterson, M.Schuette, P.Saunier, M.Wistey, D.Jena, and H.Xing. MBE-Regrown Ohmics in InAlN HEMTs with a Regrowth Interface Resistance of 0.05 Ω.mm. IEEE ELECTRON DEVICE LETTERS, VOL. 33, NO. 4, APRIL 2012.

Improving the Performance of AlInN/GaN and AlInGaN/GaN HEMTs by Using a Triethylgallium-Grown Channel Layer and Barrier

Indraneel Sanyal[1], Yen-Chang Lee[1], Yu-Chuan Lin[1] and Jen-Inn Chyi[1,2]

[1] *Department of Electrical Engineering, National Central University, Taiwan R.O.C*
[2] *Centre for Applied Sciences, Academia Sinica, Taiwan R.O.C*

$Al_xIn_yGa_{(1-x-y)}N$/GaN heterostructure is gaining increasing popularity for high power millimeter (mm)-wave applications because of its superior electron transport properties. Alloy scattering and interface roughness scattering play a significant role to limit the transport properties of this heterostructure. Ways, such as using an AlN spacer and low temperature growth, have been proposed to overcome the scattering issues. In this work, we carry out a comparative study on the transport properties of $Al_xIn_yGa_{(1-x-y)}N$/GaN high electron mobility transistors (HEMTs) with their GaN channels grown by either triethylgallium (TEG) or trimethylgallium(TMG) precursor using metal-organic chemical vapor deposition (MOCVD).

Hall-effect measurements indicate that by changing TMG to TEG precursor for the channel of AlInN/AlN/GaN HEMTs, the electron mobility increases from 1,740 cm^2/V.s to 1,820 cm^2/V.s, the corresponding 2DEG concentration increases from 1.15×10^{13} cm^{-2} to 1.26×10^{13} cm^{-2} and sheet resistance (R_{sh}) decreases from 312 $\Omega/\square$ to 271 $\Omega/\square$. Replacing the AlInN barrier by a slightly tensile strained 9 nm $Al_{0.73}In_{0.08}Ga_{0.19}N$ barrier, its room temperature electron mobility increases up to 1910 cm^2/V.s with 2DEG concentration of 1.33×10^{13} cm^{-2}, resulting a low R_{sh} of 248 $\Omega/\square$. The electron mobility reaches as high as 13,700 cm^2/V.s with R_{sh} of 34 $\Omega/\square$ at 13K. These results are among the best reported values obtained on AlInGaN HEMTs grown on Si [1]. These improved transport properties are attributed to lower unintentional carbon doping in the TEG-grown GaN channel as evidenced by secondary ion mass spectroscopy (SIMS).

The DC and RF performance of AlInN/AlN/GaN HEMTs reported elsewhere confirms the advantage of using TEG for the GaN channel [2]. These observations are in line with their transport properties and reveal the significance of controlling background impurities and defects in the GaN-based HEMTs. Further study on the dynamic performance by pulsed I_d-V_g measurement shows a positive threshold voltage shift of 26%, 23% and 12% in the TMG AlInN, TEG AlInN and TEG AlInGaN HEMT, respectively, signifying a negative charge trapping under the gate. This implies that trap density in the channel/barrier of these devices is reduced. The significant reduction in trap density in the devices with a quaternary barrier could be attributed to the reduced compositional inhomogeneity and indium segregation.

Reference:

[1] I. Sanyal et al., Photonics West, San Francisco, U.S.A., 2018.
[2] E.-S. Lin et al., Compound semiconductor week, Cambridge, USA, 2018.
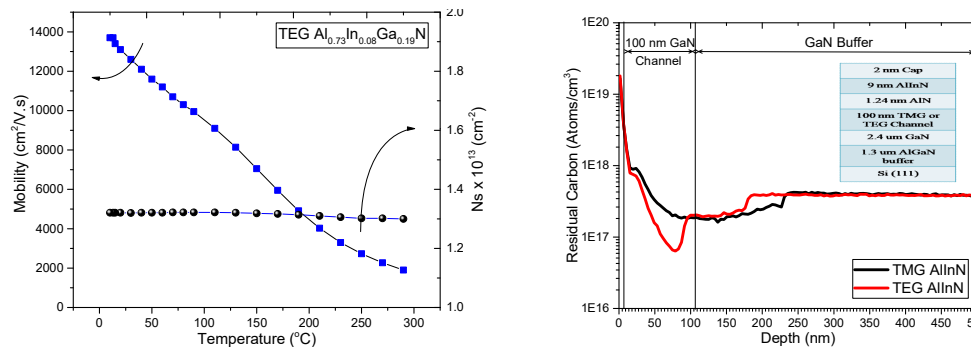
Invited lecture

Characterization of Threading Dislocations in Thick GaN Films Using Multiphoton-Excitation Photoluminescence

Tomoyuki Tanikawa, Kazuki Ohnishi, Tatsuya Fujita and Takashi Matsuoka

Institute for Materials Research, Tohoku University, Katahira 2-1-1, Aoba-ku, Sendai, Japan

III-nitride semiconductors have attracted attention as materials for power devices. In order to suppress undesirable current leakage, the device should include less crystalline defects. The GaN bulk substrate is commercially available, but the substrates has high-density threading dislocations of the order of 10^6 cm^{-2}. The homoepitaxially-grown device also contain high-density threading dislocations. In order to realize high-performance power devices, bulk GaN substrates with low defect density are indispensable. To achieve much less threading dislocations in bulk GaN, it is important to clarify how TDs propagate in the GaN crystal. In this study, multiphoton excitation photoluminescence was proposed as a novel method for characterizing threading dislocations, and three-dimensional imaging of threading dislocations in GaN films was demonstrated [1].

The distribution of threading dislocations in GaN films grown by hydride vapor phase epitaxy was characterized using multiphoton-excitation photoluminescence. Figure 1 shows a schematic illustration of the multiphoton-excitation photoluminescence system. A Ti:Al$_2$O$_3$ laser with a wavelength of 800 nm was used as an excitation source. It was focused on the sample with an objective lens. Photoluminescence occurs at the focal point in the GaN film, which was detected with a photomultiplier tube. A band-pass filter is used to correct the near-band-edge emission of GaN. Three-dimensional photoluminescence images were obtained by scanning the focal point of the laser beam in both directions of the in-plane and the depth.

In the in-plane photoluminescence image, dark spots appeared. Since threading dislocations act as nonradiative centers, photoluminescence intensity decreases around them. A three-dimensional photoluminescence image is shown in Fig. 2. In the three-dimensional photoluminescence image, each dark spots, which are observed in the in-plane image, are connected with each other to form dark lines. By using this method, multiscale characterization of threading dislocations is possible without any destructive sample preparation. In this paper, we will introduce several results obtained using multiphoton-excitation photoluminescence.

[1] T. Tanikawa, K. Ohnishi, M. Kanoh, T. Mukai, and T. Matsuoka, *Appl. Phys. Express* **11**, 031004 (2018).
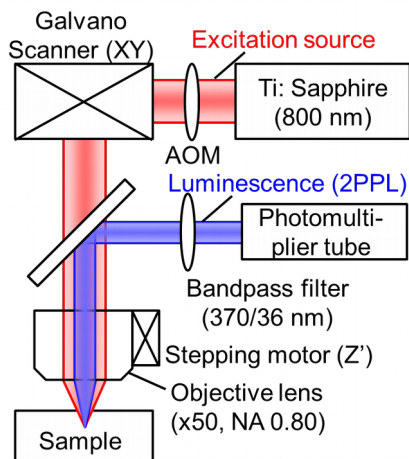
Fig. 1 Schematic illustration of multiphoton-excitation photoluminescence system.
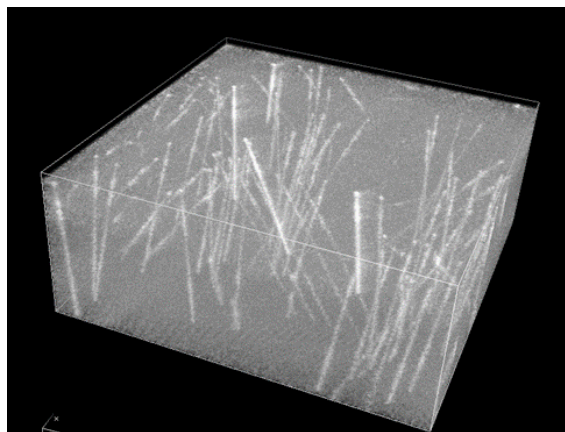
Fig. 2 Three-dimensional image of multiphoton-excitation photoluminescence. The contrast is inverted to visualize dark lines as bright ones.

Invited lecture

Observation of Dislocation Propagation in GaN on GaN Structure with a Multiphoton Excitation Photoluminescence Microscope

A. Tanaka [1,2], K. Nagamatsu [1], S. Usami [3], M. Kushimoto [3], M. Deki [1],
S. Nitta [1], Y. Honda [1] and H. Amano [1,2,4,5]

[1] *Institute of Materials and Systems for Sustainability (IMaSS), Nagoya University, Furo-cho, Chikusa-ku, Nagoya, Japan*
[2] *National Institute for Materials Science (NIMS), Namiki, Tsukuba, Japan*
[3] *Department of Electrical Engineering and Computer Science, Nagoya University, Furo-cho, Chikusa-ku, Nagoya, Japan*
[4] *Akasaki Research Center, Nagoya University, Furo-cho, Chikusa-ku, Nagoya, Japan*
[5] *Venture Business Laboratory, Nagoya University, Furo-cho, Chikusa-ku, Nagoya, Japan*

Recently, gallium nitride (GaN), single-crystal substrates with various growth methods have become available. In this study, with the assumption of vertical-type, high-voltage power devices, dislocation propagation from several GaN substrates to thick GaN epilayers on the substrates was investigated.

N-type GaN (0001) substrates of several fabrication methods Hydride Vapor Phase Epitaxy (HVPE) with a threading dislocation density (TDD) of 10^6 cm^{-2}, sodium flux (Na-flux) with a TDD of 10^4 cm^{-2} and ammonothermal substrate with a TDD of 10^3 cm^{-2} were used for this study. Before epi-layer growth, the TDD of each substrate was confirmed with synchrotron X-ray topography. Then, an undoped GaN epilayer was grown on the substrates by metalorganic vapor phase epitaxy (MOVPE). The epitaxial growth on several substrates was performed simultaneously. The temperature during epitaxial growth was 1100 °C. The thickness of the epilayer was 30 μm. Then, we observed synchrotron X-ray topography again to confirm the TDD. We also investigated dislocation propagation in the samples with a multiphoton excitation photoluminescence microscope (MEPM).

The TDD in the epilayer on HVPE and Na-flux substrates was almost unchanged. However, although it remained low, the TDD changed from 10^3 cm^{-2} in the ammonothermal substrate to 10^4 cm^{-2} in the epilayer on the same substrate. In HVPE, dislocations propagate linearly. In Na-flux, dislocations move laterally at the epi-sub interface (Fig. 1). In the ammonothermal sample, V-shape dislocations are newly generated in the epilayer (Fig. 2). Further detailed investigation found V-shape dislocation is a singular dislocation having Burgers vector of 1a. We will discuss the relationship between the difference of dislocation propagation and lattice constant of each substrate.
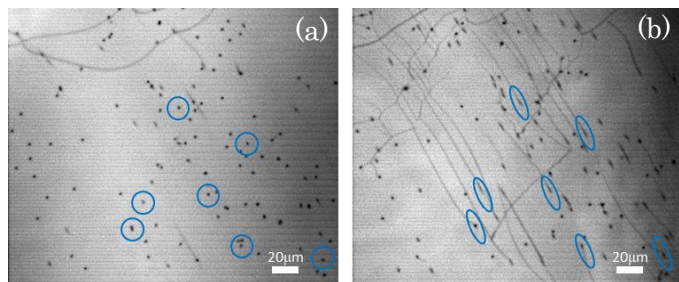
Fig.1 . MEPM image at substrate (a) and at epi-sub interface (b), respectively. Blue circles indicate dislocations that move well.
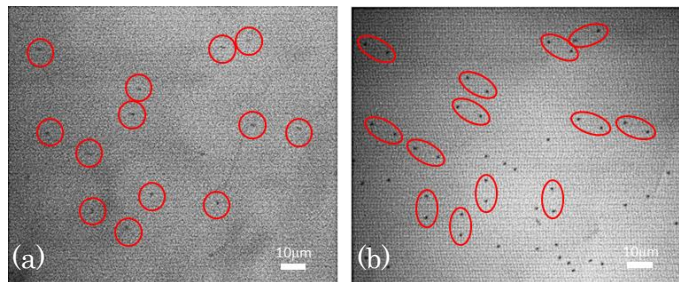
Fig.2 . MEPM image at epi-sub interface (a) and at epilayer (b), respectively. Red circles indicate dislocations that leave each other in a V shape.

Invited lecture

Evaluation of Structural Disorder and In-Gap States of III-V nitrides by Photothermal Deflection Spectroscopy

M. Sumiya [1], K. Fukuda [1,2], Y. Nakano[3], S. Ueda [1], L. Sang [1], H. Iwai [1],
T. Yamaguchi [2], T. Onuma [2], and T. Honda [2]

[1] *National Institute for Materials Science, Tsukuba Ibaraki, 305-0044, Japan*
[2] *Kougakuin Univ., Hachioji, Tokyo 192-0015, Japan*
[3] *Chubu Univ., Kasugai Aichi, 487-8501, Japan*

We use photothermal deflection spectroscopy (PDS) [1] for characterizing both valence band structure and defect states in bandgap in III-V nitrides. When electron excited by monochromatic light recombines, thermal energy can be partially generated. In PDS measurement, this thermal energy deflects the direction of laser probing on sample surface. Detecting the shift of laser spot as a function of incident photon energy, we obtain the spectrum corresponding to the integrated density of state (DOS) of GaN materials as shown in Fig. 1. The PDS detects the tail states, which are also detected by hard x-ray photoemission spectroscopy shown in the inset, corresponding to A1, A2 and A3 (2.6, 2.9 and 3.2 eV) assigned as hydrogenated Ga vacancy (V_{Ga}-H_n) by steady-state photo-capacitance spectroscopy [2].

Advantages of PDS technique are 1) no electrode (need not to care the junction property), 2) coverage of deeper levels (compared with DLTS), and 3) detection of all charge states (positive, neutral and negative) [3]. PDS was applied to evaluating the structural disorder (Urbach energy) and deep-level defects for electronically inactive and no emissive materials like ion-implanted III-V nitrides.

Figure 2 shows the PDS spectra for a SIMS standard sample of Mg ion implanted GaN film (2μm) grown on sapphire substrate. The PDS signal for as-implanted sample decreases gradually towards deep levels from the valence band maximum (VBM) at 3.4 eV. This indicates the large disorder and high defect density in the band-gap. With increase of annealing temperature, Urbach energy (reciprocal slope from the VBM) becomes smaller and defect states in the deep level become lower, indicating that structural disorder is recovered. The value of FWHM value of ω (0002) was independent of the annealing temperature. PDS method can be used for understanding and improving p-type conduction in Mg ion implanted GaN in term of structural disorder and in-gap defect states.
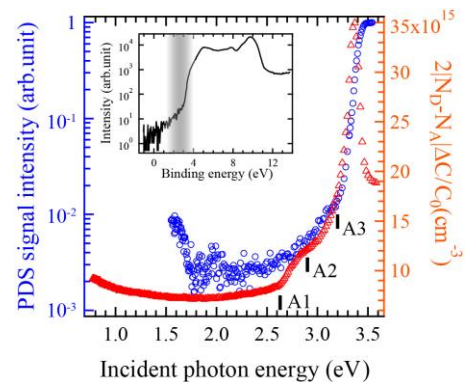
Fig. 1 PDS (blue) and SSPS (red) spectra for MOCVD-GaN film grown on c-sapphire and HVPE-GaN bulk, respectively. The inset shows the valence band spectrum for HVPE-GaN bulk observed by HAX-PES.
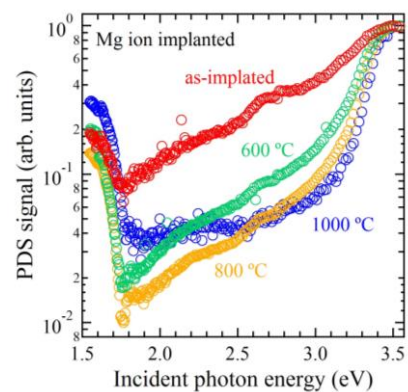
Fig. 2 PDS spectra for Mg ion implanted GaN film annealed at several temperatures. Acceleration voltage, dose quantity and peak concentration was 160 keV, 2.0×10^{14} cm^{-2}, and 1.0×10^{20} cm^{-3} at 100 nm depth, respectively.

[1] M. Sumiy et al., APEX **11**, 021002 (2018). [2] Y. Nakano et al., JVST A **33**, 043002 (2015). [3] Asano et al., PRB **70**, 5025 (1991).

Origin of the Yellow Luminescence in Be-doped GaN revealed by hydrostatic pressure studies

A. Kaminska [1,2], H. Teisseyre[1,3], J. L. Lyons[4], D. Jarosz,[1] M. Boćkowski[3], A. Suchocki[1] and C. G. Van de Walle[5]

[1] *Institute of Physics, Polish Academy of Sciences, Aleja Lotnikow 32/46, PL-02-668 Warsaw, Poland*

[2] *Cardinal Stefan Wyszynski University, College of Science, Department of Mathematics and Natural Sciences, Dewajtis 5, 01-815 Warsaw, Poland*

[3] *Institute of High Pressure Physics, Polish Academy of Sciences, Sokolowska 29/37, 01-142 Warsaw, Poland*

[4] *Center for Computational Materials Science, Naval Research Laboratory, Washington, DC 20375, USA*

[5] *Materials Department, University of California, Santa Barbara, CA 93106-5050 USA*

Before realization of the p-type doping in gallium nitride by using magnesium, beryllium had been taken into account as a natural candidate for such doping. However, so far no one was able to realize p-type conductivity in such way. On the one hand, hybrid density functional calculations [1] have shown that Be is a deeper acceptor (550 meV ionization energy) than Mg (260 meV ionization energy), and that this is the fundamental reason why Be p-type doping is ineffective. On the other hand it has been also suggested that with increasing doping level most of the beryllium is incorporated into the crystal in the interstitial position. In such position beryllium acts as a donor not as an acceptor [2]. Another model proposes that the nitrogen vacancies are responsible for self-compensations mechanism in doped gallium nitride [3].

It is well known that GaN:Be possesses two luminescence bands; one at 3.38 eV and a second near 2.2 eV at an energy that is close to that of the parasitic yellow luminescence often existing in undoped GaN crystals. In order to shed more light on this issue, we performed high hydrostatic pressure studies of bulk, Be-doped gallium nitride crystals using the diamond anvil cell technique. We observed a splitting of the yellow luminescence line under hydrostatic pressure into two components, one which is strongly dependent on applied pressure and another whose pressure dependence is more modest. Together with hybrid functional calculations, we attribute the strongly-varying component to the beryllium-oxygen complex. The second component of the yellow luminescence possesses very similar pressure behavior to the yellow luminescence observed in undoped samples grown by the same method, behavior which we find consistent with the C_N acceptor. At higher pressure, we observe the vanishing of yellow luminescence and a rapid increase in luminescence intensity of the UV line. We explain this as the pressure-induced transformation of the Be-O complex from a highly localized state with large lattice relaxation to a delocalized state with limited lattice relaxation, also observed in positron annihilation experiment as a function of temperature [4].

[1] J. L. Lyons, A. Janotti and C. G. Van de Walle, *Jpn. J. Appl. Phys.* **52**, 08JJ04-1-5 (2013).

[2] J. Neugebauer and C. G. Van de Walle, *J. Appl. Phys.* **85**, 3003-3005 (1999).

[3] J. Buckeridge, C. R. A. Catlow, D. O. Scanlon, T.W. Keal, P. Sherwood, M. Miskufova, A. Walsh, S. M. Woodley and A. A. Sokol, *Phys. Rev. Lett.* **114**, 016405-1-5 (2015)**.**

[4] F. Tuomisto, V. Prozheeva, I. Makkonen, T. H. Myers, M. Bockowski and H. Teisseyre, *Phys. Rev. Lett.* **119**, 196404-1-5 (2017).

Imaging of Surface Plasmon Polaritons of 2D Plasmons of InN Nanostructures having Surface Electron Accumulation

K. K. Madapu and S. K. Dhara

Surface and Nanoscience Division, Indira Gandhi Centre for Atomic Research, Homi Bhabha National Institute, Kalpakkam-603102, India

InN belongs to the III–nitride family and it has the unique property of possessing the surface electron accumulation (SEA). The carriers in the SEA are quantized and provide a two-dimensional electron gas (2DEG) along the surface [1]. Recently 2D plasmons, especially graphene, have generated a lot of curiosity because of its terahertz (THz) resonance frequency [2]. In this context, the frequency of the 2D plasmons of InN falls in the technologically important THz spectral regime (0.5 THz $\leq f \leq 5$ THz). InN also has the advantage of providing a spontaneous 2D electron system from the bulk material.

InN structures were grown using the atmospheric chemical vapour deposition technique via a self-seeded catalytic approach. The nucleation barrier of InN is overcome by self-seeded In nanoparticles [3]. The SEA is confirmed by Raman spectroscopic studies which are further corroborated by photoluminescence and photoelectron emission spectroscopic studies. The sheet carrier density of the SEA is varied using the growth temperature.
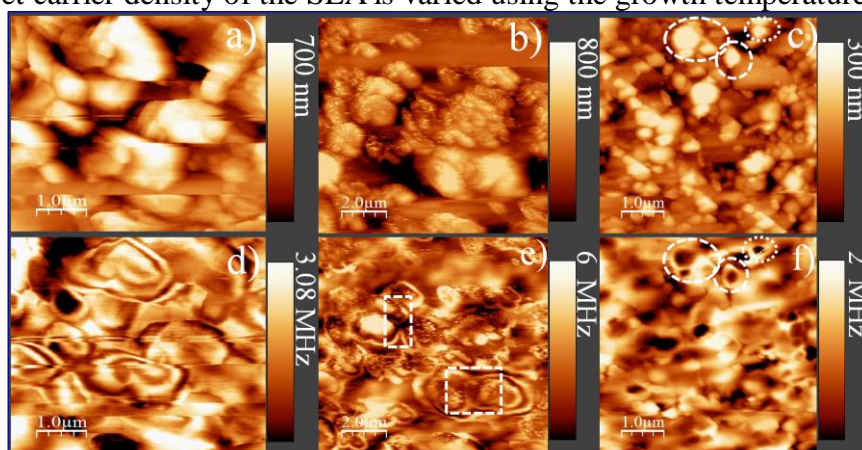
Figure 1. Topography (a, b, c) and corresponding NSOM images (d, e, f), respectively. NSOM images show periodic fringes (d), interferences of SPPs (shown by dashed rectangles) (e) and resonance enhancement (shown by dashed ellipses) (f) around the nanostructures.

Real space mapping of the surface plasmon fields of InN nanostructures is carried out using near-field scanning optical microscopy (NSOM) technique. The measurements were carried out with an aperture probe of size 100 nm. The periodic fringes (Fig. 1d) are observed in the NSOM images of InN nanostructures. The observed fringes are attributed to the interference of propagated and back reflected surface plasmon polaritons (SPPs). The observation of SPPs is solely attributed to the 2DEG corresponding to the SEA of InN. The wavelength of SPPs is estimated to be in the range of 274-500 nm. The destructive interference between the SPPs is further corroborated the wave nature of the observed fringes (Fig. 1e). A resonance kind of behavior with the intensity enhancement is observed for the nanostructures with size less than the SPP wavelength (Fig. 1f). Observation of SPPs indicates that InN with SEA can be a promising THz plasmonic material for the light confinement.

[1] C. G. Van de Wallea, and D. Segev, *J. Appl. Phys.* **101**, 081704 (2007).
[2] A. N. Grigorenko, M. Polini, and K. S. Novoselov, *Nat. Photonics* **6**, 749 (2012).
[3] K. K. Madapu, S. R. Polaki, and S. Dhara, *Phys. Chem. Chem. Phys.* **18**, 18584 (2016).

Invited lecture

Navy Application of Wide Bandgap (WBG) semiconductors enabling future Power and Energy Systems

Travis J. Anderson [1]**, Lynn Petersen** [2]

[1] *U.S. Naval Research Laboratory, 4555 Overlook Ave SW, Washington, DC USA*
[2] *Office of Naval Research, 875 N Randolph St, Arlington, VA USA*

Wide Bandgap (WBG) power devices switching greater than 100kHz enable new benchmarks in power converter performance. These converters will enable power systems where all the sources and loads are connected by converters. These new systems are multifunctional and highly-integrated. However, their realization requires research in areas such as: advanced power electronic control across many converters, concepts for distributed storage, and active filtering across many converters.

Invited lecture

Vertical Power Devices Enabled by Bulk GaN Substrates

Travis J. Anderson[1], Lunet E. Luna [1], James C. Gallagher[1], Jennifer K. Hite[1], Alan G. Jacobs[1], Boris N. Feigelson[1], Karl D. Hobart[1], and Fritz J. Kub[1]

[1] *U.S. Naval Research Laboratory, 4555 Overlook Ave SW, Washington, DC USA*

GaN is an ideal material for power applications due to its high breakdown field, high switching speed, and low switching losses. Current GaN power electronics tend to be based on the successful lateral HEMT design. The usage of the 2-dimensional electron gas (2DEG) as the channel in the device provides for high mobilities with a significant reduction in ionized impurity scattering. However, the blocking voltage in this lateral device is held between the source and drain, requiring large footprints for high power devices. In a vertical transistor the blocking voltage is sustained across the drift region into the main bulk of the chip, thus making the final device footprint significantly smaller for comparable performance. Vertical GaN p-n diodes and transistors, such as the current aperture vertical electron transistor (CAVET) and trench MOSFET devices have been demonstrated through epitaxial growth of n-p-n structures, but this process requires multiple masking and regrowth steps that leads to impurity incorporation and poor regrowth interfaces, which can degrade device performance. In many other semiconductor materials such as Si and SiC, ion implantation is a routine step in most processing sequences for selective area doping and greatly facilitates manufacturing by avoiding the complicated etch/regrowth process. The ability to implant and activate dopants, particularly p-type dopants, in GaN still remains a challenge though. The NRL-developed symmetric multicycle rapid thermal annealing (SMTRA) technique has been shown to activate up to ~10% of the implanted Mg dopant atoms using a combination of a temporary thermally stable capping layer, annealing in a nitrogen overpressure, and performing a well-optimized annealing temperature profile including multiple spike anneals. This talk will address a fundamental assessment of the impact of the capping/annealing process on material and electrical properties of GaN, address basic vertical devices such as vertical GaN junction barrier Schottky (JBS) diodes and Schottky barrier diodes (SBDs) with implanted junction termination extension (JTE) using the SMRTA process, and identify process module development toward trench MOSFET devices.

Characterizations of high-temperature Mg ion implantation in GaN

M. Takahashi[1], K. Sone[1], A. Tanaka[2,3], S. Usami[1], Y. Ando[1],
M. Deki[2], M. Kushimoto[1], S. Nitta[2], Y. Honda[2], and H. Amano[2,4,5]

[1] *Dept. of Electronics, Nagoya Univ, Furo-cho, Chikusa-ku, Nagoya, 464-8603, JAPAN,*
[2] *Nagoya Univ. IMaSS, Furo-cho, Chikusa-ku, Nagoya, 464-8603, JAPAN,*
[3] *NIMS, 1-2-1 Sengen, Tsukuba, Ibaraki 305-0047, JAPAN*
[4] *Nagoya Univ. Akasaki Research Center, Furo-cho, Chikusa-ku, Nagoya, 464-8603, JAPAN,*
[5] *Nagoya Univ. VBL, Furo-cho, Chikusa-ku, Nagoya, 464-8603, JAPAN*

GaN is expected to be useful for next-generation power devices. Ion implantation is required for selective area doping in GaN. However, the use of ion implantation to control p-type conductivity in GaN has not yet been established due to the defects generated during ion implantation and the difficulty of activating the implanted Mg ions. It has been reported that vacancy-type defects decrease when annealing is performed at higher temperatures [1]. We hypothesize that this may also be true for ion implantation, and we have therefore investigated Mg ion implantation at higher temperatures.

We first grew a 5-μm undoped GaN epilayer using metal-organic vapor phase epitaxy on the c-plane of an n-type GaN substrate. We then deposited a 40-nm layer of SiN on samples using plasma-enhanced chemical vapor deposition (PECVD). We subsequently implanted Mg ions with energies of 40 keV and 100 keV into the samples at room temperature (RT), 800 °C, 900 °C, and 1000 °C. We designed a box profile with the Mg concentration of about 1×10^{19} cm^{-3} and the Mg implantation depth of about 100 nm. After the ion implantation, we deposited a 40-nm SiN cap layer on the samples using PECVD. The samples with the SiN cap layers were annealed by rapid thermal annealing. The annealing was performed at 1250 °C for 20 s in nitrogen gas.

Fig. 1 shows the low-temperature (77 K) PL spectrums of the Mg-implanted GaN samples after annealing. The near-band-edge (NBE) at 3.47 eV (Several luminescence seems to be mixed) indicates good crystallinity and the donor-acceptor pair (DAP) at 3.28 eV shows that the Mg ions act as acceptors. The NBE and DAP were observed in both samples but were stronger for the samples that were implanted at 1000 °C. Fig. 2 shows the current-voltage (*I-V*) characteristics of vertical p-n diodes fabricated from the implanted samples. Rectification was not seen for the Mg-implanted GaN at RT. However, clear rectifying properties were observed for GaN with Mg implanted at 1000 °C. The *I-V* characteristics of the latter sample exhibit steps that can be interpreted as space-charge-limited currents. We conclude that Mg ion implantation performed at ≥1000 °C is better for producing p-type conductivity in GaN. In this presentation, we will also report other evaluations of this technique.
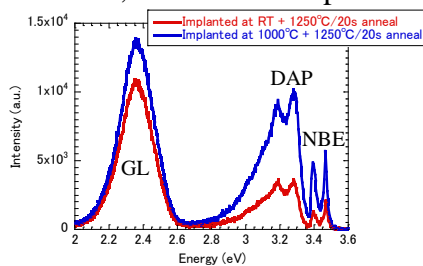
Fig. 1. Low-temperature (77 K) PL spectrums   Fig. 2. *I–V* characteristics of p–n diodes
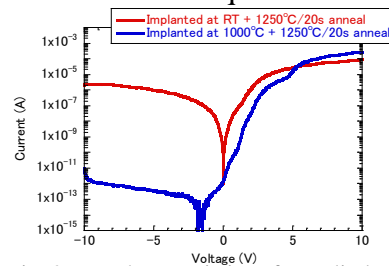
[1] A. Uedono *et al.*, Phys. Status Solidi B **252**, No. 12, 2794–2801 (2015)

Non-cap thermal activation process of Mg-ion implanted Ga-polar GaN using ultra high pressure N₂ annealing

H. Sakurai [1,2,3] , S. Yamada[1,2,3], M. Omori[1], Y. Furukawa[3], H. Suzuki[3], M. Boćkowski[1,4], J. Suda[1,2] and T. Kachi[1]

[1]*IMaSS, Nagoya University, Aichi 464-8603, Japan*
[2]*Dept. of Electronics, Grad. School of Engineering, Nagoya Univ., Aichi 464-8603, Japan*
[3]*ISET, ULVAC, Inc., Chigasaki, Kanagawa 253-8543, Japan*
[4] *Institute of High Pressure Physics Polish Academy of Sciences, 01-142 Warsaw, Poland*

For the realization of GaN power devices, ion implantation technique and annealing for carrier activation and crystal quality recovery technique to enable impurity doping into selected regions are one of important researches. Because these techniques make it possible to increase a degree of power device design, for example, can form region of p^+/n^+-contact layer, body-layer, edge termination more easily. However, Mg-ion implantation into GaN as p-type doping technique has in particularly difficult research challenges. Because it has two major research issues. The one is that some crystal defects are introduced by Mg-ion implantation process itself. The other is that pyrolysis reaction occurs on GaN surface during high temperature annealing process. That is, high carrier activation and crystal recovery require high temperature, but instead GaN surface flatness deteriorated.

To solve these research problems, we conducted research on thermal activation process of Mg-ion implanted Ga-polar GaN without protection cap layer by use of high pressure N₂ annealing. We consider that the deteriorated GaN surface during annealing process will be inhibited by using ultra high N₂ pressure annealing to maintain equilibrium condition at high temperature.

The Mg-ion implanted GaN layers with 300-nm-depth box profile of 1×10^{19} cm^{-3} on n-GaN (Si:2×10^{16}cm^{-3}) grown on a GaN substrate were used as sample. And non-capped GaN samples were annealed in 1 GPa N₂ atmosphere. The annealing temperature was from 1300 to above 1400 °C.

The low-temperature cathodoluminescence (CL) results after activation annealing comparing the conventional lamp-annealing and the high pressure N₂ annealing are shown in Fig. 1. Here, the intensity of lamp-annealing was multiplied by 20 times. It is clear from these spectra, in the lamp-annealing, the Green Luminescence (GL) as emission from vacancy defect is more dominant than Donor-Acceptor-Pair (DAP) emission, whereas in high pressure N₂ annealing, the DAP emission intensity is markedly increased. We consider that the non-radiative recombination in p-GaN layer was reduced by high pressure N₂ annealing. And the AFM images after activation annealing comparison are shown in Fig. 2. The high pressure N₂ annealed GaN surface was very smooth. Therefore we found out that carrier activation and crystal quality recovery and surface smoothness could be carried out by using high pressure N₂ annealing. The details will be discussed at the conference.
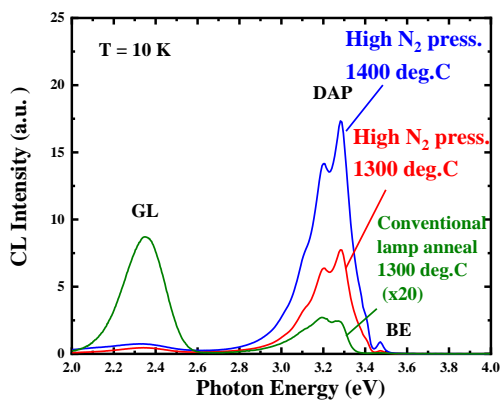
Fig.1   Low-temperature CL spectra
Ramp anneal vs. High N₂ press. anneal
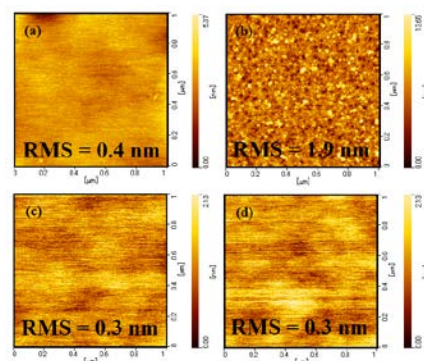
Fig.2 AFM images of p-GaN surface
(a)As Mg-implanted
(b) Conventional lamp-annealed (After removing cap layer)
(c) high N2 press. at 1300 deg.C (d) high N2 press. at 1400 deg.C

Improvement of Electrical Stability of ALD-Al$_2$O$_3$/GaN Interface by UV/O$_3$ Oxidation and Postdeposition Annealing

M. Deki[1], K. Sone[2], K. Watanabe[2], F. Miura[2], K. Nagamatsu[1], A. Tanaka[1,3], M. Kushimoto[2], S. Nitta[1], Y. Honda[1], and H. Amano[1,2,4,5]

[1] *Inst. of Materials and Systems for Sustainability, Nagoya University, Nagoya, Japan*
[2] *Dept. of Electrical Engineering and Computer Science, Nagoya University, Nagoya, Japan*
[3] *National Institute for Materials Science, Namiki, Tsukuba, Japan*
[4] *Akasaki Research Center, Nagoya University, Nagoya, Japan*
[5] *Venture Business Laboratory, Nagoya University, Nagoya, Japan*

Owing to its high breakdown electric field and high electron saturation velocity, GaN is ideal for devices requiring high-power and high-speed operation. To realize normally-off vertical GaN MOSFETs for power conversion, the deposition of insulator films with high reliability and low interface state density (D_{it}) is required. Recently, it has been reported that thin ε-Ga$_2$O$_3$ layer in the SiO$_2$/GaN interface decreases D_{it} in GaN-MOS devices [1]. However, in high temperature processes, it has problem that gallium can diffuse into SiO$_2$ layer. In this study, we investigated the effects of UV/O$_3$ oxidation and post deposition annealing (PDA) in the GaN-MOS structure to improve of D_{it} in Al$_2$O$_3$/GaN interface.

MOS capacitors were fabricated on n-type GaN epitaxial layers, which were grown on n-type c-plane GaN substrates using MOCVD. The thickness of epitaxial layer was 5 microns. The effective donor concentration of epitaxial layers was determined to be 2×10^{16} cm^{-3} from the C-V characteristics. GaN surface was exposed with UV light for 5 min in O$_3$ ambient. The wavelengths of UV light were 184.9 and 253.7 nm. After UV/O$_3$ oxidation, Al$_2$O$_3$ was deposited by atomic layer deposition (ALD) at 350 °C for the gate insulator. The thickness of Al$_2$O$_3$ was 60 nm from the accumulation condition of the C-V characteristics. To evaluate the effect of postdeposition annealing (PDA), sample was annealed in 400°C for 60 min in N$_2$ ambient. After the fabrication of the gate and back electrode, D_{it} was estimated using the Hi-Lo method at 300 K.

Figure 1 shows the 1 MHz C-V characteristics and ideal curve of GaN-MOS capacitors after UV/O$_3$ oxidation. Hysteresis was also indicated in fig.1. From the resulting C-V characteristics, there was a large flat-band voltage shift (ΔV_{FB}) to negative bias direction in as-oxidized samples. This result indicated that positive fixed charges exist in Al$_2$O$_3$/GaN interface. On the other hands, there was a decrease in the hysteresis and ΔV_{FB} of 400°C annealed samples. From the XPS measurements, since O1s peak of 400°C annealed samples increased compared with as-oxidized samples, it is considered that oxygen defects in GaO$_x$ were reduced by PDA. In addition, D_{it} of 400°C annealed samples became range of 10^{10} cm^{-2}eV^{-1} using the Hi-Lo method.

Fig.1 C-V characteristics of GaN-MOS capacitors after UV/O$_3$ oxidation

We conclude that UV/O$_3$ oxidation and 400°C PDA can lead to ALD-Al$_2$O$_3$/GaO$_x$/GaN interface structure with low D_{it}.

References [1] K. Mitsuishi *et al.,* JJAP, **56**, 110312 (2017)

Fabrication and characterization of GaN-nanowires optoelectronic devices

M. Takebayashi [1], N. Sone [1], A. Suzuki [1], K. Nokimura [1], K. Sasai [1], S. Kamiyama [1], T. Takeuchi [1], M. Iwaya [1], I. Akasaki [1, 2]

[1] *Meijo Univ., 1-501, Shiogamaguchi, Tempaku-ku, Nagoya, Japan*
[2] *Akasaki Research Center, Nagoya Univ., Furou-cho, Chikusa-ku, Nagoya, Japan*

Recently, epitaxial growth of GaN nanowires (NWs) and multi-quantum shell (MQS) active materials have attracted much attention for new optoelectronic device applications such as light-emitting diodes (LEDs) and laser diodes (LDs). Our group aims to achieve novel optoelectronic device using MQS structure. However, there have been few reports focusing on the details of processing of device fabrication. In this paper, we report on optimization of processing condition to suppress current leakage and to improve optical properties of the MQS-device.

Before the device fabrication, the NWs including n-GaN NWs, GaInN/GaN MQSs (three pairs with the thicknesses of 3 nm and 3.5 nm) and p-GaN shells were grown at the 200 nm-diameter openings of SiO_2 mask deposited on AlGaN template by metalorganic chemical vapor deposition (MOCVD). In MQS-devices, simultaneous formation of growth area of the NWs (active area) and non-growth area (electrode area) are required. We adopted the "top-down approach", which is based on the etching method to remove the NWs selectively at the electrode area, while the NWs at the active area are protected. To protect the active area, photoresist with a thickness of approximately 2 µm was spin-coated. After spin-coating, the NWs at the whole area were planarized by photoresist. Then, ICP etching was carried out. At the electrode area, small etching rate difference between the NWs and photoresist provided almost flat etching surface, and the n-AlGaN surface with a small roughness could be obtained as shown in Fig 1.

Next, spin-on-grass (SOG) material was coated to prevent from current leakage of bottom of the NWs. Then SOG was etched to expose the side wall of the NWs as shown in Fig 2. As a result, the leakage of this MQS-device could be suppressed and operation was confirmed as shown in Fig 3.

At the presentation, we will report on the details of experimental method and the results of the arrangement technique of the NWs, as well as optical properties of the MQS-device fabricated by this technique.
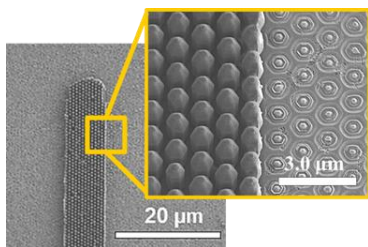
Fig 1 Formation of growth area of the NWs and non-growth area
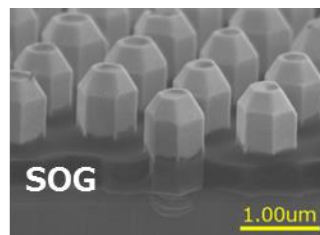
Fig 2 Spin-coated SOG to prevent from current leakage
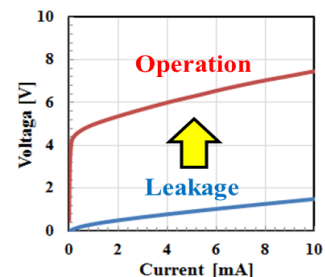
Fig 3 V-I characteristic of MQS-device

Optical simulation of GaInN-based multi-quantum-shell (MQS)-Light-Emitting-Diodes (LEDs)

Mizuki Terazawa [1], Masaki Ohya[1], Satoshi Kamiyama[1],Tetsuya Takeuchi[1],
Motoaki Iwaya[1] and Isamu Akasaki[1,2]

[1] *Meijo Univ., 501 Icchoume, Shiogamaguchi, Tenpaku-ku, Nagoya-shi, Aichi, Japan*
[2] *Akasaki Research Center, Nagoya Univ., Furou-cho, Chikusa-ku, Nagoya-shi, Aichi, Japan*

Since nitride MQS and nanowire (NW)-based LEDs have 3D active regions, the volume of the active region is larger than that of conventional planar LEDs and excellent optical properties are expected. The light extraction efficiency (LEE) of the MQS/NW-LED may be greatly dependent on the structural parameters. However, optical simulation tools for such complex structures are not available at this moment. Therefore, in this paper, we propose a new simulation method composed of finite-difference time-domain (FDTD) method, rigorous coupled-wave analysis (RCWA) method and ray tracing method (RTM), and apply it to the calculation of the optical properties of MQS-LEDs.

As a first step, we calculated the radiation characteristics per MQS pillar by the FDTD method and obtained light source data of MQS-LED. Next, distribution of transmittance/ reflectance data in periodically placed MQS active regions were acquired by RCWA method. Finally, we created a 3D model by the RTM tool, using the light source data from the FDTD method and distribution of transmittance/reflectance data from the RCWA method, and obtained the LEE of MQS-LED. The simulation model of the MQS-LED in this study is shown in Fig 1.

Figure 2 shows the calculated results of the LEE as a function of the diameter of n-GaN-NW. The pitch of the MQS active regions was varied from 800 to 1700 nm. According to calculated results, the LEE was improved as the NW diameter became smaller. We thought that this improvement may be because of the decreased volume of the absorption materials such as ITO. In the current calculation model, the pitch of 1200 nm gives the minimum LEE. The discussions regarding the structural parameter dependence of the LEE will be made in the presentation.
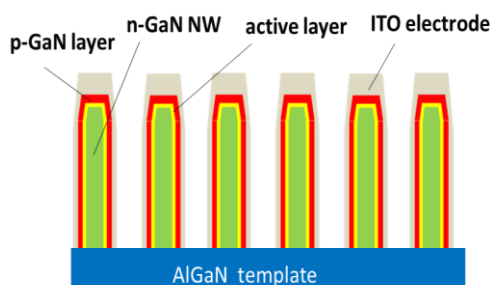
Fig.1   Simulation Model
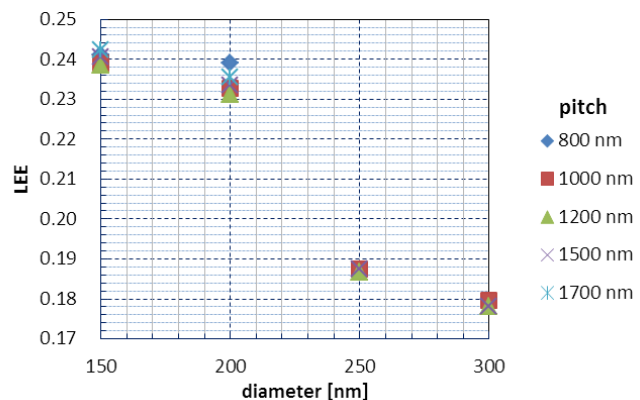
Fig.2   Structural dependence of the LEE

Self-Induced InGaN Nanowires with a Controlled Indium Composition and Selective Area Growth of InN by HVPE

G. Avit [1], M. Zeghouane [1], Y. André [1,5], C. Bougerol [2,3], E. Gil [1,5], D. Castelucci [1], P. Ferret [4], E. Roche [1], J. Leymarie [1], F. Médard [1], V. G. Dubrovskii [5], and A. Trassoudaine [1]

[1] *Université Clermont Auvergne, CNRS SIGMA Clermont, Institut Pascal, F-63000 Clermont-Ferrand, France*
[2] *Université Grenoble Alpes, F-38000 Grenoble, France*
[3] *CNRS, Institut Néel, F-38042 Grenoble, France*
[4] *CEA LETI, Département Optique et Photonique, F-38000 Grenoble, France*
[5] *ITMO University, Kronverkskiy prospekt 49, 197101, St Petersburg, Russia*

In(Ga)N material is promising for high performance optoelectronic devices due to its tunable bandgap from IR to UV by varying the indium mole fraction in the alloy. However, the growth of InGaN with high indium concentration is still challenging. This could be overcome thanks to the nanowire geometry that enables the growth of indium-rich In(Ga)N material with a low density of defects on different substrates.

In this context, we show that hydride vapour phase epitaxy (HVPE) has unique features regarding the growth of InGaN nanowires. The full range of indium composition is achieved by controlling the input partial pressures of group-III elements ($InCl_3$ and $GaCl$) and the growth temperature. X-Rays diffraction and high resolution transmission electron microscopy are used to determine the composition and the crystalline structure of the nanowires. It shows that nanowires with an homogeneous In concentration higher than 70% are nearly defect-free. Photoluminescence measurements are performed to probe the optical properties of the nanowires. Energy dispersive spectroscopy profiles on single InGaN nanowires do not reveal In segregation.

The experimental results are supported by a model which attributes the wide compositional range of InGaN nanowires within the bulk miscibility gap to a purely kinetic growth regime without macroscopic nucleation.

Thanks to the use of chloride precursors, selective area growth (SAG) of InN nanowires is also achieved. Optical and structural characterizations are discussed. First results concerning SAG-HVPE of InGaN are presented.

These findings provide a convenient method to grow homogenous In(Ga)N nanowires and could stretch further the performances of optoelectronic devices.
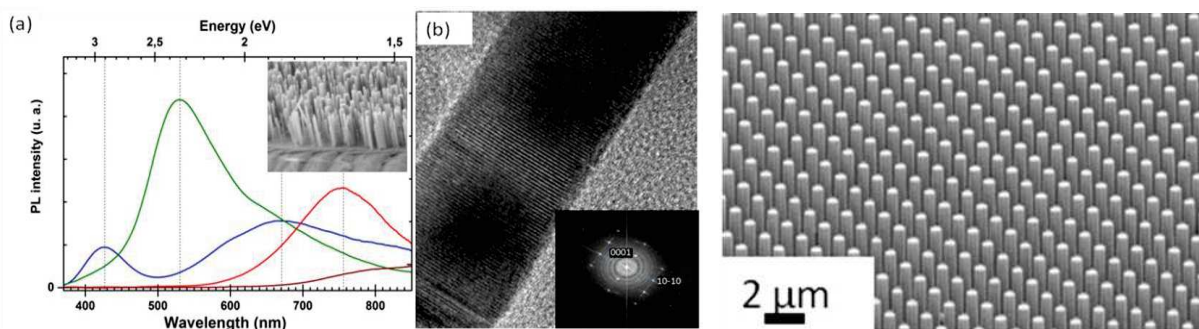
Figure 1. (a) Photoluminescence spectra of self-assembled InGaN nanowires of different compositions. (b) High resoluton TEM showing a nearly defect-free crystal stucture for an In concentration of 70%.

Figure 2. InN nanowires grown by SAG-HVPE on a masked SiN/GaN/c-sapphire substrate.

Study on emission wavelength control of GaInN multi-quantum-shell/GaN nanowire

Nanami Goto[1], Kohei Sasai[1], Kazuyoshi Iida[1], Naoki Sone[1], Atushi Suzuki[1], Kyohei Nokimura[1], Minoru Takebayashi[1], Hideki Murakami[1], Mizuki Terazawa[1], Satoshi Kamiyama[1], Tetsuya Takeuchi[1], Motoaki Iwaya[1] and Isamu Akasaki[1,2]

[1] *Meijo Univ., 501 Icchoume, Shiogamaguchi, Tenpaku-ku, Nagoya-shi, Aichi, Japan*
[2] *Akasaki Research Center, Nagoya Univ., Furou-cho, Chikusa-ku, Nagoya-shi, Aichi, Japan*

A structure composed of GaInN multi-quantum-shell (MQS) and GaN nanowire is promising active material for high performance optical devices. However, due to the tiny structures of MQS/nanowires, there is a concern that growth rate and a composition uniformity may be much differ from those of 2D-layers. It is necessary to study the method for controlling of the emission wavelength in MQS. In this study, we report the result of controlling the emission wavelength by changing growth condition of GaInN/GaN-MQS.

Before the growth of MQS, the n-GaN nanowires were grown on an $Al_{0.03}Ga0._{97}N$ template at 1,030 °C through the 30 nm-thick SiO_2 mask with 200 nm-diameter openings by the pulsed-mode MOVPE technique. The diameter and height of the nanowires are 230 nm and 1.5 μm, respectively. After that, growth of MQS was performed by the continuous-mode MOVPE at 700 °C. In the series of the growth of MQS samples, the flow rates of TMIn and TEGa were the growth parameters to control the emission wavelength of the MQS. The optical properties of the samples were characterized by cathode luminescence (CL).

Figure 1 shows the peak wavelength of the CL spectra as a function of In gas-phase ratio. To change the In gas-phase ratio, TMIn flow rate variation (closed circles) and TEGa flow rate variation (closed triangles) were examined. When the TMIn flow rate was increased, the peak wavelength was simply moved to longer wavelength. On the contrary, the change of the TEGa flow rate showed the unique behavior. When the In gas-phase is 84.4 %, the peak wavelength is shortest in this series. And both it is higher and lower than 84.4 %, the wavelength is moved to longer side, due to influence of growth rate variation. From CL image shown in Fig. 2, highest and uniform emission is obtained, when the In gas-phase ration is 89.4 %. The lower growth rate may improve the quality of MQS.
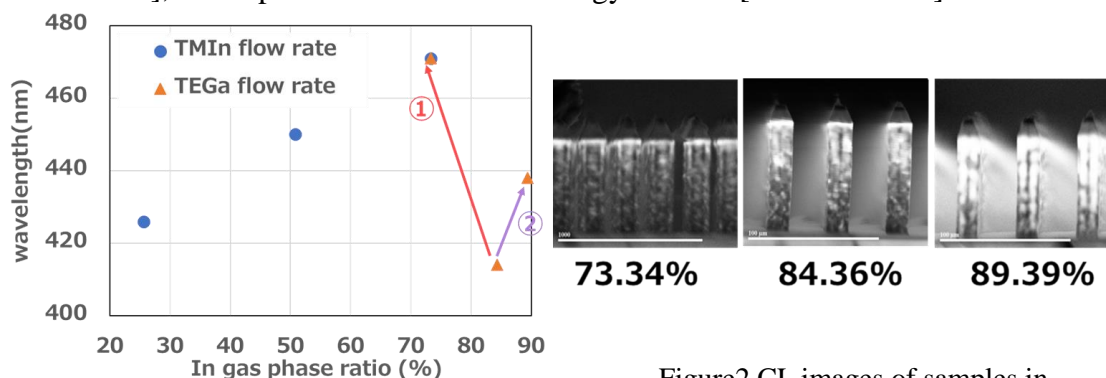
Figure1 Peak wavelength of MQS samples as a function of In gas-phase ratio.

Figure2 CL images of samples in TEGa flow rate variation.

Device fabrication of GaInN-based multi-quantum-shell LEDs

A. Suzuki [1], H.Murakami[1] , K. Nokimura [1] , M. Takebayashi [1], K. Sasai [1], N.Goto [1],
N. Sone [1] , S. Kamiyama [1], T. Takeuchi [1], M. Iwaya [1], I. Akasaki [1, 2]

[1] *Meijo Univ., 1-501, Shiogamaguchi, Tenpaku-ku, Nagoya, Japan*
[2] *Akasaki Research Center, Nagoya Univ., Furou-cho, Chikusa-ku, Nagoya, Japan*

Three-dimensional active material composed of GaN nanowires (NWs) and multi-quantum shell (MQS) are expected to have superior internal quantum efficiency (IQE) even with a high InN molar fraction in MQS, compared with conventional planer devices. Although the preliminary operation of MQS-LEDs were reported by several groups [1,2], detailed device fabrication procedures and quantitative discussions of their performance have not been presented so far. Therefore, in this paper, the fabrication technique and device characteristics of the MQS-LEDs are reported.

Before the device fabrication, the MQS-LED structure including n-GaN NWs, GaInN/GaN MQSs (three pairs) and p-GaN shells were grown at the 200 nm-diameter openings of SiO_2 mask deposited on n-AlGaN template by metalorganic chemical vapor deposition (MOCVD). A transparent electrode, made of In-Tin-Oxide (ITO) deposited by sputtering, was formed after epitaxial growth. Figure 1 shows schematic diagram of the MQS-LED. A photograph of operating MQS-LED is shown in the inset of Fig.1

The EL and PL spectra of the MQS-LED are shown in Fig. 2. The emission peak of the GaInN/GaN-MQS in EL spectrum is observed at around 460nm. On the other hand, PL spectra includes not only the MQS emission but also longer wavelength component (generally known as the yellow luminescence) is involved. By comparison with the EL spectrum, this yellow emission is not from the MQS, but is caused by nitrogen vacancies in n-GaN NWs. In the presentation, detailed device fabrication procedures and device characters will be given.

References
[1] J. Ristić, E. Calleja, M. A. Sánchez-García, J. M. Ulloa, J. Sánchez-Páramo, J. Calleja, U. Jahn, A. Trampert, and K. H. Ploog: Phys. Rev. B, 68 (2003) 125305.
[2] 20)   F. Qian, S. Gradecˇak, Y. Li, C.-Y. Wen, and C. M. Lieber: Nano Lett. 5 (2005) 2287.
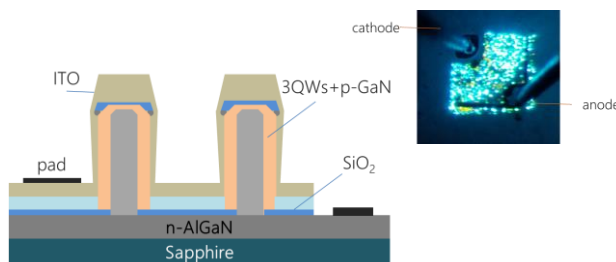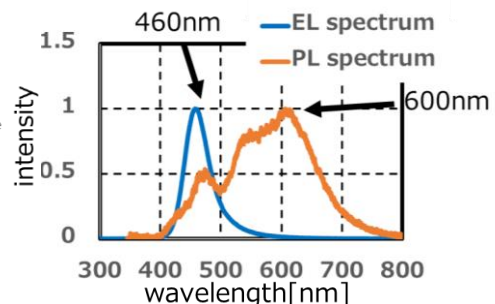
Fig 1. A schematic diagram of MQS-LED.

Fig 2. EL & PL spectra of MQS-LED.

Green/Yellow/Red Emission From *m*-plane Core-shell InGaN/GaN Nanowires

A. Kapoor[1], N. Guan[2], L. Mancini[2], C. Bougerol[1, 4], F. H. Julien[2], J.P. Barnes[5], M. Tchernycheva[2], C. Durand[1] and J. Eymery[3]

[1] *Univ. Grenoble Alpes, CEA, INAC-PHELIQS, 38000 Grenoble, France*
[2] *Center of Nanoscience and Nanotechnologies (C2N), UMR 9001 CNRS, Paris, France*
[3] *Univ. Grenoble Alpes, CEA, INAC-MEM, 38000 Grenoble, France*
[4] *Univ. Grenoble Alpes, CNRS, Institut Néel, 38000 Grenoble, France*
[5] *Univ. Grenoble Alpes, CEA, LETI, DTSI, SCMC, F-38000 Grenoble, France.*

The realization of efficient LEDs using core-shell m-plane InGaN/GaN nanowires has been mainly demonstrated for the blue emission [1,2]. Green and other longer wavelength emissions still remain a challenge for this core-shell geometry due to a lower In incorporation on the *m*-plane with respect to the *c*-plane [3]. This work demonstrates a multi-color emission from self-assembled wires with InGaN multi-quantum wells (MQWs), which are used to demonstrate flexible LEDs. Self-assembled catalyst-free GaN microwires have been grown by metalorganic vapor phase epitaxy (MOVPE) with silane addition on sapphire in situ capped with SiNx mask. This was followed by the growth of seven InGaN/GaN QWs and completed with the growth of a p-GaN shell [1,4]. The electrical and optical characterization of the flexible LED device was performed using micro electroluminescence (μEL); and photoluminescence (PL) and cathodoluminescence (at 4K) respectively.
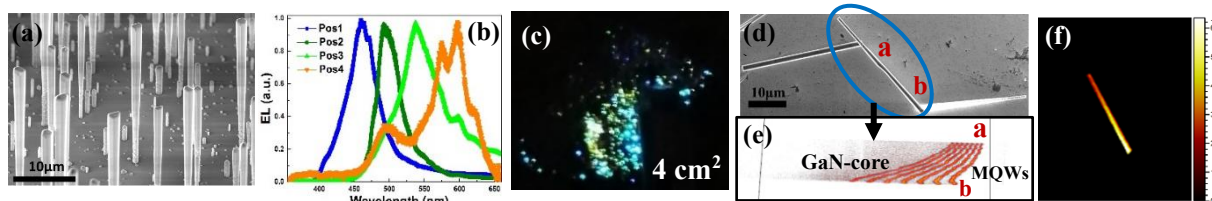
Figure 1. (a) SEM image of virgin NWs; (b) EL spectra at four different positions; (b) Emission observed during EL measurement; (d) SEM image of NWs dispersed on Si; (e) 3D mapping of In using TOF-SIMS; (f) Color profile of secondary In$^+$ counts on single NW

Fig. 1 (a) shows the SEM image of as-grown nanowires. The EL measured at injection current of 60 mA in Fig. 1(b) revealed different wavelength emission at 460 nm, 500 nm, 540 nm and 600 nm. Different color emission can be seen from the flexible LED device in Fig. 1(c) captured during current injection. Further investigations using ToF-SIMS analysis on single nanowires were also performed to quantify the indium incorporation in the InGaN/GaN core-shell structure [4]. The 'ab' section of an identified single nanowire as seen in the SEM image of Fig. 1(d) was analyzed by ToF-SIMS and the 3D profile of In present in this section can be seen in Fig. 1(e). The secondary ion count for In$^+$ in Fig. 1(f) shows a gradient of In-content along the length of the nanowire. These results indicate high and inhomogeneous In incorporation in the side-walls thus resulting in the variation in wavelength emission of the core-shell nanowires. This work highlights the possibility to obtain multi-color emission from blue to red from core-shell m-plane InGaN/GaN MQWs in GaN nanowire-based LEDs that opens the route for monolithic white flexible LED without phosphors.

References:
[1] R. Koester et al. *Nano Lett.*, vol. **11**, 4839 (2011)
[2] N. Guan et al. *ACS Photonics.*, **3**, 597−603 (2016)
[3] Y. J. Hong et al. *Adv. Mater.,* **23**, 3284–3288 (2011)
[4] X. Dai et al. *Nano Lett.*, **15**, 6958 (2015)

Insights into the Quantum Efficiency and Recombination Dynamics of InGaN/GaN Core-Shell Microrod LED Structures

H. Zhou [1,2], **P. Henning** [3], **F. A. Ketzer** [3], **L. Nicolai** [4], **H. Spende** [1,2], **J. Hartmann** [1,2], **A. Vogt** [1], **A. Avramescu** [2,5], **S. Fündling** [1,2], **H.-H. Wehmann** [1,2], **M. Hanke** [4], **A. Trampert** [4], **M. Straßburg** [2,5], **H.-J. Lugauer** [2,5], **A. Hangleiter** [3], **T. Voss** [1] **and A. Waag** [1,2]

[1] *Institut für Halbleitertechnik and Laboratory for Emerging Nanometrology, Technische Universität Braunschweig, 38092 Braunschweig, Germany*
[2] *epitaxy competence center ec², Hans-Sommer-Straße 66, 38106 Braunschweig, Germany*
[3] *Institut für Angewandte Physik, Technische Universität Braunschweig, 38106 Braunschweig, Germany*
[4] *Paul-Drude-Institut für Festkörperelektronik, Hausvogteiplatz 5-7, 10117 Berlin, Germany*
[5] *OSRAM Optosemiconductors GmbH, Leibnizstraße 4, 93055 Regensburg, Germany*

Microrod LEDs with the core-shell geometry fabricated by MOVPE have been proposed as a potential candidate for high performance solid state lighting.[1] Such structure brings several advantages, including reduced threading dislocation density and absence of polarity related electric field within the sidewall quantum wells. These two benefits are both supposed to be in favor of a high internal quantum efficiency (IQE). Indeed, very limited publications reported the IQEs of such structures. [2] What is also insufficient is the insight into the recombination dynamics of core-shell microrod structures.

InGaN/GaN core-shell microrods have been prepared by MOVPE using selective area growth. An IQE of above 40% was measured by using power-dependent and temperature-dependent photoluminescence (PL) measurements with a laser wavelength of 380 nm. Further time-resolved PL under low excitation conditions indicate a decay time of 357 ± 3 ps at a temperature of 5 K, which decreases to 190 ± 3 ps at 300 K. Meanwhile, a spectrally-dependent PL decay time variation was also observed. The optical properties of microrod structures were also correlated to their structural characteristics obtained by (scanning) transmission electron microscopy and nanofocus x-ray diffraction.
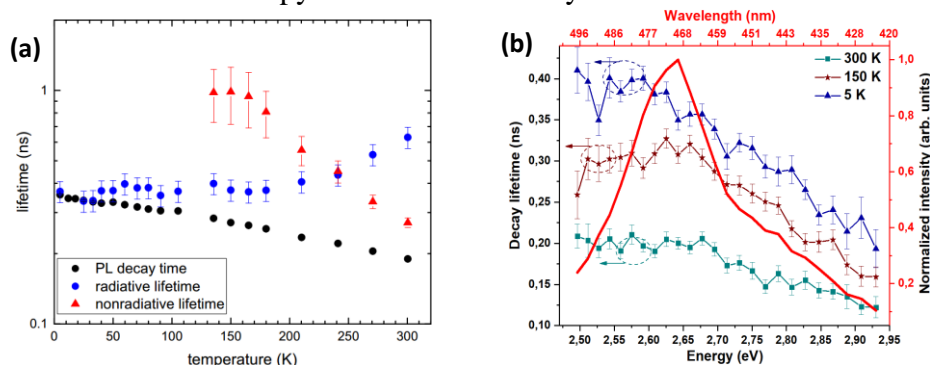
Fig 1. (a) Time-resolved PL decay time versus temperature and calculated radiative and non-radiative lifetimes. (b) Integrated PL-spectrum (at 5 K) along with the measured decay time across the spectrum at different temperatures.

[1] A. Waag, X. Wang, S. Fündling, J. Ledig, M. Erenburg, R. Neumann, M. A. Suleiman, S. Merzsch, J.D. Wei, S.F. Li, H.-H. Wehmann, W. Bergbauer, M. Straßburg, A.Trampert, U. Jahn, and H. Riechert, *Phys. Status Solidi C* **8**, 7–8 (2011).
[2] C. Mounir, T. Schimpke, G. Rossbach, A. Avramescu, M. Strassburg, and U. T. Schwarz, *J. Appl. Phys.* **120**, 155702 (2016).

In-situ observation of AlN growth on levitated Ni-Al droplet

Y. Yamagata[1], S. Hamaya[1], M. Adachi[1], A. J. Loach[2], J. S. Fada[3], L. G. Wilson[2], J.L.W. Carter[2], R. H. French[2] and H. Fukuyama[1]

[1]*Institute of Multidisciplinary Research for Advanced Materials (IMRAM), Tohoku University, 2-1-1 Katahira, Aoba-ku, Sendai 980-8577, Japan.*
[2]*Department of Materials Science and Engineering, Case Western Reserve University, 10900 Euclid Avenue, Cleveland, Ohio 44106-7204, USA.*
[3]*Department of Mechanical and Aerospace Engineering, Case Western Reserve University, 10900 Euclid Avenue, Cleveland, Ohio 44106-7204, USA.*

AlN is a promising substrate material for AlGaN-based UV-LED. Recently, we have developed an original liquid phase epitaxy (LPE) method using Ga-Al flux [1]. A fundamental understanding of the growth kinetics is necessary to improve processing parameters. We also have been seeking an alternative flux system for LPE growth to achieve high growth rate. The purpose of this study is to obtain the insight of flux selection through in-situ observation of AlN growth using an electromagnetic levitation (EML) [2] technique. By the EML, electrically conductive material droplets can be levitated without containers. It is suitable for in-situ observation of crystal formation behavior on the surface of the flux.

In this study, AlN crystals formation behavior on levitated droplets of $Ni_{(1-x)}$-Al_x alloys was investigated. The alloys were prepared using an arc melting furnace. The EML furnace was filled with Ar-5 vol%H_2 gas. The sample was levitated in a radio frequency magnetic field and heated by induction current and laser irradiation. After stable levitation of the molten sample is achieved, N_2 gas was introduced into the chamber. The levitated sample images were recorded by high-speed cameras during AlN formation on the sample surface.

Automated image analysis techniques were applied to extract nucleation and growth kinetics from the in-situ images. Nucleation and crystal growth rates of AlN were proportional to the Al composition and inversely proportional to growth temperature. In the experiments using the sample with low Al composition ratio at higher temperature, hexagonal AlN crystal formed on the surface. On the other hand, in the experiments using samples with high Al ratio at lower temperature, dendritic morphology AlN crystal appeared. It was considered that these morphology and growth behavior changes were caused by the difference of driving force of AlN formation reaction. Formed AlN crystals were characterized with X-ray diffraction, scanning electron microscopy, and transmission electron microscopy.

[1] M. Adachi, K. Maeda, A. Tanaka, H. Kobatake, and H. Fukuyama, *Phys. Stat. Sol. (a)*, **7**, 1494 (2011).
[2] M. Watanabe, M. Adachi, and H. Fukuyama, *J. Mater. Sci.*, 51, 3303 (2016).

Effect of Reaction Temperature on AlN Formation at Interface of Al Layer Deposited on GaN Substrate

Marsetio Noorprajuda, Makoto Ohtsuka, Masayoshi Adachi, and Hiroyuki Fukuyama

Institute of Multidisciplinary Research for Advanced Materials (IMRAM), Tohoku University, 2-1-1, Katahira, Aoba-ku, Sendai 980-8577, Japan

Aluminum nitride (AlN) is a good candidate material for AlGaN based UV-LED substrate owing to its wide band gap, high ultraviolet (UV) transparency, and low lattice mismatch with AlGaN. To the current technology, AlN had been fabricated using several methods on the foreign substrates owing to the scarcity of the AlN in the nature. For instances, Fukuyama, *et al*. had fabricated the AlN on the *c*- and *a*-plane sapphires using the sapphire nitridation method [1]. Ohtsuka, *et al*. had grown the AlN on a nitrided *a*-plane sapphire using the pulsed DC reactive sputtering method [2]. Adachi, *et al*. had grown the AlN on a nitrided *r*-plane sapphire using the liquid-phase epitaxy (LPE) method [3]. Kishimoto, *et al*. had grown the AlN on the *c*-plane sapphire by the elementary source vapor phase epitaxy (EVPE) method [4]. Apart from the above-mentioned methods, this is a feasibility study aiming for the novel AlN fabrication method, i.e., an AlN crystal is obtained from heat treatment of Al on GaN substrate. Here, the interfacial reaction between Al layer and GaN substrate at elevated temperatures is studied as a first step.

An Al layer was deposited on a GaN substrate in Ar gas at 294 K and 600 W using magnetron sputtering equipped with pulsed DC power source. An Al target (99.999 mass%, diameter: 101.6 mm) was used. The single crystalline GaN substrates (thickness: 350 μm) were used with a cut off angle of 0.35° toward *m*-axis. The thickness of the sputtered Al layer was 7.6 μm. Subsequently, the Al-coated substrate was placed on a heating stage in a microscope with the Al surface downward, and it was thermally treated at 823-1673 K in an Ar gas. The Ar gas flow rate was kept at 0.03 L/min. The interfacial reaction between the Al layer and the GaN substrate during the heat treatment was observed from the back side of the substrate. The crystalline orientation and quality of the obtained AlN were evaluated using an X-ray diffractometer.

The interface morphology was dramatically changed after the heat treatment at 1673 K. The AlN (0002) and (0004) peaks were clearly observed in the 2θ–ω profile from the XRD measurement after the heat treatment at 1673 K, indicating that the AlN was grown by the interfacial reaction between Al and GaN at 1673 K. The experimental details and growth mechanism will be presented at the symposium.

[1] H. Fukuyama, K. Nakamura, T. Aikawa, H. Kobatake, A. Hakomori, K. Takeda, and K. Hiraga, *J. Appl. Phys.* **107**, 043502 (2010).
[2] M. Ohtsuka, H. Takeuchi, and H. Fukuyama, *Jpn. J. App. Phys*. **55**, 05FD08 (2016).
[3] M. Adachi and H. Fukuyama, *Phys. Status Solidi B*, 1700478 (2017).
[4] K. Kishimoto, M. Funato, and Y. Kawakami, *Crystals* **7**, 123 (2017).

Evolution of morphology and crystalline quality of sputtered AlN films with high-temperature annealing

Yosuke Mogami[1,2], Shogo Motegi[1,2], Atsushi Osawa[3], Kazuto Osaki[3], Yukitake Tanioka[3], Atsushi Maeoka[3], Masafumi Jo[1], Noritoshi Maeda[1], Hiroyuki Yaguchi[2] and Hideki Hirayama[1]

[1]*RIKEN, 2-1 Hirosawa, Wako, Saitama 351-0198, Japan*
[2]*Saitama University, 255 Shimo-Okubo, Sakura-ku, Saitama 338-8570, Japan*
[3]*SCREEN Finetech Solutions Co. Ltd., 2426-1 Mikami, Yasu, Shiga 520-2323, Japan*

AlGaN-based UV light-emitting diodes (LEDs) have attracted much attention because of their wide-range applications in disinfection and bio-medical fields. Recently, high-temperature annealing (HTA) technique has been proposed to improve the crystalline quality of sputtered AlN on sapphire [1], which paves the way for high-efficiency AlGaN LEDs with low cost. During the annealing, columnar AlN with small boundaries coalesced into a uniform film, reducing the crystal mosaicity. However, the recrystallization process may also produce large hillocks if AlN islands with different crystal orientation are contained in the initial sputtered film. Here, we investigate the evolution of the surface morphology and crystalline quality of sputtered AlN films in terms of the annealing temperature.

AlN films were grown on sapphire substrates by low-inductance-antenna (LIA) assisted dc sputtering. The sputtering condition was such that "spike" structures with different crystal orientations were formed with the density of 5×10^7 cm^{-2}. The samples were then annealed at 1500-1700 °C for 1h under N$_2$ ambient. The inset in Fig. 1 shows an AFM image of the AlN surface annealed at 1700 °C, where the formation of large hillocks is visible. The height vs width of the hillocks for various annealing temperatures are plotted in Fig. 1. As the temperature increased, the size of the hillock as well as the height-width aspect ratio increased. Then, 1-µm AlN was overgrown by MOCVD to improve the flatness. The surface roughness decreased from 7.5 to 2.6 nm for the 1500°C-annealed AlN layer, whereas large hillocks remained (or increased in size) for the AlN annealed at ≥ 1650°C. As a result, the 1500°C-annealed sample showed the best XRC linewidth after the regrowth [Fig. 2]. These results indicate that the annealing condition depends on the initial morphology of the sputtered AlN.
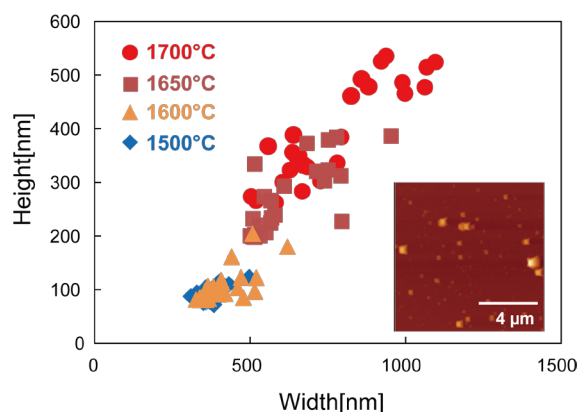
Fig. 1 Height-width plots of hillocks for HTA sputtered AlN. The inset shows a 10×10-µm AFM image of the AlN surface annealed at 1700 °C.
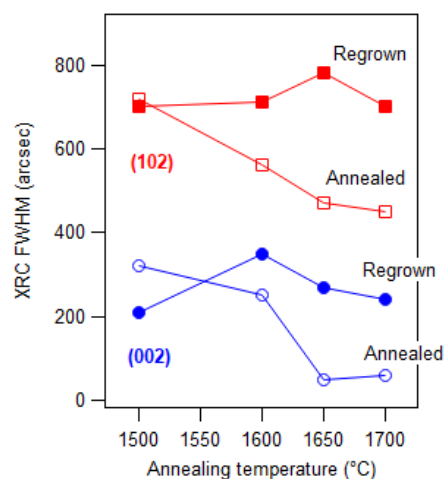
Fig. 2 FWHMs of the (002) and (102) XRC for annealed and 1-µm AlN regrown samples.

[1] H. Miyake *et. al*., J. Cryst. Growth **456**, 155 (2016).

Characteristics of highly conductive p-type GaN films prepared by pulsed sputtering

Taiga Fudetani [1], Kohei Ueno [1], Atsushi Kobayashi [1], and Hiroshi Fujioka [1,2]

[1] *Institute of Industrial Science, The University of Tokyo, 4-6-1 Komaba, Meguro, Tokyo, Japan*
[2] *JST-ACCEL, 5 Sanbancho, Chiyoda, Tokyo, Japan*

p-type doping for nitride semiconductors is quite important for fabrication of high performance optoelectronic devices. It is recently reported that pulsed sputtering deposition (PSD) technique enabled to form p-type GaN at low process temperatures at around 480 ^{o}C. [1] It is also known that as-grown Mg doped PSD GaN shows p-type conduction without any activation anneal because of its low residual hydrogen concentration. Moreover, the memory effect and the thermal diffusion of Mg atoms, which have been serious problems in MOCVD growth, are suppressed by the use of PSD because of its low growth temperatures. [1,2] For lightly Mg doped PSD-GaN, room temperature (RT) hole mobility as high as 34 cm^2 V^{-1} s^{-1} has been already reported, which indicates that it is possible to prepare high quality p-type GaN thin films with PSD. [2] In this study, we have grown heavily Mg doped GaN thin films with PSD and investigated their electrical and structural properties.

Mg-doped GaN with a thickness of 0.5 μm was grown on GaN:Fe templates by PSD. Hall effect measurements were performed at temperatures ranging from 77-650 K. Pd/Ni/Au electrodes were formed for p-type ohmic contacts by e-beam evaporation.

Figure 1 shows the resistivity of PSD-grown Mg-doped GaN as a function of the RT hole concentration, $[h^+]_{RT}$. The sample with the highest $[h^+]_{RT}$ showed a low resistivity of 0.6 Ωcm. Even for the sample with the highest $[h^+]_{RT}$, no apparent structural degradation was observed and its surface remained atomically-flat with the RMS surface roughness of 0.51 nm as shown in the inset of Fig. 1. Figure 2 shows the temperature dependence of hole concentration for samples with various $[h^+]_{RT}$. The fitting curves in this figure were obtained assuming the existence of a compensating donor. The fitted compensation ratio N_D/N_A for heavily Mg doped GaN samples were as low as 5%, which can explain low resistivity of p-type PSD GaN.

[1] E. Nakamura *et al.*, Appl. Phys. Lett. **104**, 051121 (2014). [2] Y. Arakawa *et al.*, APL Materials **4**, 086103 (2016).
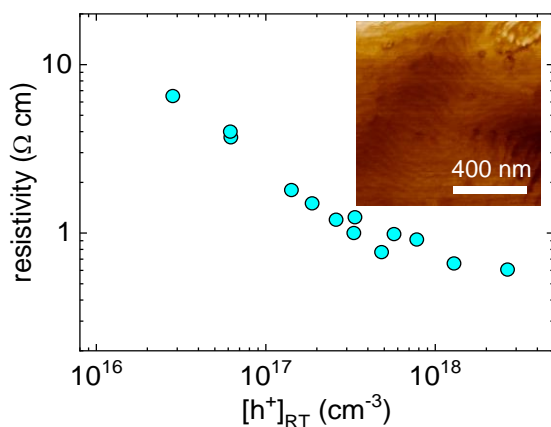
Figure 1. Resistivity of Mg-doped PSD GaN as a function of $[h^+]$ at RT. An AFM image of the sample with the lowest resistivity is shown as an inset.
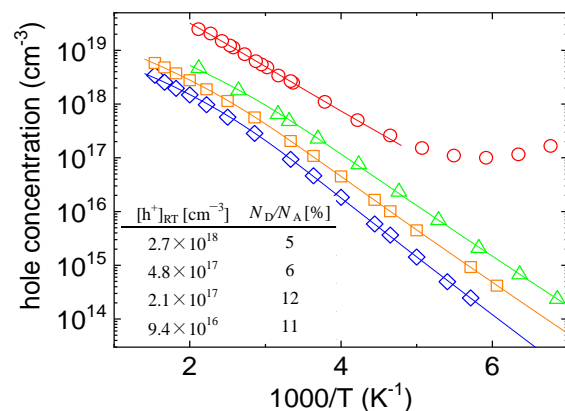

Figure 2. Temperature dependence of hole concentration for samples with various $[h^+]_{RT}$. The inset table shows compensation ratio, N_D/N_A for each $[h^+]_{RT}$.

International Symposium on Growth of III-Nitrides ISGN-7, 5-10 August 2018, Warsaw, Poland

Improvement of electron mobility of polycrystalline InN on glass substrates by AlN buffer layers

Masumi Sakamoto[1], Atsushi Kobayashi[1], Kohei Ueno[1], and Hiroshi Fujioka[1,2]

[1]*Institute of Industrial Science, The University of Tokyo, 4-6-1 Komaba, Meguro, Tokyo, Japan*
[2]*JST-ACCEL, 5 Sanbancho, Chiyoda, Tokyo, Japan*

Single crystalline InN has been regarded as a promising candidate for a material of high speed transistors since its electron velocity and mobility are highest among the group III nitride semiconductors. We have recently found that polycrystalline InN grown of glass or polyimide substrates can be also used for fabrication of thin film transistors (TFTs). [1][2] For further boost in device performance, improvement in crystalline quality of the poly InN films is inherently important. In this presentation, we will discuss a new method for controlling crystallographic orientation of polycrystalline InN grown on glass substrates, and demonstrate improved electron mobility of the *c*-axis oriented InN films.

We grew InN films on fused-silica glass substrates by pulsed sputtering deposition (PSD). AlN, HfO_2, or Al_2O_3 was inserted between the InN films and the glass substrates to control the crystallographic orientation of InN. We evaluated structural and electrical properties of InN with X-ray diffraction (XRD) and Hall effect measurements.

Figure 1 shows the XRD patterns of the InN films grown on glass substrates at 460 °C. InN films grown with AlN buffer layers exhibited XRD peaks assigned only to 0002 and 0004 diffractions, indicating formation of *c*-axis orientated InN films. Figure 2 depicts electron mobility and concentration of the InN films grown on the glass substrates. It is found that the insertion of AlN buffer layers improves electron mobility of the InN films from 100 to 350 $cm^2V^{-1}s^{-1}$ and decreases electron concentration, which should lead to improved TFT device performance.

[1] T. Itoh *et al*., Appl. Phys. Lett. **109**, 142104 (2016). [2] K. S. Lye *et al*., Appl. Phys. Lett.
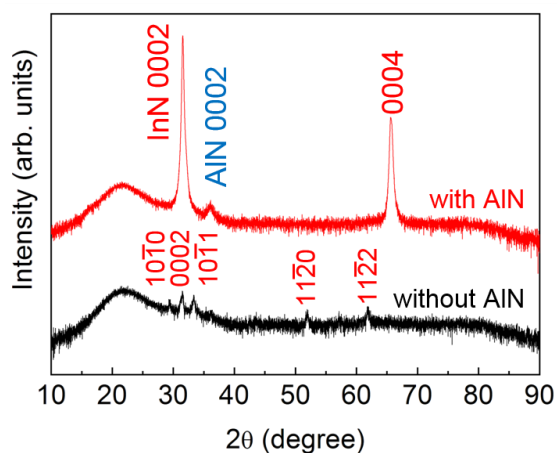
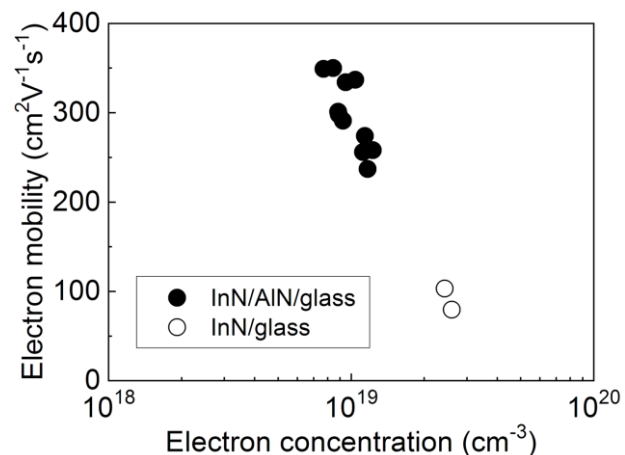Fig.1 XRD patterns of InN with and without the AlN buffer layers.

Fig.2 Electron mobility and concentration of InN on glass with and without the AlN buffer layers.

Structural and Electrical Properties of AlN and AlGaN Prepared by Pulsed Sputtering

Yuya Sakurai [1], **Kohei Ueno** [1], **Atsushi Kobayashi** [1], **Hideto Miyake**[2], **and Hiroshi Fujioka** [1,3]

[1]*Institute of Industrial Science, the University of Tokyo, 4-6-1 Komaba, Tokyo, Japan*
[2]*Graduate School of Regional Innovation, Mie University, Mie 514-8507, Japan*
[3]*ACCEL, Japan Science and Technology Agency (JST), 5 Sanbancho, Chiyoda, Tokyo, Japan*

AlGaN-based UV-LEDs have attracted much attention because they can be used for various applications such as a sterilization and water purification. For their mass-production, low cost thin film growth and doping techniques are highly sought after. It is known that a conventional MOCVD technique suffers from several serious problems, which include its high growth temperature above 1000 °C and difficulties in achieving heavily doped materials. By contrast, pulsed sputtering deposition (PSD) technique enables to form high-quality AlN epitaxial films even at room temperature and highly conductive n-type GaN with a record low resistivity. [1,2] In this presentation, we report the besic characteristics of the growth and doping technique for AlN and AlGaN with PSD.

A TEM image shown in Fig. 1 revealed densities for mixed and edge dislocations in this PSD-AlN/sapphire structure were 2.8×10^8 cm^{-2} and 4.4×10^9 cm^{-2}, respectively. No screw dislocation was observed in this image. We have found that Si-doping to AlN (0001) films prepared on sapphire by PSD allows to control n-type resistivity in the range from 1×10^2 to 1×10^3 Ωcm. Electron mobility μ_e for the AlN/sapphire is plotted as a function of the electron concentration [n] in Fig. 2. A maximum μ_e for our samples is as high as 44 cm^{2}V^{-1}s^{-1}, which is a record high value for n-type AlN prepared on sapphire, to the best of our knowledge.

We have found that the use of PSD technique also enables the precise control of the Al composition and doping profiles in AlGaN alloys because of its lower growth temperature. We have also found that we can grow highly n-type conductive Al$_x$Ga$_{1-x}$N films in whole Al composition range. These results demonstrate the potential of the highly non-equilibrium pulsed sputtering technique for the growth of conductive n-type AlN and AlGaN at low cost.
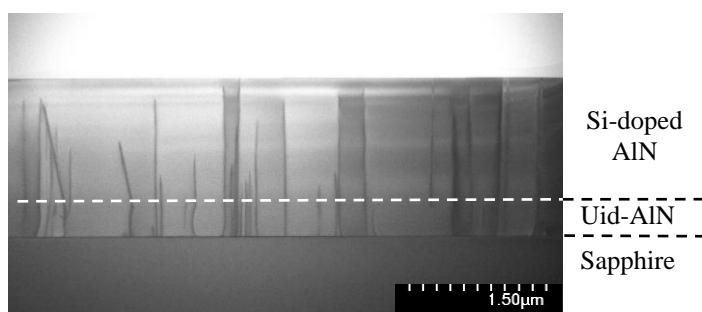
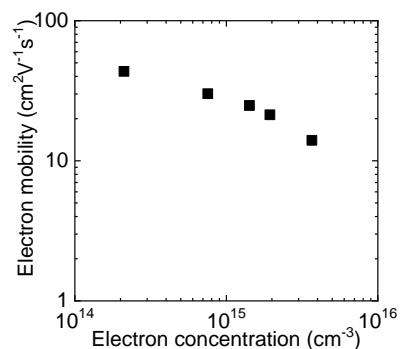Fig.1 TEM image of Si-doped AlN (0001) on sapphire prepared by PSD.

Fig.2 μ_e vs. [n] of Si-doped AlN on sapphire prepared by PSD.

[1] K. Sato *et al.*, *Appl. Phys. Express* **2**, 011003 (2009).
[2] K. Ueno *et al.*, *APL Mater.* **5**, 126102 (2017).

Surface Morphology Control and Si-Doping of MOVPE-Grown High-Al-Content AlGaN Layers

M. Tollabi Mazraehno [1,3]**, M. P. Hoffmann** [3]**, L. Cancellara** [2]**, C. Frankerl** [3]**,**
B. Neuschulz [1]**, M. J. Davies** [3]**, C. Brandl** [3]**, T. Wernicke** [1]**, M. Albrecht** [2]**, M. Kneissl** [1]**,**
and H.-J. Lugauer [3]

[1] *Institute of Solid State Physics, Technische Universität Berlin, Hardenbergstr. 36, 10623*
Berlin, Germany
[2] *Leibniz-Institut für Kristallzüchtung, Max-Born-Str. 2, 12489 Berlin, Germany*
[3] *OSRAM Opto Semiconductors GmbH, Leibnizstr. 4, 93055 Regensburg, Germany*

In this presentation we address different issues in AlGaN epitaxial growth regarding the development of deep ultraviolet (DUV) LEDs, with emphasis on the relationship between surface morphology, doping and quantum efficiency. $Al_xGa_{1-x}N$ layers with x=0.6-0.95 are grown by metalorganic vapor phase epitaxy on c-plane native AlN substrates with threading dislocation densities (TDDs) below $1\times10^4 cm^{-2}$, as well as on AlN/sapphire templates with a TDD of about $1\times10^9 cm^{-2}$. AlGaN growth on AlN/sapphire templates is dominated by growth spirals, which are formed at threading dislocations with a screw component, leading to increased surface roughening. It is shown that the density and aspect ratio of these spirals, which directly influence the surface roughness, can be reduced by decreasing the metal supersaturation during growth, in accordance with basic assumptions of the Burton-Cabrera-Frank model [1]. Si-doped high-Al-content AlGaN layers are grown under high metal supersaturation growth conditions in order to minimize the formation of compensating metal vacancies [2], leading to highly conductive but rough surfaces due to the spiral growth. In this case, the spiral height is enhanced in contrast to an AlGaN growth at low supersaturation, in which conditions spirals tend to grow flat and wide. In contrast to AlN/sapphire template, growth on native AlN substrates, due to very low TDD, is shown to be spiral free resulting in smooth surfaces with monolayer surface steps. The effect of rough AlGaN:Si layers on the active region of DUV LEDs, in terms of structural homogeneity and internal quantum efficiency, is then investigated. High resolution TEM as well as temperature dependent photoluminescence measurements are carried out to assess the structural properties and internal quantum efficiency of DUV multi-quantum-wells grown on AlGaN:Si layers.

[1] W. K. Burton, N. Cabrera, and F. C. Frank, *Philosophical Transactions of the Royal Society of London. Series A, Mathematical and Physical Sciences* **243**, 299 (1951).
[2] I. Bryan, Z. Bryan, S. Washiyama, P. Reddy, B. Gaddy, B. Sarkar, M. H. Breckenridge, Q. Guo, M. Bobea, J. Tweedie, S. Mita, D. Irving, R. Collazo, and Z. Sitar, *Appl. Phys. Lett.* **112**, 062102 (2018).

Effects of N_2 and H_2 carrier gases on the growth of AlGaN epilayers on Si(110) substrates by MOCVD

X. Q. Shen, T. Takahashi, M. Shimizu and H. Okumura

National Institute of Advanced Industrial Science and Technology (AIST)
Tsukuba, Ibaraki 305-8568, Japan

III-nitride semiconductors are promising materials for both optical and electronic device applications. Among them, AlGaN is an important material because it is indispensable to the structures both in optical device (such as UVLEDs) and electronic device (such as HEMTs). At present, the device structures are mainly grown by MOCVD technique. In MOCVD growth, H_2 and N_2 as carrier gases (CGs) are used. Many studies concerning the effect of H_2 and N_2 CGs on the GaN growth have been carried out. It is shown that high N_2 content results in more pinholes in GaN.[1] In addition, GaN growth rate decreases with an increasing fraction of N_2.[2] However, less is reported concerning the CG effect on the AlGaN growth, which is important in the above mentioned device structure fabrications.

In this study, we report the effects of H_2 and N_2 CGs on the growth of AlGaN epilayers in MOCVD. As a result, it is found that different CGs can greatly influence the surface morphology, growth rate and even Al composition of the AlGaN epilayers.

The samples were grown on the 4" Si(110) substrates by MOCVD. In-situ measurements of the reflectance were carried out by LayTec to characterize the growth rate changing under differnet CGs. AFM, HRXRD and STEM were used to characterize the morphology, the Al composition and the layer thickness of the AlGaN.

Figure 1 shows AFM images of two AlGaN samples grown under the H_2 (sample I) and the N_2 (sample II) CGs, respectively.

Fig.1 AFM images of AlGaN surface using (a) H_2 and (b) N_2 as carrier gases. Al composition is 0.61.

Many large pits are observed from the sample I, while smooth surface with small pits and mono-layer steps is obtained from sample II. This means that N_2 CG is helpful to improve the AlGaN surface morphology, which is different from the GaN case. Figure 2 illustrates the ratio of the AlGaN growth rate under N_2 and H_2 CGs at whole Al compositions measured by LayTec. It is clear that AlGaN growth rate decreases using N_2 CG and the ratio is between 0.5 and 0.6, which is similar to the previous results in GaN growth.

Details will be discussed at the conference.

[1] S. Cho, H. Hardtdegen, N. Kaluza, N. Thillosen, R. Steins, Z. Sofer, and H. Lüth, phys. stat. sol. (c) 3 (2006) 1408.
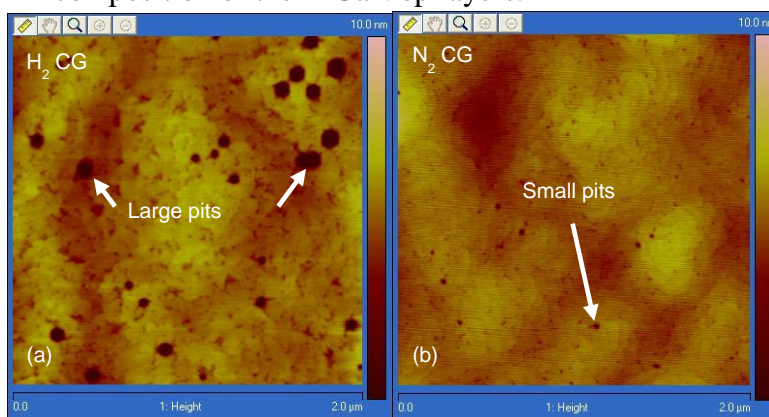[2] H. Dartsch, S. Figge, T. Aschenbrenner, A. Pretorius, A. Rosenauer, D. Hommel, J. Cryst. Growth 310 (2008) 4923.
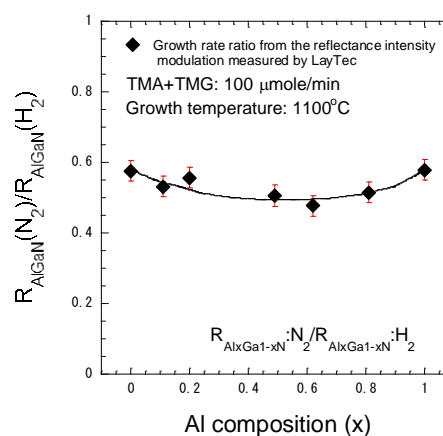
Fig.2 Dependence of the AlGaN growth rate ratio under N_2 and H_2 CGs on the Al composition.

Significantly enhanced performance for AlGaN UV LED by employing a thin BAlN electron blocking layer

Wenzhe Guo, [1] Z.-H. Zhang,[2] Haiding Sun, [1] Kaikai Liu, [1] and Xiaohang Li[1]

[1]King Abdullah University of Science and Technology (KAUST), Thuwal, 23955, Saudi Arabia

[2]Hebei University of Technology, Tianjin, 300401, China.

III-nitride based ultraviolet light emitting diodes (UV LED) has attracted many researchers in various applications. However, UV LEDs suffer from low efficiency and efficiency droop which hinder the development. These drawbacks could be originated from large electron leakage into the p-type AlGaN layer and low hole injection into the active region. To improve the performance, conventionally, a thin aluminum gallium nitride ($Al_xGa_{1-x}N$) p-type electron blocking layer (p-EBL) is inserted between the last quantum barrier and the p-type AlGaN layer. Due to the Al composition limit and large valence band offset (VBO) of AlGaN materials, $Al_xGa_{1-x}N$ p-EBL can not sufficiently suppress the electron leakage and deteriorates the hole injection. Some special designs have been proposed and demonstrated to be useful for the performance improvement, like $Al_xGa_{1-x}N$ p-EBL with graded Al content, polarization-reversed AlInGaN p-EBL and $Al_xGa_{1-x}N$ superlattice p-EBL.[1,2,3]These designs are challenging to be realized because of complex structures.

Boron aluminum nitride ($B_xAl_{1-x}N$), as a newly-emerged III-nitride ternary material, has been studied for the application in optoelectronics devices. Zhang et al. have computed the electronic properties of $B_xAl_{1-x}N$ material, including bandgap, lattice constants and effective mass, etc.[4] Liu et al. have revealed the polarization constants of $B_xAl_{1-x}N$ material.[5] Most importantly, Sun et al. have identified the band alignment between $B_{0.14}Al_{0.86}N$ and GaN layers, which indicates that the valence band edge of $B_{0.14}Al_{0.86}N$ is located 2 meV below that of GaN material. Thus, combining $B_{0.14}Al_{0.86}N$ and low-Al-content AlGaN layer can lead to zero VBO without considering the polarization effect. All these discovery on BAlN material allows us to study BAlN material in the applications of LED.

In this work, we propose to use $B_{0.14}Al_{0.86}N$ as an EBL in GaN-based UVA LED that emits at the wavelength of 360 nm. The electronic and optical characteristics of the UV LED are numerically investigated by the commercial software, Advanced Physical Models of Semiconductor Devices (APSYS), and the comparison has been made with UVA LED with conventional $Al_{0.30}Ga_{0.70}N$ EBL. We demonstrate that $B_{0.14}Al_{0.86}N$ is capable of creating large effective potential barrier for electrons and small barrier for holes, thus increasing both electron and hole concentrations in the active region. As a result, the internal quantum efficiency is improved by 42% at the current density of 400 A/cm^2 and the efficiency droop is also reduced. The output power is boosted from 10 mW to 22 mW at the current density of 400 A/cm^2. To optimize the thickness of $B_{0.14}Al_{0.86}N$ EBL, we conduct the thickness-dependent study and reveal that $B_{0.14}Al_{0.86}N$ EBL can be thinned down to 6 nm without significant influence on the UV LED performance.

[1] Y. H. Lu et al., Appl. Phys. Lett. **102**, 143504 (2013).

[2] Y. A. Chang et al., IEEE J. Quantum Electron. **49**, 553–559 (2013).

[3] Y. K. Kuo et al., IEEE J. Quantum Electron. **52**, 1-5 (2016).

[4] M. Zhang and X. Li, Phys. Status Solidi B, 1600749 (2017).

[5] K. Liu, et al., Appl. Phys. Lett. **111**, 222106 (2017)

Green - blue InGaN/GaN LED array obtained by lateral band-gap engineering.

Piotr A. Dróżdż[1,2], **Marcin Sarzyński**[2], **Krzysztof P. Korona**[1], **Robert Czernecki**[2] **and Tadeusz Suski**[2]

[1] *Faculty of Physics, University of Warsaw, Pasteura 5, 02-093 Warsaw, Poland*

[2] *Institute of High Pressure Physics "Unipress", Polish Academy of Sciences, Sokołowska 29/37, 01-142 Warsaw, Poland*

The off-cut angle of the substrate is one of the most important parameters that governs kinetic processes on the growth front and influences structural, optical and electrical properties of the structures. Our previous work showed that a controllable modification of this angle offers a valuable variety of new ideas leading to interesting applications. They rely on the effect of decreasing In-content in InGaN and simultaneous rising of hole concentration in Mg doped GaN [1] with increase of the off-cut angle of the substrate.

In the present work, we show InGaN/GaN light emitting diode (LED) arrays with a variation of wavelength originating from lateral arrangement of differently tilted substrate by use of a special photolithography and ion etching techniques. The off-cut angle was modified in the range from 0.4° to 4.5° with respect to (0001) plane of the wurtzite structure. After the growth of InGaN layers, indium concentration changed with respect to the off-cut angle, what results with the change of bandgap and the luminescence wavelength. Such lateral band-gap engineering let us to produce devices of photo- and electro-luminescence range from 2.39 to 2.72 eV (change from green to blue color of the emitted light on one wafer).

Such LED arrays are also an experimental tool for studying microscopic processes of light emission from InGaN/GaN quantum structures characterized by different concentration of indium. The light emission dynamics was studied with the use of time–resolved photoluminescence spectroscopy. It has been found that PL energy and decay time depended on voltage that changed electric field inside the structure and modified the Stark effect. The other consequence of such situation was the observation of different PL time decays in the TRPL spectra. At room temperature, the times were between 4.5 and 11 ns, for high and small angles, respectively. It is interpreted as the differences in the built-in electric field due to indium content change with off-cut angle. Low defect concentration leads to high internal efficiency of light emission in our devices.

Fig. 1: PL spectra measured at 300 K at differently tilted regions in one of our devices.

We demonstrate that our technique allows local modification of parameters and precise determination of the emitted light wavelength, suitable for practical devices.

[1] P. A. Dróżdż, M. Sarzyński, J. Z. Domagała, E. Grzanka, S. Grzanka, R. Czernecki, Ł. Marona, K. P. Korona, and T. Suski, *Phys. Stat. Solidi (a)* **214**, 1600815 (2017).
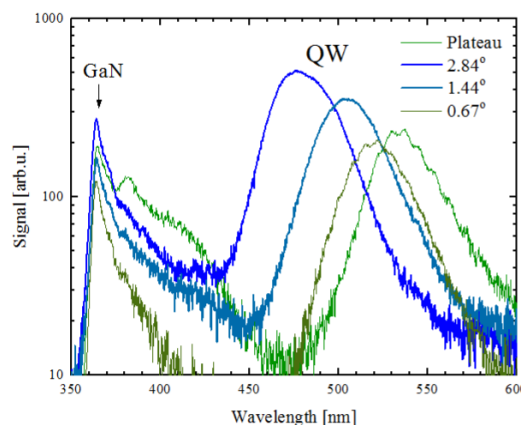
InAlN growth peculiarities on vicinal GaN substrates

Marta Sawicka [1,2], **Marcin Siekacz** [1], **Grzegorz Muzioł** [1], **Anna Feduniewicz-Żmuda** [1],
Julita Smalc-Koziorowska [1,2], **Marcin Kryśko** [1], **Žarko Gačević** [3], **Enrique Calleja** [3]
and Czesław Skierbiszewski [1,2]

[1] *Institute of High Pressure Physics Polish Academy of Sciences, Sokołowska 29/37, 01-142 Warsaw, Poland*
[2] *TopGaN Sp. z o.o., Sokołowska 29/37, 01-142 Warsaw, Poland*
[3] *ISOM-ETSIT Universidad Politécnica de Madrid, Avda. Complutense s/n, 28040 Madrid, Spain*

InAlN is a promising alternative to AlGaN and InGaN in nitride-based optoelectronic device structures. One of the most attractive features is the possibility to achieve lattice matching to GaN for $In_xAl_{1-x}N$ with indium content x ~17%. Additionally, high refractive index contrast to GaN ($\Delta n/n$ ~7%) makes it an ideal candidate for optical cladding layers in edge-emitting laser diodes (LDs) or distributed Bragg reflectors (DBRs) for vertical cavity surface emitting lasers (VCSELs) and other nitride-based devices [1].

The InAlN growth has been proven difficult due to large difference in bond strength and lattice parameters of InN and AlN. The growth-related issues leading to poor material quality are still not completely solved for this ternary compound both in metal-organic vapor phase epitaxy (MOVPE) [2] and in plasma-assisted molecular beam epitaxy (PAMBE) [3]. The observed lateral inhomogeneity in composition and formation of so-called columnar "honeycomb" microstructure (Al-rich columns along growth direction surrounded by In-rich regions) is believed to be related to insufficient diffusion of Al and N adatoms at low growth temperatures. In PAMBE the indium content in metal-polar InAlN is severely constrained by InN bonds decomposition imposing the need to grow at temperatures below 550°C to incorporate ~17% In. Dislocation-mediated alloy segregation has been also considered [4].

This work presents the InAlN layers and InAlN/InGaN structures grown by PAMBE on low dislocation density (~10^5 cm^{-2}) Ammomo-GaN substrates. The initial substrate miscut varied from 0.7° to 4°, resulting in a decrease of the atomic terrace width from ~20 nm to ~4 nm. Surface morphology, indium incorporation and InAlN homogeneity was studied as a function of growth temperature, substrate miscut and metal/nitrogen excess grown conditions. We will discuss the results obtained on high-quality GaN substrates in reference to earlier reports on GaN/Sapphire templates [5].

[1] R. Butté, J. F. Carlin, E. Feltin, M. Gonschorek, S. Nicolay, G. Christmann, D. Simeonov, A. Castiglia, J. Dorsaz, H. J. Buehlmann, S. Christopoulos, G. B. H. v. Högersthal, A. J. D. Grundy, M. Mosca, C. Pinquier, M. A. Py, F. Demangeot, J. Frandon, P. G. Lagoudakis, J. J. Baumberg, and N. Grandjean, *Journal of Physics D: Applied Physics* **40,** 6328 (2007).
[2] G. Cosendey, J.-F. Carlin, N. A. K. Kaufmann, R. Butté, and N. Grandjean, *Applied Physics Letters* **98,** 181111 (2011).
[3] S. Choi, F. Wu, R. Shivaraman, E. C. Young, and J. S. Speck, *Applied Physics Letters* **100,** 232102 (2012).
[4] Q. Y. Wei, T. Li, Y. Huang, J. Y. Huang, Z. T. Chen, T. Egawa, and F. A. Ponce, *Applied Physics Letters* **100,** 092101 (2012).
[5] S. Fernandez-Garrido, Z. Gacevic, and E. Calleja, *Applied Physics Letters* **93,** 191907 (2008).

Germanium doping of Cubic $Al_xGa_{1-x}N$ Grown by Molecular Beam Epitaxy

Michael Deppe [1], Fabian Tacken [1], Tobias Henksmeier [1], Jürgen W. Gerlach [2], Dirk Reuter [1] and Donat J. As [1]

[1] *University of Paderborn, Department of Physics, Warburger Str. 100, 33098 Paderborn, Germany*
[2] *Leibniz Institute of Surface Engineering (IOM), Permoserstr. 15, 04318 Leipzig, Germany*

Germanium has recently emerged as a well-suited alternative to silicon for n-type doping of both wurtzite and zinc blende GaN. The ternary alloy $Al_xGa_{1-x}N$ can be employed to extend the emission of nitride-based structures further into the ultraviolet spectral region. Only little work on Ge-doping of wurtzite $Al_xGa_{1-x}N$ has been published. To the best of our knowledge, no experiments on Ge-doping of zinc blende $Al_xGa_{1-x}N$ have been reported yet.

In this work, we report on the growth by plasma assisted molecular beam epitaxy and characterisation of Ge-doped cubic $Al_xGa_{1-x}N$ layers with Al mole fractions $0 \leq x \leq 0.6$. The Al mole fraction x is determined by high resolution X-ray diffraction and energy dispersive X-ray spectroscopy. For each Al content, both a Ge-doped and a nominally undoped cubic $Al_xGa_{1-x}N$ sample are grown. A constant Ge concentration of around 10^{18} cm^{-3} is targeted for all doped $Al_xGa_{1-x}N$ samples. Time-of-flight secondary ion mass spectrometry (TOF-SIMS) verifies the incorporation of Ge into the layers and by capacitance-voltage (CV) measurements a nearly constant dopant concentration N_D of about 6×10^{18} cm^{-3} is estimated in all doped $Al_xGa_{1-x}N$ samples.

However, with increasing Al content a linear increase of O impurities is found by SIMS measurements. Since O itself acts as a donor in the group III-nitrides the electrical and optical properties as revealed by CV and photoluminescence (PL) are strongly influenced by the unintentional incorporation of O at higher Al contents, e.g. the undoped samples show a strong n-type conductivity. PL spectra taken at 13 K show a broadening and a blue shift of the donor-acceptor emission due to the Ge doping and at higher Al concentrations also due to an increasing background doping. However, due to similar donor binding energies no separation in the donor-acceptor emission ascribable to the different donors can be observed.
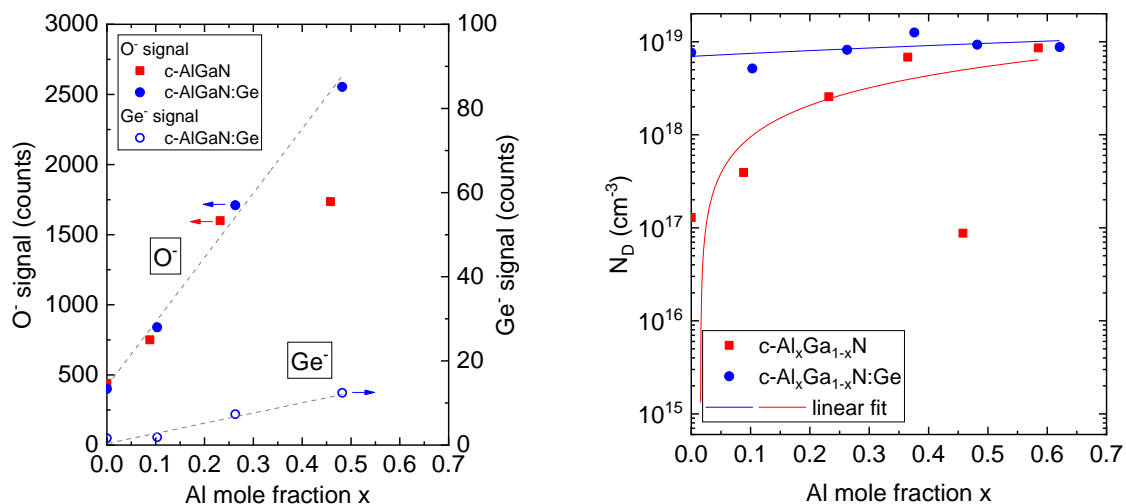

Fig 1: (left) TOF-SIMS intensities of the Ge$^-$-signal (open blue circle) and O$^-$-signal versus Al mole fraction.

(right) Donor concentration N_D measured by CV versus Al content for nominally undoped cubic $Al_xGa_{1-x}N$ samples (red squares) and Ge doped $Al_xGa_{1-x}N$ samples with an intended donor concentration of about 10^{18} cm^{-3} (blue circles).

Material Redistribution during Thermal Annealing of GaN Nanocolumns and Conditions for Their Maskless Overgrowth by MOVPE

Vitaly Z. Zubialevich [1]**, Pietro Pampili** [1,2] **and Peter J. Parbrook** [1,2]

[1] *Tyndall National Institute, University College Cork, T12 R5CP Cork, Ireland*
[2] *School of Engineering, University College Cork, Cork, Ireland*

Using bottom-up approaches, both by metalorganic chemical vapour deposition (MOCVD) and molecular beam epitaxy, with optimised conditions allow formation of GaN nanocolumns (NCs) with no extended defects (free of dislocations). However, precise control of NC doping and their dimensions (mainly height), obtaining high density arrays, and the general complexity of the techniques (nanomasking for selective are growth, pulsed MOVPE etc.) are some weak points of these bottom-up approaches. Many of the above issues can be easily addressed by various top-down or hybrid approaches [1].

We recently developed a flexible hybrid top-down–overgrowth technique using nanosphere lithography for fabrication of high fill factor, locally ordered arrays of GaN NCs with very narrow standard deviation in their height. Here we report the evolution of GaN NC profiles at thermal annealing, as part of a method to allow optimal maskless (with no passivation of areas in between NC) overgrowth of them by MOVPE.

GaN NCs prepared without capping, and with a thin SiO_2 cap on the top c-plane facet, were annealed at 300 mbar, under different temperatures and ambient gases (H_2 and N_2) in presence of ammonia (3/8 of total flow). It was found that while no significant change in NC shape happens (for both uncapped or capped NCs) until $T \geq 1000°C$ in H_2+NH_3 (10 min), those annealed (for the same time) at 900°C in N_2+NH_3 already show a perceptible deterioration of their c-plane top (uncapped) and the formation of the six non-polar facets (both capped and uncapped). The deterioration of c-plane facets (albeit without formation of the non-polar hexagonal sidewalls) for NCs annealed in ambient H_2 only becomes notable at 1050°C, and this process escalates with the further increase of temperature. Finally, at 1100°C uncapped NCs lose material from their tops so fast that the excess of Ga adatoms manage to redeposit on NCs' sidewalls forming six non-polar facets.

Surprisingly, for the uncapped NCs annealed in ambient N_2, the extent of reshaping was found to be non-monotonic with temperature, but showed a distinct maximum at 950°C. Similar to the 1100°C in H_2 case, the NCs expanded laterally, accounted for by the fast decrease in NC height. However, even capped NCs annealed at this temperature show some perceptible lateral growth. As material desorption from their capped with SiO_2 c-plane facets was supressed, the growth must be for the account of material desorbed from the regions in between NCs. This result gave a hint on identifying suitable MOVPE conditions for a maskless NC overgrowth aiming for their controlled lateral expansion.

Such an overgrowth was successfully realised resulting in NC arrays with significantly improved fill factors (Fig.). Due to capping of GaN NCs used for the overgrowth, their initial height (top level) was preserved unchanged which might be an important control measure for potential device fabrication using such uniform NC arrays.
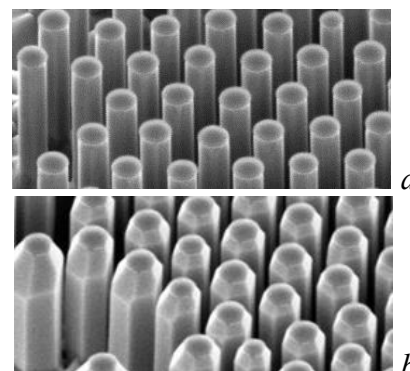

Fig. – Capped GaN NCs before (*a*) and after (*b*) the overgrowth. Actual images' width – 5 μm.

[1] P. R. Narangari, S. K. Karuturi, M. Lysevych, H. H. Tan, C. Jagadish, *Nanotechnology*, **28**, 154001 (2017).

Surface-enhanced Raman scattering in graphene induced by $Al_xGa_{1-x}N$/GaN axial heterostructure nanowire substrate

Jakub Kierdaszuk [1]**, Mateusz Tokarczyk** [1]**, Krzysztof M. Czajkowski** [1]**,**
Aleksandra Krajewska [2,3]**, Zbigniew R. Zytkiewicz** [4]**, Grzegorz Kowalski** [1]**,**
Tomasz J. Antosiewicz [1]**, Maria Kamińska** [1]**, Andrzej Wysmołek** [1]**, Aneta Drabińska** [1]

[1] *Faculty of Physics, University of Warsaw, Pasteura 5, Warsaw, Poland*
[2] *Institute of Electronic Materials Technology, Wólczyńska 133, Warsaw, Poland*
[3] *Institute of Optoelectronics, Military University of Technology,*
Kaliskiego 2, Warsaw, Poland
[4] *Institute of Physics, Polish Academy of Sciences, Lotników 32/46, Warsaw, Poland*

GaN nanowires (NWs) with equal heights were reported as an efficient platform for surface-enhanced Raman scattering in graphene [1]. The presence of local nanogating of graphene deposited on GaN NWs suggested the electromagnetic mechanism of the effect. In wurtzite GaN high spontaneous and piezoelectric polarization is present. Recently it was shown that NW structure reduces free carrier screening of polarization charges [2]. Therefore, larger aluminium content in AlGaN NWs should increase the polarization charge concentration induced at NWs top surface and furthermore increase nanogating effect of graphene. To investigate the influence of polarization charges induced by spontaneous and piezoelectric polarization on Raman spectra, graphene transferred onto GaN NWs with 100 nm $Al_xGa_{1-x}N$ caps with x varying between 0 and 1 was studied in this work (Fig. 1a). One order of magnitude enhancement of Raman spectra intensity in all the investigated samples was found, when comparing with graphene deposited on GaN epilayer (EPI) (Fig. 1b). However, analysis of the enhancement factor of each band intensity indicated no explicit correlation with aluminium content in $Al_xGa_{1-x}N$ caps (Fig. 1c). On the other hand, detailed studies of Raman bands showed that aluminium content significantly impacts carrier concentration in graphene, which confirms influence of aluminium content on polarization charge density and reduction of screening effect. For direct determination of polarization induced electric field in NWs photoreflectance measurements are in progress. Numerical simulations indicate that energy of surface plasmon in graphene is far from laser line used for Raman excitation. Therefore, our results indicate the chemical mechanism of the observed enhancement of graphene Raman spectra, in contrary to electromagnetic mechanism commonly observed in other systems.
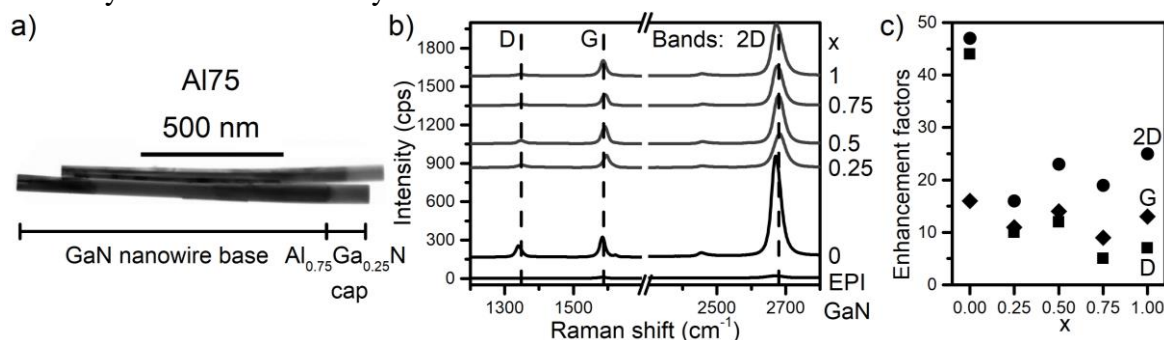

Figure 1: a) TEM image of axial heterostructure NWs, b) Raman spectra of investigated samples obtained by 532 nm laser excitation, c) enhancement factors of each graphene bands.

[1] J. Kierdaszuk, et al., *Carbon* **128**, 70 (2018)
[2] N. Jamond et al., *Nanotechnology* **27**, 325403 (2016)

Two-step epitaxial growth of GaN nanowires by MOVPE

Kohei Sasai[1], Nanami Goto[1], Kazuyoshi Iida[1], Naoki Sone[1], Atushi Suzuki[1], Kyohei Nokimura[1], Minoru Takebayashi[1], Hideki Murakami[1], Satoshi Kamiyama[1], Tetsuya Takeuchi[1], Motoaki Iwaya[1] and Isamu Akasaki[1,2]

[1] *Meijo Univ., 501 Icchoume, Shiogamaguchi, Tenpaku-ku, Nagoya-shi, Aichi, Japan*
[2] *Akasaki Research Center, Nagoya Univ., Furou-cho, Chikusa-ku, Nagoya-shi, Aichi, Japan*

Nitride-based nanowires (NWs) and multi-quantum shell (MQS) active materials have attracted much attention for high-performance optoelectronic device applications. The advantages of NW/MQS structure might be the absence of dislocations, elimination of quantum confined Stark effect by use of the non-polar m-plane, and its flexibility of MQS active area by changing the height of the NWs. However, stable and uniform growth of NWs is not so easy because of the tiny crystals. In this paper, we report the result of two-step NW growth using nucleation layer to realize in-plane uniformity and reproducibility.

Two-step GaN-NW growth is consisting of an nucleation layer growth at 940 °C by continuous supply-mode MOVPE and NW growth at high temperature (1010 and 1025 °C) by pulsed-mode MOVPE. The shape and in-plane uniformity of the NWs were examined by SEM. As a reference, the NW grown at 1010 °C without the nucleation layer was prepared.

Figure 1 (a) shows the SEM image of the NWs grown without the nucleation layer, and (b) shows the NWs grown with the nucleation layer. By using the nucleation layer, island growth was decreased by 30 %. Figure 2 shows the diameter and height of the NWs for three different growth conditions. While the first two conditions (without nucleation and two-step growth with 1010 °C) resulted in the similar height and diameter, the two-step growth at 1025 °C provided greater height and slightly smaller diameter. The nucleation layer enable the NWs to be grown at high temperature, and it enhances height-direction growth. It also suppress the island growth.
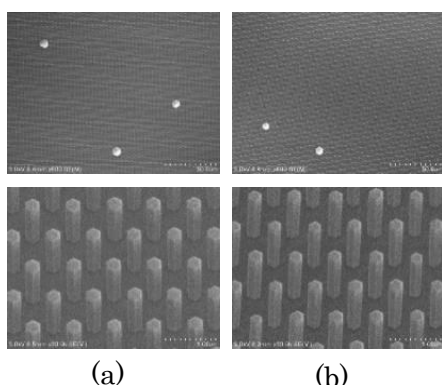
(a)   (b)

Figure 1. SEM images of NWs, (a) without nucleation layer and (b) with nucleation layer grown at 1025 °C. Upper images were taken with low magnification, and lower ones were taken with high magnification.
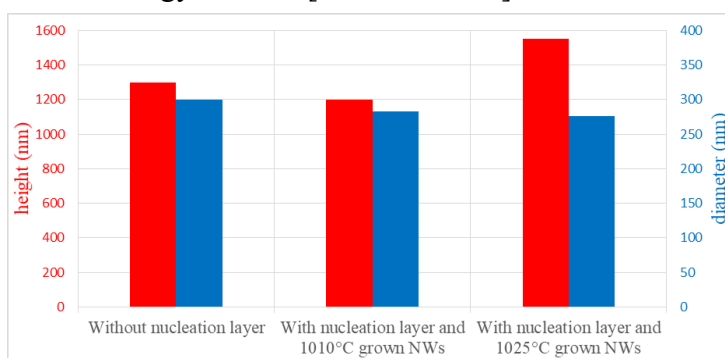

Figure 2. Diameter and height of NWs.

Invited lecture

EdgeFET Devices Fabricated on 2DEG GaN/AlGaN Heterostructures for Basic and Applied Sciences

G. Cywiński[1,2], P. Sai[1,2], D. B. But[1,2], P. Prystawko[1], M. Grabowski[1], P. Kruszewski[1], I. Yahniuk[1], P. Wiśniewski[2], B. Stonio[2], M. Słowikowski[2], B. Grzywacz[1,2], G. S. Simin[4] K. Nowakowski-Szkudlarek[1], J. Przybytek[1], S. L. Rumyantsev[3], W. Knap[1,2,5]

[1]*Institute of High Pressure Physics PAS, ul. Sokolowska 29/37, 01-142, Warsaw, Poland*
[2] *CEZAMAT, Warsaw University of Technology, 02-822, Warsaw, Poland*
[3]*National Research University of Information Technologies, St. Petersburg, 197101, Russia*
[4]*Department of Electrical Engineering, University of South Carolina, Columbia, 29208, USA*
[5]*Laboratoire Charles Coulomb, University of Montpellier, CNRS, Montpellier, 34095, France*

We report on our study of GaN/AlGaN heterostructure field effect transistors (FETs) with gates based on two lateral Schottky contacts [1]. The proposed here a new design of FET (see fig. 1), which two side gates are Schottky diodes to 2DEG, we named as EdgeFET. Due to technological developments in nitrides, even for EdgeFET devices with the mesa width 2-4 μm, we were able to completely close the 2DEG conduction channel. Moreover, for typical pinch-off voltages (which are in range of -30 V up to -15 V) we observed small values of gate currents (i.e.

Fig. 1. Schematic views of GaN/AlGaN EdgeFET under study.

low gate leakage). The main feature of this EdgeFET device is possibility of a fine tuning of the 2DEG conduction channel width by electrical field – the gate voltage – until it is fully closed. Our Synopsys Sentaurus simulations are consistent with experiment data and predict, that in the first stage, by applying the gate voltage, we are mainly changing the channel width without significant changes in the 2DEG sheet density, but in the second stage (near to pinch-off voltage) we are also changing the 2DEG density. The electrical control of the channel width in this wide range is attractive for terahertz (THz) resonant detection and emission applications. In particular: THz detection experiments showed lower responsivity and the resonant maxima were much broader than predicted by the theory [2, 3]. These effects should depend on transistor channel dimensions. We expect that one of the possible reason for this discrepancy is the existence of the oblique modes in investigated previously transistors, where the channel width is bigger than the channel length [4]. However, oblique modes can be suppressed by using the one dimensional (1D) channel and this is the first foreseen scientific task for EdgeFETs. This paves the way to the resonant THz detector, which can be tunable by the gate voltage. The second scientific task is its application for 1D transport measurements at mK range, where in the case of this electrically formed EdgeFET channel, it should not suffer of damaged sidewall effects usually noticeable in etched nanostructures.

In conclusion: our EdgeFET showed possibility to electrically control 2DEG transport down to 1D and finally to fully pinch-off it. These structures are very attractive objects for semiconductor physics towards their applications and important basic science experiments.

REFERENCES
[1] G. Cywiński, et al., *Appl. Phys. Lett.* **112**, 133502 (2018).
[2] M. I. Dyakonov, *Comp. Rend. Phys.* **11**, 413-420 (2010).
[3] W. Knap and M. Dyakonov, in "Handbook of Terahertz Technology" edited by D. Saeedkia (Woodhead Publishing, Waterloo, Canada, pp. 121-155 (2013).
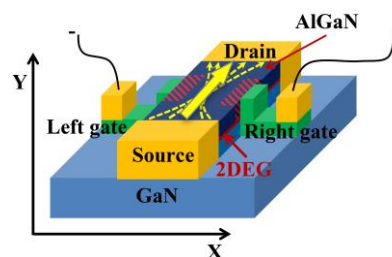[4] S. Boubanga-Tombet, et al., *Appl. Phys. Lett.* **92**, 212101 (2008).

AlGaN/GaN EdgeFET Based on Two Lateral Schottky Barrier Gates as Terahertz Detector

P. Sai[1,2], D. B. But[1,2], P. Prystawko[1], I. Yahniuk[1], P. Wiśniewski[2], B. Stonio[2], M. Słowikowski[2], B. Grzywacz[1,2], K. Nowakowski-Szkudlarek[1], J. Przybytek[1], S. L. Rumyantsev[3], W. Knap[1,2,4], G. Cywiński[1,2]

[1] *Institute of High Pressure Physics PAS, ul. Sokolowska 29/37, 01-142, Warsaw, Poland*
[2] *CEZAMAT, Warsaw University of Technology, 02-822, Warsaw, Poland*
[3] *National Research University of Information Technologies, St. Petersburg, 197101, Russia*
[4] *Laboratoire Charles Coulomb, University of Montpellier, CNRS, Montpellier, 34095, France*

We report on a study of AlGaN/GaN heterostructure field effect transistors with gate based on lateral Schottky contacts [1]. A possibility to control channel width in a wide range is interesting for terahertz (THz) resonant detection and emission application using field effect transistor (FET) [2]. Particularly, detection experiments showed lower responsivity and the resonant maxima much broader than predicted by the theory [2, 3] and depends on the transistor channel dimension. One of the possible reasons for this discrepancy is the existence of the oblique modes in the transistors with the channel width higher than the channel length [4].

Using AlGaN/GaN heterostructure, we made two types of transistors. First is field effect transistor with the fin-shaped channel (FinFET), where gate crosses whole channel and second, where unlike common two-dimensional transistors designs, the gates were deposited only in adjacent to the edges of the two-dimensional electron gas (2DEG) channel. We suggest EdgeFET short name for this device. In this case, a lateral gate based on side Schottky contacts between the gate metal and 2DEG. The lateral Schottky barriers demonstrate low leakage current in the wide range of reverse bias as shown in Fig. 1a. The typical length and width of FinFET and EdgeFET channels were
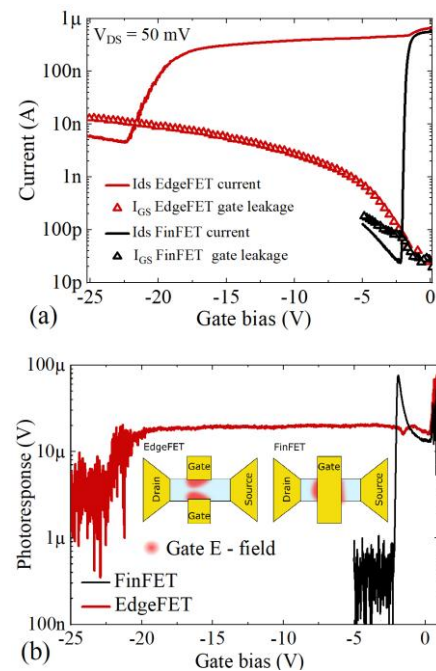

Fig. 1. a) Transport characteristics of EdgeFET and FinFET transistor and gate leakage current characteristic. b) Photoresponses as a function of gate voltage of the same devices at 140 GHz. The inset shows the schematic drawings of a FinFET and a EdgeFET.

in range of 2-4 μm. Figure 1. a. shows transport characteristics of EdgeFET and FinFET. The Edge-FET demonstrated stable photoresponse signal at 140 GHz in the wide range of reverse biasing from -20 V to -5 V (see Fig. 1b).

Control of the side gates of Edge-FET allows changing the width of 2D electron gas and forming a wire-channel, which could be beneficial for observation of plasma wave resonances in THz range [2, 3].

[1] G. Cywiński, et al., *Appl. Phys. Lett.* **112**, 133502 (2018).
[2] M. I. Dyakonov, Comp. Rend. Phys. **11**, 413-420 (2010).
[3] W. Knap and M. Dyakonov, in "Handbook of Terahertz Technology" edited by D. Saeedkia (Woodhead Publishing, Waterloo, Canada, pp. 121-155 (2013).
[4] S. Boubanga-Tombet, et al., *Appl. Phys. Lett.* **92**, 212101 (2008).

A Study on 2DEG Properties of AlGaN/GaN Structures Formed on Stepped GaN Surfaces for Vertical Power Devices

A. Yamamoto, K. Kanatani, S. Makino, and M. Kuzuhara

Graduate School of Engineering, University of Fukui, 3-9-1 Bunkyo, Fukui 910-8507, Japan

GaN-based vertical FETs with a trenched MIS gate are extensively studied for power applications[1]. Such FETs, however, have problems of small drain current due to low electron mobility[2] and of large hysteresis due to high interface states[3] at the insulator/semiconductor interface. Provided that an AlGaN layer with excellent interface properties is grown directly on the trenched GaN surface, the MIS gate can be replaced by an AlGaN/GaN gate with a 2DEG channel. This replacement is expected to give effective solutions to the main problems in MIS-gate vertical FETs. In order to realize such vertical HEMTs, we have to establish technologies for the regrowth of an AlGaN layer with excellent interface properties and a uniform thickness on a GaN trench. Recently, we have succeeded in obtaining an electron mobility as high as 1350 cm^2/Vs in an AlGaN/GaN structure with an AlGaN layer grown directly on an RIE-treated c-plane GaN surface[4].

In this paper, the MOVPE growth of AlGaN on stepped GaN substrates and the 2DEG properties of the AlGaN/GaN structures prepared were studied. As a substrate, c^+-plane n^--GaN (6 μm thick) on sapphire was used. Figure1 shows the sample structure for the evaluation of 2DEG properties of stepped surface. Figure 2 shows a cross-sectional view of a 100-nm thick AlGaN layer (with an n^+-GaN cap) regrown on a trenched GaN. This sample was prepared to check the uniformity of AlGaN thickness. One can see that an AlGaN layer with a relatively uniform thickness (the fluctuation is within ±20 % through the top, slope and bottom of the trench) was successfully grown. In order to evaluate the 2DEG properties of AlGaN/GaN structure, samples (with a 30 nm-thick AlGaN) having a different number of step (1~7) were prepared. Figure 3 shows the resistance of the samples as a function of number of steps. The $R_{step=0}$ and slope/step give the $n_s \cdot \mu$ products of the c-plane (top and bottom regions) and of the step, respectively. Table 1 summarizes the $n_s \cdot \mu$ products for the flat (c-plane) and the inclined plane and their ratio, obtained from Fig. 3. It was found that the flat plane (c-plane) had a $n_s \cdot \mu$ product of about 1 x 10^{16} 1/Vs and that of the inclined plane with an angle of about 45˚ was 30 % of that of the c-plane. Thus, the results obtained in this study give important information to the design and fabrication of a 2DEG-channel vertical power device.

Refs. 1) Appl. Phys. Express **7**, 021002 (2014), 2) Appl. Phys. Express **9**, 121001 (2016), 3) IEEE Trans. Electron Devices **64**, 1554 (2017), 4) Jpn. J. Appl. Phys. **57**, 045502 (2018).
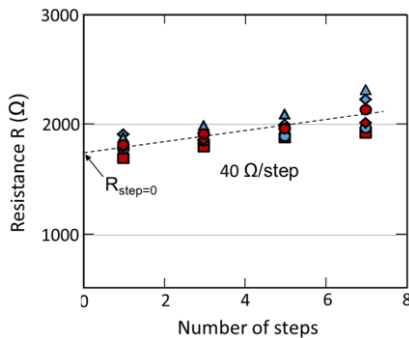

Fig.3. Resistance R of the samples with a step height of 1.4 μm, as a function of number of steps.
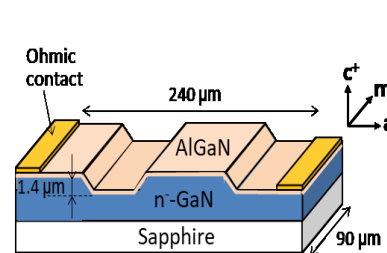

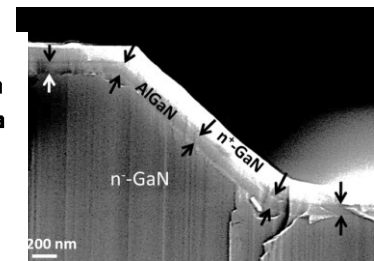Fig 1. Sample structure for the evaluation of 2DEG properties of stepped surface.

Fig.2. Cross-sectional SEM view of a 100-nm thick AlGaN layer grown on trenched GaN. Arrows show the boundary of the AlGaN layer.

Table 1. $n_s \cdot \mu$ products for the flat (c-plane) and the inclined planes and their ratio, obtained from Fig. 3.

$n_{sc} \cdot \mu_c$ product for flat regions (c plane) (1/Vs)	$n_{si} \cdot \mu_i$ product for inclined plane (1/Vs)	Ratio $n_{si} \cdot \mu_i / n_{sc} \cdot \mu_c$
9.6 x 10^{15}	2.9 x 10^{15}	0.30

Modified Small-Signal Model for the High Frequency GaN-on-Si HEMT with the Leaky Buffer

Yung-Ting Ho[1], Kai-Chieh Hsu[2], Li-Cheng Chang[2], and Chao-Hsin Wu[1,2]

[1] *Graduate Institute of Photonics and Optoelectronics, National Taiwan University,*
[2] *Graduate Institute of Electronics Engineering, National Taiwan University,*
No. 1, Sec. 4, Roosevelt Road, Taipei City, 10617, Taiwan (R.O.C)

GaN-based high electron mobility transistors (HEMTs) have excellent material properties for high power and high frequency amplifiers [1,2]. In recent years, power microwave device using GaN HEMTs on Si substrate attracts much attention due to the combination of high performance and low-cost production. However, because of the large lattice mismatch between (Al)GaN and Si, large amounts of buffer trap is induced which affects the device characteristics especially in the high frequency regime. Power loss induced by the leaky buffer leads to an unacceptable deviation of S-parameter extraction from the conventional small-signal model. In this work, a modified small-signal model with consideration of the leaky buffer is proposed to improve the accuracy of the modeling during the S-parameter fitting.

Device is started with Ohmic contact with Ti/Al/Ni/Au metallization followed by mesa isolation through ICP-RIE. Afterward, e-beam lithography is implemented to define rectangular gate and thick gate stack Ni/Au (15/300 nm) is used to reduce gate resistance. Finally, a standard back-end process is formed including polyimide planarization and thick Au-plated process with common source GSG probing layout. The device characterization was performed on devices with geometries of $L_G/L_{GS}/L_{GD}/W_G$ = 0.1/1/1/75 µm.

The transfer characteristics are shown in Fig. 1, the threshold voltage is -6.2 V and peak g_m is 226 mS/mm. Fig. 2 shows the modified small-signal model we proposed with the consideration of leaky buffer. The additional capacitance and resistance compared to the conventional model (dashed square) are added to improve the fitting accuracy of S-parameter [3]. Fig. 3 shows the Smith chart of OPEN test structure and the measurement is in a frequency of 0.04-40 GHz. The red line indicates the measurement result of test structure and fitting result with the modified model exhibit consistent trend to the measurement data. Fig. 4 shows the |h21| and U at bias point of V_d = 6 V and V_g = -5.4 V. The f_T of 62.66 GHz and f_{max} of 39.15 GHz are obtained by extrapolating under slope of -20 dB/dec.

In conclusion, we proposed a modified small-signal model with consideration of leaky buffer which can improve the fitting accuracy of S-parameter. The additional capacitance and resistance in the modified model lead to highly consistent between measurement and fitting result. The de-embedding f_T and f_{max} of the device with modified model is 62.66 and 39.15 GHz respectively.
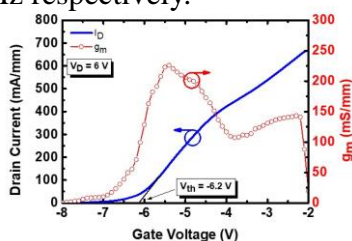

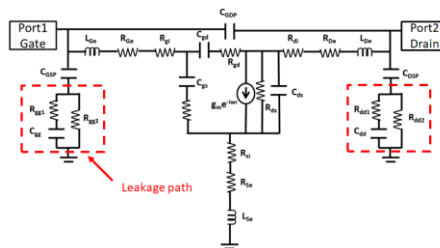Fig. 1. The transfer characteristics of the device

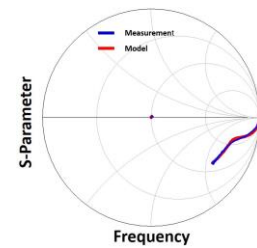Fig. 2. Modified small-signal model with the additional capacitance and resistance.

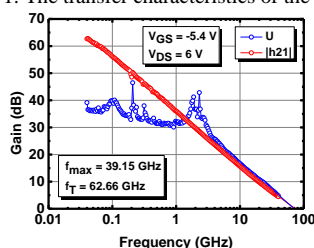Fig. 3. Smith chart of measurement data and fitting result with modified model .

Fig. 4. f_T and f_{max} of device after de-embedding with modified model

Reference: [1] P. D. Christy *et al.*, *Electronics Letters*, vol. 51, no. 17, pp. 1366-1368, 8 20 2015. [2] W. Xing et al., *IEEE Electron Device Letters*, vol. 39, no. 1, pp. 75-78, Jan. 2018. [3] Yaser A. Khalaf, Doctoral dissertation, July 2000.

Schottky Barrier Diodes Fabricated on Miscut *m*-plane Substrates

**Yuto Ando[1], Kentaro Nagamatsu[2], Atsushi Tanaka[2, 3], Manato Deki[2],
Ousmane 1 Barry[1], Shigeyoshi Usami[1], Maki Kushimoto[1], Shugo Nitta[2],
Yoshio Honda[2], and Hiroshi Amano[2, 3, 4, 5]**

[1] *Department of Electrical Engineering and Computer Science, Nagoya University, Furo-Cho,
Chikusa-ku, 464-8603 Nagoya, Japan*
[2] *Institute of Materials and Systems for Sustainability, Nagoya University, Furo-Cho,
Chikusa-ku, 464-8603 Nagoya, Japan*
[3] *National Institute for Materials Science, 1-1, Namiki, 305-0044 Tsukuba, Japan*
[4] *Akasaki Research Center, Furo-Cho, Chikusa-ku, 464-8603 Nagoya, Japan*
[5] *Venture Business Laboratory, Furo-Cho, Chikusa-ku, 464-8603 Nagoya, Japan*

Non-polar GaN is promising for applications in power-switching devices, because there is no polarization-induced charge at an heterojunction interface, and enhancement- mode HEMTs can be fabricated.[1] Also we reported that impurity incorporation into unintentionally doped epi-layers can be suppressed below the SIMS detection limit using *m*-plane a miscut substrate, indicating that the vertical structure devices with a very low-impurity-concentration drift layer can be realized on *m*-plane.[2] The proposed study aims to investigate and characterize the Si doped layers grown on several miscut *m*-plane substrates by fabricating Schottky barrier diodes (SBDs) on the substrates and comparing them with *c*-plane devices.

We used miscut *m*-plane substrates with the following three types of angles and directions: 5° toward [0001] (*c*+5), 5° toward [000−1] (*c*−5) and 0.5° toward [−12−10] (*a* 0.5) prepared by slicing *c*-plane HVPE-grown bulk GaN (N_D-N_A=2×10^{17} cm^{-3}). We used MOVPE to grow 5µm layers of Si-doped GaN on each substrate. We formed backside ohmic contacts by depositing Ti/Al/Ti/Au and sintering. We then patterned Ni/Au Schottky contacts on the surface using a metal shadow mask. We prepared reference devices simultaneously on the *c*-plane by the same process.

Fig. 1 shows the result of a SIMS analysis of the epi-layer. The C concentration for *c*−5 is less than that for the other miscut substrates. The Si concentrations are independent of the miscut and are almost the same, i.e., 2×10^{16} cm^{-3}. Fig. 2 shows measured and calculated reverse current-voltage characteristics of the SBDs. The calculation is based on thermionic-field-emission (TFE) theory using the barrier heights obtained from the forward characteristics. [3] The characteristics for *c*−5 are not close to the calculation due to its surface roughness. On the contrary, we obtained flat surfaces for the *c*-plane and *a* 0.5 SBDs, and they were in agreement with the TFE current. Thus, although *c*−5 has good impurity concentrations, the surface morphology must be improved for device fabrication.
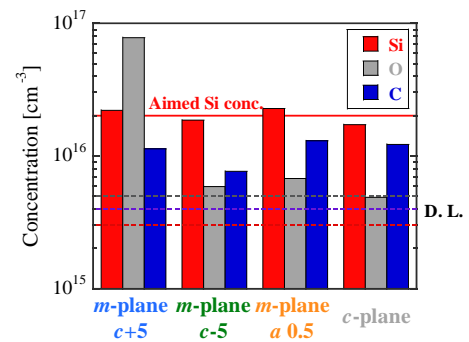

Fig.1 Impurity concentrations in epi-layers analyzed by SIMS.
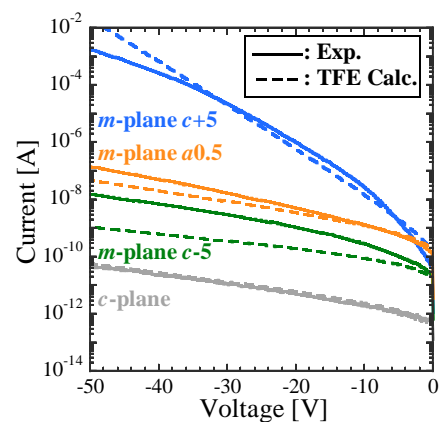
Fig.2 Measured and calculated reverse current-voltage characteristics of SBDs.

[1] T. Fujiwara *et al.*, Appl. Phys. Exp. **4**, 096501 (2011).
[2] A. Tanaka *et al.*, Phys. Status Solidi A 1700645 (2017). [3] J. Suda *et al.*, Appl. Phys. Exp. **3**, 101003 (2010).

AlGaN/GaN HEMT Heterostructures Grown by Ammonia and Combined Plasma-Assisted/Ammonia MBE on Sapphire Substrates

Evgenii V. Lutsenko [1], Mikalai V. Rzheutski [1], Aliaksei G. Vainilovich [1], Illia E. Svitsiankou [1], Varvara A. Shulenkova [1], Gennadii P. Yablonskii [1], Alexey N. Alexeev [2], Stanislav I. Petrov [2] and Ahmed Y. Alyamani [3]

[1] *Institute of Physics of NAS of Belarus, 68 Nezalezhnasti Ave. 220072, Minsk, Belarus*
[2] *SemiTEq JSC, 27 Engels Ave. 194156, Saint-Petersburg, Russia*
[3] *KACST, National Nanotechnology Center. P.O. BOX 6086, 11442 Riyadh, Saudi Arabia*

While one of the most important tasks of nitride epitaxy is a low-defect growth on Si substrates, an epitaxy on sapphire substrates is also an actual task for some applications (e. g. sensors). In this work we report on optimization of ammonia molecular beam epitaxy (MBE) of buffer AlN layers on sapphire substrates as well as demonstrate high electron mobility transistor (HEMT) heterostructures grown by both ammonia and combined plasma-assisted (PA) /ammonia MBE on STE3N SemiTEq MBE system. In addition, luminescence properties and stimulated emission were measured for the heterostructures.

A series of 0.28 μm thick AlN layers was grown on 2-inch sapphire substrates in a STE3N MBE system at different growth conditions (NH_3 flow and substrate temperature T_{gr} were varied from 30 to 200 sccm and from 800°C to 1190°C respectively). A substantial improving of surface morphology with increase of NH_3 flow from 30 to 100 sccm was observed by atomic force and scanning electron microscopes. The lowest root-mean-square roughness of 0.7 nm was measured for AlN layer grown at 100 sccm NH_3 flow and $T_{gr} = 1085°C$. A further increase of NH_3 flow to 200 sccm didn't improve surface quality significantly. Ammonia flow of 100 sccm and $T_{gr} = 1085°C$ were accepted as near optimal values providing growth of well-ordered AlN layer with satisfactory surface smoothness. The optimal substrate temperature for growth of GaN and AlGaN layers $T_{gr} = 945°C$ was determined which corresponds to the beginning of GaN thermal decomposition.

Using the determined optimal growth conditions, two HEMT heterostructures were grown. An active structure contained 200 nm thick GaN layer and 25 nm thick $Al_{0.3}Ga_{0.7}N$ barrier layer including Si-doped interlayer. Buffer structure consisted of 700 nm thick AlN, 280 nm thick $Al_{0.3}Ga_{0.7}N$ and 420 nm thick $Al_{0.1}Ga_{0.9}N$ separated by gradient-composition AlGaN layers. The active and buffer layers were grown by ammonia MBE for both samples. The only difference between the heterostructures was growth conditions of a 70 nm thick nucleation AlN layers. While the AlN nucleation layer for the first structure was grown in ammonia MBE mode, the nucleation layer for the second one was grown by PA MBE using migration-enhanced epitaxy approach [1]. The HEMT heterostructure grown by the combined PA/ammonia MBE demonstrated slightly better two-dimensional electron gas (2DEG) properties (mobility of ~2000 cm^2/Vs at density of 1.2×10^{13} cm^{-2}). In the figure, the results are given in comparison with our older ones [2]. Optical, photoluminescent and laser properties of HEMT heterostructures were investigated and discussed.
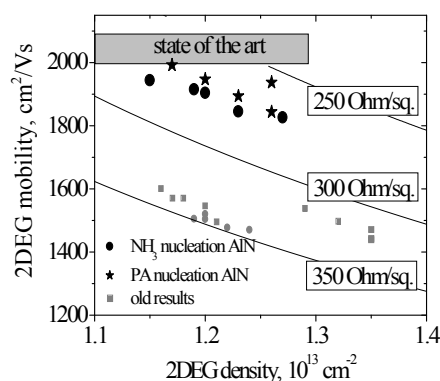
[1] V. N. Jmeric, et al., *J. Mater. Res.* **30** 2871 (2015).
[2] E. V. Lutsenko, et al., *Phys. Stat. Sol. A* Published online DOI: 10.1002/pssa.201700602.

MOCVD of Boron Nitride Films on Sapphire

J. M.Baranowski and P.A.Caban, P.P.Michalowski, J.Gaca, M.Wójcik and P.Ciepielewski

Institute of Electronic Materials Technology, Warsaw, POLAND

Boron nitride films were grown on 2-inch sapphire substrates by MOCVD method. The growth was done at temperature 1050^0C using various pressures and V/III ratios. Pulsed source injection mode with triethylborane (TEB) and ammonia (NH_3) precursors were applied. The growth was performed under Ar or H_2 flow.

It was observed, in agreement with previous results [1], that there may be realized two kind of growth modes of BN films: the continuous and self-terminated one. The continuous one is connected with 3D growth and leads to relatively thick, of 10-100nm thickness films, however, with a poor morphology of the surface. The self-terminated mode leads to very thin BN films of the order of 2nm thickness with atomic smooth surfaces. Transition between continuous 3D and self-terminated growth mode predominantly depends on the V/III ratio.

The grown BN films were characterized by a wide range of experimental techniques such as SIMS, XRD, XRR, XPS, TEM, SEM, AFM, Raman, ATR spectroscopy. The hexagonal sp^2 structure of grown BN films was confirmed by XRD and TEM. It was also found that hBN films grown under Ar flow are not uniform and are strongly contaminated with carbon. The contamination with C of the order of a few percent established by SIMS and technique, for both continuous and self-terminated growth modes. Different properties of BN films have been obtained for BN films grown under H_2 flow. SIMS measurements revealed also that BN films grown under H_2 flow are very uniform and have substantial reduced carbon concentration by about five orders of magnitude. It was shown that mechanism of C contamination is connected with reactions between TEB and NH_3 which takes place in the presence of Ar. The mechanism of elimination excess of carbon from BN films is connected with reaction of C with H_2. That reveals the essential role of H_2 in the BN growth.

[1] Q.Paduano, M.Snure, D.Weyburne, A.Kiefer, G.Siegel, and J.Hu, *J.Crystal Growth*, **449**, 148 (2016)

Investigation of MOVPE Boron Nitride Growth

K. Pakuła, M. Tokarczyk, A. Dąbrowska, J. Borysiuk, G. Kowalski, K. Korona, A. Wysmołek, R. Stępniewski

Faculty of Physics, University of Warsaw, Pasteura 5, 02-093 Warsaw, Poland

Boron nitride was grown on sapphire substrates by metalorganic vapor phase epitaxy (MOVPE) with triethylboron and ammonia as B and N precursors. Continuous [1] and pulsed growth methods [2,3] were investigated. Growth was performed by covering a wide range of thermodynamic parameters to establish their influence on the synthesis efficiency and epilayer properties.

The obtained BN layers were characterized using several methods: X-ray diffraction, Raman spectroscopy and a variety of microscopic techniques such as scanning electron microscopy, transmission electron microscopy and atomic force microscopy. These investigations provided thorough information about the crystallographic lattice properties including subsequent layer alignment, as well as bonding type, structural defects and built-in strain in the grown material. Optical methods including absorption and photoluminescence provided information about band structure and optically active defects in the boron nitride layers.

Some unusual dependencies concerning the BN synthesis kinetic originating from complex reactions between boron and nitrogen compounds in gas-phase and on the crystal surface, were observed. Depending on the MOVPE process conditions different types of BN layers can be grown, ranging from nano-polycrystalline, through micro-crystalline with different grain shapes, to monocrystalline material. Different crystallographic structure from semi-amorphous, through turbostratic to rhombohedral and hexagonal can be obtained. A strong influence of the growth conditions on the concentration of optically active mid-band-gap point defects was observed.

The quality of the monocrystalline h-BN layers, presented at this work, is similar to best material reported recently in literature [4,5]. Our material displayed a good crystallographic structure and orientation correlated with the sapphire substrate. Two types of nano-metric objects were observed on the layer surface by AFM - irregular islands caused by non-stoichiometry during the growth, and wrinkles related to the thermal expansion coefficient differences between h-BN and sapphire. Solution of these problems is a main challenge at the current stage of BN growth technology.

The performed technological experiments substantially broadened our understanding of the growth thermodynamics of BN layers. Our findings allow us to implement new methods aiming at a further improvement of the quality of MOVPE grown boron nitride, which is crucial for any possible application.

[1]   Y. Kobayashi, T. Akasaka - J. Cryst. Growth **310** (2008) 5044–5047.
[2]   Y. Kobayashi, T. Akasaka, T. Makimoto - J. Cryst. Growth **310** (2008) 5048–5052.
[3]   S. Majety, T. C. Doan, J. Li, J. Y. Lin, and H. X. Jiang - AIP ADVANCES **3**, 122116 (2013).
[4]   Xin Li, Suresh Sundaram, Youssef El Gmili, Taha Ayari, Renaud Puybaret, Gilles Patriarche, Paul L. Voss, Jean Paul Salvestrini, and Abdallah Ougazzaden - Cryst. Growth Des. (2016), **16**, 3409−3415
[5]   Xu Yang, Shugo Nitta, Kentaro Nagamatsu, Si-Young Bae, Ho-Jun Lee, Yuhuai Liu, Markus Pristovsek, Yoshio Honda, Hiroshi Amano – J. Cryst. Growth **482** (2018) 1–8

Growth of BN thin films by MBE: effect of post thermal annealing

F. Liu[1], P. Wang[1], X. Rong[1], T. Wang[1], Z. Chen[1], B. Sheng[1], X. Zheng[1], S. Sheng[1], F. Xu[1], B. Shen[1] and X. Wang[1]*

[1]*State Key Laboratory for Artificial Microstructure and Mesoscopic Physics, School of Physics, Peking University, Beijing 100871, China*
*Corresponding author's E-mail: wangshi@pku.edu.cn

BN has attracted tremendous interest over the past decades due to the alternative sp^3 (3D) and sp^2 (2D) hybridization, and its promising applications in efficient deep ultraviolet optoelectronics devices [1]. Compared with other III-nitride materials, BN exhibits intrinsic p-type conduction, which provides a new approach to solve the p-type contact bottleneck in AlGaN-based UV-LEDs [2]. Besides, the large exciton binding energy of BN is suitable for realization of high temperature emitting devices. Despite many efforts have been devoted to growth of BN epilayers, there are still severe challenges on the crystal quality and doping controllability in non-metallic substrates [3].

In this work, BN films are grown on sapphire substrates by plasma assisted molecular beam epitaxy (PA-MBE). Reflection high energy electron diffraction (RHEED) is used to in-situ monitor growth behavior. The sp^2 hybridization of the grown BN has been confirmed by X-ray photoelectron spectroscopy (XPS) and Raman scattering measurement. However, it is very difficult to directly crystalline BN layers, as evidenced by the hollow RHEED pattern during growth and the non-detectable diffraction peaks in XRD measurement after growth. This is ascribed to the relatively low temperature in our MBE chamber. We then annealed the as-grown samples in a tubular furnace at 1700°C under nitrogen ambient, which is similar as the case of AlN [4]. The BN (002) diffraction peak is observed at 26.2° after thermal annealing, showing 2D-BN crystallinity. A band gap energy of ~5.50 eV is estimated from XPS measurement, which agrees well with the theoretical predicted and previous reported values [5]. Meanwhile, the DUV emission at 227 nm is also detected by low-temperature cathodeluminescence (CL) measurement. Our work indicates that high temperature will benefit for BN epitaxy. And the combination of MBE and thermal annealing provides an alternative way for high quality 2D-BN.

[1] K. Watanabe et al., *Nature Photonics* **3**, 591 (2009).
[2] T. Tran et al., *Nature nanotechnology* **11**, 37 (2016).
[3] H. Jiang et al., *Semicond. Sci. Technol.* **29**, 084003 (2014).
[4] H. Miyake et al., *Applied physics Express* **9**, 025501 (2016).
[5] M. Silly et al., *Physics Review B* **75**, 085205 (2007).

Invited lecture

Excitonic spectra of ultra-thin epitaxial boron nitride layers grown by MOCVD

A. Grempka, P. Tatarczak, M. Wojtczak, A. Dąbrowska, K. Pakuła, M. Tokarczyk, G. Kowalski, J. Borysiuk, R. Stępniewski, A. Wysmołek

[1] *Faculty of Physics, University of Warsaw, Pasteura 5, 02-093 Warsaw, Poland*

Boron nitride (BN) due to its exceptional physical properties such as high chemical stability, thermal conductivity and wide bandgap energy is a very promising candidate for optoelectronic applications in the deep ultraviolet spectral range. A negative electron affinity makes BN a very promising material for novel thermoemission applications. A large cross section for neutron capture renders BN an outstanding candidate for neutron detectors, while a reported effective p-type doping opens new possibilities of application as a transparent contact in UV emitting devices based on nitrides. The growing interest in BN results also from the fact that it is an excellent substrate, as well as insulating barrier material for hybrid structures composed of graphene, transition metal dichalcogenides and other 2D materials.

The development of various applications based on BN requires high quality layers. It is obvious that the development of technology is strongly correlated with the knowledge of the properties of the material. Despite the growing interest in BN the knowledge regarding its basic properties is still very limited. Here, one should mention longstanding and still vivid discussion about the direct/indirect band gap character of hexagonal boron nitride. [1]

In this work we show that by using ultra-thin, high quality epitaxial layers, detailed absorption studies in the bandgap spectral region of BN can be performed. Epitaxial BN layers with thicknesses in the range of 2-100 nm, were grown by Metal Organic Vapor Deposition (MOCVD) on sapphire. X-ray measurements prove sp^2 ordering, as expected for hexagonal (h-BN) and romboedric (r-BN) structures. Optical measurements performed at low temperature (6K) revealed a very well resolved excitonic absorption line at around 6.15 eV. As verified for several layers with different thicknesses, the absorption coefficient corresponding to this transition is of about 2×10^6 cm^{-1}, which is one order of magnitude larger than for GaN. The spectral shape of the observed excitonic transition resembles the shape observed for direct bandgap semiconductors. A direct character of this transition is confirmed by temperature dependence of the excitonic absorption energy in the temperature range 6-340 K, which is very similar to homoepitaxial GaN.

At first glance, the observation of a direct character of the excitonic absorption in BN would suggest a contradiction to theoretical predictions and recent photoluminescence experiments [1], which clearly show an indirect character of the excitonic emission in h-BN. However, in our opinion these two results are not contradictory, but confirm that the direct excitonic bandgap in BN is slightly higher in energy than the indirect bandgap. A very similar effect is seen in indirect AlGaAs alloys with high Al content, for which direct excitonic transitions dominate the absorption spectra, whereas luminescence shows the characteristic behavior of indirect bandgap semiconductors. [2]

The measurements performed for layers with different thicknesses allow us to discuss the role of the interaction with the sapphire substrate, especially the role of an AlN buffer layer in the context of an anomalous thermal expansion coefficient of BN, strain generation and structural properties of epitaxial BN layers.

[1] G. Cassabois, P. Valvin and B. Gil, Nature Photonics 10, 262 (2016).
[2] B. Monemar, K. K. Shih, and G. D. Pettit, J. Appl. Phys. 47, 2604 (1976).

Novel BAlN/Al$_x$Ga$_{1-x}$N heterostructures for optical and power devices

Haiding Sun[1,*], Kuang-Hui Li[1], Young Jea Park[2], Theeradetch Detchprohm[2], Russell D. Dupuis[2], Xiaohang Li[1]

[1] *King Abdullah University of Science and Technology (KAUST), Thuwal, 23955 Saudi Arabia*
[2] *School of Electrical and Computer Engineering, Georgia Institute of Technology, Atlanta, Georgia 30332, USA*

Boron aluminum nitride (BAlN) is an emerging III-nitride alloy that has a large bandgap comparable to that of AlN and Al-rich AlGaN. It is promising for deep-ultraviolet emitters and power electronics. Despite the potential of BAlN, the scope of experimental studies has been limited, especially in terms of the growth of single-phase wurtzite BAlN layers with a high B content and large thickness. Recently, we demonstrated a significant increase in the thickness (i.e., 100 nm) and B content to 14.4% for single-phase wurtzite BAlN layer. Furthermore, we found that the bandgap of BAlN transitioned from direct to indirect as the B content increased to 12%. This result indicates that it is unlikely for BAlN to be the sole material for the active layer. Therefore, BAlN would probably have to be integrated with Al-rich AlGaN to form heterostructures for application. Thus far, there have been limited experimental reports concerning the structural characterization and band alignment of BAlN/AlGaN heterostructures with a high B content. Here we grew B$_{0.14}$Al$_{0.86}$N/Al$_{0.70}$Ga$_{0.30}$N and B$_{0.14}$Al$_{0.86}$N/GaN heterostructures using MOCVD. We conducted detailed characterizations related to the microstructure, defect formation, and strain within the BAlN and AlGaN layers. [1] Furthermore, we measured the conduction and valence band offset in such heterojunctions. [2] Our experimental analysis provides insights for future research and development of the BAlN/AlGaN heterostructures for optical and power electronics.
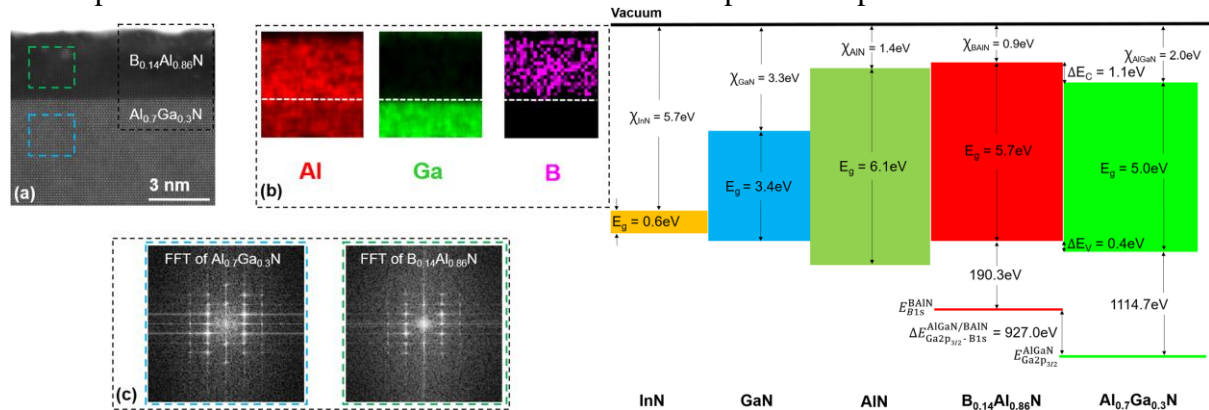

Figure 1. (a) A cross-sectional HAADF-STEM [11-20] image at the heterojunction interface. (b) Element map of Al, Ga, B. (c) The Fourier transform (FFT) patterns from the blue and green boxes of the Al$_{0.70}$Ga$_{0.30}$N and B$_{0.14}$Al$_{0.86}$N layer in (a), respectively. Schematic of the band alignment of B$_{0.14}$Al$_{0.86}$N/Al$_{0.70}$Ga$_{0.30}$N heterojunction.

High resolution TEM confirmed the high structural quality of the heterojunction with an abrupt interface and uniform element distribution, as shown in Figure 1. The valence band offset was determined to be 0.40 ± 0.05 eV. As a consequence, we identified a staggered-gap (type-II) heterojunction with the conduction band offset of 1.10 ± 0.05 eV. The determination of the band alignment of the B$_{0.14}$Al$_{0.86}$N/Al$_{0.70}$Ga$_{0.30}$N heterojunction along with InN, AlN, GaN is plotted in Figure 2, which facilitates the design of optical and electronic devices based on such junctions.

[1] H. Sun. et al., Appl. Phys. Express 11, 011001 (2018).
[2] H. Sun et al., Appl. Phys. Lett. 111, 122106 (2017).

Nitrogen Plasma Effects on MBE Growth of GaN on Graphitic Substrate

Ukyo Ooe, Shingo Arakawa, Shinichiro Mouri, Yasushi Nanishi, Tsutomu Araki

Ritsumeikan University, Nojihigashi1-1-1, Kusatsu, Shiga, Japan

Heteroepitaxy of III-nitrides on graphene is an effective way to obtain single crystal transferable onto arbitral foreign substrates[1-3]. We reported the growth of GaN on the graphene substrate by RF-MBE, but the coalescence of crystals was not enough to achieve high performance optical or electronic devices[4]. Understanding of plasma effects on graphitic surface is a key issue to control nucleation density which is one of the important parameters to improve coalescence of crystals. In this paper, we study the role of nitrogen plasma during MBE growth of GaN on graphene using RF- and ECR-MBE.

We prepared CVD graphene on SiO_2/Si substrate (Graphenea Co.). Then, GaN crystals were grown on it by RF-MBE and ECR-MBE. The growth temperatures were 770℃ and 750℃, respectively. We deduced the nucleation mechanism of GaN on graphene from SEM images at the initial stage of the growth.

Fig. 1(a) and (b) show the SEM images of GaN grown on graphene by RF-MBE and ECR-MBE for 10 min and 1 min respectively, which are much less than the time to obtain nearly continuous film. As-prepared graphene is composed of many pieces of graphitic domain as shown in Fig. 2. GaN crystals were grown densely along the domain boundary of graphene in both cases. However, the feature on the graphitic region is quite different. In the case of RF-MBE, the number of crystals grown on graphitic region was small. On the other hand, in the case of ECR-MBE, crystallites were grown on the whole graphitic region in a higher density.

These results suggest the difference of nitrogen plasma damage on graphene between RF- and ECR-MBE. The ionization rate of nitrogen plasma in ECR-MBE is two or three orders of magnitudes larger than that of RF-MBE. The ionized plasma could effectively introduce the defects on the graphitic surface[5] which becomes nucleation sites of GaN. In the presentation, we will also discuss on the control of nucleation density by applying bias on the substrate.
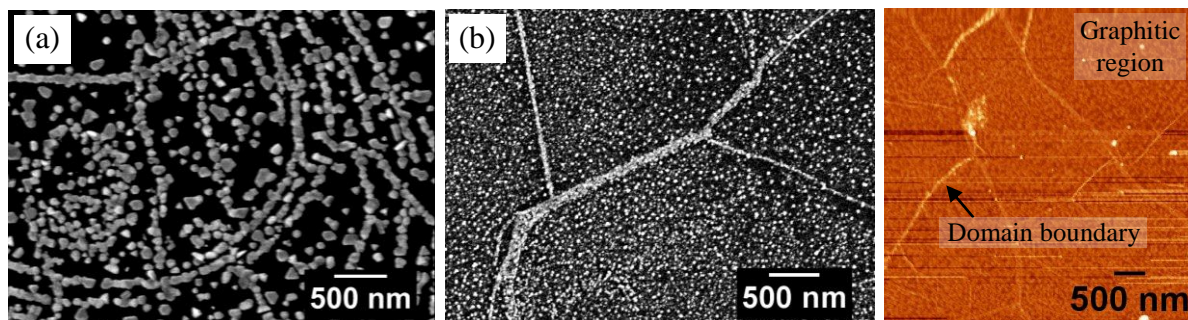

Fig. 1 SEM images of GaN crystals grown on graphene
for (a) 10 min by RF-MBE and (b) 1 min by ECR-MBE

Fig. 2 AFM image
of graphene surface

[1] J. W. Shon et al., Appl. Phys. Exp. **7**, 085502 (2014).
[2] J. Kim et al., Nature Communications **5**, 4836 (2014).
[3] K. Chung et al., Science **330**, 6004 (2010).
[4] T. Araki et al., Appl. Phys. Exp. **7**, 071001 (2014).
[5] Z. Y. Al Balushi et al., Surface Science **634**, 81 (2015).

New AlScN growth and annealing for used as lattice matched substrate for deep UV LEDs

Jason Schmitt[1], Peng Lu[1], Mark Kennard[1], Dominik Jaeger[2], Lutz Kriste[3]

[1] *Nitride Solutions INC, 3333 W. Pawnee St, Wichita, KS USA*
[2] *Evatec AG, Hauptstrasse 1a, CH-9477 Trubbach, Switzerland*
[3] *Fraunhofer Institute for Applied Solid State Physics, Tullastrasse 72, 79108 Freiburg, Germany*

ScAlN has recently been proposed as a lattice matched, pseudomorphic substrate for the growth of high Al content (90% to 60%) AlGaN used in deep UVLEDs and power electronics. Unfortunately, no practical method for the commercial manufacturing of ScAlN substrates exists. In this paper we will investigate a new promising method to produce commercially viable 2-inch and 4-inch AlScN substrates for these devices.

Invited lecture

InGaN still to be discovered

M. Anikeeva,[1] T. Schulz,[1] L. Lymperakis[2], C. Freysoldt[2], P. Wolny[3], M. Sawicka[3], C. Cheze[4],
F. Bertram[5], G. Schmidt[5], F. Mahler[3], J. Tomm[6], C. Skierbiszewski[3], J. Christen[5], Neugebauer[2],
and M. Albrecht[1]

[1]*Leibniz-Institut für Kristallzüchtung, Max-Born-Str. 2, Berlin, Germany*
[2] *Max-Planck-Institut für Eisenforschung, Düsseldorf, Germany*
[3]*Institute for High Pressure Physics, Polish Academy of Sciences, Poland*
[4] *Paul-Drude-Institut, Berlin, Germany*
[5]*Otto von Guericke Universität Magdeburg, Magdeburg, Germany*
[6]*Max-Born-Institut, Berlin, Germany*

The discovery of (In,Ga)N quantum wells (QW) as active material was among the key findings that enabled for the success of III-Nitrides for light emitting devices. The discussion on the physics that could explain the high efficiency of InGaN based structures is ongoing since then. Phase separation, spinodal decomposition and the length scale of alloy fluctuations that would influences optical properties governed the discussion in the last two decades. A major drawback when studying the relation between optical and structural properties of quantum wells grown on c-plane sapphire comes from the intricate interrelation of composition and strain with optical properties due to the presence of the quantum confined Stark effect. Compositional fluctuations and quantum well thickness both influence confinement and piezoelectric fields.

In this presentation we study the relation between structure and optical properties of short period superlattices. In such structures quantum wells are monolayer thick and the influence of the quantum confined Stark effect can be neglected. By changing the composition of the wells and the barrier thickness between the wells allows to study carrier localization and delocalization independent on the piezoelectric fields. Our structures are grown by molecular beam epitaxy consist of monlayer thick InGaN quantum wells, embedded in GaN barriers. Aberration corrected transmission electron microscopy of samples from series of dedicated growth experiments reveals that In is incorporated into these layers in form of laterally confined patches with lateral extension of few nm up to 50 nm. With increasing growth time, the density and size of these patches increases until the layer is closed. Cathodoluminescence in the transmission electron microscope show quantum dot like spectra at low coverages. The wavelength shifts with patch size due to lateral confinement. With increasing density of patches, the sharp spectra merge in a broad spectrum.

Monolayer stacks with barrier thickness ranging from 6 to 50 MLs are used to study interwell coupling. Time resolved PL shows the smallest decay time evidencing the highest recombination rate and a suppression of the PL intensity for the 6 ML superlattice by a factor of 20 compared with 50 ML thick barriers. This is consistent with DFT calculations that show a considerable decrease of the hole effective masses at a barrier thickness ≤5 MLs while the electron wavefunction is indifferent to barrier width changes. On the other hand, the overlap integral of the electron and hole wavefunctions significantly increases with the decrease of the barrier, i.e. we find a stronger coupling of the QWs and therefore a more efficient recombination. From the study of superlattices we thus gain insights into the processes that govern carrier recombination in conventional InGaN quantum wells.

Invited lecture

Differences in the mechanism of strain relaxation of InGaN buffer layers deposited on GaN/sapphire templates and GaN bulk substrates

J. Smalc-Koziorowska [1,2], J. Moneta[2,3], E. Grzanka[1,2], G. Staszczak[1], G. Targowski[1,2], T. Suski [1]

[1] *Institute of High Pressure Physics, PAS, Sokołowska 29/37, 01-142 Warsaw, Poland*
[2] *TopGaN Ltd. Sokołowska 29/37, 01-142 Warsaw, Poland*
[3] *Leibniz Institute for Crystal Growth, Max-Born-Str. 2, 12489 Berlin, Germany*

The realization of nitride optoelectronic devices emitting light in green and infrared range of wavelengths still encounters problems due to difficulties in introduction of higher amount of In into InGaN layers. Theoretical works show that epitaxial growth of such layers requires substrates with higher lattice constant than that of bulk GaN. [1] It could be realized by growth of such structures on the InGaN buffer layers, which are plastically relaxed. In this work we present the structural studies of 100 nm thick $In_{0.18}GaN$ buffer layers grown on GaN/sapphire templates and on bulk GaN substrates by metal-organic vapour phase epitaxy. We carried out investigations on such structures using transmission electron microscopy, cathodoluminescence spectroscopy and x-ray diffraction. The InGaN layers deposited on various substrates exhibit differences in a way of strain relaxation. We observe that the layers grown on GaN/sapphire templates relax via formation of V-pits at **a+c** threading dislocations (TD) (Fig.1a) and by inclination of **a**-type threading dislocations. While the buffer layers grown on bulk GaN substrates relax by the introduction of **a+c** dislocation half-loops at the growing surface and formation of trigonal network of misfit dislocations (MD) at the GaN/InGaN interface (Fig. 1b). We observe that the InGaN layers grown on templates exhibit lower state of relaxation than the InGaN layers of the same thickness and composition deposited on bulk GaN substrates. Both mechanisms of relaxation have implications in the generation of defects in the InGaN buffer layers and in the structures deposited on these buffers. We observe formation of agglomeration of stacking fault domains[2] in less relaxed buffers grown on templates, while they were not formed in the buffer layers grown on bulk GaN. This observation indicates that the formation of stacking fault domains may be related to state of the layer relaxation. In the InGaN layers grown on bulk GaN substrates, the gliding **a+c** misfit dislocations leave traces in the layer in a form of high In content inclusions. Presence of such inclusions leads to the formation of nanopipes, which eventually open into V-pits (Fig. 1b).
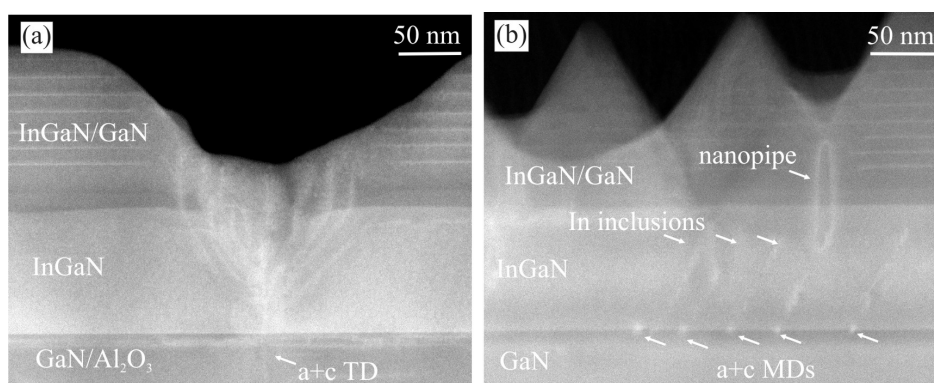

Fig.1 STEM images of InGaN buffer layers deposited on (a) GaN/sapphire template; (b) on GaN bulk substrate.

[1] A.I. Duff, L. Lymperakis, J. Neugebauer, Physical Review B, 89 (2014).
[2] J. Smalc-Koziorowska, C. Bazioti, M. Albrecht, G.P. Dimitrakopulos, Applied Physics Letters, 108 (2016) 051901.

Investigation of the spontaneous crystallographic degradation in nearly lattice-matched InAlN layers to GaN

Ranim MOHAMAD[1], Hichem BEN AMMAR[1], Piero Gamarra[2], Cédric Lacam[2], S. Kret[3], Jun CHEN[1] and Pierre RUTERANA[1]

[1] *CIMAP, ENSICAEN 6 boulevard du Marechal Juin and Pôle universitaire d'Alençon, Campus de Damigny, 61250 DAMIGNY, Université de Caen Normandie, Caen, France*

[2] *III-V Lab, 1 Avenue Augustin Fresnel, Campus Polytechnique, Palaiseau, France*

[3] *Institute of Physics, Polish Academy of Sciences, al. Lotników 32/46, Warsaw, Poland*

High Electronic mobility transistors (HEMTs) based on GaN are very important devices for amplification and detection of the microwave power signals. The binary compounds of group III nitride (InN, AlN and GaN) and their alloys are used for numerous applications such as light emitting diode (LEDs), diode laser (LDs) and transistors with high electronic mobility (HEMTs). In particular, the ternary compound InAlN has recently attracted much research interest due to the possibility of lattice matching it to GaN for an indium composition of around 18%. In addition, the higher 2DEG charge density in InAlN/GaN HEMTs results in higher output current density and, potentially, higher power density [1,2]. Moreover, the band gap of $In_xAl_{1-x}N$ alloys covers the widest range of semiconductor alloy system from 0.67 eV (InN) to 6.2 eV (AlN). Recently, it has been pointed out that, the $In_{0.18}Al_{0.82}N$ alloy is in the immiscibility gap; however, it was claimed also that biaxial strain could modify the miscibility gap [3]. Therefore, it is important to investigate the main factors that may influence the layer quality in these heterostructures.

In this work, we have used a combination of microscopy techniques and theoretical modelling in a detailed study of InAlN layers grown on GaN. The theoretical modelling is carried out using ab-initio methods (DFT), along with molecular dynamics for large systems. The microstructure of the defects was studied by conventional transmission electron microscopy and Scanning transmission electron microscopy at atomic resolution for chemical sensitive imaging and local composition determination. From this investigation, it comes out that the spontaneous degradation of nearly lattice-matched InAlN layers to GaN is based on the effect of native defects that play a critical role on the In segregation and subsequent accumulation of the local strain.

[1] F. Medjdoub, J. F. Carlin, M. Gonschorek, E. Feltin, M. A. Py, D. Ducatteau, and E. Kohn, "Can InAlN/GaN be an alternative to high power/high temperature AlGaN/GaN devices?" in Proceeding of the 2006 International Electron Devices Meeting, Vol 1 and 2, P. 673 (2006).

[2] J. W. Chung, O. I. Saadat, J. M. Tirado, X. Gao, S. Guo, and T. Palacios, "Gate-Recessed InAlN/GaN HEMTs on SiC Substrate With Al2O3 Passivation" IEEE Electron Device Lett., vol. 30, no. 9, pp. 904-906 (2009).

[3] R. Mohamad, A. Béré, J. Chen, and P. Ruterana. "Investigation of strain effects on phase diagrams in the ternary nitride alloys (InAlN, AlGaN, InGaN)", Phys. Status Solidi A 1600752 (2017).

The Upper Limit for InGaN Plastic Relaxation –
– Could We Obtain Fully Relaxed InGaN Layer?

J. Moneta[1,2,3], E. Grzanka[2,3], M. Siekacz[2], M. Albrecht[1] and J. Smalc-Koziorowska[2,3]

[1] *Leibniz Institute for Crystal Growth, Max-Born-Str. 2, 12489 Berlin, Germany*
[2] *Institute of High Pressure Physics, Polish Academy of Sciences, Sokolowska 29/37,
01-142 Warsaw, Poland*
[3] *Top GaN Ltd, Sokolowska 29/37, 01-142 Warsaw, Poland*

The growth of high indium content InGaN layers remains one of the challenges in III-nitrides development. There are theoretical studies showing that introduction of higher amounts of In in the InGaN layers requires substrates with higher lattice constant than bulk GaN.[1] The idea of using relaxed InGaN layers deposited on GaN templates as pseudo-substrates for the growth of InGaN-based structures emerge during last years.[2] In this work we study strain relaxation of InGaN layers via misfit dislocation generation and we show that there are upper limits for the achievable state of the relaxation.

InGaN layers grown at 630°C by molecular beam epitaxy on bulk GaN substrates and GaN/sapphire templates were analyzed by high-resolution X-ray diffractometry, cathodoluminescence imaging and transmission electron microscopy.

We find an upper limit for relaxation of layers grown on GaN/sapphire template: 100 nm $In_{0.2}Ga_{0.8}N$ layer show 25% relaxation which does not change with increasing the thickness to 500 nm. While 17% and 35% degrees of relaxation have been evidenced for respectively 100 nm and 500 nm $In_{0.18}Ga_{0.82}N$ layers grown on bulk GaN substrates. We attribute this upper limit for relaxation to blocking of threading segments of new created dislocation half-loops by preexisting threading dislocations through repulsive interactions. This mechanism is especially crucial in the case of layers grown on GaN/sapphire templates with initial threading dislocation densities of 10^8 cm^{-2}.

We performed post-growth annealing at 800°C (the temperature higher than the growth temperature) for 100 nm InGaN layers grown on both substrates to overcome existing kinetic barriers for the dislocation formation and movement. After 0.5 h annealing we observe 27% relaxation for both structures, i.e. the degree of relaxation does not change much for the layer grown on GaN/sapphire template and increase by about 60% for the layer grown on bulk GaN substrate. After 1 h annealing we find that the degree of relaxation does not change for the layer grown on GaN/sapphire template, while for the layer grown on bulk GaN the degree of relaxation is 30%, i.e. has increased by about 10% in respect to the state after 0.5 h annealing.

Our results indicate that the upper limit for InGaN plastic relaxation depends on substrate threading dislocation density. The achievable degree of relaxation is higher for InGaN grown on bulk GaN substrate than on GaN/sapphire template. We find the upper limit for plastic relaxation of $In_{0.2}Ga_{0.8}N$ grown on GaN/sapphire template to be about 27%. Our samples grown on bulk GaN substrates exhibit a maximum degree of relaxation of 35% for 500 nm $In_{0.18}Ga_{0.82}N$ layer.

[1] A. I. Duff et al., *Physical Review B* **89**, 085307 (2014).
[2] K. Hestroffer et al., *Semiconductor Science and Technology* **30**, 105015 (2015).

Structural Studies of the Processes Occurring During Thermal Annealing of InGaN Quantum Wells

A. Lachowski[1,3]*, E. Grzanka[1,2],J. Smalc-Koziorowska[1,2],Sz. Grzanka[1,2], Ł. Marona[1,2], R. Czernecki[1,2], G.Staszczak[1] , S.Kret[4], M. Leszczyński[1,2]

[1] *Institute of High Pressure Physics, Polish Academy of Sciences, Sokolowska 29/37, 01-142 Warsaw, Poland*
[2] *TopGaN Ltd., Sokolowska 29/37, 01-142 Warsaw, Poland*
[3] *Faculty of Materials Science and Engineering, Warsaw University of Technology, Wołoska 141, 02-507 Warsaw, Poland*
[4] *Institute of Physics, Polish Academy of Sciences, Al.Lotnikow 29/37, 02-668 Warsaw, Poland*

One of the main problems with the epitaxial growth of InGaN/GaN Quantum Wells (QWs) with high In content is their thermal instability. The thermal decomposition of InGaN QWs is observed in the growth of blue and green laser diodes by metal-organic vapour phase epitaxy (MOVPE), when the InGaN QWs are overgrown by p-type layers, which are grown at the temperatures much higher than the growth temperatures of InGaN QWs. We performed structural studies of LED structures with QWs grown by MOVPE method on sapphire templates and GaN bulk substrates. To investigate how the growth temperature of p-type layers alter the QWs emitting light in the blue-green region, p-type overgrowths were performed in temperatures range from 780ºC to 930ºC.

In the studies of electroluminescence (EL) from the structures with InGaN QWs with p-type layer grown at subsequent temperatures (from 830 °C to 905° C) we observe an increase in the intensity of the emitted light, the light is blue-shifted and the FWHM of the emission peak becomes narrower. While the decomposition of QWs and abrupt worsening of the emission is observed for the structure with p-type layer grown at 930°C. The observed changes in the characteristics of emitted light indicate that there is a structural change of the quantum wells. What is also observed in XRD investigations, where we first observe a shift in the amount of indium in InGaN QWs to lower compositions and then radical change of XRD curves, when the decomposition occurs. The mapping of cathodoluminescence emission of the InGaN structures shows, that first signs of thermal decomposition (areas of lower intensity of emission) occur in the sample with p-type grown at 905°C. In the TEM studies we observe distinct change of the structure of QWs in the sample with p-type layer grown at 930°C. TEM results also show, that the thickness of the InGaN QWs before degradation does not change, what indicates that there is no diffusion of In atoms to GaN quantum barriers.

The above observations indicate, that before the thermal degradation of InGaN QWs, a sort of homogenization process is taking place inside InGaN QWs, when they are kept at elevated temperatures. Such clear stages of the initial improvement of the structural quality of InGaN QWs are well observed in case of structures deposited on GaN/sapphire templates, while it seems that these processes occur more rapidly in the layers deposited on bulk GaN structures, and we do not observe there the stages of homogenization.

To investigate how the homogenization process affects the indium distribution in the QWs, we employed a chemical mapping method based on scanning transmission electron microscopy (STEM). This imaging technique combined with high resolution STEM image simulation, makes feasible obtaining precise information on indium content in each atomic column visible in high-resolution pictures. We used this method to track indium atom rearrangement with increasing temperature of p-type growth and to observe the evolution of the microstructure of InGaN QWs.

Invited lecture

Ultralow-sheet-resistance high-electron-mobility transistor structures with strain-controlled high-Al-composition AlGaN barrier

Atsushi Yamada, Junji Kotani, and Norikazu Nakamura

Fujitsu Laboratories Ltd., 10-1 Morinosato-Wakamiya, Atsugi, Kanagawa, 243-0197, Japan

GaN-based high-electron-mobility transistors (HEMTs) have been demonstrated to exhibit higher breakdown voltages with higher cut-off frequencies than other material-based devices, enabling the fabrication of high-power and high-efficiency amplifiers. Over the past few decades, the goal of most studies on AlGaN-HEMTs was the improvement of output power and it was found that increasing the aluminum (Al) composition in the AlGaN barrier is beneficial for this purpose. However, further improvement, especially for Al compositions over 0.40, is expected to be difficult because of strain-related issues. In this study, we investigated the effects of the AlGaN-barrier's growth conditions on the electrical characteristics and successfully achieved ultralow-sheet-resistance HEMT structures with a high-Al-composition AlGaN barrier.

The sample structures comprised a 2-nm GaN cap, a 6-nm AlGaN barrier, a 2-nm $Al_{0.65}Ga_{0.35}N$ spacer, a 1.3-μm GaN channel, and a buffer layer on a semi-insulating SiC substrate. The AlGaN barriers were grown under different conditions: a high temperature (980°C) with H_2 as a carrier gas (HT-H_2), a low temperature (755°C) with H_2 (LT-H_2), and 755°C with N_2 (LT-N_2). To protect the AlGaN surfaces, GaN caps were grown continuously on the top of AlGaN barriers without changing the conditions of the reactor temperature and the carrier gases. The $Al_{0.65}Ga_{0.35}N$ spacers were grown at 980°C with H_2 as a carrier gas for all samples. Figures 1 and 2 show the sheet resistance (R_s) and electron mobility (μ), respectively, as a function of the Al composition in the AlGaN barriers. For the samples grown with HT-H_2, minimum R_s was obtained at an Al composition of 0.43. R_s increases at a greater Al composition owing to a drastic decrease in electron mobility, which in turn is probably due to an increased lattice strain. Similarly, low electron mobility was measured for the sample grown with LT-H_2. By contrast, much higher electron mobility was obtained for the samples grown with LT-N_2 even at a high Al composition, over 0.50, resulting in an ultralow R_s value of 211 Ω/sq at an Al composition of 0.71. It is likely that lattice strain in AlGaN barriers will reduce when the AlGaN barrier is grown with LT-N_2.

We believe that our results may pave the way for a new technology using improved GaN HEMTs with AlGaN barrier layers.
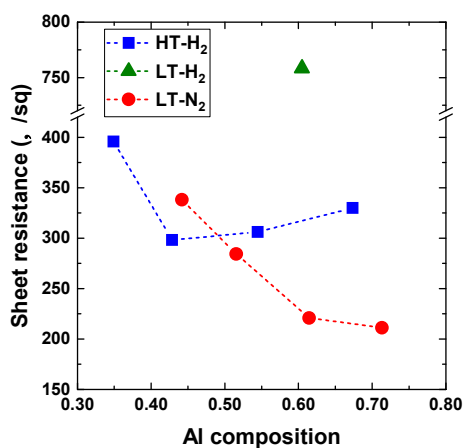

Fig. 1 Sheet resistance versus Al composition.
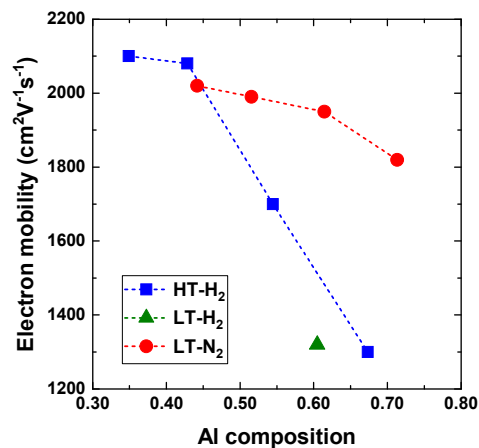

Fig. 2 Electron mobility versus Al composition.

Leakage current analysis for individual dislocations in the modified Na-flux GaN bulk single crystal

T. Hamachi[1], S. Takeuchi[1], T. Tohei[1], M. Imanishi[2], Y. Mori[2], and A. Sakai[1]

[1] *Graduate School of Engineering Science, Osaka University, 1-3 Machikaneyama-cho, Toyonaka, Osaka, Japan*
[2] *Graduate School of Engineering, Osaka University, 2-1 Yamadaoka, Suita, Osaka, Japan*

A Na-flux GaN bulk single crystal grown with a multipoint-seed-GaN (MPS-GaN) technique is one of promising materials to produce high-quality freestanding GaN wafers for power device applications.[1] Recently, we have clarified the electrical conduction mechanism through individual threading dislocations (TDs) in the Na-flux GaN grown on the MPS-GaN template by conductive atomic force microscopy (C-AFM).[2] The leakage current conduction behavior strongly depends on the sites in the Na-flux GaN, such as a *c*-growth sector (*c*GS), a faceted-growth sector (FGS), and boundary regions of *c*GS/FGS and FGS/FGS. TDs in the *c*GS exhibited extremely low leakage compared with TDs in the other sites. In this study, we have investigated the relationship between the leakage current conduction behavior, dislocation morphology, and inner local structures in a modified Na-flux GaN crystal entirely composed of *c*GS.

The modified Na-flux GaN crystal was grown on a Na-flux GaN/MPS-GaN template.[3] To identify the locations of TDs in the Na-flux GaN, etch pits (EPs) were formed on the surface by using a wet chemical etching method with a KOH-NaOH solution. Pt was locally deposited on the EPs by using a focused ion beam system to make a conformal Schottky contact. The backside surface was coated by In to make an Ohmic contact. C-AFM analyses were performed to investigate the electrical conduction through individual TDs. Multi-photon excitation photoluminescence microscopy (MPPL) and transmission electron microscopy were used to identify the dislocation morphology and structures around each EP in the Na-flux GaN.

Figure 1 shows current-voltage (I-V) curves for EP1 and EP2 obtained by C-AFM. Although both EPs had similar size, depth and shape (see the inset), I-V characteristics at EP1 and EP2 were significantly different. In particular, under the reverse bias condition, the leakage current was detected at EP2 whereas that at EP1 was under the detection limit in our C-AFM system. Figure 2 shows surface MPPL images around the EPs. In contrast to the case of EP1, EP2 was clearly observed to be located on a wavy bright contrast region which is the micro-FGS (μ-FGS) locally formed in the *c*GS. This indicates that the inner local structures having high concentration of impurities[3] are crucially responsible for the current leakage phenomena. Correlation with the TD structure and morphology, and the electrical conduction mechanism will be also discussed.
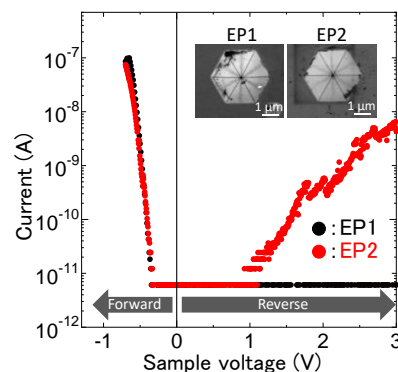

Fig. 1. I-V characteristics for EP1 and EP2. Inset shows scanning electron microscopy images of EP1 and EP2 after the wet chemical etching.
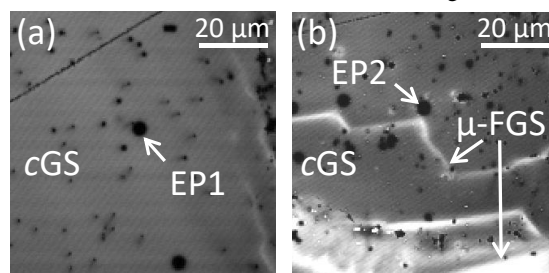
Fig. 2. Surface MPPL images of the modified Na-flux GaN around (a) EP1 and (b) EP2.

Dependency of the reverse leakage current on the MOVPE growth pressure of vertical p–n diodes on a GaN free-standing substrate

S. Usami[1], A. Tanaka[2,3], H. Fukushima[1], Y. Ando[1], M. Deki[2],
M. Kushimoto[1], S. Nitta[2], Y. Honda[2], and H. Amano[2,4,5]

[1] *Dept. of Electronics, Nagoya Univ, Furo-cho, Chikusa-ku, Nagoya, 464-8603, JAPAN,*
[2] *Nagoya Univ. IMaSS,* [3] *NIMS,* [4] *Nagoya Univ. ARC,* [5] *Nagoya Univ. VBL*

Recently, with the development of high quality GaN substrates, high-performance GaN vertical power devices have been actively developed. However, the threading dislocation density (TDD) of the GaN free-standing substrate is as high as 10^6 cm^{-2}, and it is known that these threading dislocations affect the reverse leakage current [1]. The threading dislocation is generally considered to propagate through the epitaxial layer directly from the GaN substrate during homoepitaxial growth. On the other hand, we observed that the growth pressure also affects the leakage current in vertical p–n diodes (PNDs) when we used MOVPE to conduct homoepitaxial growth. This observation indicates that the growth pressure could vary the propagation behavior of the threading dislocations. Here, we investigate the threading dislocation's propagation dependency on the growth pressure of MOVPE during homoepitaxy.

A PND structure with 10-µm n-type drift layer (Si: 2×10^{16} cm^{-3}) was epitaxially grown by MOVPE on a 2-inch n-type GaN free-standing substrate with a TDD of 1×10^6 cm^{-2} under two different growth pressure conditions, a low pressure (LP) of 500 hPa, and an atmospheric pressure (AP) of 1000 hPa. We call them LP- and AP-PND structure, respectively. Further, the mesa structure was formed by ICP dry etching, and the p-type layer was thermally activated. Both p- and n-type ohmic contacts were further added, and a 100-nm Al$_2$O$_3$ passivation layer was finally formed by atomic layer deposition. The measured reverse I–V characteristics of a φ100-µm device are exhibited in figure 1. 70% of the measured LP-PNDs exhibited a large leakage current. Figure 2 depicted the leakage spots in a φ500-µm device that was observed by emission microscope. The observed leakage spot (red circled) density in the LP-PNDs was observed to be higher by an order of magnitude than that of AP-PNDs. When etch pits were formed during KOH etching, two sizes of etch pit (large and small) were obtained; a portion of the large pit coincided with the leakage spots. Because the substrate properties were uniform, it was considered that the dislocation propagation behavior into the epilayer was altered by the growth pressure. The dislocation propagation behavior was observed using a two−photon excitation microscopy system [2], which revealed that some types of adjacent dislocations were converted forming the large pits either by splitting or merging. It was concluded that the initial stage growth mode was related to the change in the dislocation propagation behavior.
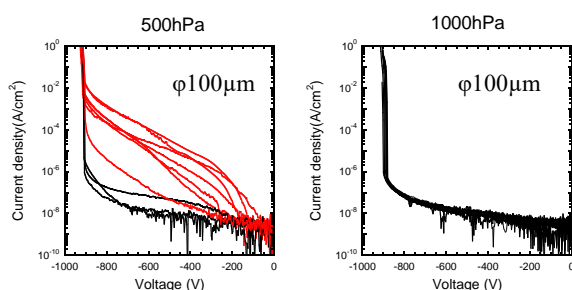

Fig. 1 I–V characteristics of LP-PNDs(left) and AP-PNDs (right).
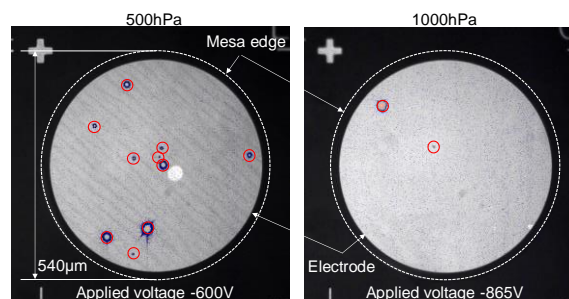

Fig. 2 Emission images of LP-PND (left) and AP-PND (right).

[1] B. Kim *et al.*, Appl. Phys. Lett. **104**, 102101 (2014).
[2] T. Tanikawa *et al.*, Appl. Phys. Exp. **11**, 031004 (2018).

Reduction of Carrier Concentration Increase near the Surface of Silicon Substrate after GaN Growth

Koji Matsumoto [1,2], **Toshiaki Ono** [1], **Yoshio Honda** [3], **Kazuhisa Torigoe** [1], **Maki Kushimoto** [2], **and Hiroshi Amano** [3,4,5]

[1] *SUMCO Corporation, 1-52 Kubara, Yamashiro-cho, Imari 849-4256, Japan*
[2] *Department of Electrical Engineering and Computer Science,* [3] *Institute of Materials and Systems for Sustainability,* [4] *Venture Business Laboratory,* [5] *Akasaki Research Center, Nagoya University, Chikusa-ku, Nagoya 464-8603, Japan*

Gallium nitride (GaN) on silicon substrate is expected to be used as the material for high power devices and high frequency devices owing to the advantages of silicon substrate, such as large wafer size, and low cost. However, because it is difficult to grow the thick GaN film on the silicon substrate due to the large mismatch of the lattice constants and the thermal expansion coefficient difference, horizontal devices like high electron mobility transistors (HEMT) are generally applied for the GaN on silicon substrates. In regarding to the GaN HEMT for the power device, it was reported that the breakdown voltage was improved by increasing the thickness of the GaN film [1]. In addition, a local silicon substrate removal was proposed to enhance blocking voltage of the GaN-on-silicon HEMT [2, 3]. These results suggest the presence of the leakage current passing through a silicon substrate, and it is preferred to use a high resistivity substrate for the power HEMTs. For the high frequency applications, a low resistivity substrate causes the parasitic capacitance between the device and the substrate, and a high resistivity substrate is also desirable. However, it was found that the carrier concentration of the surface of the silicon substrate was influenced by aluminum and gallium diffusions during the growth of GaN and aluminum nitride (AlN) buffer layer. In this study, the causes of the diffusion of aluminum and gallium were investigated, and the processes to suppress the diffusion were examined.

The GaN layer was grown by using a metal organic chemical vapor deposition (MOCVD) system. Trimethyl-aluminum (TMAl), trimethyl-gallium (TMGa), and ammonia (NH_3) were used as precursors. The carrier gas was hydrogen (H_2). Two-inch silicon(111) wafers grown by float-zone (FZ) technique were used as substrates, and those resistivity was more than 1000 Ωcm. A 100nm-AlN layer was grown on the silicon substrate as a buffer layer for the GaN layer growth at 1140°C. After AlN growth, a 1μm-GaN layer was grown at 1050°C. The sample which had only 100nm-AlN layer without the GaN layer was also prepared in order to investigate the cause of the impurities diffusion. The reactor was cleaned with H_2 and NH_3 before the next growth. The impurity concentrations in silicon substrate were evaluated by secondary ion mass spectrometry (SIMS), and the carrier concentrations were measured by spreading resistance analysis (SR).

The gallium diffusion into the silicon substrate was detected in the sample without GaN layer. This result reveals that the gallium diffusion comes from the GaN deposition on the reactor wall, and it is found that the gallium diffusion into the silicon substrate was reduced by applying the proper cleaning conditions to the reactor wall. In comparison, it appeared that the aluminum diffusion was affected by the AlN growth conditions. Therefore, the aluminum diffusion has been suppressed by optimizing the AlN growth procedure.

[1] S. Iwakami, O. Machida, M. Yanagihara, T. Ehara, N. Kaneko, H. Goto, and A. Iwabuchi, *Jpn. J. Appl. Phys.* **46**, L587 (2007).
[2] N. Herbecq, I. Roch-Jeune, N. Rolland, D. Visalli, J. Derluyn, S. Degroote, M. Germain, and F. Medjdoub, Appl. Phys. Exp. **7**, 034103 (2014).
[3] E. Dogmus, M. Zegaoui, and F. Medjdoub, Appl. Phys. Exp. **11**, 034102 (2018).

RF-Loss Suppression of AlGaN/GaN-on-Si HEMT With Superlattice Buffer

**Yu-En Jeng [1], Li-Cheng Chang [2], Kai-Chieh Hsu[2], Yung-Ting Ho[1]
and Chao-Hsin Wu [1,2]**

[1] *Graduate Institute of Photonics and Optoelectronics, National Taiwan University, Taipei 106, Taiwan*
[2] *Graduate Institute of Electronics Engineering, National Taiwan University, Taipei 106, Taiwan*

GaN-on-Si attracts a lot of attention because of superior properties for high-speed and high-power electronics applications. Compared to SiC or sapphire substrate, GaN-on-Si offers price benefits over the other substrate[1-2]. However, due to the large lattice mismatch between (Al)GaN and Si, buffer layers between (Al)GaN and Si become a critical issue. In this work, we have fabricated two different of AlGaN/GaN-on-Si HEMTs with gradient $Al_xGa_{1-x}N$ stacked buffer and AlGaN/GaN superlattice buffer. The comparison of DC and RF characteristics indicates that although the DC performance of both devices is similar, the structure with superlattice buffer shows less signal loss with higher frequency response.
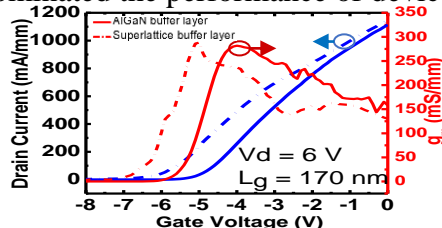
Device structures of two different buffers us shown in fig (1). Both device is carried out with the same process and the fabrication is started from source and drain metal deposition with Ti/Al/Ni/Au, followed by rapid thermal annealing at 875 °C for 40 s in N_2. Then, mesa isolation is formed by Cl_2/BCl_3 plasma. Rectangular gate is defined by e-beam lithography with Ni/Au metallization. Finally, the standard back-end process included polyimide planarization and GSG probing layout metallization is carried out. Both two devices are characterized by 170 nm gate length and 1.86 μm source-to-drain distance with equal gate-to-source and gate-to-drain distance.

DC transfer characteristics are shown in Fig (2). For the device with stacked $Al_xGa_{1-x}N$ buffers, the threshold voltage (V_{TH}) is -6.02 V and peak g_m is 288 mS/mm. For device with superlattice buffer, V_{TH} is -4.96 V and peak g_m is 281 mS/mm. According to the results, both devices exhibit similar peak g_m suggests that both AlGaN barrier and AlGaN buffer do not affect the peak g_m significantly. The difference of V_{TH} between two structures might be caused by the different conduction band alignment between AlGaN barrier and GaN channel. Fig (3) shows the f_T and f_{max} of both devices. The S-parameters of device are measured in a frequency of 0.04−40 GHz, the f_T/f_{max} of device with stacked AlGaN buffer and AlGaN/GaN superlattice is 36.59/49.78 GHz and 41.63/126.46 GHz, respectively which are obtained by extrapolating under the slope of −20 dB/dec. The device with stacked $Al_xGa_{1-x}N$ buffer shows lower f_T/f_{max} than the device with superlattice buffer and this is attributed to the signal loss form the buffer layer. Inset of Fig (3) shows the S-parameter of both devices. The open-pad S-parameters also confirmed that device with stacked exhibits higher signal loss from buffer.

In conclusion, we fabricate the AlGaN/GaN-on-Si HEMTs with the fabrication and different buffer layers. The similar peak g_m of both devices suggests that layer structure does not play an important role to the DC characteristics. However, lower f_T/f_{max} of stacked $Al_xGa_{1-x}N$ buffer which is attributed to the buffer loss indicates that buffer engineering in high frequency operation really dominated the performance of device.

Fig(1) schematic layer structure of the (a)AlGaN buffer layer(b)superlattce buffer layer

Fig(2) Common source DC transfer characteristics of AlGaN buffer layer and superlattce buffer layer
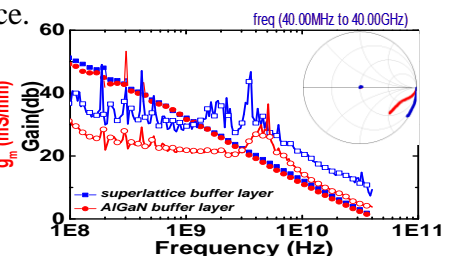
Fig(3) Smith chart of open mode (inset) and small signal RF performance at a quiescent bias of Vgs = -3.8 V, Vds = 12 V after de-embedding

[1] A. Eblabla *et al*., *IEEE Electron Device Lett.*, vol. 36, no. 9, pp. 899-901, Sep. 2015.
[2] P. Altuntas *et al*., *IEEE Electron Device Lett.*, vol. 36, no. 4, pp. 303-305, Apr. 2015.

Growth and Characterization of InAlN/AlGaN Heterostructures

J. S. Xue, J. C. Zhang and Y. Hao

Key Laboratory of Wide Bandgap Semiconductor Materials and Devices, School of Microelectronics, Xidian University, Xi'an, People's Republic of China

(In)AlN-based device has been studied extensively in last decade for high frequency millimeter wave application. Up to now, a high current cut-off frequency of 454GHz has been demonstrated for AlN/GaN HEMTs in virtue of advanced device process and high quality material. However, the breakdown voltage for InAlN barrier device is too low to operate at high voltage. To address this issue, adopting wide bandgap AlGaN instead of GaN channel is a viable scheme due to high breakdown electrical field. On the other hand, the high gate leakage current can be suppressed by adding the insulator layer under the gate electrode.

In this work, we report the growth and characterization of InAlN/AlGaN heterostructures grown by metal organic chemical vapor deposition. By changing the ratio of TMGa to TMAl, a series of AlGaN channel layer with different composition is successfully grown. Based on the growth of AlGaN channel, InAlN/AlGaN are subsequently epitaxied and characterized by XRD, AFM, Hall effect and TEM. It is found that the composition of AlGaN channel influences the surface morphology of InAlN barrier obviously, even though the surface morphology of AlGaN channel layer depend on its composition incompletely. For the electron transport properties of 2DEG at the interface of InAlN/AlGaN heterostructures, with the increase of AlGaN channel Al composition the sheet resistance significantly reduced owing to the decreased electron mobility, which is ascribed to the strong alloy disorder scattering for high Al composition AlGaN channel. Besides, application of the grown heterostructures is verified by demonstration high electron mobility transistors.

Invited lecture

Determination of the Fermi Level in Doped GaN by Contactless Electroreflectance

Łukasz Janicki and Robert Kudrawiec

[1] *Faculty of Fundamental Problems of Technology, Wrocław University of Science and Technology, Wybrzeże Wyspiańskiego 27, 50-370 Wrocław, Poland*

Determination of the Fermi level in GaN doped with atoms which make the material semi-insulating is generally not an easy task since it is usually done in an electrical way by e.g. measuring an *I-V* or *I-T* characteristic of a Schottky diode. In this work an alternative approach is presented that the Fermi level can be determined by optical spectroscopy studies. A modulation spectroscopy technique (contactless electroreflectance) is used to study the built-in electric field in specially designed samples. The field is dependent on the Fermi level position in the doped part of the structure. The analysis of the band profile of the structure allows to determine the Fermi level position.

This approach has been applied to study the Fermi level position in GaN:Mn, GaN:Zn, and GaN:Fe. All of those dopants act as acceptors in GaN making the material semi-insulating and all of them have been proposed to compensate the residual carriers in GaN base layers in III-N transistors. The Fermi level position in doped GaN was studied on GaN(undoped)/GaN:X structures by contactless electroreflectance where X stands for an appropriate dopant. A well-defined Franz-Keldysh oscillation (FKO) is present in optical spectra obtained for those structures which results from the built-in electric field present in the near-surface undoped layer. Using the field values estimated from FKO band profiles were calculated with the Fermi level in the doped part treated as a free parameter. The Fermi level position in GaN:Mn, GaN:Zn, and GaN:Fe is found to be at 1.4 eV, 1.1 eV, and 2.6 eV above the valence band maximum, respectively. For GaN:Mn 1.4 eV corresponds to a $Mn^{2+/3+}$ level.[1] For GaN:Zn 1.1 eV coincides with level corresponding to Zn on N sites either uncharged or with a single captured electron.[2] In GaN:Fe 2.6 eV corresponds to a $Fe^{2+/3+}$ level.[3] The surface Fermi level of all structures is located in the middle of the band gap, that is in the lower singularity of (0001) GaN surface density of states.[4] This agrees well with predictions for GaN/GaN:X structures doped with an acceptor.

[1] L. Janicki, G. Kunert, M. Sawicki, E. Piskorska-Hommel, K. Gas, R. Jakiela, D. Hommel, R. Kudrawiec, *Sci. Rep.* **2017**, *7*, 41877.

[2] L. A. Marasina, A. N. Pikhtin, I. G. Pichugin, A. V. Solomonov, *Phys. Status Solidi A* **1976**, *38*, 753.

[3] J. Dashdorj, M. E. Zvanut, J. G. Harrison, K. Udwary, T. Paskova, *J. Appl. Phys.* **2012**, *112*, 013712.

[4] Ł. Janicki, M. Gładysiewicz, J. Misiewicz, K. Klosek, M. Sobanska, P. Kempisty, Z. R. Zytkiewicz, R. Kudrawiec, *Appl. Surf. Sci.* **2017**, *396*, 1657.

Alloying as an effective way to increase Mg incorporation into Nitrides

Henryk Turski [1], Grzegorz Muzioł [1], Paweł Wolny [1], Marcin Siekacz [1], Krzesimir Nowakowski-Szkudlarek [1], Anna Feduniewicz-Żmuda [1], and Czesław Skierbiszewski [1,2]

[1] *Institute of High Pressure Physics, PAS, Sokolowska 29/37, 01-142 Warsaw, Poland*
[2] *Top GaN Ltd., Sokolowska 29/37, 01-142 Warsaw, Poland*

Molecular beam epitaxy (MBE) offers an interesting alternative to metal organic vapor phase epitaxy in the growth of Mg-doped layers because p-type conductivity does not need to be activated after the growth and can be realized at much lower growth temperatures. Those facts enable the use of MBE to grow p-type layers after active region of long wavelength light emitters [1] and also for structures such as tunnel junctions were p-type layers lay buried in the crystal [2,3]. To achieve high Mg concentration in GaN growth temperature needs to be significantly reduced. We show that Mg incorporation can be influenced by simultaneously incorporating In or Al atoms into the layer.

In this work, Mg doping of InGaN and AlGaN layers by plasma-assisted MBE in metal-rich conditions on c-plane bulk GaN substrates is studied. AlGaN layers where grown at 750°C in Ga-rich conditions while InGaN at 670°C in In-rich conditions. Mg concentration obtained for Ga(Al)N layers grown using different growth rates with other growth conditions constant is shown in Fig 1(a) (Al flux was adjusted to obtain similar compositions). Higher Mg incorporation into AlGaN than GaN was observed with no dependency on the growth rate[4]. Graded InGaN:Mg layers where used to compare Mg incorporation into pure GaN vs low In content InGaN. Obtained results indicating higher Mg incorporation into InGaN than GaN are shown in Fig 1(b). Secondary ion mass spectroscopy (SIMS) measurements confirmed.

Possible origins of the higher Mg incorporation into nitride alloys than into pure GaN will be discussed. Comparison of hole concentration for doped layers will be presented.
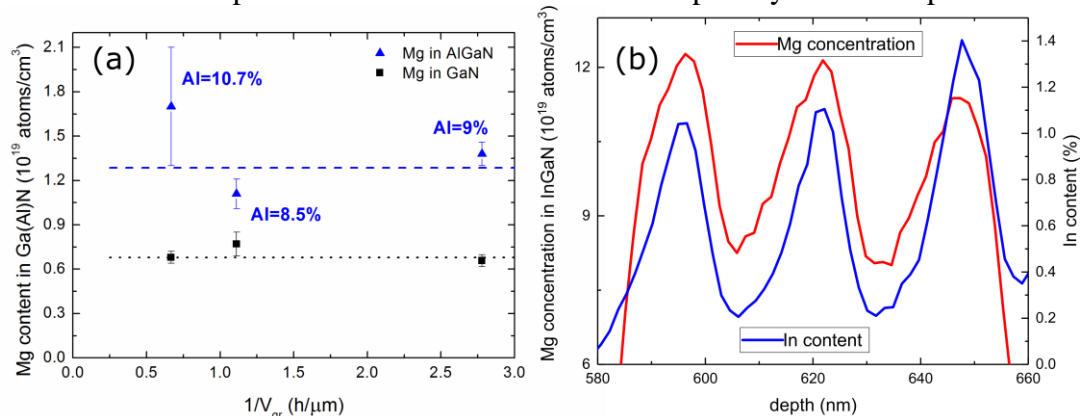

Fig. 1 Mg content obtained by SIMS for (a) Ga(Al)N as a function of inverted growth rate and (b) Ga(In)N as a function of depth in the graded layer. For InGaN growth Ga cell temperature was adjusted to obtain In content modulated between ~1.5% and ~0%.

[1] M. Malinverni, C. Tardy, M. Rossetti, A. Castiglia, M. Duelk, C. Vélez, D. Martin, and N. Grandjean, *Applied Physics Express* **9** (2016).
[2] C. Skierbiszewski, et al., *Applied Physics Express* **11** (2018).
[3] S. J. Kowsz, E. C. Young, B. P. Yonkee, C. D. Pynn, R. M. Farrell, J. S. Speck, S. P. DenBaars, and S. Nakamura, *Opt Express* **25**, 3841 (2017).
[4] H. Turski, et al., *Journal of Crystal Growth* **482**, 56 (2018).

Self-Compensation of Carbon in AlGaN

Ben Rackauskas[1], Michael J. Uren[1], Steve Stoffels[2], Ming Zhao[2], Stefaan Decoutere[2], Martin Kuball[1]

[1]*Center for Device Thermography and Reliability, University of Bristol, UK*
[2]*Inter-University Micro-Electronics Centre, Belgium*

Carbon is often incorporated in the buffer and strain relief layers of AlGaN/GaN HEMTs for power applications to suppress buffer conduction and short channel effects. However, despite its frequent use, the mechanism by which it achieves Fermi level pinning deep in the band gap is not completely clear. Here we demonstrate for the first time that it is strongly self-compensated, a key result for accurate device simulations [1].

Theoretical models indicate the dominant mechanism of carbon incorporation in AlGaN is substitution on aluminium, gallium and nitrogen sites resulting in two main traps; C_N, an acceptor at $E_v+0.9eV$ for GaN increasing to $E_V+1.88eV$ for AlN and C_{AlGa}, a donor at E_c [2–4]. The incorporation of carbon on the two sites depends strongly on the position of the Fermi level during growth and due to intrinsic and extrinsic donors in MOCVD growth, C_N is favoured over C_{AlGa} resulting in Fermi level pinning near the C_N level [2,3]. This work evidences that carbon is self-compensating (both C_N and C_{AlGa} present) following the investigation of two AlGaN/GaN epitaxies differing only by the carbon doping in the 8% AlGaN back-barrier. The silicon substrate was used as a back gate, with the 2DEG conductivity during the negative ramp shown in Fig. 1. The substrate bias independence of the undoped sample means none of the vertical field was dropped over the channel. This can only be caused by the accumulation of positive charge somewhere below the channel and is reasonably inferred to be a 2DHG at a buried interlayer [5]. Conversely when carbon is incorporated at this heterointerface, the 2DEG depletes proportionally to the substrate bias indicating the 2DHG is not present with carbon. The 2DHG can only be suppressed by donors indicating this suppression is caused by C_{AlGa}. The structures were simulated, with an interlayer composition profile based on STEM data. By varying the compensation ratio in the simulated structure to match experimental data in Fig. 1, we put a lower bound on the carbon self-compensation ratio at $N_d/N_a > 0.4$ – the ratio required for 2DHG suppression in the simulation and to recover the observed experimental behaviour in Fig. 1. In a compensated material, it is the compensation ratio, N_d/N_a rather than the total density, which determines the position of the Fermi level and hence, the resistivity [6]. Bulk resistivity is linked to properties such as leakage, breakdown and trapping time-constants. Therefore, knowledge of this ratio is essential for accurate simulation and device understanding.

[1] B. Rackauskas et al., IEEE Trans. Electron Devices (2018). doi: 10.1109/TED.2018.2813542
[2] J.L. Lyons et al., Phys. Rev. B **89**, 35204 (2014). doi:
[3] M. Matsubara et al., J. Appl. Phys. **121**, 195701 (2017).
[4] A.Y. Polyakov et al., Mater. Sci. Eng. R Reports **94**, 1 (2015).
[5] A. Nakajima et al., Appl. Phys. Express **3**, (2010).
[6] J.S. Blakemore, *Semiconductor Statistics* (Pergamon Press, 1962).
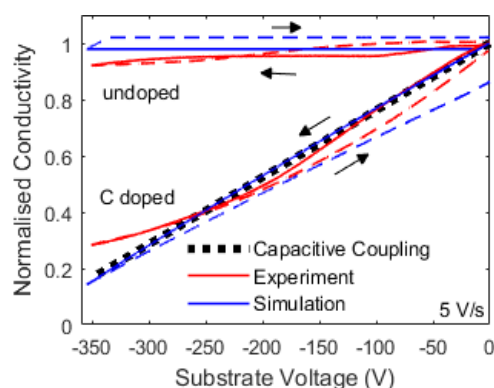
Fig. 1. Experimental and simulated 2DEG conductivity as the Si substrate is ramped. The capacitive coupling line corresponds to the expected response of an ideal dielectric buffer.

Controlling Si Doping Limits in Al Rich AlGaN: Knee Behavior and Low Doping Limits

Ramón Collazo[1], Pramod Reddy[1,2], Shun Washiyama[1], Felix Kaess[1], Ronny Kirste[2], Seiji Mita[2], and Zlatko Sitar[1]

[1] *Department of Materials Science and Engineering, North Carolina State University, Raleigh, NC 27695-7919, USA.*
[2] *Adroit Materials, Inc., 2054 Kildaire Farm Rd., Cary NC 27518, USA*

Significant challenges in point defect control in AlGaN epitaxy have precluded commercialization of AlGaN based devices. Si is typically employed as n-type dopant in AlGaN and exhibits a low activation energy (<50 meV) in $Al_xGa_{1-x}N$ with x<0.8. However, Si doped AlGaN exhibits a "knee behavior" resulting in a conductivity and carrier concentration maxima at a specific Si concentration. Hence a high doping limit exists for Si in AlGaN that lowers the maximum achievable carrier concentrations that are necessary for AlGaN based power electronics. Similarly, a low doping limit (a minimum achievable carrier concentration with a corresponding maximum mobility) exists in AlGaN similar to that in GaN which precludes implementation of AlGaN power electronics that require low doped drift regions. Hence a major "point defect problem" exists in AlGaN that needs to be solved for implementation of AlGaN technology.

In this work, we demonstrate a systematic chemical potential control (CPC) based point defect control (PDC) where we relate the growth environment variables with the defect formation energy by determining and controlling the Al,Ga,N and impurity chemical potentials and optimize the growth environment accordingly for minimal point defect incorporation or generation [1]. Here, we develop and employ a theoretical framework that provides quantitative relationship between point defect formation energies and growth process parameters including V/III ratio, diluent gases and temperature. CPC based targeted reduction requires knowledge of the defects responsible and accordingly, we identify the point defects responsible for knee behavior in n-type AlGaN as most likely vacancy-silicon complexes and low doping limit as C_N. Utilizing the vacancy-silicon complex and C_N in $Al_{0.7}Ga_{0.3}N$ as a case study, we demonstrate control over the knee behavior (improving the peak carrier concentration to state of the art 2.5×10^{19} cm^{-3} by impeding the formation V_{III}-Si_{III} complexes) and low doping limit (achieving lower carrier concentrations by reducing the compensating impurity (C_N) density) in $Al_{0.7}Ga_{0.3}N$ by controlling the chemical potentials of III/N and growth temperature with excellent agreement with quantitative theoretical predictions.
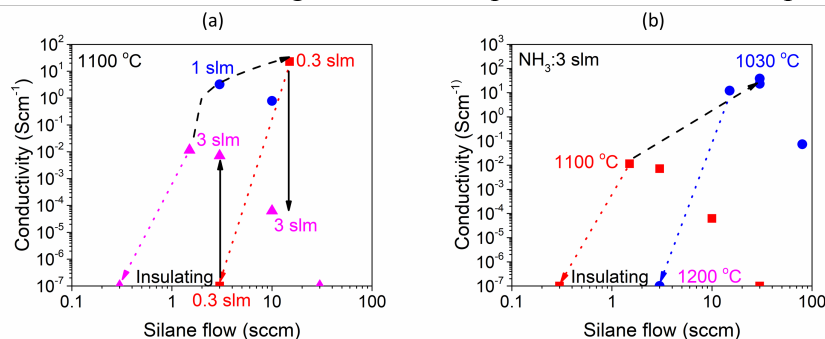

Figure 1: (a) Conductivity as a function of silicon incorporation (silane flow) at different ammonia flows at a constant growth temperature being 1100 °C. (b) Conductivity as a function of silicon incorporation (silane flow) at different growth temperatures at a constant ammonia flow (3 slm). The dotted lines represent a decrease in conductivity to an insulating behavior.

[1] P. Reddy et al., *J. Appl. Phys.* **122**, 245702 (2017).

Growth and Device Characterization of III-N Deep-Ultraviolet Avalanche Photodiodes and Arrays

Mi-Hee Ji[1], Marzieh Bakhtiary-Noodeh[2], Hoon Jeong[1], Jeomoh Kim[3], Theeradetch Detchprohm[1], Shyh-Chiang Shen[1], Parminder Ghuman[4], Sachidananda Babu[4], Ashok K. Sood[5], and Russell D. Dupuis[1,2]

[1]*Center for Compound Semiconductors and School of Electrical and Computer Georgia Institute of Technology, Atlanta, Georgia 30332, USA*
[2]*Center for Compound Semiconductors and School of Materials Science and Engineering Georgia Institute of Technology, Atlanta, Georgia 30332, USA*
[3]*Materials and Devices Advanced Research Institute, LG Electronics, Seoul, South Korea*
[4]*NASA Earth Science Technology Office, Goddard Space Flight Center, Greenbelt, MD 2077*
[5]*Magnolia Optical Technologies, Inc., Woburn, MA 01801, USA*

Wide-bandgap III-N-based avalanche photodiodes (APDs) are primary candidates for compact, high-sensitivity, photodetection in the ultraviolet (UV) spectral region. Because of the intrinsic detection capability of these direct-bandgap III-N materials and their stability in harsh environments, they are well suited for operation in the solar-blind UV spectral region, $\lambda < 280$ nm in harsh environments. For the realization of deep-UV solar-blind APDs with high gain and sensitivity, high quality and highly conductive n- and p-type $Al_xGa_{1-x}N$ wide-bandgap materials ($x > 0.5$) are essential. However, the epitaxial growth of high-Al-content $Al_xGa_{1-x}N$ layers have been hampered by high dislocation densities originating from epitaxial layers grown on lattice- and thermally-mismatched substrates, surface roughening, and crack formation as well as limitation in their doping properties. It is well known that achieving highly conductive high-Al-content p-$Al_xGa_{1-x}N$ alloys is difficult with increasing Al content because of the increase in the ionization energy of the dopants with Al mole fraction.

In this work, we studied the growth of $Al_xGa_{1-x}N$ epitaxial layers on AlN/(0001) sapphire templates by metalorganic chemical vapor deposition (MOCVD) with AlN mole fractions, $x > 0.50$, corresponding to an absorption cut-off wavelength below 280 nm. In order to achieve crack-free growth, two-step $Al_xGa_{1-x}N$/AlN short-period superlattice layers (SPSLs) were grown between the AlN buffer layer and the n-type $Al_{0.6}Ga_{0.4}N$ layer as a strain management scheme. In addition, the growth and doping conditions for $Al_xGa_{1-x}N$ epitaxial layers were investigated to achieve improved crystalline and structural quality by modifying the growth parameters such as growth temperature, pressure, and V/III ratio. We studied the structural, compositional, optical, and electrical properties of $Al_xGa_{1-x}N$ epitaxial layers. Also in this study, front-illuminated p-i-p-i-n SAM-APD array structures were grown by Metalorganic Chemical Vapor Deposition (MOCVD) on c-axis n-type bulk GaN:Si substrates. The epitaxial structure consisted of an n-GaN:Si layer, an i-GaN:ud multiplication layer, a p-GaN:Mg charge layer with linearly graded [Mg] up to ~7.5×10^{18} cm-3, an i-GaN:ud absorption layer, a p-Al0.05Ga0.95N:Mg window layer, and a heavily doped p-Al0.05Ga0.95N:Mg++ contact layer. The SAM-APD arrays were defined into mesas size of 100×100 µm2 by inductively coupled plasma (ICP) etching. Metal stacks of Ti/Al/Ti/Au and Ni/Ag/Ni/Au were evaporated on the n- and p-type layers, respectively. A SiO2 passivation layer was applied on the arrays. In order to evaluate the uniformity of a 4×4 SAM-APD array, the dark current and photocurrent of 16 individual SAM-APDs in the array were measured. The SAM-APD array showed uniform distribution of dark current density of JDark=$(5.1 \pm 0.8) \times 10$-8 A/cm2 at reverse bias of -46 V except for two of them. Also, the average onset point of breakdown voltages of the SAM-APD array was -73.1±0.21V. Multiple reverse-bias I-V scans were performed for selected devices in the SAM-APD array to verify the reliability and stability. The detailed growth, device fabrication processing and device characterization including spectral response will be further discussed.

Alternative Growth Approaches of *p*-Type Doped AlGaN Epitaxial Structures

Sebastian Zlotnik [1], **Krzysztof Rosiński** [1], **Jakub Sitek** [1], **Paweł Michałowski** [1] **and Mariusz Rudziński** [1]

[1] *Institute of Electronic Materials Technology, Wolczynska 133, 01-919 Warsaw, Poland*

Inorganic materials for light-emitting diodes (LEDs) covering wide spectrum of radiation have undergone a significant evolution over last two decades, becoming crucial semiconductor systems [1]. Among them are III-nitrides (AlGaInN) emitting green, cyan, blue and violet light as well as ultraviolet (UV) radiation. AlGaN alloys have emerged as the most promising compounds for deep UV emitters in order to replace traditional UV sources, *e.g.* Hg lamps, and find application ranging from water purification to biomedical utilization [2]. However, unlike III-nitrides for visible light technology (GaInN), the wide-bandgap semiconductor devices posses fundamental limitations caused mainly by a strong asymmetry between n-type and p-type properties, in particular in the case of Al-rich AlGaN. The reason is related to low hole concentration and mobility, and associated to chemical deactivation of Mg acceptors by hydrogen atoms and a high Mg thermal activation energy [3]. The acceptor activation has been commonly conducted by post-growth thermal annealing.

In this work, a careful optimization of growth conditions for p-type doping of AlGaN, during metalorganic vapor phase epitaxy (MOVPE) was performed. Conventional MOVPE epitaxial growth is carried out under continuous flow of metalorganic precursors, simultaneously injected into reactor chamber. Alternative concepts are proposed based on a modified surface engineering – a pulsed-growth approach (δ-doping) with various periodical interruption of metalorganic sources combined with co-doping. It was reported that In-surfactant-assisted δ-doping method leads to more effective Mg incorporation due to reduced acceptor activation energy and valence-band modulation [4]. Here, we aimed to directly compare different δ-doping approaches and their effects on structure, surface morphology, chemical composition and electrical parameters, by implementing various characterization techniques: high resolution X-ray diffraction (HR-XRD), electron microscopy (SEM, TEM), atomic force microscopy (AFM), secondary-ion mass spectrometry (SIMS), temperature-dependent Hall effect measurements, *etc*. The following sequences of pulsed-growth experiments were conducted (in all cases NH_3 was always constantly introduced in the reactor): i) continuous Cp_2Mg flow with alternatively opening and closing the TMAl and TMGa sources with intervals varying from 2 to 10 sec, ii) alternative TMAl/TMGa with Cp_2Mg flow, iii) additional 2 sec-purging cycle to the previous process, and iv) co-doping. The achieved results show that all these non-conventional approaches have a beneficial effect on Mg incorporation and consequently rise of hole concentration in AlGaN.

[1] J. H. Park, D. Y. Kim, E. F. Schubert, J. Cho, and J. K. Kim, *ACS. Energy Lett.* **3**, 655 (2018).
[2] M. H. Crawford, *Semicond. Semimet.* **96**, 3, 2017.
[3] P. Pampili, and P. J. Parbrook, *Mater. Sci. Semicond. Proc.* **62**, 180, 2017.
[4] Y. Chen, H. Wu, E. Han, G. Yue, Z. Chen, Z. Wu, G. Wang, and H. Jiang, *Appl. Phys. Lett.* **106**, 162102, 2015.

Design of InGaN/GaN MQW structure for scintillator applications

Alice Hospodková[1], Tomáš Hubáček[1,2], Markéta Zíková[1], Filip Dominec[1], Jiří Oswald[1], Karla Kuldová[1], František Hájek[1], Tomáš Vaněk[1,2], Vitězslav Jarý[1]

[1] *Institute of Physics, CAS, Cukrovarnická 10, Praha 6, Czech Republic*
[2] *Crytur, s r.o., Na Lukách 2283, Turnov, Czech Republic*

Nitride semiconductor heterostructures are widely used for light emitting and laser diodes as well as for high power and high frequency applications. Recently, new application for InGaN/GaN multiple quantum well (MQW) heterostructures has emerged [1,2]. It was shown that these heterostructures, if properly designed, can work as very efficient fast scintillators with long lifetime due to their radiation resistance. Although this application does not have such a massive market as LEDs, LDs or HEMTs, there is still very strong demand for fast scintillators and detectors of ionizing radiation due to the expansion of new diagnostic methods in medicine, electron microscopy and nuclear physics. Especially, there is a lack of fast scintillators with short decay time in the order of few nanoseconds. This new application with diverse requirements needs completely different design of heterostructure and opens new problems which were not solved, yet. First, due to the penetration depth of ionizing radiation, the active region has to be much thicker with high number of QWs, see example in Fig. 1. We will discuss the consequences of thick active region, e.g. formation of huge V-pits (see V-pit profiles in Fig. 2), their influence on photoluminescence (PL) properties and possibilities to suppress their size. While for LED structures high level of excitation brings a problem with non-radiative Auger recombination, in the case of scintillator an opposite problem, extremely low intensity of excitation, has to be solved. Under such conditions the excitonic QW luminescence (3.2 eV) can have even lower intensity than different kind of defect bands originating either in GaN (yellow band 2.2 eV) or in InGaN QWs (2.6 eV), see cathodoluminescence (CL) results in Fig. 3. Since they have slow decay times, defect bands are detrimental for fast scintillator applications. The origin of these bands and different ways how to suppress their intensity will be discussed. Surprisingly, some of defect bands are very sensitive to polarization field in InGaN/GaN heterostructure, which can be influenced by doping or by structure design. Scintillator structure design will be based on results obtained from PL spectra and excitation-emission maps, AFM, HRTEM, CL, SIMS and band structure simulations by NextNano software.
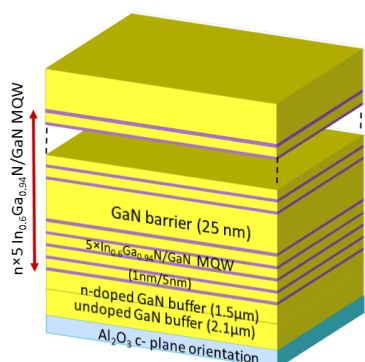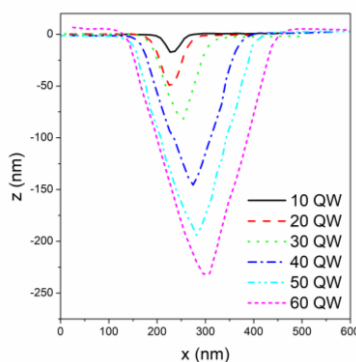
Fig. 1. Example of scintillator structure

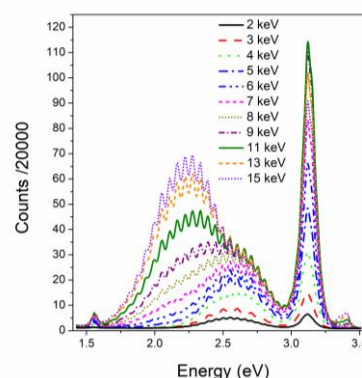Fig. 2. V-pit profiles for different QW number

Fig. 3. CL of MQW sample for different energy of electrons

[1] G. Balakrishnan, Nanotechnology **26**, 090501 (2015).
[2] A. Hospodková, et al, Nanotechnology **25**, 455501 (2014).

Burying surface defects in InGaN underlayer to increase blue LED efficiency

Camille Haller, Wei Liu, Jean-François Carlin, Gwénolé Jacopin, Denis Martin, Raphaël Butté, and Nicolas Grandjean

Institute of Physics, Ecole polytechnique fédérale de Lausanne (EPFL), Switzerland

Blue light emitting diodes (LEDs) currently exhibit impressive performance, i.e. a wall plug efficiency exceeding 80%. The active region of those devices consists in an InGaN/GaN multiple quantum well (MQW) structure. The high internal quantum efficiency (IQE) of these heterostructures has been ascribed for a long time to carrier localization in random alloy disorder induced potential fluctuations. However, another factor seems at play since commercial high brightness LEDs usually feature an InGaN layer, which is underneath the MQW structure. This underlayer (UL) has been shown to increase the efficiency of blue LEDs. Several explanations have been proposed like screening of threading dislocations due to V-pit formation [1], decrease of the internal electric field in the InGaN/GaN QWs due to band bending [2], or improved carrier injection [3]. Another hypothesis is that the InGaN UL reduces the density of deep levels in the QW active region [4,5].

In this presentation, we will present a comprehensive study of the effect of InGaN UL on the IQE of InGaN/GaN QWs. We will show that the role of this layer is to incorporate surface defects, which lie at the GaN surface. The origin of those defects will be discussed in view of secondary ion mass spectroscopy analysis.
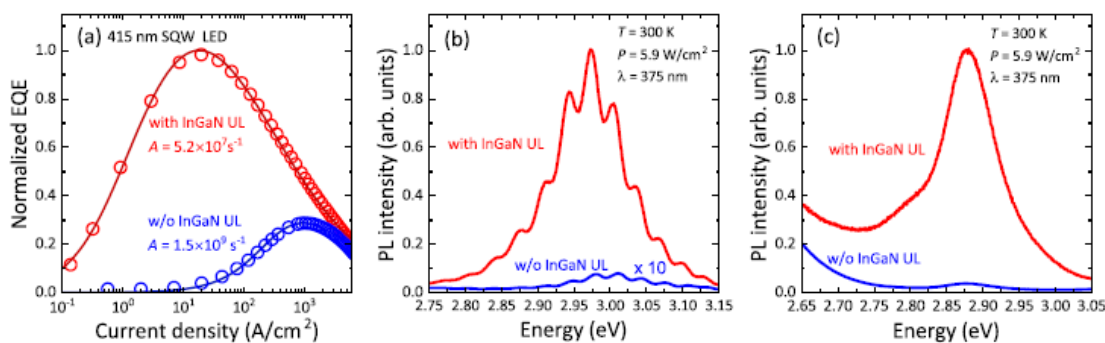

Figure 1: External quantum efficiency versus current density of single QW LEDs (a) and 300K PL intensity of an $In_{0.12}Ga_{0.88}N$/GaN sinlge QW grown on sapphire substrate (b) and on FS GaN substrate (c), with (red lines) and without (blue lines) an InGaN UL

[1] A. Hangleiter, F. Hitzel, C. Netzel, D. Fuhrmann, U. Rossow, G. Ade, and P. Hinze, Phys. Rev. Lett. 95, 127402 (2005)

[2] M. J. Davies, P. Dawson, F. C.-P. Massabuau, A. L. Fol, R. A. Oliver, M. J. Kappers, and C. J. Humphreys, Phys. Status Solidi B 252, 866 (2015)

[3] J.-W. Ju, E.-S. Kang, H.-S. Kim, L.-W. Jang, H.-K. Ahn, J.-W. Jeon, I.-H. Leea, and J. H. Baek, J. Appl. Phys. 102, 053519 (2007)

[4] T. Akasaka, H. Gotoh, T. Saito, and T. Makimoto, Appl. Phys. Lett. 85, 3089 (2004)

[5] A. M. Armstrong, B. N. Bryant, M. H. Crawford, D. D. Koleske, S. R. Lee, and J. J. Wierer, J. Appl. Phys. 117, 134501 (2015)

[6] C. Haller, J.-F. Carlin, G. Jacopin, D. Martin, R. Butté, and N. Grandjean, Appl. Phys. Lett. 111, 262101 (2017)

ISGN-7

August 5-10, 2018
Warsaw, Poland

Technology Trust Teamwork

FINANCIAL SUPPORT

PAN
POLISH ACADEMY OF SCIENCES

Ministry of Science
and Higher Education
Republic of Poland

Mazovia.
heart of Poland

UNIVERSITY
OF WARSAW

Malvern
Panalytical

Takatori
The Power of "T"
Technology Trust Teamwork

AdroitMaterials